The Dynamic Interplay of Microbiota and Mucosa Drives Establishment of Homeostasis in Conventionalized Mice

Sahar El Aidy

Thesis committee

Thesis supervisor
Prof. dr. M. Kleerebezem
Professor of Bacterial Metagenomics, Wageningen University

Thesis co-supervisors
Dr. ir. P. van Baarlen
Assistant professor, Host-Microbe Interactomics, Wageningen University
Dr. E. G. Zoetendal
Assistant professor, Laboratory of Microbiology, Wageningen University

Other members
Prof. dr. Michael Muller, Wageningen University
Prof. dr. Dirk Haller, Technische Universität München, Germany
Prof. dr. Albert K. Groen, Groningen University, The Netherlands
Dr. Annick Mercenier, Nestlé Research Centre, Lausanne, Switzerland

This research was conducted under the auspices of the Graduate School
VLAG (Voeding, Levensmiddelentechnologie, Agrobiotechnologie en Gezondheid).

The dynamic interplay of microbiota and mucosa drives establishment of homeostasis in conventionalized mice

Sahar El Aidy

Thesis
submitted in fulfillment of the requirements for the degree of doctor
at Wageningen University
by the authority of the Rector Magnificus
Prof. dr. M.J. Kropff,
in the presence of the
Thesis Committee appointed by the Academic Board
to be defended in public
on Friday 17 February 2012
at 4 p.m. in the Aula.

Sahar El Aidy
The dynamic interplay of microbiota and mucosa drives establishment of homeostasis in conventionalized mice,
176 pages.

Thesis, Wageningen University, Wageningen, NL (2012)
With references, with summaries in English, Dutch, and Arabic

ISBN 978-94-6173-195-1

SUMMARY

The intimate interplay between gut microbiota, host, and nutrient flow is crucial in defining the health status of the host. During microbial conventionalization of germfree mice, tightly regulated molecular responses assure the establishment of homeostasis and immune tolerance towards the microbiota. To decipher the temporal and regional dynamics of host-microbiota communication during the process of conventionalization, a combination of transcriptomics, (immune-)histology, metabonomics (tissue, urine, and plasma), as well as MITChip (Mouse Intestinal Tract Chip) based microbiota profiling was employed. To this end, C57/BL 6 J germfree mice were conventionalized with mouse fecal microbiota and responses were followed in a time-resolved manner for thirty days. The colonizing microbiota was characterized by a shift from low towards higher diversity of its composition, over the period of conventionalization. Microbial colonization was rapidly (after one day) reflected by increased concentrations of specific urine and jejunal metabolites as well as by biologically relevant changes in jejunal tissue transcriptome profiles. Conversely, ileal and colonic transcriptome responses could be measured later, after four days post-conventionalization, and led towards stable molecular profiles at sixteen and thirty days of conventionalization, albeit with region-specific differences. The major molecular responses included strong induction of innate immune response followed by stimulation of adaptive and regulatory immune functions, as well as modulation of metabolic pathways involved in lipid, carbohydrate, and anabolic metabolism. Conventionalization was characterized by two stages separated by one stage of a single day which, particularly in the colon, resembled a transient stage of inflammation, based on transcriptomes, histology and transiently elevated levels of specific plasma markers. This state coincided with temporal domination of specific microbial groups that have previously been identified as “pathobionts”, suggestive of a transient state of dysbiosis. Extensive transcriptome profile analyses throughout the GI tract enabled the identification of central gene regulatory networks that govern the molecular responses during conventionalization and are proposed to serve as genetic signatures for the control of intestinal homeostasis in mice. Nearly all genes in these regulatory networks have human orthologues, suggesting that the biological findings of this study is also relevant for human intestinal biology. In support of this hypothesis, in the jejunum, the identified gene regulatory network appeared to be strongly associated with human metabolic disorders. This notion also suggests that at least in mice, possibly also in human, there is a prominent role of the proximal small intestine in systemic metabolic control.
This thesis exemplifies the pivotal role of the dynamic molecular interactions between the microbiota and the intestinal mucosa, in the establishment and maintenance of mucosal homeostasis in healthy mice. The molecular signatures obtained from these studies in mice may provide novel diagnostic tools and/or therapeutic targets in humans for specific disorders associated with intestinal dysbiosis and loss of mucosal homeostasis.

KEYWORDS: C57/BL6 J mice, conventionalization, transcriptomics, (immune-)histology, metabonomics, microbiota.

TABLE OF CONTENTS

Chapter 1

General Introduction

Gut Microbiota and the Balance between Health and Disease

Sahar El Aidy and Michiel Kleerebezem

In preparation

Overview of the Mammalian Gastrointestinal Tract, its Cellular Architecture and Renewal

The gastrointestinal (GI) tract of an adult human consists of a muscular tube that starts from the oral cavity, where the food enters through the mouth, passes through the pharynx, the upper GI-tract, which consists of the oesophagus, stomach, and the first part of the small intestine (duodenum), the lower GI tract, which consists of the rest of the small intestine (jejunum and ileum), and the large intestine (cecum to which the appendix is attached, and the colon (ascending, transverse, descending, and sigmoid flexure)) to end with the anus and rectum, where the food waste is expelled (Martini 2001). Each part of the intestine has a different function. During swallowing, the food passes from the oral cavity to the stomach via the oesophagus. The main function of the stomach is the secretion of digestive enzymes and acids to help food digestion. From the duodenum onward, the dietary components are in close contact with the intestinal mucosa that fulfills the most important absorptive function and provide a barrier between the luminal contents and the rest of the body. The duodenum is the site where stomach acids are neutralized, and where the dietary materials are mixed together with the digestive enzymes mixture that catalyzes the break-down of the food into proteins and fats to facilitate their absorption. The main function of the jejunum is the passive transport of monosaccharides and active transport of amino acids, small peptides, vitamins, lipids, and glucose (Wilson 2004). The ileum absorbs the digestive products that were not absorbed by jejunum and secretes the enzymes required for the final stages of protein digestion (Sheehy 1964). The digested nutrients absorbed via the small intestine represent nearly 90% of the energy uptake from the diet (Walter and Ley 2011). The small intestine (terminal ileum) is separated from the large intestine (colon) by the ileocecal valve. The colon reabsorbs water and inorganic salts from the solid wastes before they are excreted from the body. Unlike the small intestine, no digestive enzymes are secreted in the colon. Instead, the colon is home to trillions of intestinal commensal microbes which break down unabsorbed material and produce fermentation products in the form of short chain fatty acids (SCFAs) which, in turn, are used by colonocytes as a major source of energy (Cummings and MacFarlane 1997).

The three segments of the small intestine have the same basic histological organization, mucosa and submucosa (Figure 1.1B). The mucosa is composed of the lumen-exposed monolayer of epithelium that covers the gastrointestinal wall and overlays the lamina propria (a layer of connective tissue) and the muscularis mucosae (a thin layer of smooth muscle). The entire mucosa has finger like projections (known as villi) which extrude into the lumen and cover the inner surface and are much longer in the jejunum than in the duodenum or ileum. The villi are lined with epithelial cells which in their turn have a large number of microvilli at the apical side, the brush border region, whereby the surface area of mucosa that is in contact with the intestine lumen is maximized (see also below). Such structural features of the mucosa support the main function of the small intestine, the absorption of digested food. The ileal villi contain large number of capillaries that transport the amino acids and glucose as end products of digestion to the hepatic portal vein. Crypts of Lieberkühn (simple tubular glands) are found between the intestinal villi and extend down to the muscularis mucosae through the lamina propria which is rich with lymphocytes and other immune cells. Together, the crypt-villus units (also known as crypt-to-villus axis) play an important role in control of cell proliferation, differentiation, migration, and apoptosis (Ahuja, Dieckgraefe et al. 2006). Conversely, the surface of the large intestine is relatively smooth with no extruding villi and longer and straighter crypts of Lieberkühn as compared to the small intestine (Stappenbeck, Hooper et al. 2002). Only a limited lamina propria is present in the large intestine, which is located between the crypts.

The submucosa is comprised of connective tissue, blood and lymphatic vessels, and nerves to supply and support the intestinal mucosa (Barrett 2006).
Under physiological, healthy conditions, the gut is covered by the largest epithelial surface in the body (Tlaskalova-Hogenova, Stepankova et al. 2011), which in humans equals the size of a tennis-court (approximately 200 m^2 in humans). This single layer consists of interconnected, polarized cells reinforced together by associated areas of protein strands known as the tight junctions, to form the major barrier of the intestinal mucosa. Tight junctions participate in determining the shape and structure of epithelial cells (Fasano 2008) . Epithelial cells are continuously shed and generated *de novo* by multipotent stem cells located at the base of crypts of Lieberkühn (Figure 1.1C). Each active stem cell differentiates into progenitor cells which give rise to two cell-populations, (i) the absorptive enterocytes, and (ii) the secretory epithelial cells, including goblet, enteroendocrine, and Paneth cells (Bjerknes and Cheng 1981) (Figure 1.1C). Enterocytes are the most abundant cells present in both the small and large intestine. They are involved in water and electrolyte absorption and form an important physical barrier to the luminal microbes (Ahuja, Dieckgraefe et al. 2006). Goblet cells are present in both the small and large intestine but are relatively more abundant in the large intestine. They help protect the mucosal surface by secreting mucins (glycosylated proteins) that form a protective layer that lies over the epithelial surface and prevents or restricts direct contact between the epithelial cells and gut content, particularly in the large intestine. Moreover, the mucus layer acts as a lubricant to facilitate the peristaltic movement of the intestine and its luminal content. The thickness of the secreted mucus increases along the GI tract (150-300 μm in the small intestine up to 800 μm in the large intestine) (Medema and Vermeulen 2011). Enterendocrine cells are a complex and specialized population of intestinal epithelial cells that can produce a variety of gut hormones and neurotransmitters such as serotonin, cholecystokinin (CCK), and glucagon-like peptides 1, 2 (GLP-1,-2) (Liddle 2010). Enteroendocrine cells are positioned in the mucosa in a way that allows them to sense luminal signals, including microbial metabolites, which can elicit cellular responses that in their turn function as signals to modulate other mucosal cells (Bienenstock and Collins 2010). The signals derived from enteroendocrine cells play an important role in the modulation of host energy metabolism, mucus secretion and intestinal motility (Cani and Delzenne 2009). The three cell lineages described above complete their differentiation by migrating out of the crypt to a cellular extrusion zone located near the tip of each villus which takes 2 to 5 days to be completed (Stappenbeck, Hooper et al. 2002). The fourth cell lineage, Paneth cells (Barker, van de Wetering et al. 2008), are essential in the antimicrobial defense and are located at the base of the small intestinal crypts (Figure 1.1C), while they appear to be absent from the large intestinal mucosa. Paneth cells contain secretory granules in which different antimicrobial peptides such as α-defensins, lysozymes, RegIIIγ, and phospolipase A_2 are present. The vital role that these humoral components of the innate (non-specific) immune response play in mucosal barrier function is now well-recognized (Tlaskalova-Hogenova, Stepankova et al. 2011; Vaishnava, Yamamoto et al. 2011). Defensins (also known as cryptidins) are the principle defense molecules of Paneth cells (Wilson, Ouellette et al. 1999), they interact with phospholipids in bacterial cell membranes and form pores that disrupt the membrane function and cause cell lysis (Ayabe, Satchell et al. 2000). In order to maintain the protective function of the mucosal epithelia, the cellular turn-over needs to be tightly controlled without disrupting the epithelial cell-cell tight-junctions, to prevent breaches in the epithelial barrier function (Mentor-Marcel, Bobe et al. 2009).

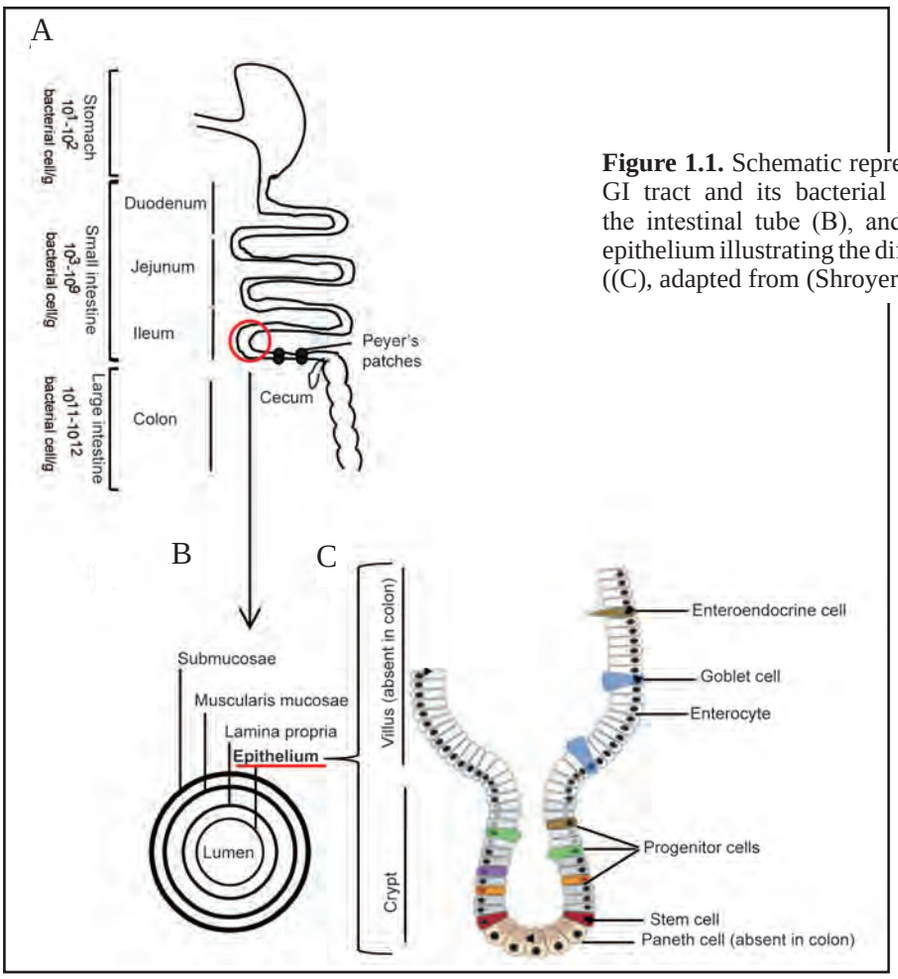

Figure 1.1. Schematic representation of the mammalian GI tract and its bacterial load (A). Cross section of the intestinal tube (B), and crypt and adjoining villus epithelium illustrating the different epithelial cell lineages ((C), adapted from (Shroyer, Wallis et al. 2005)).

The Immune System of the Gastrointestinal Tract

The enormous surface area of the GI tract that is exposed to the environment requires a balanced defense system to prevent the translocation of antigens from the lumen (Mestecky 2005). A multitude of activities contribute to defense, including the innate and adaptive (specific) immune system, as well as detoxification enzymes, and bile salts which have bactericidal effect (Cummins 1911). Collectively, the immune system of the GI tract is largely organized in the gut-associated lymphoid tissue (GALT), which is the largest mass of lymphoid tissue in the human body (Isolauri, Sutas et al. 2001). The GALT comprises different types of lymphoid tissues including the Peyer's patches (Mestecky 2005). Only the ileum has abundant Peyer's patches that contain large numbers of lymphocytes and other immune cells. Peyer's patches are aggregations of lymphoid tissue which appear as elongated thickenings of the ileal tissue (Figure 1.1A) and play a major role in the development and maintenance of the immune system. The Peyer's patches are located in the lamina propria layer of the mucosa and are covered by microfold cells (M cells), which sample antigens from the GI tract lumen that are processed by antigen presenting cells located in the Peyer's patches such as macrophages, dendritic cells, natural killer cells, B-and T-lymphocytes (Brandtzaeg, Kiyono et al. 2008) (Figure 1.2). M cells are absent from the isolated lymphoid follicles of the large intestine. In addition, sampling of antigens from the intestinal lumen can also be carried out by a subset of dendritic cells that have been reported to sample directly by dendrites that penetrate between the epithelial cells and protrude into the lumen (Rescigno, Urbano et al. 2001). Dendritic cells and macrophages

represent important members of the innate immune system; they internalize partially degraded luminal compounds and present them to cells of the adaptive immune system. In particular, antigens are presented to naive and memory T cells leading to their activation in a process known as antigen-processing and presentation (Lee, Starkey et al. 1985) (Figure 1.2). Naive T cells can differentiate into T helper (Th) cells (Th1, Th2, and Th17), which are co-regulated with regulatory T cells (T_{regs}) (Hooper and Macpherson 2010). The differentiation of B cells leads to cells that produce immunoglobulin A (IgA), which plays a vital role in mucosal immunity and is produced extensively in mucosal linings. Epithelia express the polymeric IgA receptor (pIgA) to transport IgA across the epithelial cells to be released into the lumen where the IgA are involved in neutralization of luminal antigens (Macpherson and Uhr 2004). The mesenteric lymph nodes are part of the intestinal lymphatic system and lie in the peritoneal membrane that separates the jejunum and ileum from the abdomen. The mesenteric lymph nodes prevent the translocation of the luminal antigens to the systemic immune compartment to avoid eliciting damaging immune responses to the harmless luminal antigens (Macpherson and Harris 2004).

Microbiota of the (human) Gastrointestinal Tract in Health and Disease

There is an intimate contact of the microbes (collectively known as microbiota) that live in and on the surface areas of mammalian bodies, including the mucosal surfaces of the GI tract. Colonization of the GI tract is initiated during and after birth (Hallstrom, Eerola et al. 2004). Typically, a high degree of variation in the gut microbiota composition during the first few days to weeks after birth is observed (Harmsen HJ 2000; Palmer, Bik et al. 2007). In healthy adults, the colonizing microbiota reaches a climax community with a total number of approximately 10^{14} microbial cells that collectively weigh more than 1kg.

A typical microbe includes archaea, fungi, viruses, and protozoa, but is largely predominated by bacteria. This number of microbial cells is several orders of magnitude larger than the estimated 10^{12} parenchymal cells in an average human body (excluding the blood cells and neurons) (Todar 2004). The very low pH of the stomach allows the survival of very limited number of microbiota (10^{1}-10^{2} cells/g, with *Helicobacter pylori* as the most well-known example) (O'Hara and Shanahan 2006) (Figure 1.1A). In the proximal small intestine the luminal pH is neutralized so that the number of residing bacteria can increase gradually along the GI tract. In the small intestine, the rapid luminal flow and the secretion of bile salts limit the bacterial density (between 10^{3}-10^{5} cells/g in the proximal part of the small intestine; duodenum and jejunum).

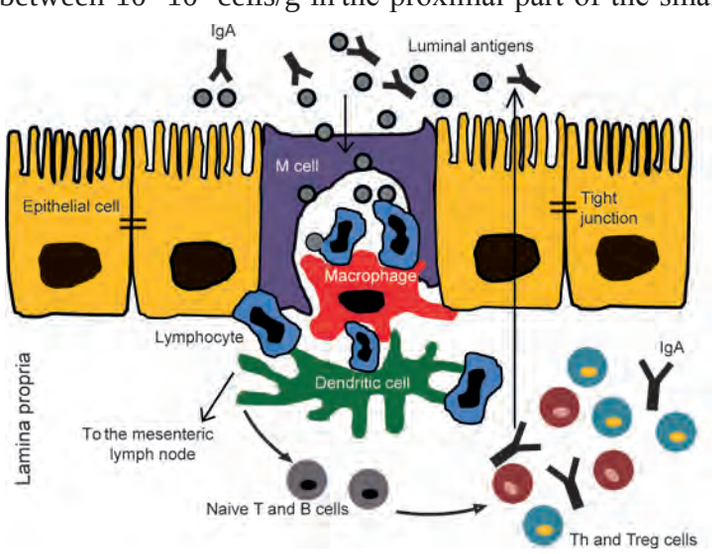

Figure 1.2. Schematic diagram of the intestinal mucosal immune system. The effector compartment consists of lamina propria and epithelial cells. M cells act as an entry port to facilitate the uptake of luminal antigens and their subsequent processing by the lymphoid tissues, particularly involving dendritic cells and macrophages. Antigen presentation and processing leads to the activation and differentiation of naive T and B cells into T helper (Th), T regulatory (T_{regs}), and IgA-producing B-cells, respectively.

Such low number of colonizing microbiota allows the host to limit direct competition with the microbiota for the absorption of ingested nutrients which is the main function of the proximal small intestine (Walter and Ley 2011). In contrast, the distal part of the small intestine and the large intestine have significantly slower luminal flow, which allows for the colonization by a more dense microbiota (nearly 10^7 -10^{12} bacterial cell/g) (Figure 1.1A) (O'Hara and Shanahan 2006).

Despite the high microbial population density, a peaceful coexistence (homeostasis) is maintained between the intestinal microbiota and its (healthy) host. The molecular basis of this partnership involves bacterial signals that are recognized by host receptors to mediate host's tolerance towards the commensal microbiota, which facilitates beneficial outcomes for both the microbiota and host (Lee and Mazmanian 2010). The microbiota contributes to diverse mammalian processes that include the defense against pathogens, thereby enhancing the barrier function of the gut mucosa. In addition, the microbiota ensures *de novo* synthesis of essential nutrients and the fermentation of non-digestible dietary materials, which result in enhanced recovery of energy from the diet by the host (Hooper, Bry et al. 1998; Xu and Gordon 2003). Only microbial population that are capable of establishing a mutualistic relation with the host can be maintained in the gut ecosystem (Bäckhed, Ley et al. 2005), creating a habitat that exerts restrictive selection on its microbial inhabitants. This restrictive selection of specific microbial groups is illustrated clearly by the relatively low phylum-level diversity observed in the microbiota of the GI tract of many mammalian organisms, including mice and humans, which is dominated by the phyla of the Bacteroidetes (e.g., the genus *Bacteroides*), the Firmicutes (e.g., the genera *Clostridium* and *Eubacterium*), (Bäckhed, Ley et al. 2005; Eckburg, Bik et al. 2005; Ley, Hamady et al. 2008) and Actinobacteria. The actual number of the latter group are probably under-estimated by PCR based approaches but appear to make up a high proportion of the gut microbiota based on Florescent *in situ* hybridization (FISH) approaches (Zoetendal, Vaughan et al. 2006) . Notwithstanding the relatively low diversity of the gut microbiota at the phylum level, the diversity at the genus and species levels is enormous and is shaped by the host genotype, the variation in early-life environmental exposure that includes the mode of delivery (Zoetendal 2001; Hallstrom, Eerola et al. 2004) and nourishing regime of neonates (Dai D 1999), and later in life by factors like dietary habits, antibiotic therapy, hygiene and infection (Fanaro, Chierici et al. 2003).

Molecular strategies to create inventories of the human intestine microbiota species composition commonly target the universal 16 S ribosomal RNA (16 S rRNA) gene as a universal marker to discriminate bacterial species. These studies have demonstrated strikingly high variability within and between the individuals (Zoetendal 1998; Eckburg, Bik et al. 2005). In an attempt to define a common core of microbiota members in the fecal samples of healthy individuals, Tap and colleagues reported that 2.1% of the identified bacterial groups were encountered in more than 50% of the individuals (designated "core microbiota"), while the rest were individual-specific (Tap, Mondot et al. 2009). However, more recent studies have debated the concept of a common core microbiota that can be recognized at the phylogenetic level, pointing out that the depth of analysis may play an important role in the differences in the outcomes of these analyses (Turnbaugh, Hamady et al. 2009; Jalanka-Tuovinen, Salonen et al. 2011). The molecular profiling of microbiota community composition in healthy volunteers in comparison to cohorts of diseased individuals show associations between diseases and aberrations in the intestinal microbiota composition (Zoetendal, Vaughan et al. 2006). While these associations are highly intriguing and postulate that there is potential for health management through the

(targeted) modulation of the microbiota composition, in many cases the exact causal relations within these associations remain to be established. More recently, metagenomic approaches allowed in depth insight in the functional diversity of the dominant microbial composition and its genetic potential (Gill, Pop et al. 2006; Qin, Li et al. 2010) and have revealed that despite the variation of species composition, the microbial communities encompass a relatively similar set of (metabolic) functions in healthy individuals, which is referred to as "core microbiome" (Turnbaugh, Hamady et al. 2009; Qin, Li et al. 2010). Subsequent function-based comparative analysis of the function-microbiome of individual humans has allowed the detection of distinct subgroups of people that can be classified on basis of their microbiome composition, so-called enterotypes (Arumugam, Raes et al. 2011). The three enterotypes detected could be discriminated on basis of a single discriminating genus (*Bacteroides* [enterotype 1], *Prevotella* [enterotype 2], or *Ruminococcus* [enterotype 3]) (Arumugam, Raes et al. 2011), and did not appear to correlate with particular host properties like body mass index (BMI), gender, age or dietary habits. Moreover, distinct abundances of specific functional markers (microbiome functions) could be correlated with either the enterotype classification or with some of the host-phenotype data like age and BMI. These microbiome functional markers may provide diagnostic tools for detecting (enterotype specific) markers for specific health aberrations within the intestinal microbiome (Arumugam, Raes et al. 2011). A recent study suggested that enterotypes could be specifically linked to long-term dietary pattern, although only two enterotypes could be discriminated (Wu, Chen et al. 2011). Taken together, the human microbiome studies confirm the significant difference in the microbial composition of healthy and diseased individuals and highlight the importance of the human gut microbiome in human (and animal) health and disease. Despite these advances, the molecular mechanisms by which the microbiota may influence human health remain largely unknown, and it will require a substantial effort to unravel these mechanisms to a level that enables the use of this knowledge for the definition of species- or functional- microbiome-markers for diagnostic purposes or as targets for therapeutic and/or dietary interventions that aim at maintaining or may be even improving host health.

In Vivo Animal Models as Simplified Host Models

Simplified in vivo and in vitro models have been instrumental in the first steps towards unraveling the molecular basis of the complex and dynamic interrelations underlying the healthy homeostatic relation between the microbiota and the intestinal mucosa, as well as the deviations in these interrelations that may lead to dysbiosis and disease. In vitro and ex vivo models frequently employ animal and human cell culture systems such as cell-line models, Ussing chambers, organotypic models (which include all intestinal cell types), and isolated and perfused intestinal segments. These models have been widely used to study host-microbe interactions, particularly, the functioning of the intestinal epithelium and its role in absorption, metabolism, drug detoxification, and microbial recognition (Le Ferrec, Chesne et al. 2001). These approaches provide relatively simple models, but the extrapolation of the results obtained in these in vitro and ex vivo systems to real life is far from trivial. These simplified models consistently lack the systemic in vivo interplay that is found within a complete organism, but in most cases also fail to accurately mimic the in vivo anatomical and biochemical characteristics. For instance, the use of tumor-derived cell lines (e.g.; Caco-2 and HT-29) may introduce artifacts due to the hyperproliferative nature of the tumor cells employed. Therefore, in vivo models are crucial to better understand the molecular bases by which the microbiota shapes the host's physiology. However, it is virtually impossible to perform such molecular studies in vivo in human subjects

due to the experimental and ethical limitations. To overcome this, (ex-) germfree, gnotobiotic, and genetically modified animals provide attractive and genetically defined, simplified models to study the in vivo responses to commensal bacteria. The most frequently employed animal models in such studies are zebra fish, *Drosophila spp.*, and rodents, with the largest number of published studies on germfree mice. Germfree (and genetically modified) mice have allowed the study of the role of specific genes and functions in the interplay between (specific) microbial species and the mouse physiology, and these models have been extensively used to study the relations between microbiota and different hosts, including healthy hosts and models for diseases like obesity, diabetes, and cardiovascular dyslipidaemia (Bäckhed, Ding et al. 2004; Turnbaugh, Ley et al. 2006; Cani, Amar et al. 2007; Cani, Neyrinck et al. 2007). The basic studies on germfree life were initiated in the United States by J.A. Reyniers at the Lobund laboratories-University of Notre Dame in 1928 (Wiseman 1965). Germfree animals are bred and maintained without exposure to bacteria of any kind (Gordon 1968), they live in flexible-film isolators that are essentially plastic bubbles inflated with sterile filtered air using elevated atmospheric pressure. All food, water, and bedding are autoclaved and introduced to the isolator using aseptic protocols. Initiator animals for a germfree colony must be aseptically delivered by Caesarean section, but later they can be interbred within the sterile environment (Gordon 1968; Smith, McCoy et al. 2007). If colonized with single microbial species (mono-association), or a microbiota of low or high complexity, the animals will allow the establishment of a bacterial community in the intestine and other body surfaces within days. This process can be considered to share similarities with the process encountered by a conventionally born mammal that becomes rapidly colonized by microbial communities after leaving the uterus (Macpherson and Uhr 2004). Histological and molecular experiments performed on germfree animals illustrated that the presence of the microbiota causes extensive changes in the host biology that includes altered epithelial cell gene expression, changes in the composition and activity of the mucosal immune system, metabolism, angiogenesis, bile acid cycle, intestinal motility, and overall animal behavior (Heneghan 1963; Evrard, Charlier et al. 1964; Dahlqvis.A, Bull et al. 1965; Reddy, Pleasant et al. 1969; Yolton, Stanley et al. 1971; Cebra 1999; Hooper 2001; Hooper, Wong et al. 2001; Stappenbeck, Hooper et al. 2002; DiBaise, Zhang et al. 2008) (Table 1.1). For example, the intestinal mucosal morphology of the germfree animals differs from that of their conventional counterparts in several ways, including the total mass of the intestine (Levenson and Tennant 1963) and the total surface area of the small intestine, both of which are decreased in germfree animals (Gordon and Brucknerkardoss 1961; Meslin and Guenet 1973). Simplified and defined microbiotas composed of single or several bacterial species and/or strains have been used in germfree mice to define the impact of a specific member of the bacterial community on the host functions. Mono- and bi-association are attractive models of gnotobiotic animals based on their high degree of definition and consistency. *Bacteroides thetaiotaomicron*, an abundant, genetically tractable member of the normal human and mouse microbiota (Salyers, Bonheyo et al. 2000) represents the most widely used mono-associated model in mice. *B. thetaiotaomicron* was used to study the microbial polysaccharide metabolism in the gut (Bry, Falk et al. 1996; Hooper, Xu et al. 1999; Xu, Bjursell et al. 2003) and showed to be able to degrade a wide variety of host-derived glycans (glycoconjugates) that provided a nutrient source for the initial colonization of the neonate intestine (Salyers, Vercellotti et al. 1977; Karlsson 1989; Falk, Roth et al. 1994; Hooper, Midtvedt et al. 2002). In a pioneering study, Hooper and co-workers showed how the mono-association of germfree mice with *B. thetaiotaomicron* modulated the cellular, kinetic, and spatial features of fucosylated glycans in

a way that bears similarity to the effects of total microbial communities in conventionally raised animals during weaning (Hooper, Wong et al. 2001). Interestingly, the metabolic activity of *B. thetaiotamicron* in situ in the intestine of mice as well as the mouse immune responses were shown to be significantly influenced by the presence of specific additional members of the microbiota (Sonnenburg, Chen et al. 2006; Sonnenburg, Zheng et al. 2010), illustrating the importance of microbial interplay in the interaction with the host system. Mono-association of mice with *Bacteroides fragilis* demonstrated the strong impact of this microbe on mucosal immune responses, in particular its role in the stimulation of anti-inflammatory T regulatory cell development (Mazmanian, Round et al. 2008). Another intriguing example was provided by mono-association experiments using segmented-filamentous bacteria (SFB). SFB are strictly anaerobic, gram-positive bacterial groups that inhabits the intestinal tracts of many species (Klaasen, Koopman et al. 1992). Mono-association studies of SFB in mice illustrated the potent role of this bacteria in the stimulation of the gut mucosal immune system including the induction of germinal center reactions and activation of effector T cells in Peyer's patches (Talham, Jiang et al. 1999; Gaboriau-Routhiau, Rakotobe et al. 2009). Besides mono-associations, colonization of mice by multiple groups has also been performed. Schaedler and co-workers developed a reduced standardized microbiota (referred to as altered Schaedler flora or ASF) (Orcutt, Gianni et al. 1987) to colonize germfree mice in order to avoid the variations in the microbial composition among conventionally raised mice purchased from different sources (Gaboriau-Routhiau, Rakotobe et al. 2009; Ivanov and Manel 2010). Unfortunately, even such a standardized microbial community is unlikely to provide an accurate representation of the complexity of the total microbial community. These examples highlight the usefulness of simplified (ex-) germfree animal models for the study of molecular interactions between the intestinal mucosa and the colonizing bacteria. Notably, without such animal model studies it is virtually impossible to decipher molecular interaction models that accurately describe host microbe interactions in the mammalian intestine. However, it remains essential that mechanisms of interaction deduced from these simplified animal models are translated to hypotheses for the molecular basis of human host-microbe homeostasis in the intestine that can be verified in vivo in human intervention studies. Importantly, recent controlled dietary interventions in healthy human volunteers have illustrated the feasibility of the accurate measurement of mucosal transcriptional responses after consumption of probiotics (van Baarlen, Troost et al. 2011).

Gut Microbiota Shapes the Host Immune System in Health and Disease

In healthy individuals, the gut epithelia are in continuous contact with different kinds of stressors, including the gut microbiota, but succeed to maintain homeostasis. During early and later stages of life, the gut microbiota shapes the molecular profile of the gastrointestinal immune system (Lee and Mazmanian 2010). The beneficial and adverse interactions between the immune system and microbiota (Macpherson and Harris 2004; Garrett, Gordon et al. 2010) have been extensively studied in in vivo animal models. These studies showed that the host intestinal immune system requires the presence of commensal microbes for its development and proper functioning. The first line of defense for the intestinal mucosa (GALT) is defective in germfree mice that have smaller Peyer's patches and reduced cellularity of the lamina propria with lower $Cd4^+$ and $Cd8^+$ T cells (Glaister 1973; Falk, Hooper et al. 1998). Plasma cells and intraepithelial lymphocytes are rare in the small intestine mucosa of germfree mice and secretory IgA levels are significantly lower (Fahey and Sell 1965; Crabbe, Nash et al. 1970; Moreau, Ducluzeau et al. 1978) (Table 1.1). Germfree mice exhibit reduced expression

Table 1.1. Selected examples of germfree animal associated characteristics (adapted from (Norin E. 2000; Smith, McCoy et al. 2007; Round and Mazmanian 2009)).

Parameter	Germfree associated characteristics	Reference
Intestinal motility	-Increased transit time of contents -Altered myenteric neurons -Increased muscular tissue	(Abrams, Sprinz et al. 1963) (Dupont, Jervis et al. 1965) (Gordon 1968)
Intestinal function	-Altered absorption rate of ingested material -Decreased fatty acids in intestinal content -Excrete largely unsaturated fatty acids -Excrete large amount of mucin in feces -Increased bilirubin in feces	(Heneghan 1963) (Evrard, Charlier et al. 1964) (Evrard, Charlier et al. 1964) (Carlstedtduke, Hoverstad et al. 1986) (Gustafsson and Lanke 1960)
Absorption function	-Increased absorption of vitamins and minerals	(Heneghan 1963)
Intestinal morphology	-Decreased intestinal total mass -Decreased total surface area of small intestine -Altered villus and crypt length -Larger cecum with thinner cecal wall -Thinner lamina propria with less cellularity	(Levenson and Tennant 1963) (Gordon and Brucknerkardoss 1961) (Glaister 1973) (Jervis and Biggers 1964; Gordon 1968) (Glaister 1973)
Intestinal epithelium	-More uniform with longer microvilli -Slower rate of turn over -Decreased cellular renewal rate in Peyer's patch -Reduced expression of antimicrobial peptides in Paneth cells	(Abrams, Sprinz et al. 1963) (Lesher, Sacher et al. 1964) (Abrams, Sprinz et al. 1963) (Round and Mazmanian 2009)
Mucosal immunity	-Decreased IgA -Very few plasma cells in small intestine -Decreased expression of activation markers on immune cells -Decreased histamine and increased 5-HT in small intestine -Decreased MHC II on epithelial cells of small intestine - Fewer $CD8^+$T cells in intestinal epithelial lymphocytes with reduced cytotoxicity -Fewer $CD4^+$T cells in lamina propria	(Fahey and Sell 1965) (Glaister 1973) (Mikkelsen, Garbarsch et al. 2004) (Beaver and Wostmann 1962) (Umesaki, Okada et al. 1995) (Glaister 1973; Round and Mazmanian 2009) (Round and Mazmanian 2009)
Metabolism	-Increased nitrogen in feces and cecal content -Little ammonia and more urea in intestinal content -Decreased basal metabolic rate	(Evrard, Charlier et al. 1964) (Evrard, Charlier et al. 1964) (Wostmann, Bruckner.E et al. 1968)
Nutritional differences	-Requires Vitamin B and K in diet -Decreased body fat percentage	(Wostmann 1981) (Levenson and Tennant 1963)

of activation markers of intestinal macrophages (Mikkelsen, Garbarsch et al. 2004), Toll-like receptors (TLRs), and major histocompatibility complex II (MHC II) which are involved in microbial sensing and antigen presentation (Matsumoto, Setoyama et al. 1992; Lundin, Bok et al. 2008). Reconstitution of germfree animals leads to re-localization of intestinal immune cells to both inductive sites (e.g.; Peyer's patches, colonic patches, and mesenteric lymph nodes) and effector sites (epithelia and lamina propria) (Ley, Hamady et al. 2008).

Commensal and pathogenic bacteria share the same conserved molecular patterns (designated microbe associated molecular patterns or MAMPs) that are recognized by and bind to host receptors of the innate immune system (known as pattern recognition receptors or PRRs), involved in bacterial recognition (Falk, Hooper et al. 1998; Bäckhed and Hornef 2003). PRRs are classified according to their function into signaling (such as TLRs and NOD-like receptors) and endocytic pattern recognition receptors which are found on phagocytic cells and promote attachment, engulfment, and destruction of microorganisms without depending on intracellular signaling (Mestecky 2005). Binding of MAMPs to PRRs activates a cascade of reactions that control the expression of genes that are associated with defense mechanisms including the production of anti-microbial peptides and the expression of pro- and anti-inflammatory genes, but also influence cell migration, proliferation, and apoptosis (Falk, Hooper et al. 1998; Cario, Rosenberg et al. 2000; Bäckhed and Hornef 2003). It remains obscure how the microbial sensing by the host immune system discriminates between the development of tolerance that is stimulated by the commensal gut microbiota and other benign luminal antigens, and mounting of cytotoxic responses towards undesired pathogens. The role of adaptive immune response in mounting balanced pro- and anti-inflammatory responses depending on the nature or subcellular position of a particular antigen could be a mechanism by which the host immune system tolerates or defends against the microbiota and pathogens, respectively. Surface expression of receptors by dendritic cell populations that can activate regulatory T cells (T_{regs}) may determine the direction of the mucosal immune response either towards inflammatory responses or tolerance (Coombes and Powrie 2008). For example, pathogenic bacteria induces the maturation of dendritic cell populations that activate the effector T cell subpopulation and results in strong cytotoxic, inflammatory responses (Rescigno and Di Sabatino 2009). Ignorance of recognition is another suggested mechanism that could underlie tolerance development, and it has been shown that the gut epithelium can inactivate some TLRs ligands via their delocalization (Bates, Erwin et al. 2002). The gut microbiota itself (e.g., *Bacteroides* species (Ley, Hamady et al. 2008)) may play a role in TLR inactivation, providing a mechanism by which inappropriate inflammatory responses could be avoided. One of the suggested mechanisms by which the microbiota shapes the immune balance during health is via the induction of T_{regs} activity, including the production of transforming growth factor beta (*Tgfß*) , interleukin 10 (*Il-10*), and forkhead box P3 (*Foxp3*) (Round and Mazmanian 2009) (Figure 1.3). Ivanov and co-workers demonstrated that especially the commonly abundant phylum of Bacteroidetes is essential to restore the immunological tolerance in germfree mice (Ivanov, Frutos et al. 2008). Another proposed mechanism involves bacterial DNA that is known to be able to trigger some TLRs, which leads to redirecting of the differentiation of T cell populations that supports a decreased susceptibility to infection (Lee, Lyons et al. 2011). Intriguingly, conventionally raised mice that were deliberately colonized by a defined mix of *Clostridium* strains in their early life were more resistant to colitis, which involved in particular the clusters IV and XIVa of *Clostridium* that stimulated the development of T_{regs} in the colon mucosa (Atarashi, Tanoue et al. 2011). In addition, *Faecalibacterium prausnitzii* has been proposed to promote anti-inflammatory responses that can protect against

2, 4, 6-trinitrobenzene sulfonic acid (TNBS) induced colitis in a mouse colitis model (Sokol, Pigneur et al. 2008). These experiments using simplified microbial interaction models in ex-germfree and conventional animal models, have provided elegant examples of the role of the intestinal microbiota in the shaping of the host immune system by instructing T helper cell differentiation, by bringing about shifts in the balance between regulatory and inflammatory immune responses (Lee and Mazmanian 2010). These findings also have illustrated that an intact epithelial barrier and a balanced innate and adaptive immune system are prerequisites for the maintenance of intestinal homeostasis. Gross deviations from homeostasis elicit detrimental effects in the host's physiology, and altered or aberrant microbial composition (also called dysbiosis) may include the decreased abundance of anti-inflammatory microbes and/or the increased abundance of potentially pathogenic symbionts, or pathobionts (Chow and Mazmanian 2010) that can trigger inflammatory responses. Such microbiota aberrations can lead to inadequate immune functioning and inflammatory responses by an imbalance between regulatory and pro-inflammatory T cells (Th1 and Th17) (Figure 1.3), which may especially occur in genetically susceptible hosts (Lee and Mazmanian 2010; Zhu, Yao et al. 2011). In these situations, the gut microbiota becomes harmful to its host and ultimately in an interplay with the host genotype and environmental triggers (Packey and Sartor 2009) may lead to a variety of diseases, including inflammatory bowel disease (a collective term for Crohn's disease and ulcerative colitis), autoimmunity, rheumatic diseases, cardiovascular diseases and atherosclerosis, allergy, autism, as well as cancer (Sekirov, Russell et al. 2010). The favorable response of inflammatory bowel disease patients to antibiotic treatment (Round and Mazmanian 2009) supports the fundamental role of microbiota in the pathology of the disease. Analogously, animal models for colitis depend on the presence of an intestinal microbiota and animals that are living under germfree conditions do not develop disease symptoms (Burczynski, Peterson et al.

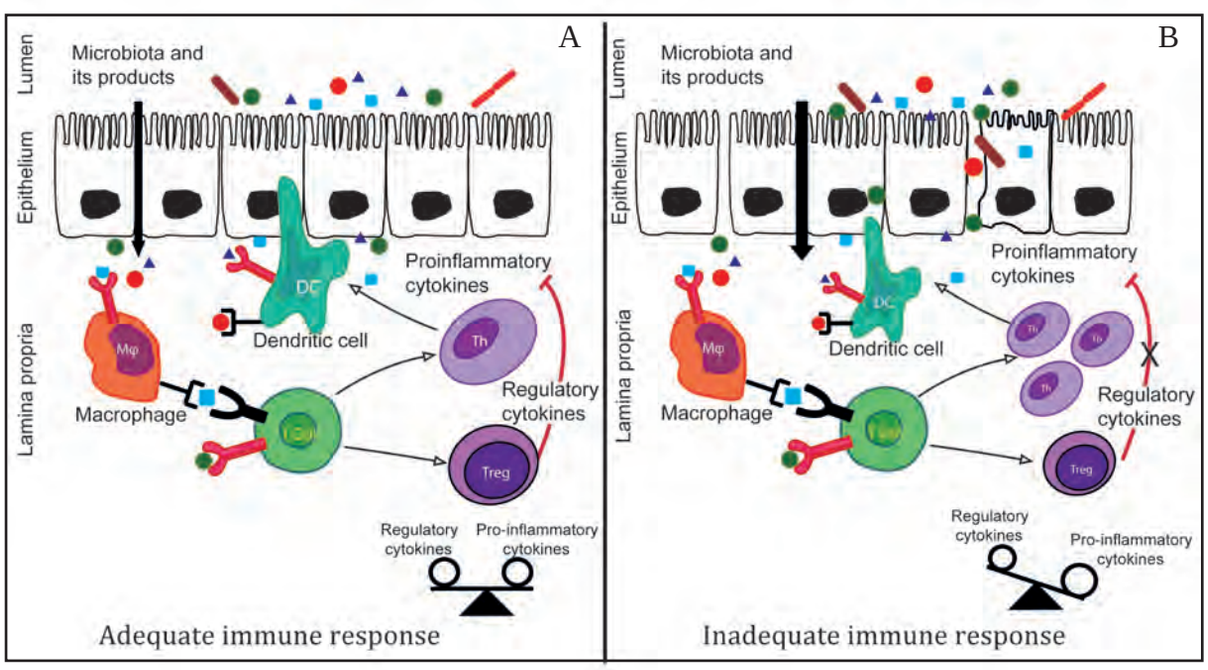

Figure 1.3. A schematic model of microbiota-mediated immune response. (A) Adequate gut immune defense is achieved in the presence of balanced microbial community and an associated regulated immune response. (B) Inadequate gut immune defense as a result of dysbiosis during which the number of pathobionts increases, loss of intestinal barrier and the consequent loss of well-balanced immune response, which would lead to inflammation.

2006). Inflammatory responses in the gut of humans as well as animal models for inflammatory bowel disease have been shown to be strongly associated with increased abundance levels of certain bacterial groups including *Escherichia coli* (Zhu, Yao et al. 2011), *Clostridium, Enterococcus,* and *Helicobacter* (Chow, Tang et al. 2011), and decreased abundance of microbes like *Faecalibacterium prausnitzii* (Sokol, Pigneur et al. 2008). In addition, Crohn's disease was found to be associated with reduced diversity of gut microbiota (Manichanh, Rigottier-Gois et al. 2006; Qin, Li et al. 2010; Lepage, Haesler et al. 2011) including a decrease in the mucolytic bacteria, *Akkermansia* (Png, Linden et al. 2010), and Firmicutes, in particular the *Clostridium leptum* group (Manichanh, Rigottier-Gois et al. 2006). These findings support a pivotal role of microbial dysbiosis in inflammatory diseases (Garrett, Lord et al. 2007; Swidsinski, Doerffel et al. 2011), particularly in combination with host genetic and environmental alterations.

The Role of Gut Microbiota in Host Metabolism, Energy Harvest, and Metabolic Diseases

The gut microbiota is able to perform chemical transformations of diet and host derived compounds that are of significant importance to the host metabolism (Nicholson, Holmes et al. 2005). The microbiota were proposed to be a "metabolically active organ" inside the human body (O'Hara and Shanahan 2006). This microbial community has a profound effect on the intestinal metabolic functions and drives metabolic adaptations in the host tissues both locally (in the intestine), but also systemically (Figure 1.4) (Bäckhed, Ley et al. 2005).

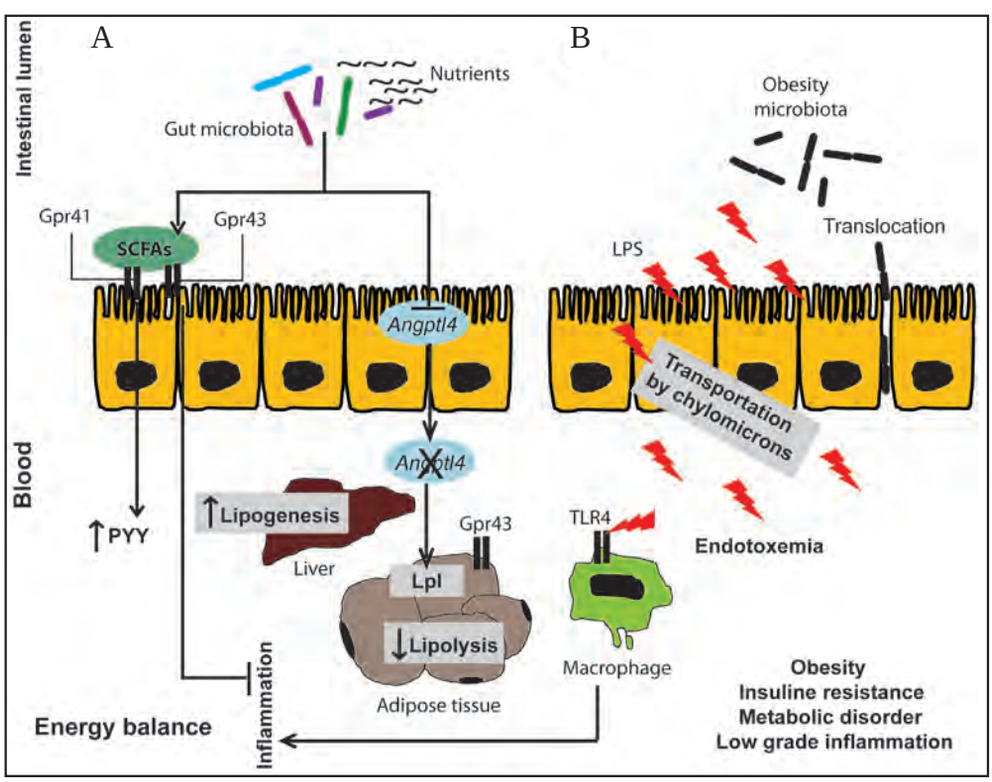

Figure 1.4. A schematic model illustrating the impact of gut microbiota on host metabolism. (A) Colonization by gut microbiota leads to the production of SCFAs that bind to GPR41 and 43 receptors to control energy balance, partly via the induction of the gut-derived hormone PYY, and anti-inflammatory responses. Microbial signals inhibit the expression of *Angptl4* , thereby promoting the peripheral Lpl-fat storage. (B) High levels of LPS (endotoxemia) observed in obese and diabetic patients are transported from the intestine to the blood leading to impaired gut integrity and activation of macrophages which in turn causes low-grade inflammation. Adapted from (Delzenne, Neyrinck et al. 2011; Tilg and Kaser 2011).

The microbiota stimulates glucose uptake in the small intestine, leading to substantial elevation of serum glucose and insulin levels, which in its turn stimulates hepatic lipogenesis (Towle 2001; Bäckhed, Ding et al. 2004; Delzenne and Cani 2010). Moreover, the gut microbiota in the large intestine contributes to the degradation of complex carbohydrates from the diet, making these components accessible for the host as an energy source (Varki 1993; Ley, Bäckhed et al. 2005). This fermentation process results in the production of SCFAs and the gases CO_2 and H_2 (Flint, Bayer et al. 2008). The most predominant SCFAs are acetate (taken up by peripheral tissues (Cummings, Pomare et al. 1987) or used by adipocytes for lipogenesis (Bergman 1990), propionate (transported to the liver), and butyrate (metabolized by intestinal epithelium into ketone bodies or oxidized to CO_2), but may also include fermentation end-products with higher energy contents like lactate or succinate. SCFAs represent the main energy source of the large intestine epithelium (Cummings and Macfarlane 1991) and their presence in the large intestine lumen leads to a lowering of the local pH, which may cause changes in the microbial composition that may include expansion of the *Bificobacterium spp.* and *Lactobacillus spp.* that are supposed to contribute to the host's health (Kleerebezem and Vaughan 2009). Several studies highlighted the role of SCFAs in human health. Butyrate has been the focus of many studies aiming to unravel its suggested role in cancer prevention (Cummings, Pomare et al. 1987; Hamer, Jonkers et al. 2008) and overall impact on the human physiology. Butyrate plays a vital role in epithelial cell proliferation and differentiation whereas it inhibits the growth of colorectal cancer cells (Blottiere, Buecher et al. 2003). SCFAs signal via the G-protein coupled receptors 41 and 43 (Gpr41,43). Gpr43 plays an important role in immune modulation (Maslowski, Vieira et al. 2009) and has a pivotal role in the regulation of energy balance (Bjursell, Admyre et al. 2011). Gpr41 is expressed in enteroendocrine cells and influences the production of specific gut peptides such as peptide YY (PYY), ghrelin, and glucagon-like peptide-1 (GLP-1), which have been proposed to modulate insulin secretion, lipid and glucose metabolism, and food intake (Cani, Hoste et al. 2007) (Figure 1.4A).

Using germfree animal models, the microbiota has been shown to stimulate fat storage processes in the animals through the modulation of its key regulator, angiopoietin like protein-4 *(Angptl4*, also known as *Fiaf*), which signals that there is a change in the host energy supply, shifting from lipid rich to polysaccharide rich diet (Bäckhed, Ding et al. 2004). Suppression of *Fiaf* elicits a subsequent increase in the activity of lipoprotein lipase enzyme (Lpl) that catalyzes adipogenesis and lipogenesis (Bäckhed, Ding et al. 2004; Cani and Delzenne 2009) (Figure 1.4). Bäckhed and co-workers found that the increase in microbiota-induced body fat storage coincides with an increase in the adipocyte-derived hormone leptin (Pelleymounter, Cullen et al. 1995; Bäckhed, Ding et al. 2004), which in addition to its role in reducing food intake and increasing energy expenditure (Pelleymounter, Cullen et al. 1995), also has an impact on the immune response (La Cava and Matarese 2004) preventing excessive inflammatory responses to microbial infection (Guo, Roberts et al. 2011). These findings exemplify the close interrelation between host metabolism and immune response.

Microbial colonization and its role in host energy homeostasis in conventionalized germfree mice has been linked to increased fat storage and weight gain (Bäckhed, Ding et al. 2004), which underpinned earlier observations of increased caloric intake in germfree animals compared to their conventionally raised counterparts (Wostmann, Larkin et al. 1983). With the increasing prevalence of obesity especially among Western populations and its link to associated diseases like hypertension, cardiovascular disease, type 2 diabetes, and cancer (Haslam and James 2005) this finding has stimulated many research approaches to unravel the underlying mechanisms

and microbial interactions. Several recent studies have aimed to illustrate the link between gut microbiota and obesity and have, to a certain extent, generated conflicting results. Initial studies by Ley and co-workers, using a leptin deficient *ob/ob* mouse model for obesity, associated obesity to a shift in the ratio of Firmicutes over Bacteroidetes (Ley, Bäckhed et al. 2005). In contrast, Turnbaugh and colleagues showed that gut microbiota transplantation from obese donor (*ob/ob* genotype) to lean acceptor (wild-type) mice resulted in increased fat deposition and weight gain in the transplanted mice, indicating that the microbiota played a causal role in the obesity phenotype in this model (Turnbaugh, Ley et al. 2006). Later studies from the same group confirmed that the differences observed in obese and lean mouse microbiotas were conserved in obese people and could be influenced by caloric restriction (Ley, Turnbaugh et al. 2006). However, other studies could not directly confirm these initial findings and suggests that obesity may be associated with more subtle changes in the microbiota composition (Duncan, Lobley et al. 2008; Zhang, DiBaise et al. 2009; Schwiertz, Taras et al. 2010). In addition, some studies have related the changes observed in the microbial composition of obese patients to high fat, high energy diet (Cani, Amar et al. 2007). Moreover, Cani and co-workers correlated the increase in the lipid content in high energy diets to low-grade inflammation, which was found to be associated with obesity and was proposed to be triggered by elevated plasma levels of bacterial lipopolysaccharides (LPS) that was designated "metabolic endotoxemia" (Gregor and Hotamisligil 2011) (Figure 1.4B). High energy diets have been proposed to cause an impairment of the epithelial barrier and a subsequent increased diffusion of bacterial LPS and their increased transport via chylomicrons into the submucosal tissues and blood. This rupture of the gut epithelial barrier may lead to an activation of macrophages and a type of low-grade inflammation, that is typical for obesity (Delzenne 2011). These findings again illustrate the strong correlations between metabolic and immune processes.

In conclusion, the gut microbiota intimately interacts with the host and plays a key-role in shaping the host's physiology, with an impact on health and disease. The post-conventionalization period during which germfree animals are exposed to the colonizing microbiota is assumed to resemble the post natal period during which neonate mucosal surfaces become gradually colonized after emerging from the sterile environment of the mother's uterus. This neonatal stage represents the most critical period during which the host is influenced by the microbiota (Macpherson and Uhr 2004; Palmer, Bik et al. 2007; Tlaskalova-Hogenova, Stepankova et al. 2011). Analysis of microbiota in newborns illustrates the relatively unstable colonization during early stages of life, characterized by low diversity, facultative anaerobes. This early community is followed by a dynamic and unstable succession of low diversity microbial composition (Palmer, Bik et al. 2007; Adlerberth and Wold 2009) until the establishment of a relatively stable, complex and host-specific microbial community towards adulthood. Together with the great post-natal development of the metabolic profile and immune system which marks the first years of life (Round and Mazmanian 2009), these findings suggest that any deviation from the normal development of microbiota during this early stage of life may affect the host physiological homeostasis and result in predisposing individuals to disease in later stages of life. Our knowledge of host-gut microbe interactions is accelerated by rapidly expanding genomics based molecular techniques such as transcriptomics, metabonomics, and metagenomics, especially in combination with the use of in vivo host models such as germfree animals. The research described in this thesis aims to define the temporal and region-specific dynamics of establishing the microbial community which colonizes germfree mice during their

conventionalization. In addition, the investigation of microbial development is paralleled by deciphering the molecular host responses over time, which may provide important insights in the microbial impact on host metabolism and immune system, and gene regulatory programs involved in establishing a homeostatic state that accommodates the microbiota.

THESIS OUTLINE AND AIMS

The work presented in this thesis was embedded in a larger Top Institute of Food and Nutrition (TIFN) funded project, "Nutritional and microbial modulation of intestinal epithelial integrity". Within this framework, this project aimed at understanding the molecular dynamics of the mouse intestinal mucosa responses to the gut microbial community and its role in maintenance of mucosal homeostasis. To study this, C57/BL6 J male, germfree mice were used as a reductionist model. The germfree mice were colonized with bacterial suspension obtained from freshly collected fecal material of conventionally raised mice, and the molecular responses in the intestine of these conventionalized mice were followed at different time-points over a period of 30 days. The analyses that were included addressed both the dynamics of mucosal transcriptome responses, and the parallel metabonome changes occurring in these mucosal tissues and plasma, with the simultaneous determination of the colonizing microbiota (Figure 1.5). The specific objectives that are addressed in each chapter are listed below.

Chapter 2 aimed to decipher the genetic regulation of the dynamics of host immune response to the colonizing microbiota throughout the GI tract. Time-resolved transcriptome and (immune)-histochemical analyses were evaluated in three different intestinal regions, jejunum, ileum, and colon, after microbial conventionalization of germfree mice during 30 days. The combined analyses revealed a sequential development of the innate and adaptive immune arms in the mucosa of the mice, and enabled the identification of a core gene network that controls the dynamic, region-specific establishment of intestinal immune homeostasis during conventionalization. The results of this study highlighted the high responsiveness of the proximal small intestine to the presence of the microbiota, which was the focus of **Chapter 3.** In this chapter, histological, transcriptome, and ^{1}H NMR metabonome analyses, as well as microbial profiling were employed to provide insight in the detailed molecular dynamics by which the presence of the microbiota coopts the metabolic function of the jejunal tissue. In addition, mining of the jejunal transcriptomes allowed the reconstruction of a core gene regulatory network that is proposed to orchestrate the jejunal metabolic changes in response to the colonizing microbiota, and which displays strong correlation to insulin-coordinated responses in tissue, supporting a prominent diet and microbiota sensing role of the jejunal mucosa. In **Chapter 4** we monitored the succession of microbial groups during conventionalization by determining the time-resolved composition of colon microbial communities in detail, in parallel with the colon mucosa transcriptomes, and the colon and urine metabonomes. The latter data were determined by ^{1}H NMR spectroscopic profiling of the complete mucosal tissue and urine. Computational modeling was applied to correlate the obtained multi-variate data from germfree and conventionalized mice. This study enabled an overall description of transient and more permanent alterations in the colon-microbiome-metabonome interaction. **Chapter 5** focused on a transient mucosal state that was characterized by a transient loss of immune homeostasis, which was identified within the time frame studied in **Chapter 2**. This transient state appeared to reflect the boundaries of tolerance of the mucosal immune system towards the luminal microbiota. Colon tissue transcriptomes, gut microbiota composition, and specific plasma metabolites were employed to enable multi-variate analysis of this transition state during conventionalization. Microbiota profiling illustrated the

dominance of specific microbial groups that have previously been identified as "pathobionts" which appeared to play a role in the subsequent activation of the adaptive immune response. Finally, **Chapter 6** summarizes and discusses the contribution of this work to the current knowledge of the host-microbe interrelations with an emphasis on future directions.

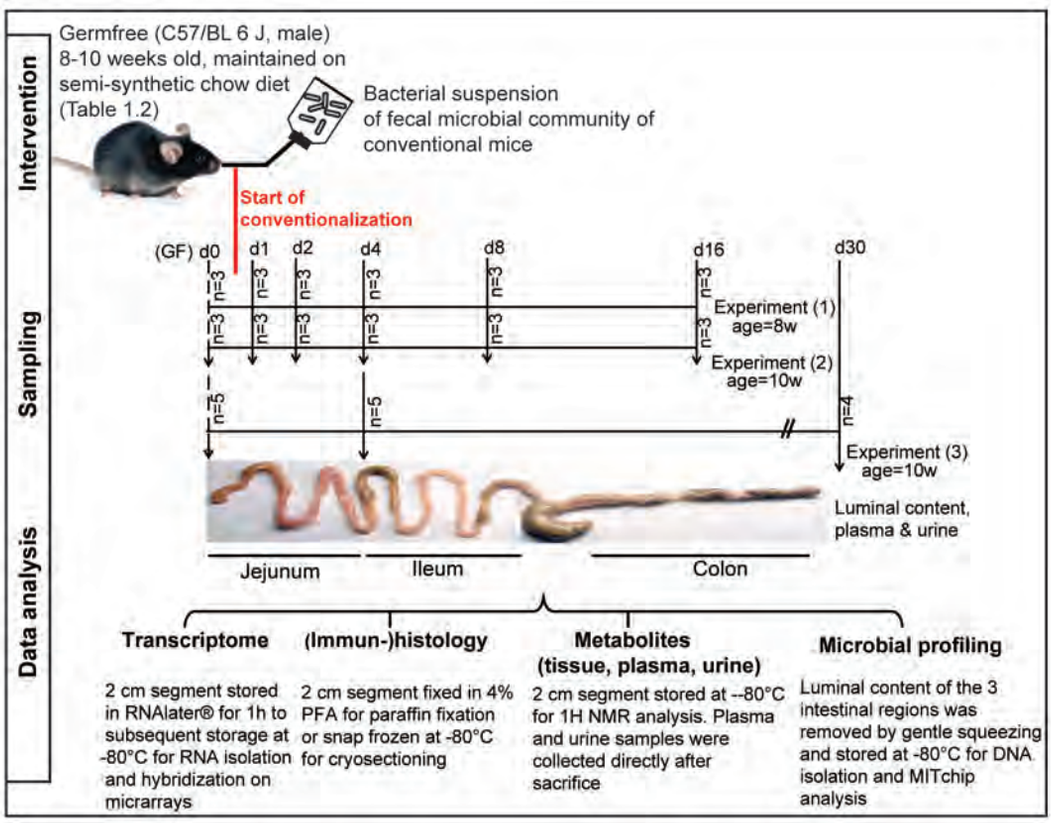

Figure 1.5. Outline of the conventionalization experiments performed on C57/BL 6 J germfree mice in this study.

Table 1.2. Composition of the semi-synthetic chow diet. (*) Nurish 1500 (DuPont Protein Technologies), (#) Analyses were performed by Eurofins scientific.

Ingredients	**Gram (%)**	**Analytical components(#)**	
Corn starch	28.985	Dry matter	91.48%
Smashed potato	29.000	Energy	17.39%
Sucrose		Protein	17.06%
Casein	5.000	Fat	6.09%
Soy isolate*	12.000	Ash	5.06%
Corn oil	3.000	Cellulose	2.17%
Lard	3.000		
Cholesterol	0.015		
Cellulose	6.000		
Mineral mix	7.000		
Vitamin mix	1.000		
Total	100.000		

References

Abrams, G. D., H. Sprinz, et al. (1963). "Influence of normal flora on mucosal morphology and cellular renewal in ileum - a comparison of germ-free and conventional mice." Laboratory Investigation **12**(3): 355-364.

Adlerberth, I. and A. E. Wold (2009). "Establishment of the gut microbiota in Western infants." Acta Paediatrica **98**(2): 229-238.

Ahuja, V., B. K. Dieckgraefe, et al. (2006). "Molecular biology of the small intestine." Current Opinion in Gastroenterology **22**(2): 90-94.

Arumugam, M., J. Raes, et al. (2011). "Enterotypes of the human gut microbiome." Nature **473**(7346): 174-180.

Atarashi, K., T. Tanoue, et al. (2011). "Induction of colonic regulatory T cells by indigenous clostridium species." Science **331**(6015): 337-341.

Ayabe, T., D. P. Satchell, et al. (2000). "Secretion of microbicidal alpha-defensins by intestinal Paneth cells in response to bacteria." Nature Immunology **1**(2): 113-118.

Bäckhed, F., H. Ding, et al. (2004). "The gut microbiota as an environmental factor that regulates fat storage." Proceedings of the National Academy of Sciences of the United States of America **101**(44): 15718-15723.

Bäckhed, F. and M. Hornef (2003). "Toll-like receptor 4-mediated signaling by epithelial surfaces: necessity or threat?" Microbes And Infection **5**(11): 951-959.

Bäckhed, F., R. E. Ley, et al. (2005). "Host-bacterial mutualism in the human intestine." Science **307**(5717): 1915-1920.

Barker, N., M. van de Wetering, et al. (2008). "The intestinal stem cell." Genes & Development **22**(14): 1856-1864.

Barrett, K. E., Fayez K. Ghishan , Juanita L. Merchant , Hamid M. Said, Jackie D. Wood, Leonard R. Johnson (2006). Physiology of the gastrointestinal tract, Elsvier Academic press.

Bates, M. D., C. R. Erwin, et al. (2002). "Novel genes and functional relationships in the adult mouse gastrointestinal tract, identified by microarray analysis." Gastroenterology **122**(5): 1467-1482.

Beaver, M. H. and B. S. Wostmann (1962). "Histamine and 5-Hydroxytryptamine in intestinal tract of germ-free animals, animals harbouring 1 microbial species and conventional animals." British Journal of Pharmacology and Chemotherapy **19**(3): 385-393.

Bergman, E. N. (1990). "Energy contributions of volatile fatty-acids from the gastrointestinal-tract in various species." Physiological Reviews **70**(2): 567-590.

Bienenstock, J. and S. Collins (2010). "99th Dahlem conference on infection, inflammation and chronic inflammatory disorders: Psycho-neuroimmunology and the intestinal microbiota: clinical observations and basic mechanisms." Clinical and Experimental Immunology **160**(1): 85-91.

Bjerknes, M. and H. Cheng (1981). "The stem-cell zone of the small intestinal epithelium .1. Evidence from Paneth cells in the adult-mouse." American Journal Of Anatomy **160**(1): 51-63.

Bjursell, M., T. Admyre, et al. (2011). "Improved glucose control and reduced body fat mass in free fatty acid receptor 2-deficient mice fed a high-fat diet." American Journal of Physiology-Endocrinology and Metabolism **300**(1): E211-E220.

Blottiere, H. M., B. Buecher, et al. (2003). "Molecular analysis of the effect of short-chain fatty acids on intestinal cell proliferation." Proceedings of the Nutrition Society **62**(1): 101-106.

Brandtzaeg, P., H. Kiyono, et al. (2008). "Terminology: nomenclature of mucosa-associated lymphoid tissue." Mucosal Immunology **1**(1): 31-37.

Bry, L., P. G. Falk, et al. (1996). "A model of host-microbial interactions in an open mammalian ecosystem." Science **273**(5280): 1380-1383.

Burczynski, M. E., R. L. Peterson, et al. (2006). "Molecular classification of Crohn's disease and ulcerative colitis patients using transcriptional profiles in peripheral blood mononuclear cells." Journal of Molecular Diagnostics **8**(1): 51-61.

Cani, P. D., J. Amar, et al. (2007). "Metabolic endotoxemia initiates obesity and insulin resistance." Diabetes **56**(7): 1761-1772.

Cani, P. D. and N. M. Delzenne (2009). "The Role of the gut microbiota in energy metabolism and metabolic disease." Current Pharmaceutical Design **15**(13): 1546-1558.

Cani, P. D., S. Hoste, et al. (2007). "Dietary non-digestible carbohydrates promote L-cell differentiation in the proximal colon of rats." British Journal of Nutrition **98**(1): 32-37.

Cani, P. D., A. M. Neyrinck, et al. (2007). "Selective increases of bifidobacteria in gut microflora improve high-fat-diet-induced diabetes in mice through a mechanism associated with endotoxaemia." Diabetologia **50**(11): 2374-2383.

Cario, E., I. M. Rosenberg, et al. (2000). "Lipopolysaccharide activates distinct signaling pathways in intestinal epithelial cell lines expressing toll-like receptors." Journal of Immunology **164**(2): 966-972.

Carlstedtduke, B., T. Hoverstad, et al. (1986). "Influence of antibiotics on intestinal mucin in healthy-subjects." European Journal of Clinical Microbiology & Infectious Diseases **5**(6): 634-638.
Cebra, J. J. (1999). "Influences of microbiota on intestinal immune system development." American Journal Of Clinical Nutrition **69**(5): 1046S-1051S.
Chow, J. and S. K. Mazmanian (2010). "A Pathobiont of the microbiota balances host colonization and intestinal inflammation." Cell Host & Microbe **7**(4): 265-276.
Chow, J., H. Tang, et al. (2011). "Pathobionts of the gastrointestinal microbiota and inflammatory disease." Current Opinion in Immunology **23**(4): 473-480.
Coombes, J. L. and F. Powrie (2008). "Dendritic cells in intestinal immune regulation." Nature Reviews Immunology **8**(6): 435-446.
Crabbe, P. A., D. R. Nash, et al. (1970). "Immunohistochemical observations on lymphoid tissues from conventional and germ-free mice." Laboratory Investigation **22**(5): 448-457.
Cummings, J. H. and G. T. Macfarlane (1991). "The control and consequences of bacterial fermentation in the human colon " Journal of Applied Bacteriology **70**(6): 443-459.
Cummings, J. H. and G. T. MacFarlane (1997). "Colonic microflora: Nutrition and health." Nutrition **13**(5): 476-478.
Cummings, J. H., E. W. Pomare, et al. (1987). "Short chain fatty-acids In human large-intestine, portal, hepatic and venous-blood." Gut **28**(10): 1221-1227.
Cummins, S. L. (1911). "The anti-bactericidal action of bile salts." The Journal of hygiene **11**(3): 373-380.
Dahlqvis.A, B. Bull, et al. (1965). "Rat intestinal 6-Bromo-2-Naphthyl glycosidase and disaccharidase activities .I. Enzymic properties and distribution in digestive tract of conventional and germ-free animals." Archives of Biochemistry and Biophysics **109**(1): 150-158.
Dai D, W. W. (1999). "Protective nutrients and bacterial colonization in the immature human gut." Adv. pediatr. **46**: 353-382.
Delzenne, N., M. , Audrey M Neyrinck, Patrice D Cani (2011). "Modulation of the gut microbiota by nutrients with prebiotic properties: consequences for host health in the context of obesity and metabolic syndrome." Microbial Cell Factories **10**(1): 1-11.
Delzenne, N. M. and P. D. Cani (2010). "Nutritional modulation of gut microbiota in the context of obesity and insulin resistance: Potential interest of prebiotics." International Dairy Journal **20**(4): 277-280.
Delzenne, N. M., A. M. Neyrinck, et al. (2011). "Targeting gut microbiota in obesity: effects of prebiotics and probiotics." Nature reviews. Endocrinology **7**(11): 639-646.
DiBaise, J. K., H. Zhang, et al. (2008). "Gut microbiota and its possible relationship with obesity." Mayo Clinic Proceedings **83**(4): 460-469.
Duncan, S. H., G. E. Lobley, et al. (2008). "Human colonic microbiota associated with diet, obesity and weight loss." International Journal of Obesity **32**(11): 1720-1724.
Dupont, J. R., H. R. Jervis, et al. (1965). "Auerbachs Plexus of rat ceum in relation to germfree state." Journal of Comparative Neurology **125**(1): 11-&.
Eckburg, P. B., E. M. Bik, et al. (2005). "Diversity of the human intestinal microbial flora." Science **308**(5728): 1635-1638.
Evrard, E., H. Charlier, et al. (1964). "Faecal lipids in germ-free + conventional rats." British Journal of Experimental Pathology **45**(4): 409-414.
Fahey, J. L. and S. Sell (1965). "Immunoglobulins of mice .v. metabolic (catabolic) properties of 5 immunoglobulin classes." Journal of Experimental Medicine **122**(1): 41-58.
Falk, P., K. A. Roth, et al. (1994). "Lectins are sensitive tools for defining the differentiation programs of mouse gut epithelial-cell lineages." American Journal Of Physiology **266**(6): G987-G1003.
Falk, P. G., L. V. Hooper, et al. (1998). "Creating and maintaining the gastrointestinal ecosystem: What we know and need to know from gnotobiology." Microbiology And Molecular Biology Reviews **62**(4): 1157-1170.
Fanaro, S., R. Chierici, et al. (2003). "Intestinal microflora in early infancy: composition and development." Acta Paediatrica **92**: 48-55.
Fasano, A. (2008). "Physiological, pathological, and therapeutic implications of zonulin-mediated intestinal barrier modulation living life on the edge of the wall." American Journal of Pathology **173**(5): 1243-1252.
Flint, H. J., E. A. Bayer, et al. (2008). "Polysaccharide utilization by gut bacteria: potential for new insights from genomic analysis." Nature Reviews Microbiology **6**(2): 121-131.
Gaboriau-Routhiau, V., S. Rakotobe, et al. (2009). "The Key role of segmented filamentous bacteria in the coordinated maturation of gut helper T cell responses." Immunity **31**(4): 677-689.
Garrett, W. S., J. I. Gordon, et al. (2010). "Homeostasis and inflammation in the intestine." Cell **140**(6): 859-870.
Garrett, W. S., G. M. Lord, et al. (2007). "Communicable ulcerative colitis induced by T-bet deficiency in the innate immune system." Cell **131**: 33-45.

Gill, S. R., M. Pop, et al. (2006). "Metagenomic analysis of the human distal gut microbiome." Science **312**(5778): 1355-1359.
Glaister, J. R. (1973). "Factors affecting lymphoid-cells in small intestinal epithelium of mouse." International Archives of Allergy and Applied Immunology **45**(5): 719-730.
Gordon, H. A. (1968). Is the germ free animals normal? . London and New York: Academic press.
Gordon, H. A. and E. Brucknerkardoss (1961). "Effect of normal microbial flora on intestinal surface area." American Journal of Physiology **201**(1): 175-178.
Gregor, M. F. and G. S. Hotamisligil (2011). Inflammatory mechanisms in obesity. Annual Review of Immunology, Vol 29. W. E. L. D. R. Y. W. M. Paul. **29:** 415-445.
Guo, X., M. R. Roberts, et al. (2011). "Leptin signaling in intestinal epithelium mediates resistance to enteric infection by Entamoeba histolytica." Mucosal Immunology **4**(3): 294-303.
Gustafsson, B. E. and L. S. Lanke (1960). "Bilirubin and urobilins in germfree, ex-germfree, and conventional rats." Journal of Experimental Medicine **112**(6): 975-981.
Hallstrom, M., E. Eerola, et al. (2004). "Effects of mode of delivery and necrotising enterocolitis on the intestinal microflora in preterm infants." European Journal of Clinical Microbiology & Infectious Diseases **23**(6): 463-470.
Hamer, H. M., D. Jonkers, et al. (2008). "Review article: the role of butyrate on colonic function." Alimentary Pharmacology & Therapeutics **27**(2): 104-119.
Harmsen HJ, W.-V. A., Raangs GC, Wagendorp AA, Klijn N, Bindels JG, Welling GW (2000). "Analysis of intestinal flora development in breast-fed and formula-fed infants by using molecular identification and detection methods." J Pediatr Gastroenterol Nutr. **30**(1): 61-67.
Haslam, D. W. and W. P. T. James (2005). "Obesity." Lancet **366**(9492): 1197-1209.
Heneghan, J. B. (1963). "Influence of microbial flora on xylose absorption in rats and mice." American Journal of Physiology **205**(3): 417-420.
Hooper, L. V., L. Bry, et al. (1998). "Host-microbial symbiosis in the mammalian intestine: exploring an internal ecosystem." Bioessays **20**(4): 336-343.
Hooper, L. V., Gordon JI (2001). "Commensal host-bacterial relationships in the gut." Science **292**(5519): 1115-1118.
Hooper, L. V. and A. J. Macpherson (2010). "Immune adaptations that maintain homeostasis with the intestinal microbiota." Nature Reviews Immunology **10**(3): 159-169.
Hooper, L. V., T. Midtvedt, et al. (2002). "How host-microbial interactions shape the nutrient environment of the mammalian intestine." Annual Review of Nutrition **22**: 283-307.
Hooper, L. V., M. H. Wong, et al. (2001). "Molecular analysis of commensal host-microbial relations hips in the intestine." Science **291**(5505): 881-884.
Hooper, L. V., J. Xu, et al. (1999). "A molecular sensor that allows a gut commensal to control its nutrient foundation in a competitive ecosystem." Proceedings of the National Academy of Sciences of the United States of America **96**(17): 9833-9838.
Isolauri, E., Y. Sutas, et al. (2001). "Probiotics: effects on immunity." American Journal of Clinical Nutrition **73**(2): 444S-450S.
Ivanov, II, R. D. Frutos, et al. (2008). "Specific microbiota direct the differentiation of IL-17-producing T-helper cells in the mucosa of the small intestine." Cell Host & Microbe **4**(4): 337-349.
Ivanov, II and N. Manel (2010). "Induction of gut mucosal Th17 cells by segmented filamentous bacteria." M S-Medecine Sciences **26**(4): 352-355.
Jalanka-Tuovinen, J., A. Salonen, et al. (2011). "Intestinal microbiota in healthy adults: temporal analysis reveals individual and common core and relation to intestinal symptoms." Plos One **6**(7).
Jervis, H. R. and D. C. Biggers (1964). "Mucosal enzymes in cecum of conventional + germfree mice." Anatomical Record **148**(4): 591-597.
Karlsson, K. A. (1989). "Animal glycosphingolipids as membrane attachment sites for bacteria." Annual Review of Biochemistry **58**: 309-350.
Klaasen, H., J. P. Koopman, et al. (1992). "Intestinal, segmented, filamentous bacteria " Fems Microbiology Reviews **88**(3-4): 165-179.
Kleerebezem, M. and E. E. Vaughan (2009). Probiotic and gut lactobacilli and bifidobacteria: molecular approaches to study diversity and activity. Annual Review of Microbiology. **63:** 269-290.
La Cava, A. and G. Matarese (2004). "The weight of leptin in immunity." Nature Reviews Immunology **4**(5): 371-379.
Le Ferrec, E., C. Chesne, et al. (2001). "In vitro models of the intestinal barrier - The report and recommendations of ECVAM Workshop 46." Atla-Alternatives to Laboratory Animals **29**(6): 649-668.
Lee, J. C., P. A. Lyons, et al. (2011). "Gene expression profiling of CD8+ T cells predicts prognosis in patients with Crohn disease and ulcerative colitis." The Journal of clinical investigation **121**(10): 4170-4179.

Lee, S. H., P. M. Starkey, et al. (1985). "Quantitative-analysis of total macrophage content in adult-mouse tissues-Immunochemical studies with monoclonal-antibody F4/80." Journal of Experimental Medicine **161**(3): 475-489.
Lee, Y. K. and S. K. Mazmanian (2010). "Has the microbiota played a critical role in the evolution of the adaptive immune system?" Science **330**(6012): 1768-1773.
Lepage, P., R. Haesler, et al. (2011). "Twin study indicates loss of interaction between microbiota and mucosa of patients with ulcerative colitis." Gastroenterology **141**(1): 227-236.
Lesher, S., G. A. Sacher, et al. (1964). "Generation cycle in duodenal crypt cells of germ-free + conventional mice." Nature **202**(493): 884-886.
Levenson, S. T. and B. Tennant (1963). "Contributions of intestinal microflora to nutrition of host animal - some metabolic and nutritional studies with germfree animals." Federation Proceedings **22**(1P1): 109-119.
Ley, R. E., F. Bäckhed, et al. (2005). "Obesity alters gut microbial ecology." Proceedings of the National Academy of Sciences of the United States of America **102**(31): 11070-11075.
Ley, R. E., M. Hamady, et al. (2008). "Evolution of mammals and their gut microbes." Science **320**(5883): 1647-1651.
Ley, R. E., P. J. Turnbaugh, et al. (2006). "Microbial ecology - Human gut microbes associated with obesity." Nature **444**(7122): 1022-1023.
Liddle, R. A. (2010). Gastrointestinal hormones and neurotransmitters. Sleisenger and Fordtran's Gastrointestinal and Liver Disease. L. S. F. Mark Feldman, and Lawrence J. Brandt. **1:** 2480.
Lundin, A., C. M. Bok, et al. (2008). "Gut flora, Toll-like receptors and nuclear receptors: a tripartite communication that tunes innate immunity in large intestine." Cellular Microbiology **10**(5): 1093-1103.
Macpherson, A. J. and N. L. Harris (2004). "Interactions between commensal intestinal bacteria and the immune system." Nature Reviews Immunology **4**(6): 478-485.
Macpherson, A. J. and T. Uhr (2004). "Induction of protective IgA by intestinal dendritic cells carrying commensal bacteria." Science **303**(5664): 1662-1665.
Manichanh, C., L. Rigottier-Gois, et al. (2006). "Reduced diversity of faecal microbiota in Crohn's disease revealed by a metagenomic approach." Gut **55**(2): 205-211.
Martini, F., William, C. Ober, Claire W. Garrison , Kathleen Welch, Ralph T. Hutchings (2001). Fundamentals of anatomy & physiology, Prentice Hall.
Maslowski, K. M., A. T. Vieira, et al. (2009). "Regulation of inflammatory responses by gut microbiota and chemoattractant receptor GPR43." Nature **461**(7268): 1282-U1119.
Matsumoto, S., H. Setoyama, et al. (1992). "Differential induction of major histocompatibility complex-molecules on mouse intestine by bacterial-colonization." Gastroenterology **103**(6): 1777-1782.
Mazmanian, S. K., J. L. Round, et al. (2008). "A microbial symbiosis factor prevents intestinal inflammatory disease." Nature **453**(7195): 620-625.
Medema, J. P. and L. Vermeulen (2011). "Microenvironmental regulation of stem cells in intestinal homeostasis and cancer." Nature **474**(7351): 318-326.
Mentor-Marcel, R. A., G. Bobe, et al. (2009). "Inflammation-associated serum and colon markers as indicators of dietary attenuation of colon carcinogenesis in ob/ob mice." Cancer Prevention Research **2**(1): 60-69.
Meslin, J. C. and J. L. Guenet (1973). "Action of Bacterial-Flora on Morphology and Mucous Surface of Small-Intestine of Rat." Annales De Biologie Animale Biochimie Biophysique **13**(2): 203-214.
Mestecky, J., Lamm, M. E. , Strober, W., Bienenstock, J., McGhee, J.R., Mayer, L. (2005). Mucosal Immunology, Elsevier academic press.
Mikkelsen, H. B., C. Garbarsch, et al. (2004). "Macrophages in the small intestinal muscularis externa of embryos, newborn and adult germ-free mice." Journal of Molecular Histology **35**(4): 377-387.
Moreau, M. C., R. Ducluzeau, et al. (1978). "Increase in population of duodenal immunoglobulin-a plasmocytes in axenic mice associated with different living or dead bacterial strains intestinal origin." Infection and Immunity **21**(2): 532-539.
Nicholson, J. K., E. Holmes, et al. (2005). "Gut microorganisms, mammalian metabolism and personalized health care." Nature Reviews Microbiology **3**(5): 431-438.
Norin E., M. T. (2000). "Interactions of bacteria with the host Alteration of microflora-associated characteristics of the host; non-immune functions " Microbial Ecology in Health and Disease **12**(2): 186-193.
O'Hara, A. M. and F. Shanahan (2006). "The gut flora as a forgotten organ." Embo Reports **7**(7): 688-693.
Orcutt, R. P., F. J. Gianni, et al. (1987). "Development of an altered schaedler flora for NCI gnotobiotic rodents " Microecology and Therapy, Vol 17 **17**: 59-59.
Packey, C. D. and R. B. Sartor (2009). "Commensal bacteria, traditional and opportunistic pathogens, dysbiosis and bacterial killing in inflammatory bowel diseases." Current Opinion in Infectious Diseases **22**(3): 292-301.

Palmer, C., E. M. Bik, et al. (2007). "Development of the human infant intestinal microbiota." Plos Biology **5**: 1556-1573.
Pelleymounter, M. A., M. J. Cullen, et al. (1995). "Effects of the obese gene-product on body-weight regulation in Ob/Ob mice." Science **269**(5223): 540-543.
Png, C. W., S. K. Linden, et al. (2010). "Mucolytic bacteria with increased prevalence in IBD mucosa augment In vitro utilization of mucin by other bacteria." American Journal of Gastroenterology **105**(11): 2420-2428.
Qin, J., R. Li, et al. (2010). "A human gut microbial gene catalogue established by metagenomic sequencing." Nature **464**(7285): 59-U70.
Reddy, B. S., Pleasant.Jr, et al. (1969). "Effect of intestinal microflora on calcium, phosphorus and magnesium metabolism in rats." Journal of Nutrition **99**(3): 353-362.
Rescigno, M. and A. Di Sabatino (2009). "Dendritic cells in intestinal homeostasis and disease." Journal of Clinical Investigation **119**(9): 2441-2450.
Rescigno, M., M. Urbano, et al. (2001). "Dendritic cells express tight junction proteins and penetrate gut epithelial monolayers to sample bacteria." Nature Immunology **2**(4): 361-367.
Round, J. L. and S. K. Mazmanian (2009). "The gut microbiota shapes intestinal immune responses during health and disease." Nature Reviews Immunology **9**(5): 313-323.
Salyers, A. A., G. Bonheyo, et al. (2000). "Starting a new genetic system: lessons from bacteroides." Methods-a Companion to Methods in Enzymology **20**(1): 35-46.
Salyers, A. A., J. R. Vercellotti, et al. (1977). "Fermentation of mucin and plant polysaccharides by strains of Bacteroides from human colon." Applied and Environmental Microbiology **33**(2): 319-322.
Schwiertz, A., D. Taras, et al. (2010). "Microbiota and SCFA in lean and overweight healthy subjects." Obesity **18**(1): 190-195.
Sekirov, I., S. L. Russell, et al. (2010). "Gut microbiota in health and disease." Physiological Reviews **90**(3): 859-904.
Sheehy, T. W., Martin H. Floch (1964). The small Intestine: its function and diseases, Hoeber.
Shroyer, N. F., D. Wallis, et al. (2005). "Gfi1 functions downstream of Math1 to control intestinal secretory cell subtype allocation and differentiation." Genes & Development **19**(20): 2412-2417.
Smith, K., K. D. McCoy, et al. (2007). "Use of axenic animals in studying the adaptation of mammals to their commensal intestinal microbiota." Seminars in Immunology **19**(2): 59-69.
Sokol, H., B. Pigneur, et al. (2008). "Faecalibacterium prausnitzii is an anti-inflammatory commensal bacterium identified by gut microbiota analysis of Crohn disease patients." Proceedings of the National Academy of Sciences of the United States of America **105**(43): 16731-16736.
Sonnenburg, E. D., H. Zheng, et al. (2010). "Specificity of polysaccharide use in intestinal Bacteroides species determines diet-induced microbiota alterations." Cell **141**(7): 1241-U1256.
Sonnenburg, J. L., C. T. L. Chen, et al. (2006). "Genomic and metabolic studies of the impact of probiotics on a model gut symbiont and host." Plos Biology **4**(12): 2213-2226.
Stappenbeck, T. S., L. V. Hooper, et al. (2002). Laser capture microdissection of mouse intestine: Characterizing mRNA and protein expression, and profiling intermediary metabolism in specified cell populations. Laser Capture Microscopy and Microdissection. **356:** 167-196.
Swidsinski, A., Y. Doerffel, et al. (2011). "Acute appendicitis is characterised by local invasion with Fusobacterium nucleatum/necrophorum." Gut **60**(1): 34-40.
Talham, G. L., H. Q. Jiang, et al. (1999). "Segmented filamentous bacteria are potent stimuli of a physiologically normal state of the murine gut mucosal immune system." Infection and Immunity **67**(4): 1992-2000.
Tap, J., S. Mondot, et al. (2009). "Towards the human intestinal microbiota phylogenetic core." Environmental Microbiology **11**(10): 2574-2584.
Tilg, H. and A. Kaser (2011). "Gut microbiome, obesity, and metabolic dysfunction." Journal of Clinical Investigation **121**(6): 2126-2132.
Tlaskalova-Hogenova, H., R. Stepankova, et al. (2011). "The role of gut microbiota (commensal bacteria) and the mucosal barrier in the pathogenesis of inflammatory and autoimmune diseases and cancer: contribution of germ-free and gnotobiotic animal models of human diseases." Cellular & Molecular Immunology **8**(2): 110-120.
Todar, K. (2004). "The Good, the bad, and the deadly." Science-Netwatch **304**(5676): 1421.
Towle, H. C. (2001). "Glucose and cAMP: adversaries in the regulation of hepatic gene expression." Proceedings Of The National Academy Of Sciences Of The United States Of America **98**(24): 13476-13478.
Turnbaugh, P. J., M. Hamady, et al. (2009). "A core gut microbiome in obese and lean twins." Nature **457**(7228): 480-U487.
Turnbaugh, P. J., R. E. Ley, et al. (2006). "An obesity-associated gut microbiome with increased capacity for energy harvest." Nature **444**(7122): 1027-1031.

Umesaki, Y., Y. Okada, et al. (1995). "Segmented filamentous bacteria are indigenous intestinal bacteria that activate intraepithelial lymphocytes and induce MHC Class-II Molecules and Fucosyl Asialo Gm1 glycolipids on the small-intestinal epithelial-cells in the ex-germ-free mouse." Microbiology and Immunology **39**(8): 555-562.

Vaishnava, S., M. Yamamoto, et al. (2011). "The antibacterial lectin RegIII gamma promotes the spatial segregation of microbiota and host in the intestine." Science **334**(6053): 255-258.

van Baarlen, P., F. Troost, et al. (2011). "Human mucosal in vivo transcriptome responses to three lactobacilli indicate how probiotics may modulate human cellular pathways." Proceedings of the National Academy of Sciences of the United States of America **108**: 4562-4569.

Varki, A. (1993). "Biological roles Of Oligosaccharides - all of the theories are correct." Glycobiology **3**(2): 97-130.

Walter, J. and R. Ley (2011). "The human gut microbiome: ecology and recent evolutionary changes." Annual Review of Microbiology **65**: 411-429.

Wilson, C. L., A. J. Ouellette, et al. (1999). "Regulation of intestinal alpha-defensin activation by the metalloproteinase matrilysin in innate host defense." Science **286**(5437): 113-117.

Wilson, M. (2004). Microbial inhabitants of humans, Cambridge books.

Wiseman, R. F. (1965). "Gnotobiotics and germ-free animal " Bioscience **15**(3): 187-&.

Wostmann, B. S. (1981). "The germ-free animal in nutritional studies." Annual Review of Nutrition **1**: 257-279.

Wostmann, B. S., Bruckner.E, et al. (1968). "Cecal enlargment cardiac output O2 consumption in germfree rats " Proceedings of the Society for Experimental Biology and Medicine **128**(1): 137-&.

Wostmann, B. S., C. Larkin, et al. (1983). "Dietary-intake, energy-metabolism, and excretory losses of adult male germfree Wistar rats." Laboratory Animal Science **33**(1): 46-50.

Wu, G. D., J. Chen, et al. (2011). "Linking long-term dietary patterns with gut microbial enterotypes." Science **333**(6052): 105-108.

Xu, J., M. K. Bjursell, et al. (2003). "A genomic view of the human-Bacteroides thetaiotaomicron symbiosis." Science **299**(5615): 2074-2076.

Xu, J. and J. I. Gordon (2003). "Honor thy symbionts." Proceedings Of The National Academy Of Sciences Of The United States Of America **100**(18): 10452-10459.

Yolton, D. P., C. Stanley, et al. (1971). "Influence of indigenous gastrointestinal microbial flora on duodenal alkaline phosphatase activity in mice." Infection and Immunity **3**(6): 768-773.

Zhang, H., J. K. DiBaise, et al. (2009). "Human gut microbiota in obesity and after gastric bypass." Proceedings of the National Academy of Sciences of the United States of America **106**(7): 2365-2370.

Zhu, Y., S. Yao, et al. (2011). "Cell surface signaling molecules in the control of immune responses: A tide model." Immunity **34**(4): 466-478.

Zoetendal, E. G., Akkermans AD, De Vos WM. (1998). "Temperature gradient gel electrophoresis analysis of 16S rRNA from human fecal samples reveals stable and host-specific communities of active bacteria." Appl Environ Microbiol. **64**(10): 3854–3859.

Zoetendal, E. G., Antoon D. L. Akkermans, Wilma M. Akkermans-van Vliet, J.Arjan G. M. de Visser and Willem M. de Vos (2001). "The host genotype affects the bacterial community in the human gastrointestinal tract." Microbial Ecology in Health and Disease **13**: 129–134.

Zoetendal, E. G., E. E. Vaughan, et al. (2006). "A microbial world within us." Molecular Microbiology **59**(6): 1639-1650.

Chapter 2

Identification of the Core Gene-Regulatory Network that Governs the Dynamic Establishment of Intestinal Homeostasis during Conventionalization in Mice

Sahar El Aidy*, Peter van Baarlen*, Muriel Derrien, Dicky J. Lindenbergh-Kortleve, Guido Hooiveld, Florence Levenez, Joël Doré, Jan Dekker, Janneke N. Samsom, Edward E.S. Nieuwenhuis, and Michiel Kleerebezem

* Contributed equally

Submitted

ABSTRACT

During microbial conventionalization of germfree mice, molecular responses of the intestinal mucosa initiate and maintain a balanced immune response. However, the genetic regulation of appropriate responses to microbiota is obscure. To better understand the genetic regulation of the dynamics of this balanced response toward the colonizing microbiota, transcriptomic profiles were determined at different time-points and in three different intestinal regions after microbial conventionalization of germfree mice. Combined analyses of germfree and conventionalized mice revealed that the major molecular responses could be detected initiating at day 4 post-conventionalization, with a strong induction of innate immune functions including the production of antimicrobial peptide molecules followed by stimulation of adaptive immune response at later stages of conventionalization. A central regulatory network that controls the dynamic, region-dependant mucosal responses to the colonizing microbiota could be identified. Some of the genes within this regulatory network have known roles in mucosal inflammatory diseases in mouse and human. Our data suggest that the identified central regulatory network could serve as a genetic signature for control of intestinal homeostasis in healthy mice and may help to decipher the genetic basis of pathway dysregulation in human intestinal inflammatory diseases.

INTRODUCTION

Mammals are germfree in utero and become colonized by microbes during and after birth following a dynamic process that results in taxonomically diverse bacterial populations that establish a symbiotic relationship with the host (Falk, Hooper et al. 1998). After colonization is completed, the intestine of conventionally raised mice is in continuous contact with a vast diversity of microbes, collectively termed as gut microbiota. Notwithstanding the exposure to trillions of microbiota, the intestinal mucosa maintains a state of homeostasis which involves tightly controlled immune responses. To achieve this, epithelial cells and immune cells of the lamina propria mount innate and adaptive immune responses that sustain tolerance to microbiota but at the same time will detect and kill infiltrating pathogens (Sansonetti and Di Santo 2007). Maintenance of mucosal immune homeostasis is essential for intestinal health. For example, in human, disproportionate immune responses that cause loss of homeostasis may lead to inflammatory bowel diseases (Baumgart and Carding 2007; Abraham and Cho 2009). Gut microbiota is proposed to play a crucial role in the establishment and maintenance of adaptive immunity and homeostasis (Lee and Mazmanian 2010), in which the complexity of the microbial community elicits an equally complex immunological response in the host. This host response is established by microbial cross-talk with the mucosal immune system through a variety of highly integrated signaling pathways and gene regulatory networks. Notwithstanding our knowledge on signaling pathways that play roles in the mucosal immune system (West, Koblansky et al. 2006; Hayden and Ghosh 2008; Chen, Shaw et al. 2009; Zhu, Yao et al. 2011), our understanding of the genetic regulation of homeostasis is still very incomplete. In healthy animals, maintenance of homeostasis is a dynamic process where changes in the gut microbiota composition will lead to appropriate, tolerant responses in the mucosa. Comparative studies of germfree mice and their conventionalized counterparts that have been inoculated with microbial communities from conventionally raised donors, established a prominent role of the microbiota in guiding immune cell development, maturation, and function (Macpherson and Harris 2004).

In a hallmark study by Gaboriau-Routhiau and colleagues (Gaboriau-Routhiau, Rakotobe et al. 2009), it was reported that nearly 50% of the genes differentially expressed in the intestine of gnotobiotic mice during microbial conventionalization regulated T cell development and responses to gut microbiota. Especially a particular member of the microbial community, the segmented filamentous bacteria, was capable of eliciting an immune response in the mucosa that resembled the response to conventionalization. The study of (Gaboriau-Routhiau, Rakotobe et al. 2009) aimed to unravel the mechanisms by which segmented filamentous bacteria induced mucosal adaptive immune responses, with the main focus on the terminal ileum. In the current study we present the time-resolved, genome-wide immune-related gene expression programs that are elicited in the mucosa of jejunum, ileum, and colon in germfree mice upon their conventionalization, and the validation of these programs by immunohistochemistry. Our findings show that conventionalization of germfree mice induced multigenic defense- and immune-related transcriptional responses that reflect the sequential activation of innate and adaptive immune responses, most pronounced processes associated with T cell development and maturation. The intestinal transcriptomes enabled the reconstruction of a core gene regulatory network that is proposed to govern the dynamic intestinal response to the microbiota and thereby play a key-role in maintenance of mucosal homeostasis. The human counterparts of some of the genes in this regulatory network have been associated with human mucosal inflammation and

diseases. This finding suggests that the expression pattern of these network-genes could serve as a genetic signature for the control of mucosal-homeostasis in healthy mice, which may aid the unraveling of the genetic basis of pathway dysregulation in human intestinal inflammatory diseases.

RESULTS

Changes in the Intestinal Physiology and Morphometry during Conventionalization

This study was aimed at identifying the time-resolved intestinal mucosal changes in germfree and conventionalized mice as measured in three independent experiments where intestinal tissues as well as luminal content were sampled after short and longer term conventionalization periods (for an experimental set-up, see: Chapter 1- Figure 1.5). As a typical hallmark of conventionalization, the cecal weight was 80% reduced upon conventionalization when compared to germfree mice (Figure 2.1A); this difference was measured from day 4 post-conventionalization onward. Intestinal morphometric analysis revealed clear, time-dependent alterations in mucosal tissue morphology upon conventionalization. An initial significant increase ($p < 0.01$) in the intestinal crypt depth was observed in the small intestine and the colon of conventionalized mice 4 days post-conventionalization, which was not yet visible on days 1 and 2. In the small intestine, crypt depth increased continuously during the first 16 days to decline at 30 days of conventionalization; at day 30, small intestinal crypt depth remained higher as compared to the germfree mice. In contrast, the colon crypt depth reached a maximum level from day 8 to day 16 but at day 30, had returned to crypt depths that were also measured in the germfree mice (Figure 2.1B). Concomitant to the lengthening of the crypts, the lamina propria in both the jejunum and ileum expanded by a global increase in connective tissue cells combined with the infiltration of lymphocytes and other mononuclear cells (Figure S2.1A).

Conventionalized mice at days 4, 8, and 16 had significantly ($p <0.05$) higher number of Ki-67-positive cells compared to germfree (Figure 2.1C). Ki-67 positive cells predominantly localized in the crypts, but were also seen in the intervillus region and in the lamina propria of the small intestine at day 30. Relative enumeration of Ki-67-positive and –negative cells in colonic crypt epithelia revealed a maximal percentage of positive cells on days 4 and 8, followed by a decline at day 16 post-conventionalization (Figure S2.1B). Notably, the percentage of proliferating cells had declined further at day 30 but remained significantly ($p <0.05$) higher than in the germfree (not shown).

To obtain global information on induction of innate immunity at day 4 post-conventionalization, the day at which the largest transcriptome shift was initiated; High Iron Diamine-Alcian Blue (HID-AB) staining of mouse intestinal sections was performed. The HID-AB stain detects the mucin load of goblet cells and discriminates between sialylated and sulfated mucins. The results showed that in jejunum and colon (but not ileum), less mucin-filled goblet cells were observed at day 4; in the colon, day 4 was also characterized by a transient domination of sialylated over sulfated mucin-containing goblet cells (Figure 2.1D). Taken together, these results clearly illustrate the region-specific transient and permanent changes in the intestinal morphology and cell proliferation as a consequence of microbial colonization. These changes did become most pronounced from day 4 post-conventionalization onward.

Establishment of the Gut Microbiota during Conventionalization

In order to get insight in the dynamics of the establishment of the microbiota in the gastrointestinal (GI) tract of conventionalized mice, samples from jejunum, ileum, and colon were collected

at days 1, 2, 4, 8, and 16 post-conventionalization and were compared for 16S RNA gene diversity among each other and with the inoculum. Quantitative (qPCR) detection of 16S rRNA gene copies in colon samples indicated that a full-sized microbial community was very rapidly established, i.e., already on day 1 post-conventionalization the microbial community contained approximately 11.6±0.5 16S rRNA copies/g colon content (expressed as log10). This community size-estimate did not significantly change during the experiment, indicating that the microbial community reached its climax size in a single day. Molecular fingerprinting of the composition of the colonizing microbiota was performed using MITChip analysis, a 16S rRNA-based phylogenetic array specifically designed to classify murine microbiota (Geurts, Lazarevic et al. 2011). These analyses revealed that the colon microbial diversity remained relatively low during days 1 and 2 and significantly increased ($p=0.001$) at later time-points of conventionalization, reaching a stable diversity level on days 8 and 16. This diversity resembled that of the original inoculum (Figure 2.2A). Pearson correlation based similarity analysis of MITChip profiles of the colon samples indicated that the similarity of the colon microbiota relative to the inoculum increased from approximately 60 % to 80 % during the course of conventionalization (Figure 2.2B), indicating that the climax community was indeed comparable to that of conventional mice. This level of similarity is comparable to what is commonly found when the microbiota of individual conventionalized mice was compared (not shown). MITChip analysis also allows more detailed evaluation of the dynamics of colonization by specific phylogenetic groups, revealing that day 1 was characterized by a higher relative abundance of Gram-negative Bacteroidetes while later stages of conventionalization (days 8 and 16) showed an expansion of the relative abundance of the Gram-positive Firmicutes (Figure 2.2C). The expansion of the Firmicutes phylum was particularly large for the members of *Clostridium* clusters IV and XIVa, while the initial abundance of the bacilli (days 1 and 2) declined upon prolonged conventionalization (Figure S2.2A). Finally, multi-variate analysis (RDA) of colon and small intestine derived microbiota profiles (jejunum and ileum) clearly established that each intestinal location did harbor different microbial consortia; especially the diversity of the small intestine community appeared to be significantly lower than that encountered in the colon (Figures S2.2B,C). These data indicate that microbial colonization of the intestine proceeds via the rapid appearance of early colonizers, followed by the establishment of a stable community that resembles the microbiota of the conventional donor animals. This outcome clearly indicates efficient colonization of the GI tract in the conventionalized mice.

Mucosal Transcriptomes Reveal Temporal and Region-Specific Immune Responses

In order to investigate the pathways underlying the mucosal changes observed, tissue gene expression patterns of jejunum, ileum, and colon at all time-points post-conventionalization were compared to day 0 (germfree state). Taking into account the time series experimental design used, the Short Time series Expression Miner (STEM) software program was used to identify genes with similar, time-dependent gene expression patterns over the 30-days timespan of conventionalization. Clustering of genes was determined separately for each location of the GI tract. STEM significantly fitted the small intestine and colon data to different expression profiles models (Figure S2.3). In these profiles, immune-related gene ontology (GO) categories were strongly enriched ($p<0.001$; nearly 40% of the genes regulated in response to conventionalization were annotated with immune-related GO terms). Interestingly, the expression patterns of immune related genes were different in the small intestine and colon (Figure S2.3). STEM output was confirmed by GO-enriched bayesian clustering which demonstrated that the most strongly upregulated GO categories included immune system processes and cell differentiation,

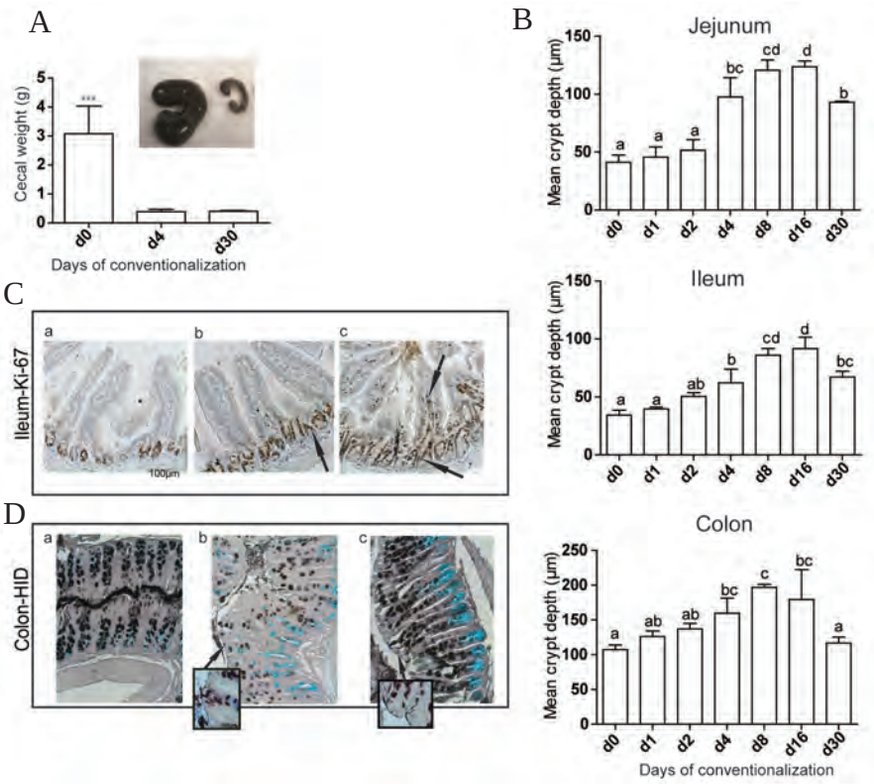

Figure 2.1. Effect of microbial colonization on the intestinal physiology and morphology. (A) Total cecal weight determined as a measure of bacterial colonization, and the insert shows a photograph of cecum at day 0 (left) and day 4 (right), respectively. (***= $p < 0.001$ compared to germfree). (B) Mean crypt depth measured from villi and crypts from the jejunum, ileum, and colon in germfree, conventionalized mice at six time-points post- conventionalization. Results are presented as means ± SD. Significant differences between time-points are indicated by distinctive characters above measurement groups. (C) IHC detection of Ki-67 positive cells using Mib-1 antibody in ileal tissues in germfree (a), days 4 (b), and 30 (c) post-conventionalization.(D) Representative HID-stained colon sections, showing the dynamics of mucin subtypes distribution in germfree (a), days 4 (b), and 16 (c) post-conventionalization. Sialylated mucins stain blue, while sulfated mucins stain brown/black.

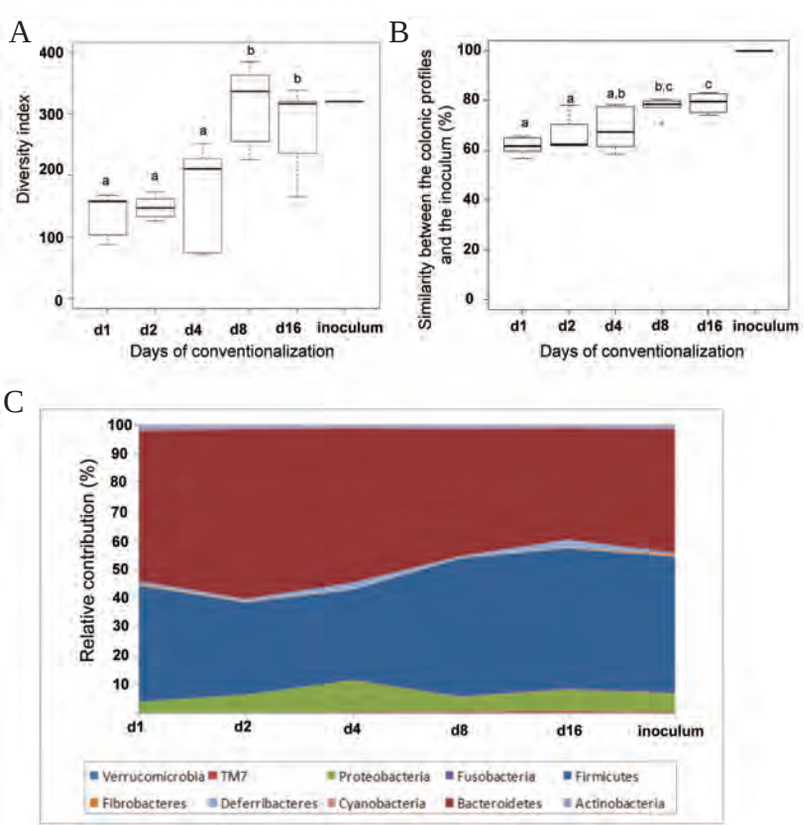

Figure 2.2 Establishment of the gut microbiota during conventionalization. (A) Diversity of the total colon microbiota at different time-points post-conventionalization, expressed as Simpson index of the hybridization profiles analyzed by the MITChip. (B) Pearson correlation similarity index of the MITChip profiles from colon samples at different time-points post-conventionalization, including the comparison to the inoculum. Significant differences between time-points are indicated by distinctive characters above the measurement groups. (C) Dynamics of the relative contribution of different microbial groups (level 0, which is similar to phylum level phylogeny) to the overall microbiota in the colon of mice at different time-points post-conventionalization, and in comparison to the inoculum. d=day.

especially of immune cells (Figure S2.4). Among the upregulated categories was one gene set annotated with GO category "immune response" which was induced on 72% of the arrays used. Collectively, these results showed that the majority of the differentially expressed genes during conventionalization participate in the immune response, in a time- and region-dependent manner.

Induction of Local Antimicrobial Defense and Surface Receptors at Day 4 Post-Conventionalization

STEM time-series analysis identified gene clusters assigned to GO-terms associated with innate immunity as a major response category. GO enrichment analysis (supplemental information) highlighted the induction of expression of surface receptors involved in microbial recognition at day 4 post-conventionalization throughout the GI tract. These receptors included

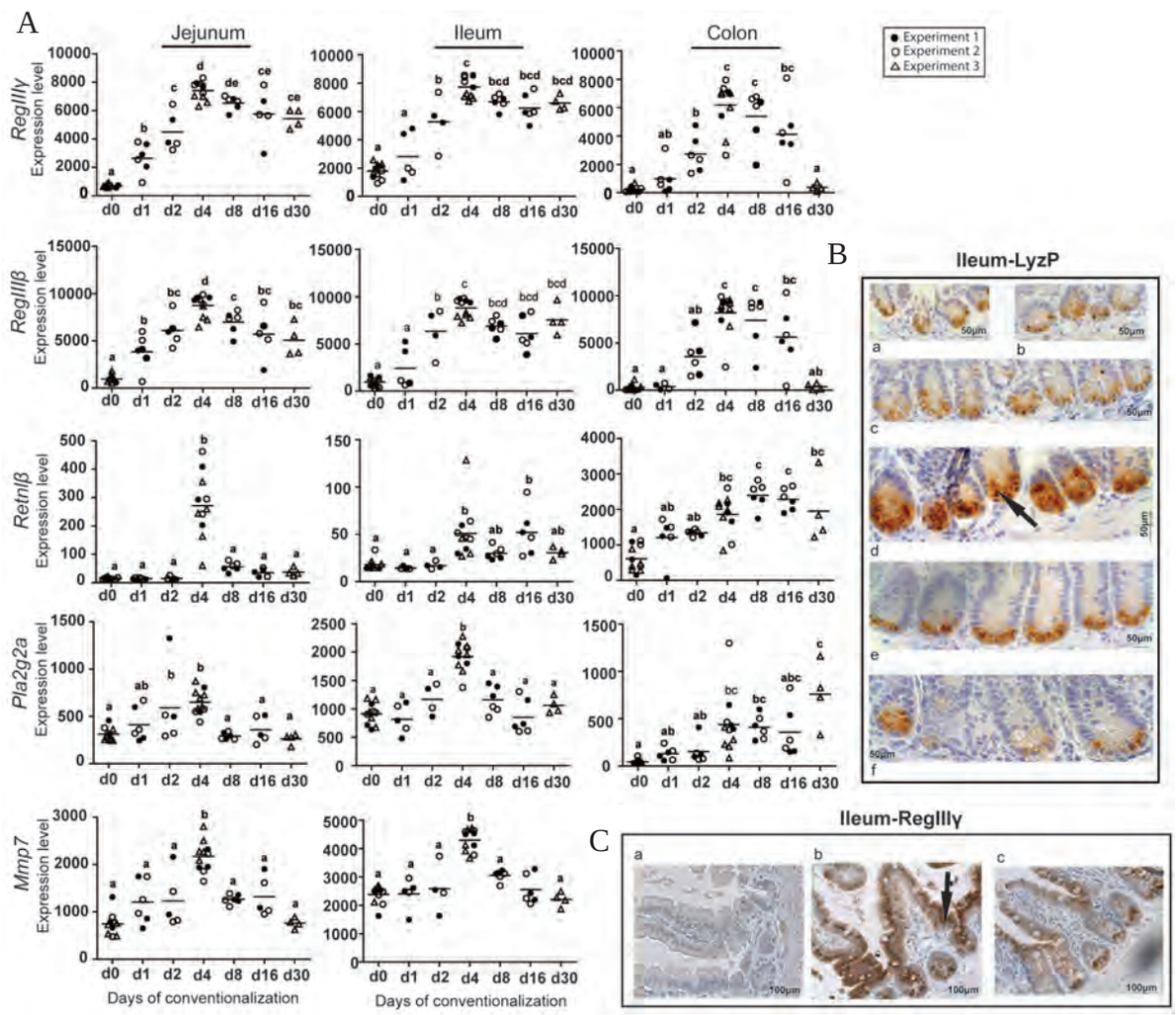

Figure 2.3. Dynamics of induction of innate immune molecules during conventionalization. (A) Gene expression levels of *RegIIIγ, RegIIIβ, Retnlβ*, and *Pla2g2a*, in jejunal, ileal, and colonic tissues, and *Mmp7* in jejunal and ileal tissues from germfree and conventionalized mice at indicated days post-conventionalization. Individual values determined in the animals and their medians are shown. Significant differences between time-points are indicated by distinctive characters above the measurement groups ($p < 0.05$). (B) Representative IHC of lysozyme-P in ileum tissues from germfree (a), days 1 (b), 2 (c), 4 (d), 8, and 16 (f) post-conventionalization. (C) Representative IHC of RegIIIγ in ileum tissues from germfree (a), days 4 (b), and 30 (c) post-conventionalization. Arrows indicate positively stained cells.

the lipopolysaccharides (LPS) receptor (*Cd14*), the intracellular signaling adaptor protein (*Myd88*) and the toll-like receptors *Tlr1, 2, 8, 9,* and *12* but not *Tlr4* or *5* (Figures S2.5A,B). In parallel, the expression levels of several antimicrobial peptides, including lysozyme P (*LyzP*), regenerating islet derived protein (*Reg*) *IIIβ* and *-γ*, resistin like beta (*Retnlβ*) and phospholipase A2 (*Pla2g2a*) had clearly increased (Figure 2.3A). The fold-changes related to these innate immune responses increased gradually during days 1 and 2 followed by a strong increase at day 4 post-conventionalization in both the small intestine and colon. Notably, prolonged exposure to microbiota (30 days) retained increased expression levels of *RegIIIβ* and *-γ* in the small intestine, but returned to the germfree-level in the colon. In contrast, the expression levels of *Retnlβ* and *Pla2g2a* returned to germfree-levels in the small intestine, but remained high in the colon. These results suggest that mucosal innate immunity is based on different molecules in the small intestine versus the colon. Indeed, immunohistochemical (IHC) analysis verified the *LyzP* loading of secretory granules in the Paneth cells in the small intestine of day 4 (Figure 2.3B), which is in agreement with the coinciding increase of expression of matrix metalloprotease 7 (*Mmp7*) (Figure 2.3A) that regulates the activity of defensins in intestinal mucosa (Wilson, Ouellette et al. 1999). IHC analysis also confirmed the peak production of *RegIIIγ* at day 4 (Figure 2.3C). The gene expression and IHC data show that transient induction of innate immune factors is region-dependent and was most pronounced after 4 days of conventionalization.

Antigen Presentation and Pro-inflammatory Cytokine Production at Day 4 Activates Local B and T Cells during Later Days of Conventionalization

To further assess the induction of innate and adaptive immune responses during conventionalization, the expression patterns of cytokines were used as markers for the release of pro-inflammatory signals and attraction of immune cells. Tumor necrosis factor alpha (*Tnf-α*), and interferon gamma (*Ifn-γ*), a strong activator of microbicidal function in macrophages and adaptive immunity (Schroder, Hertzog et al. 2004), were significantly higher expressed throughout the intestine upon conventionalization (Figure 2.4A). In the small intestine, their expression increased from day 4 onward, and peaked at day 16 post-conventionalization, while in the colon, peak induction occurred at day 4 followed by a decline of expression at later time-points and a gradual return to the levels seen in germfree mice (Figure 2.4A). To investigate whether elevated expression of pro-inflammatory cytokines coincided with the expected induction of surface expression of MHC class I and II complexes, the dynamics of expression of the associated genes were investigated. Members of the MHC class I complex and their activators were induced from day 4 onward throughout the GI tract, while the induction of members of the MHC class II complex and their transactivator (*Ciita*) appeared to occur at later time-points, mainly peaking at days 8 and 16 post-conventionalization (Figures 2.4A,B).

Adaptive Immune System Development

As anticipated, the increased expression of pro-inflammatory cytokines and MHC class I and II molecules during the later stages of conventionalization elicited the induction of expression of genes required for T cell function and development on day 8 (colon) and day 16 (small intestine) post-conventionalization. The most prominent among these genes were those coding the T cell accessory molecules that participate in antigen response, inflammatory chemokine ligands (*Cxcl9, 10, Ccl2, 3,* and *5*) and chemokine receptors (*Cxcr3, Ccr2,* and *5*) (Figure S2.6). Increased expression of these genes coincided with the increased villus width and lamina propria cellularity in the small intestine that were observed in hematoxylin and eosin-stained tissue sections (Figure S2.1A).

Ingenuity Pathways Analysis (IPA) (www.ingenuity.com) and GO-enriched bayesian clustering were employed to further detail the biological functions and signaling pathways involved in the time- and region-dependent events related to immune (T) cell activation and development. According to IPA, (positive) regulation of lymphocyte activation, T cell selection and positive thymic T cell selection were among the most significantly enriched ($p < 0.001$) GO categories throughout the intestine (Figure S2.7A). Using Genomica (described in supplemental information), detailed inspection of the gene set annotated with GO category "T cell activation" (Figures S2.7B,C) allowed to further exploring the tissue distribution of T cells. This gene set was upregulated from day 4 onward in ileum and from day 8 to 30 throughout the intestine (Figure S2.7C) and included the surface markers of T cell infiltration (DeJarnette, Sommers et al. 1998); *Cd3ε, Cd4,* and *Cd8*.

IHC was used to verify that the suggested gradual increase of T cells expressing the mentioned surface markers, with the largest numbers in the small intestine, did indeed occur. Microscopic inspection of sections hybridized with the appropriate antibodies showed increased numbers of cells positive for the T-cell maturation markers *Cd3ε* and *Cd8* from day 8 onward and highlighted the prominent localization of Cd8 positive cells along the epithelial lining of the small intestine (Figure 2.5). Compared to $Cd8^+$ and Cd3ε cells, cells positive for the $Cd4^+$ marker were observed at lower numbers in the lamina propria of the small intestine at day 16 post-conventionalization (Figure 2.5) suggesting a lower $Cd4^+$ T cell influx . Notably, prolonged conventionalization (day 30) revealed that the increase in T cell numbers (especially $Cd8^+$) had continued in the small intestine but had already reached a more steady level in the colon between days 8 and 16. Gene expression data demonstrated that the influx of $Cd4^+Cd8^+$ T cells was associated with increased expression levels of perforins (*Prf1*) and granzymes (*Gzm*) (data not shown), molecules that are typically produced by activated T cells. Altogether, the increased numbers of cells positive for typical markers of T cell activation and maturation indicate activation and development of the adaptive arm of the immune system. Development of adaptive immunity appeared to have reached a climax level on day 8 in the colon and day 16 post-conventionalization in the small intestine and appeared to follow the strong activation of innate immune response that was apparent at day 4.

Negative Regulation of the Activated Immune Response

So far, pro-inflammatory signals have been shown to activate innate and adaptive immunity in response to the microbiota. No signs of disease were noticed in the mice during conventionalization and no microscopic signs of damage to the intestine or the associated infiltration of immune cells were identified. The tolerant immune responses therefore were assumed to have been induced by the microbiota, implying negative regulation of the immune response. To investigate this, the expression profiles of immune-suppressive cytokines were analyzed. As expected, the induction of immune responses coincided with elevation of expression of tolerance-associated molecules, starting on day 8 post-conventionalization and continuing during later time-points with a climax level on day 8 in the colon and day 16 post-conventionalization in the small intestine. These molecules included the forehead box P3 (*Foxp3*), the marker for T_{regs} cells (Hori, Nomura et al. 2003), Interleukin-10 (*Il10*), which enforces immune tolerance (Fujio, Okamura et al. 2010), and *Tbx21* (*T-bet*), a transcription factor that drives Th1 cell maturation (Miller and Weinmann 2010) (Figure 2.6). In addition, the increased expression of cytotoxic T-lymphocyte-associated protein 4(*Ctla4)* and Fas ligand (*Fasl*), in particular at day 8 in the colon and day 16 post-conventionalization in the small intestine, suggested that apoptotic pathways were

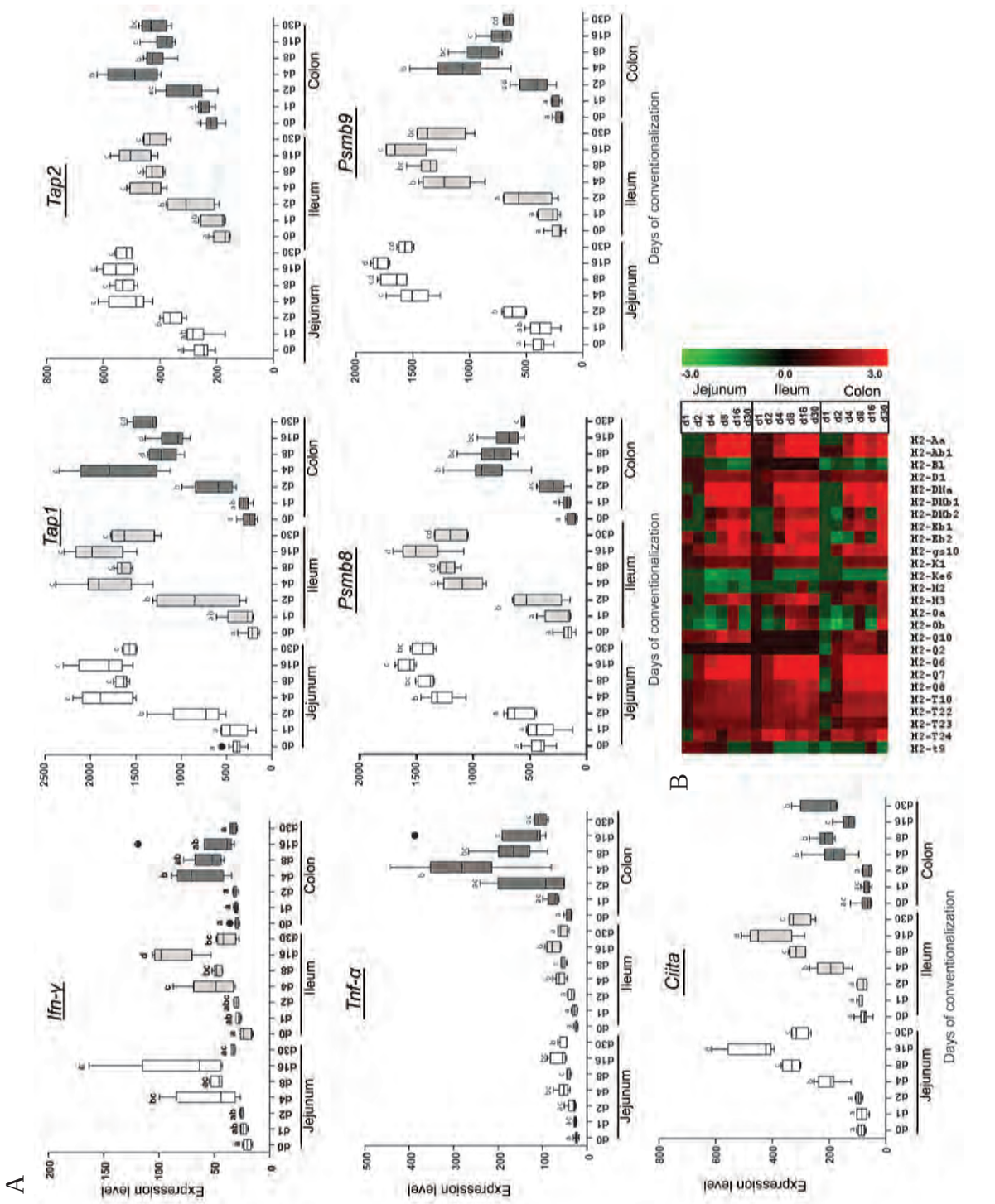

Figure 2.4. Expression of *TNF-α, Ifn-γ* and MHC class I and II complexes. (A) Jejunum, ileum, and colon gene expression levels of *TNF- α* and *Ifn-γ*, and MHC class I and II complex activators were analyzed in germfree and conventionalized mice at indicated days post-conventionalization. Values are depicted as box and whisker diagrams (top-to-bottom, maximum value, upper quartile, median, lower quartile, and minimal value, respectively). Any data not included between the whiskers is plotted as an outlier with a dot. Significant differences between time-points are indicated by distinctive characters above the measurement groups ($p < 0.05$). (B) Heat map generated from the significantly expressed MHC class I and II genes ($p < 0.05$) between the germfree and conventionalized mice at the indicated time-points.

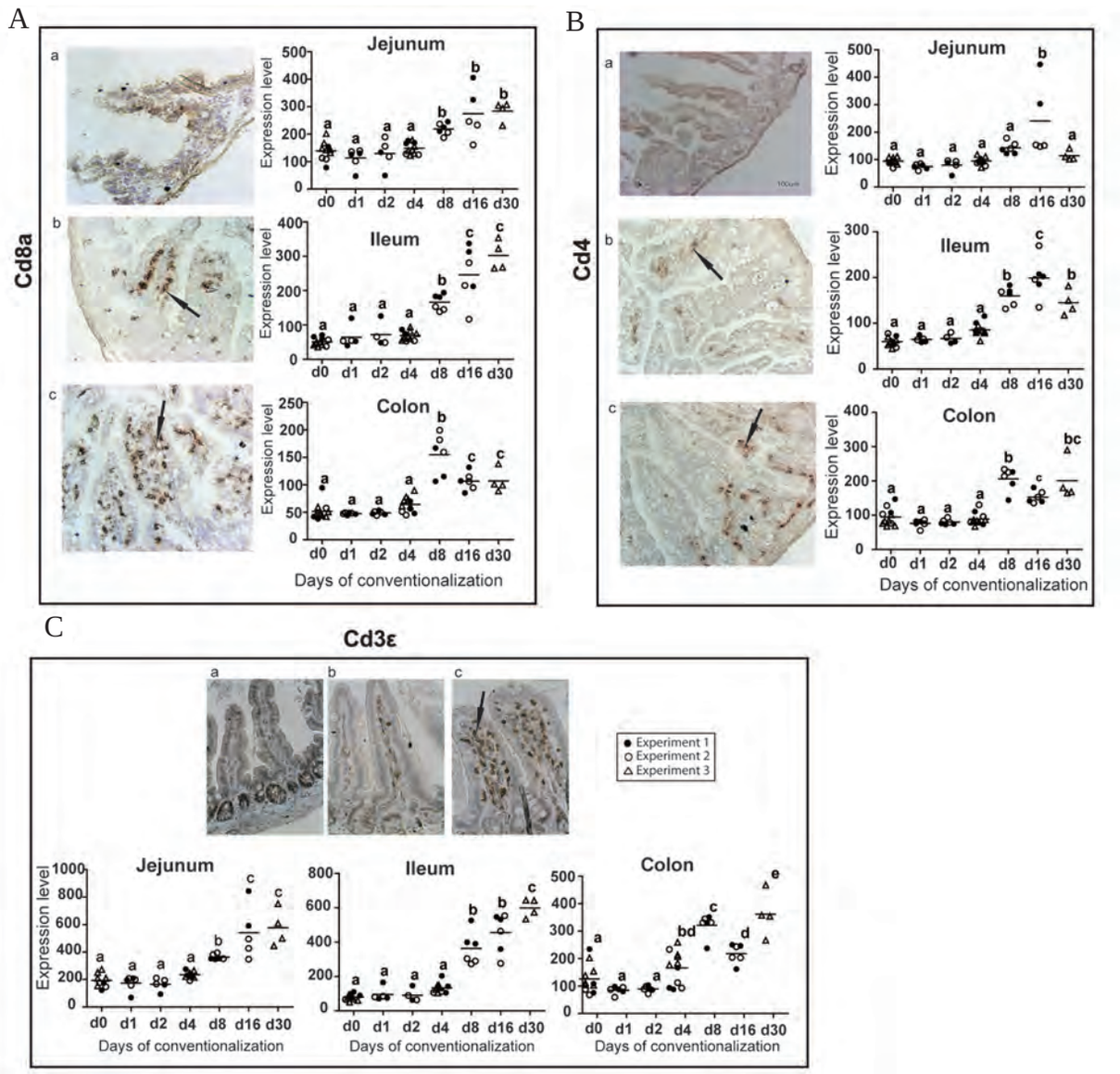

Figure 2.5. Regional variation of increasing T cell numbers and maturation. Representative IHC of Cd8a (A), Cd4 (B), and Cd3ε (C) in ileal tissues from germfree (a), days 16 (b), and 30 (c) post-conventionalization. Dot plots represent the expression levels of *Cd8a*, *Cd4*, and *Cd3ε* in jejunal, ileal, and colonic tissues in germfree and conventionalized mice at the indicated days post-conventionalization. Individual values and medians are shown. Significant differences between time-points are indicated by distinctive characters above the measurement groups ($p < 0.05$). All panels are shown at the same magnification; arrows indicate positively stained cells (brown color).

induced in the tissues harboring proliferating immune cells as a regulatory mechanism to avoid accumulation of cytotoxic T cells (Figure 2.6). Collectively, the gene expression profiles and IHC studies appear to correlate with the region-specific induction of pro- and anti-inflammatory signals that together drive a balanced, tolerant type of adaptive immune response that is required to ensure appropriate responses to the microbiota.

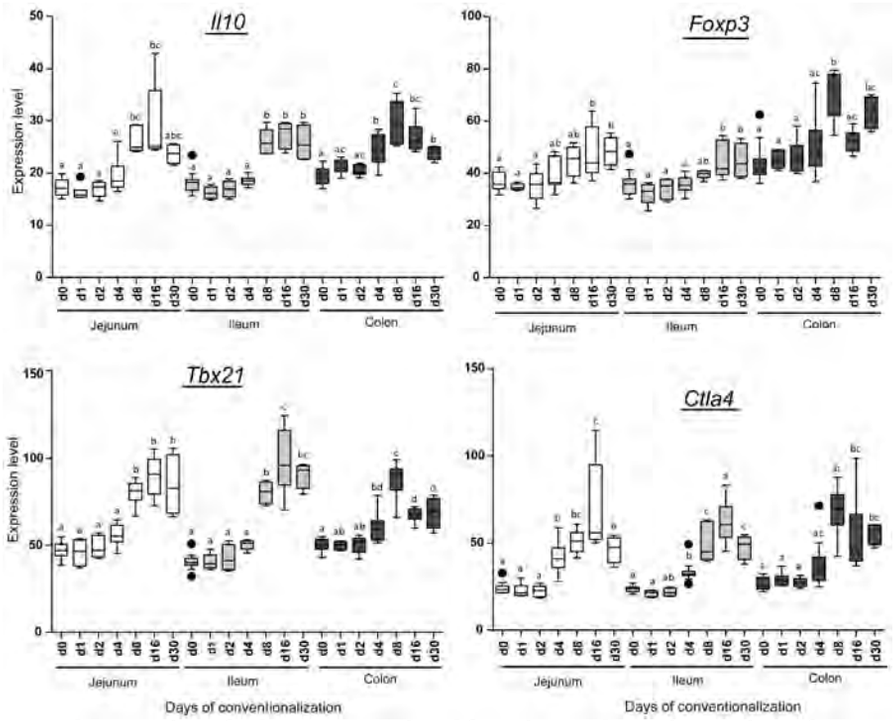

Figure 2.6. Increased expression of tolerance associated functions at later time-points of conventionalization. Jejunum, ileum, and colon gene expression levels of regulatory cytokines were analyzed in germfree and conventionalized mice at the indicated days post-conventionalization. Values are depicted as box and whisker diagram (top-to-bottom; maximum value, upper quartile, median, lower quartile, and minimal value, respectively). Any data not included between the whiskers is plotted as an outlier with a dot. Significant differences between time-points are indicated by distinctive characters above the measurement groups ($p < 0.05$).

A Universal, Core Regulatory Network Orchestrates the Immune Responses towards the Microbiota

From the STEM and GO-enriched bayesian clustering results, we hypothesized that there might be a common gene regulatory network that governs the re-establishment of mucosal homeostasis upon conventionalization throughout the GI tract. The genes that are part of such a network were further assumed to show differential expression during all time-points of conventionalization. Therefore, STEM time series analysis output sets were mined for genes that display the same expression profiles in jejunum, ileum, and colon, and these genes were used to construct a protein-protein interaction network in IPA. The resulting network illustrated the strong impact of conventionalization on both innate and adaptive immune gene expression (Figure 2.7), encompassing several central regulatory nodes that control the induction of innate and adaptive immune responses. The IPA-derived network combined the major gene categories that were identified by STEM and were strongly induced from day 4 post-conventionalization onward, including nodes belonging to bacterial recognition (*Cd14*), pro-inflammatory cytokines (*Tnf-α, Ifn-γ*), chemokines (*Ccl5, Ccr5, Cxcl9, Cxcr3, Ccl8*), and MHC Class I (*Psmb8, 9, Tap1,2, H2-Q*). The network also included nodes representing MHC Class II molecules (*Ciita, H2-Ab1, H2-DMa, H2-DMb1*), T cell differentiation and maturation (*Lck, Lat, Zap70*), cell surface markers (*Cd3ε, Cd4, Cd8*), and B cell differentiation (*Ptprc*). These nodes showed an increased expression at later time-points, i.e. day 8 in the colon and day 16 in the small intestine (Figure 2.7B). Notably that repression of the genes in this network only occurred during the early days; at 8, 16, and 30 days post conventionalization, all genes in this network were induced (Figure 2.7B).

In parallel, a protein-protein interaction map was generated from the cluster-driven time series analysis of GO categories using bayesian statistics (Figure S2.8). This network combined genes that belong to T cell differentiation and maturation (e.g. the kinases *Lck* and *Zap70*), innate immune effectors (*C2, C3*), chemokines (*Cxcl2, Il10, Tnf-α*), MHC (*H2-Q*) and cell surface markers (*Cd3ε, Cd4, Cd8*). These two latter analyses showed that T cell selection, - induction and - differentiation pathways were among the most important induced mucosal pathways during mouse conventionalization. Notably, the two core regulatory networks, constructed using very different approaches and statistical methods, contained identical major regulatory nodes, supporting the prominent roles of these nodes during immune system development.
IPA found 13 associated genes in the core network with known roles in inflammatory bowel disease (indicated with arrows in Figure 2.7A). These findings support the biological relevance of the central nodes within this regulatory network in maintenance of homeostasis. We propose that these genes are key regulators of appropriate immune interactions with the gut microbiota

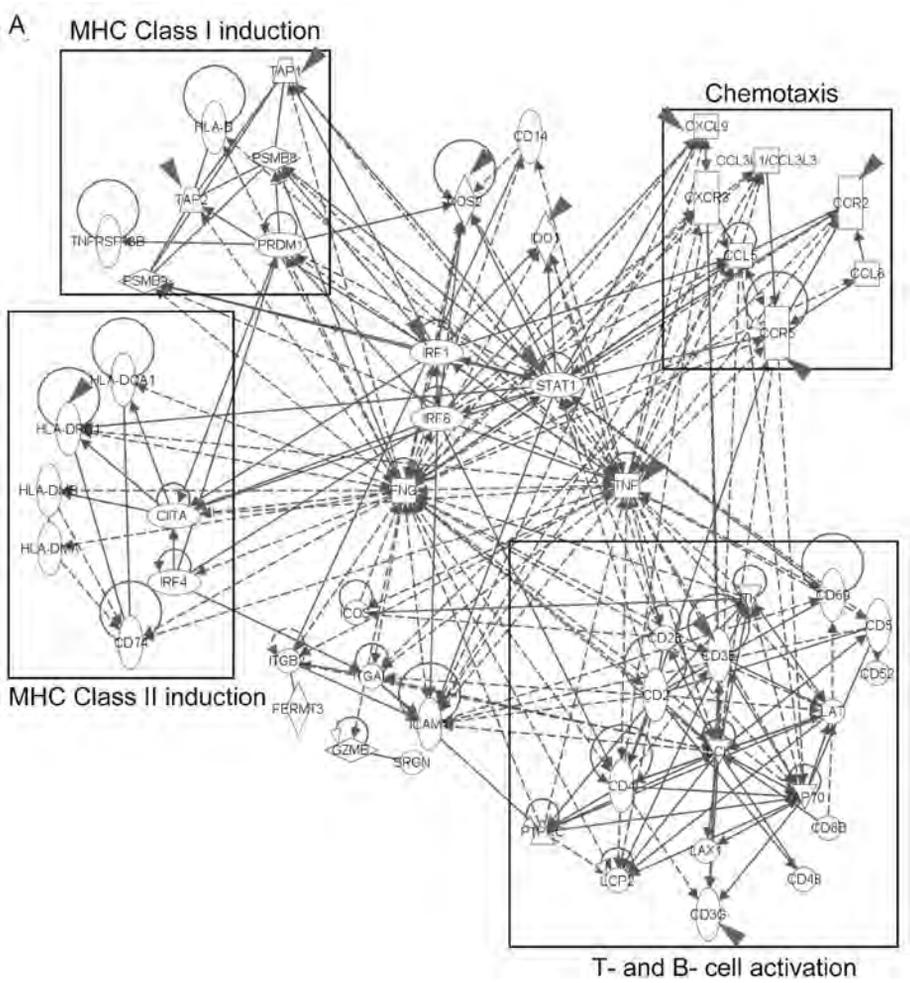

Figure 2.7. Core regulatory network that governs the dynamic establishment of intestinal homeostasis during conventionalization. (A) The ingenuity protein-protein interaction network derived by plotting STEM output genes that occur in the profiles involved in immune response in the jejunum (J), ileum (I), and colon (C). Transcriptional data was projected onto the interaction map. Arrows refer to associated genes with known role in inflammatory bowel disease. (B) Heat map of the genes that constitute the core regulatory network. The heat map in panel B is placed on the next page (38).

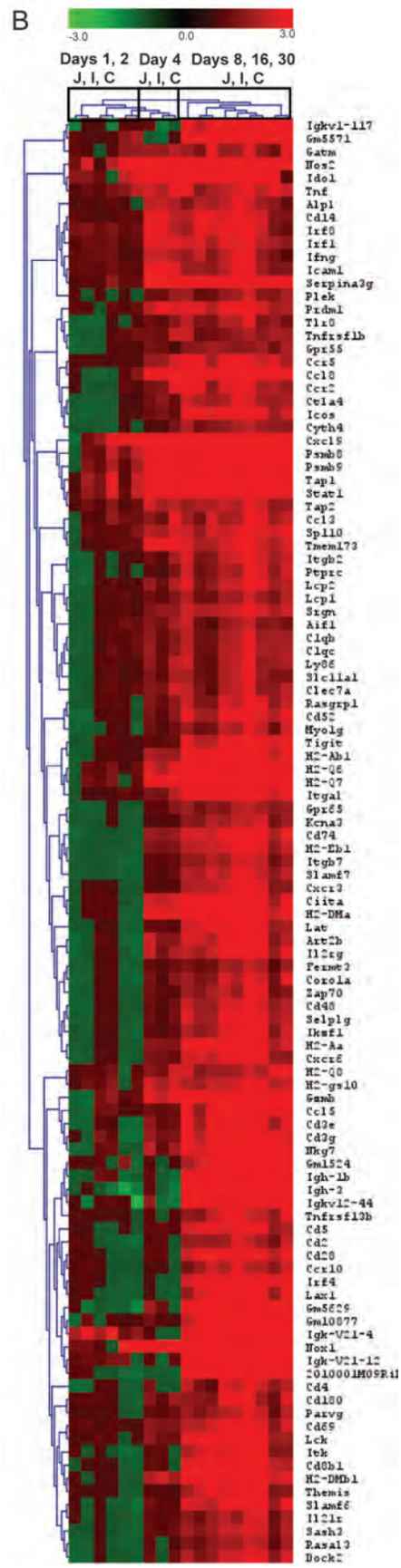

and that the expression profiles of these genes may be used to construct a molecular signature of mucosal control of homeostasis.

DISCUSSION

It has been widely recognized that the interplay between gut microbiota and the host is crucial for proper development of the (adaptive) immune system (Lee and Mazmanian, 2010) and that dysregulation of this interaction contributes to the development of inflammatory bowel disease symptoms (Abraham and Cho 2009). There is a clear requirement for the balanced genetic regulation of appropriate, tolerant responses to the microbiota (Bouma and Strober 2003; Geuking, Cahenzli et al. 2011). This is also supported by the finding that mutated forms of genes involved in regulation of basal immunological processes such as microbial uptake are strongly associated with inflammatory bowel disease phenotypes (Deretic and Levine 2009).

The present study implemented profiling the genome-wide expression of genes involved in local (jejunum, ileum, and colon) mucosal immune system development in a time-resolved (6 time-points) manner, in germfree mice upon conventionalization. Our study corroborated several important findings from the study by Gaboriau-Routhiau and colleagues (Gaboriau-Routhiau, Rakotobe et al. 2009). In both studies, it was found that the largest category of genes that is regulating the response to microbial colonisation is the immune response, and that T cells (not B cells) play key roles in the mucosal response to microbial colonization of germfree mice. Transcriptomic analysis including gene ontology (GO) enrichment and pathway and (gene regulatory) network analysis, showed that there was a time- and region-dependent enrichment of genes involved in balanced innate and adaptive immune responses. These tolerant responses ensured that a novel state of homeostasis was reached within 30 days of conventionalization. Strikingly, both transcriptomic and immunohistochemical analyses for cytokines, chemokines, T cell surface markers and immune cell transcription factors and histological stainings of innate immune parameters showed that a novel homeostasis had been reached in the colon within 8 to 16 days, whereas establishment of homeostasis in the small intestine required 16 to 30 days of conventionalization.

Remarkably, the shift in the microbiota composition (day 4) coincided with the shift in host responses. Microbial

profiling of the colon microbiota during conventionalization indicated that initially colonizing microbial communities are characterized by low diversity and higher abundance of Bacteroidetes (days 1 and 2), while the stable community established on day 8 is more diverse and dominated by Firmicutes (particularly the *Clostridium* clusters IV and XIVa).

Day 4 post-conventionalization consistently stood out in the transcriptome analyses and was characterized by drastic changes in gene transcription. For instance, gene expression could switch from induction to repression and vice versa; and some genes were no longer expressed while others were expressed for the first time. At this time-point, the activation of cascades of genes involved in innate immunity activation and initiation of adaptive immune responses was most pronounced.

No changes in the expression level of Il-17 were noticed throughout the GI tract during the process of conventionalization (not shown) suggesting that the colonization of the C57BL/6 J mice with their normal fecal microbiota did not induce Th17 differentiation, which corroborates the results of Ivanov *et al.* who reported that colonization of C57BL/6 mice purchased from the Jackson laboratories (J) was not sufficient to induce Th17 differentiation in their lamina propria due to the absence of segmented filamentous bacteria (Ivanov, Atarashi et al. 2009). As recently reported (Geuking, Cahenzli et al. 2011), our data support the notion that inflammatory tissue conditions were avoided by T_{regs}, inferred from increased expression of *Foxp3,* and *Il10* markers for tolerance-promoting T_{regs} that were induced especially from day 8 onward. Interestingly, these two and other cytokine markers showed a tendency towards increasing expression in jejunum and ileum throughout the experiment. However in the colon, expression of the same tolerance markers clearly peaked at day 8 and subsequently declined at days 16 and 30 post-conventionalization but remained higher than the levels observed in the germfree and early days of conventionalization. Notably, the climax expression level of T_{regs} at day 8 post-conventionalization in the colon coincides with the colonization of *Clostridium* groups which were previously reported to stimulate the expression of colonic regulatory T cells (Atarashi, Tanoue et al. 2011).

Similar differential expression in small intestine versus colon was also observed for six inflammatory chemokine ligands and the corresponding three receptors. We propose that the expression of these chemokines contributes to T cell chemotaxis. IHC showed that at day 8, $Cd8^+$ T cells were predominantly localized near the mucosal epithelia, which likely resulted from epithelial chemokine secretion and expression of MHC class I molecules. This timing of $Cd8^+$ T cell accumulation in response to accumulation of Th1 chemokines in “danger zones” is in line with the results reported by Valbuena *et al*. during bacterial infection of mice (Valbuena, Bradford et al. 2003). Moreover, the faster accumulation of $Cd8^+$ T in the lamina propria of the colon at day 8 but at day 16 in the small intestine illustrates an important location difference that is relevant in the context of establishing homeostasis.

Epithelia contain, in addition to the common enterocytes that are mainly involved in metabolic functions, specialized Paneth cells that secrete high amounts of a broad range of antimicrobial pepides, and goblet cells that secrete mucins. One of the broad spectrum antimicrobials secreted by Paneth cells, *RegIIIγ*, was induced in this study in agreement with Gaboriau-Routhiau *et al.* (Gaboriau-Routhiau, Rakotobe et al. 2009), together with the related *RegIIIβ*. The expression of these two peptides appeared to peak at day 4 post-conventionalization, in particular in the ileum as supported by IHC analysis. This could reflect a pronounced induction of acute innate immune responses at day 4 post-conventionalization, corroborated by peak expression levels of the genes encoding the innate immune molecules *Retnlβ* and *Pla2g2a*, and the coinciding

lyzP load of secretory granules in Paneth cells. Although innate immunity was clearly induced in every location of the GI tract, its dynamics over time was distinct per location. For example, *RegIIIβ* and *RegIIIγ* expression peaked at day 4 post-conventionalization in both small intestine and colon, and high level expression was retained in the small intestine but declined to germfree levels in the colon at later time-points. Conversely, expression of *Retnlβ* and *Pla2g2a* peaked also at day 4 but returned to germfree levels in the small intestine whereas expression remained high in colon. These data suggest that *RegIIIβ* and *RegIIIγ* are important to keep microbes at bay in the small intestine whereas this antimicrobial function is predominantly exerted by *Retnlβ* and *Pla2g2a* in the colon. This is in agreement with the presence of Reg3 peptide-producing Paneth cells in the small intestine and their absence in the colon. In contrast, *Pla2g2a* and *Retnlβ* are exclusively secreted by goblet cells (Fijneman, Peham et al. 2008; Krimi, Kotelevets et al. 2008). These results show that, in healthy germfree mice and during bacterial colonization, innate immune responses are the first line of defence against microbiota, and that this response displays location (small intestine versus colon) differences in terms of molecules and expression levels. Other responses of epithelia to increasing bacterial colonization were the increased proliferation of crypt epithelial cells and villus connective tissue cells, measured as Ki-67 expression starting at day4 post-conventionalization and the transient lengthening of the crypts, measured as crypt depth also starting at day 4. Our data corroborate results obtained by Cherbuy and co-workers demonstrating the role of microbial colonization in maturation of epithelial cells in gnotobiotic animals (Cherbuy, Honvo-Houeto et al. 2010).

The change in biochemistry of colon mucins at day 4 post-conventionalization, characterized by a reduction in the amounts of sulfated, thus stronger antimicrobial mucins, compared to sialylated, less antimicrobial mucins (Deplancke and Gaskins 2001; Linden SK 2008), could have led to a more intense contact between microbiota and epithelia. This could indeed be shown using the bacterial FISH EUB338 probe (Figure S2.9). It seems that the biochemical changes of the mucin barrier at day 4 post-conventionalization may have allowed a more intense contact between the microbiota and the mucosa, which then primed innate immune responses that were followed by adaptive immune responses four days later.

This study provides a solid catalogue of genes, pathways, and histology of intestinal adaptations of germfree mice to microbial colonization, thereby providing an important resource that complements various other studies of mouse intestinal colonization by microbiota. Taken together, the data presented here show that within 30 days following their conventionalization, the germfree mice established a novel state of immune homeostasis in the intestine that accommodates the microbiota. Notably, this novel state of homeostasis was reached earlier in the colon (days 8 and 16) as compared to the jejunum and ileum (days 16 and 30).

The extensive transcriptomic datasets for jejunum, ileum, and colon enabled us to reconstruct a central gene regulation network that governed the major transcriptome changes throughout the intestine during the 30-day conventionalization. This network included several genes of which the human orthologues are inflammatory bowel disease-associated genes that have also been discovered in genome-wide association studies (GWAS). We propose that this network could be exploited as a genetic signature to further investigate genes and pathways that are dysregulated in inflammatory bowel disease patients.

Experimental Procedures

Animals, Experimental Design, and Sampling

All procedures were carried out according to the European guidelines for the care and use of laboratory animals and with permission 78–122 of the French Veterinary Services. Germfree and conventionalized mice (male, C57 BL/6 J) were maintained in sterile conditions, on a commercial laboratory chow diet (diet composition is described in Chapter 1, Table 1.2). Three independent biological experiments were performed using mice of different age. After 2 weeks of acclimatization and diet adaptation, a first set of germfree mice (n=3) were randomly assigned to sacrifice by oral anesthesia using isoflurane. The remaining germfree mice were conventionalized by oral gavage with 0.5ml of mixed fecal suspension obtained from 0.2g of freshly obtained fecal material of conventionally raised mice (C57 BL/6 J) diluted 100-folds in Brain Heart infusion (BHI) broth. In the first 2 experiments; conventionalized mice were sacrificed at days 1, 2, 4, 8 and 16 post-conventionalization (n=3 per group per experiment). In the third experiment; conventionalized mice were sacrificed at days 4 and 30 post-conventionalization (n=4-5 per group). Small intestine; (jejunum, and ileum), and colon from each mouse were removed. The 2 segments of the small intestine and the entire colon were then divided into 2 cm segments that were immediately: stored in RNAlater® at room temperature for 1 hour prior to subsequent storage at -80°C for RNA isolation, fixed overnight (O/N) in 4% (wt/vol) paraformaldehyde (PFA) or snap frozen and stored at -80°C for IHC procedures. Luminal content from intestinal segments was removed by gentle squeezing, snap frozen, and stored at -80°C for microbiota analysis.

Histology and Immunohistochemistry

The 2 cm intestinal segments fixed in 4% (wt/vol) PFA and paraffin-embedded. 4 μm-thick cross sections were stained with haematoxylin (Vector Laboratories, Burlingame, CA) and eosin (Sigma-Aldrich, Zwijndrecht, the Netherlands). To detect morphometric differences, 12-15-well oriented villi and crypts were chosen per intestinal segment and measured. Mucin histochemistry was performed using HID-AB as described (Bogomoletz, Williams et al. 1987). For Lysozyme-P detection, sections were incubated with anti-Lysozyme P (1:50 in PBS, DakoCytomation, Denmark). For Cd3ε and Ki-67 detection, sections were incubated with anti-Cd3ε (DAKO, Heverlee, Belgium) or anti-Ki-67 (NovoCastra Laboratories, Newcastle upon Tyne, UK), respectively. Expression of RegIIIγ was detected using a custom-made antibody (detailed descriptions are presented in the supplemental material). For Cd4-8 detection, cryostat sections were incubated with anti-Cd4 and anti-Cd8 (DakoCytomation). Primary antibodies were detected using VECTASTAIN ABC Elite kit (Vector Laboratories), including biotinylated Donkey anti-rat serum (Sigma-Aldrich) using the manufacturer's instructions. For all stainings, nuclei were counterstained with haematoxylin (Vector Laboratories). Stained tissues were examined using a Nikon Microphot FXA microscope (for detailed descriptions see supplemental material). All data were presented as means ± SD for the number of animals indicated above. Comparisons of data were performed at each time-point using one-way analysis of variance (ANOVA) followed by Tukey's Studentized range test (SPSS program, Chicago, IL). For all parameters $p < 0.05$ was considered the level of significance.

Microbial Profiling of Intestinal Luminal Contents

Luminal contents from jejunum, ileum, colon, as well as inoculum were analyzed by Mouse

Intestinal Tract Chip (MITChip), a diagnostic 16S rRNA arrays that consists of 3,580 unique probes especially designed to profile murine gut microbiota (Rajilic-Stojanovic, Heilig et al. 2009; Geurts, Lazarevic et al. 2011).
Quantification of total bacteria was performed using qPCR detection of 16 S rRNA-gene copies while Fluorescent *in situ* hybridization (FISH) was used to detect bacteria from tissue samples (for detailed descriptions see supplemental material).

Transcriptome Analysis
High quality total RNA was obtained from a 2 cm segment of jejunum, ileum, and colon by extraction with TRIzol reagent, followed by DNAse treatment and column purification. Samples were hybridized on Affymetrix GeneChip Mouse Gene 1.1 ST arrays. Quality control and statistical analysis were performed using Bioconductor packages integrated in an on-line pipeline (Lin, Kools et al. 2011). Probesets were redefined according to (Irizarry, Bolstad et al. 2003; Heber and Sick 2006). Expression estimates of probesets were computed by robust multiarray (RMA) analysis (Dai, Wang et al. 2005). ComBat (Johnson, Li et al. 2007), an empirical Bayes method, was used to correct for the systematic error introduced during labeling. Differentially expressed probe sets were subsequently identified using linear models, applying moderated t-statistics that implement intensity-dependent Bayes regularization of standard errors (Storey and Tibshirani 2003; Sartor, Tomlinson et al. 2006). Data were corrected for multiple testing using a false discovery rate (FDR) method (Storey and Tibshirani 2003). Only genes with a fold-change of at least 1.2 (up/down) and FDR < 0.05 % were considered to be significantly regulated.
Several complementary methods were used for the biological interpretation for the transcriptome data; gene clustering using Multi-experiment Viewer (MeV) software (Saeed, Hagabati et al. 2006), overrepresentation analysis of Gene Ontology (GO) terms using temporal and location comparative analysis using STEM (Ernst and Bar-Joseph 2006), Bayesian clustering using Genomica, and construction of biological interaction networks using IPA (for detailed descriptions see supplemental material).

Accession Numbers
The mouse microarray dataset is deposited in the Gene Expression Omnibus (GEO) with accession number GSE32513.

ACKNOWLEDGMENTS

The authors thank the technical staff in the animal facilities in the lab of J. Doré (INRA, Jouy en Jossas) for assistance with animal sacrifice and sampling. R. Raatgeep and C. L. Menckeberg (Department of Pediatrics, Erasmus Medical Center), A. Taverne-Thiele and H. Schipper (Cell biology and immunology, Wageningen University), S. Brugman (Pediatric Gastroenterology, University Medical Center Utrecht) are acknowledged for their excellent assistance with immunohistochemical staining and data analyses. J. Jansen, M. Grootte-Bromhaar, M. Boekschoten and P. de Groot (Division for Human Nutrition, Wageningen University) for their technical support in microarray hybridization and microarray data-quality control and processing. L. Loonen and J. Wells (Host-Microbe Interactomics, Wageningen University) are thanked for providing the RegIIIγ antibody.

CHAPTER 2
Supplemental Material

Identification of the Core Gene-Regulatory Network that Governs the Dynamic Establishment of Intestinal Homeostasis during Conventionalization in Mice

SUPPLEMENTAL EXPERIMENTAL PROCEDURES

Animals, Experimental Design, and Sampling

Germfree and conventionalized mice (male, C57 BL/6 J) were purchased from the Centre de Recherché, Institute National de la Recherche Agronomique (Jouy-en-Josas, France). All mice were maintained in sterile conditions. Mice had ad libitum access to sterilized water and were maintained on a commercial laboratory chow diet (UAR 1016C Laboratory Chow, UAR, SAFE, Route de Saint-Bris, F-89290 Augy, France) that was sterilized by gamma irradiation (45KGy). The first and second experiments of the three performed independent biological experiments included 36 mice obtained in 2 biologically independent batches of 18 mice each, aged 8 and 10 weeks, respectively. The third experiment included 15 mice, aged 10 weeks old (Chapter 1, Figure 1.5).

Immunohistochemistry

For immunohistochemistry, 4 μm-thick cross sections were deparaffinized and treated with 3% hydrogen peroxide in methanol (20 min, room temperature). Antigen retrieval was performed by microwave treatment (citrate buffer, 10 mM, pH 6.0). For Lysozyme-P detection, sections were blocked for 1 h in 1% Blocking reagent (Roche, Almere, The Netherlands) and incubated O/N at 4˚C with anti-Lysozyme P (1:50 in PBS, DakoCytomation, Denmark). For Cd3ε and Ki-67 detection, sections were blocked with 10 mM Tris, 5 mM EDTA, 0.15 M NaCl, 0.25% gelatine, 0.05% Tween-20 (TENG-T), 10% normal mouse serum (NMS) or TENG-T, 10% normal goat serum (NGS), respectively. Sections were incubated O/N at 4˚C with anti-Cd3ε (DAKO, Heverlee, Belgium) or anti-Ki-67 (NovoCastra Laboratories, Newcastle upon Tyne, UK) at dilutions of 1:400 and 1:200, respectively, in PBS containing 1% BSA and 0.1% Triton X-100. Expression of RegIIIγ was detected using a custom-made antibody (1:25,000 in PBS containing 1% BSA and 0.1% Triton X-100). RegIII-γ antibodies (custom made by Eurogentec, Seraing, Belgium), were generated in rabbits against synthetically produced peptides, using the peptide sequences GEDSLKNIPSARISC (RegIIIβ) and EVAKKDAPSSRSSC (RegIIIγ). The chosen peptide sequences correspond to unique sequences within the REGIII protein and allow differentiation between the RegIII-β and -γ proteins. Serum from immunized rabbits was affinity purified using the same peptides. The signal of the secondary HRP-conjugated antibody (Goat-anti-Rabbit HRP, 1:100000, Jackson ImmunoResearch, Suffolk, UK) was detected by using the ECL Plus chemiluminescent detection kit (GE Healthcare, Den Bosch, the Netherlands). Primary antibodies were detected using VECTASTAIN ABC Elite kit (Vector Laboratories, Burlingame, CA), including biotinylated goat anti-rabbit serum (Sigma-Aldrich, Zwijndrecht, the Netherlands) using the manufacturer's instructions.

Cd4-8 staining: 6 μm-thick cryostat sections were fixed in hydrogen peroxide and acetone and blocked for 1 h in 1% Blocking reagent (Roche) and incubated O/N at 4˚C with anti-Cd4 and anti-Cd8 (DakoCytomation) diluted 1:5 in PBS containing 1% BSA and 0.1% Triton X-100. Primary antibodies were detected using VECTASTAIN ABC Elite kit (Vector Laboratories), including biotinylated Donkey anti-rat serum (Sigma-Aldrich) using the manufacturer's instructions. Nuclei were counterstained with Haematoxylin (Vector Laboratories).

Fluorescent *In Situ* Hybridization (FISH)

Paraffin slides were deparaffinized, rehydrated and were subjected to lysozyme treatment for 60 min (20 mg/ml Tris-HCL, pH. 8.2; Sigma-Aldrich, Zwijndrecht, the Netherlands), washed in

demineralized water, and dipped briefly in 96 % ethanol. Once dry, a probe mixture containing 20 µl FITC-labeled oligonucleotide general probe EUB338 (Eurogentec-the Netherlands) (100 ng/µl) (, 20 µl Milli-Q (Millipore), and 160 µl hybridization buffer (52 g NaCl, 20 ml Tris-HCL, pH 7.2, 10 ml 10% SDS in 1 liter demineralized water, filtered through 0.2 µm filter) was applied to the slides. Subsequently, slides were incubated at 50˚C O/N in a dark moist chamber in an incubator (Marius), and the next day, slides were washed in washing buffer (hybridization buffer without SDS) for 30 min at 50˚C, and, after briefly rinsing in ultrapure water, slides were air dried rapidly. Slides were DAPI stained (Sigma), washed in 1x PBS, and rinsed shortly in ultrapure water. After rapid drying, slides were mounted with VECTASHIELD (Vector Laboratories) and evaluated under the fluorescent microscope (Leica DM5500; Leica Microsystems).

Microbiota Analysis

Microbial DNA was isolated from intestinal lumen samples (jejunum, ileum, colon, and inoculum) using the Fast DNA Spin kit (Qbiogene, Inc, Carlsbad, CA, USA), applying 0.05 to 0.1 g of luminal content and eluting the DNA yield in in 50 µl DES.

Quantification of total bacteria was performed in each sample using qPCR detection of 16 S rRNA-gene copies using universal primers, Bact-1369-For (5´-CGGTGAATACGTTCYCGG-3´) and Prok-1492-Rev (5´-GGWTACCTTGTTACGACTT-3´)(Suzuki, Taylor et al. 2000). QPCR was executed on an IQ5 Cycler apparatus (Bio-Rad, Veenendaal, The Netherlands). Reactions were performed in triplicate in a single run. Samples were analyzed in a 25 µl reaction mixture consisting of 12.5 µl Bio-Rad master mix SYBR Green (50 mM KCl, 20 mM Tris-HCl, pH 8.4, 0.2 mM of each dNTP, 0.625 U iTaq DNA polymerase, 3 mM MgCl2, 10 nM fluorescein), 0.1 µM of each primer and 5 µl of template DNA diluted 10 times (jejunum) and 100 times (ileum and colon). Standard curves of 16 S rRNA PCR product from *Lactobacillus casei* as a standard pure culture were generated using serial 10-fold dilution of the purified PCR product corresponding to 10^8 to 10^0 16 S rRNA copies. Amplification employed the following set-up: 95°C for 10 min, followed by 35 cycles of denaturation at 95°C for 15 sec, annealing temperature for 20 sec, extension at 72°C for 30 sec and a final extension step at 72°C for 5 min. A melting curve was determined at the end of each run to verify the specificity of the PCR amplicons. Data analysis was performed using the Bio-Rad software.

The Mouse Intestinal Tract Chip (MITChip) design was carried out in analogy as described for the Human Intestinal Tract Chip (HITChip) (Rajilic-Stojanovic, Heilig et al. 2009). Briefly, over 9,000 mouse intestine derived full-length 16 S rRNA sequences obtained from the public databases were reduced to 1,885 Operational taxonomic units (OTUs) or phylotypes, sharing <98% sequence similarity, and represent the so-called level 3 groups. These level-3 groups were grouped into 94 genus-like (level-2) clusters, sharing > 90%, which in turn were clustered into 27 order-like groups (level-1), and 10 phylum-like groups (level-0). Sequences from the variable V1 and V6 regions from each OTU were extracted and reverse-complemented, before being divided into six tiling probes that were printed on an Agilent oligonucleotide array (Agilent Technologies, Palo Alto, CA). In order to profile jejunum, ileum, and colon microbiota, 20 ng of DNA extract was used to amplify the 16S rRNA genes with the primers *T7prom*-Bact-27-for (5'-TGAATTGTAATACGACTCACTATAGGGGTTTGATCCTGGCTCAG-3') and Uni-1492-rev (5'-CGGCTACCTTGTTACGAC-3'). The PCR program used was: pre-denaturation of 2 min at 94°C followed by 35 cycles of 94°C during 30 sec (denaturation), 52°C during 40 sec (annealing), 72°C during 90 sec (elongation) and a final extension at 72°C for 7 min.

PCR products were purified (High Pure PCR Cleanup Micro Kit, Roche Diagnostics GmbH, Mannheim, Germany) and the DNA concentration was measured using a NanoDropÒ ND-1000 spectrophotometer (NanoDrop Technologies, Wilmington, DE, USA). The 16S rRNA genes carrying the T7-promoter were transcribed using the Riboprobe System (Promega, La Jolla, USA). The amplicon (500 ng) together with rATP, rGTP, rCTP and a 1:1 mix of rUTP and aminoallyl-rUTP (Ambion, Austin, TX, USA) were incubated at room temperature for 2h; afterwards possible DNA present was digested with the Qiagen RNAse-free DNAse kit (Qiagen, Hilden, Germany). Purification of RNA was done using the RNeasy Mini-Elute Kit (Qiagen) and concentration was quantified using NanoDrop. Subsequently, an in vitro transcription and labeling with Cy3 and Cy5 dyes was performed as previously described (Rajilic-Stojanovic, Heilig et al. 2009). The Cy3/Cy5-labeled target mixes were fragmented using 10× fragmentation reagent (Ambion) and fragmented material was hybridized on the arrays at 62.5˚C for 16 h in a rotation oven (Agilent Technologies). Slides were washed at room temperature in 2× SSC with 0.3% SDS (10 min) followed by 0.1× SSC + 0.3% SDS at 38°C (10 min) and 0.06× SSPE (5 min). The slides were washed and dried before scanning. Signal intensity data were obtained from the microarray images using Agilent Feature Extraction software, version 9.1 (http://www.agilent.com). Microarray data normalization and further analysis were performed using a set of R-based scripts (http://r-project.org) in combination with a custom-designed relational database, which operates under the MySQL database management system (http://www.mysql.com), as previously described (Rajilic-Stojanovic, Heilig et al. 2009).

Microbial diversity, similarity of the microbiota profiles, and gene copy numbers, were analyzed by a one-way analysis of variance (ANOVA) in SPSS Statistics 17.0 (SPSS Inc., Chicago, IL), with the group distinction as a fixed factor and time-points as the dependent variable, followed by Tukey's post hoc test. Diversity of microbial profiles obtained by MITChip analysis was expressed as Simpson's reciprocal index of diversity (1/D)(Simpson 1949). Diversity was calculated with the equation $D= 1/\Sigma Pi^2$, where Pi is the proportion of i^{th} taxon. This is the proportion of each probe signal compared to the total signal for each sample. A higher Simpson's index value indicates a higher degree of diversity.

Multi-variate analysis was carried out in SPSS Statistics 17.0 (SPSS Inc., Chicago, IL). A p value < 0.05 was considered to be statistically significant. In order to relate the change of the microbiota to environmental variables (experiment, days, anatomical locations), representational difference analysis (RDA) was used, as implemented in the CANOCO 4.5 software package (Biometris, Wageningen, the Netherlands), on average signal intensities for 94 bacterial groups (levels 2). All environmental variables were transformed as log (1+X). The environmental variables tested were the anatomical regions jejunum, ileum, and colon. The Monte Carlo Permutation Procedure (MCPP) as implemented in the Canoco package was used to assess statistical significance of the variation in large datasets. A Monte-Carlo permutation test based on 499 random permutations was used to test the significance, and p-values < 0.05 were considered significant.

Transcriptome Analysis

RNA quantity and quality was assessed on the total RNA obtained from jejunum, ileum, and colon spectrophotometrically (ND-1000, NanoDrop Technologies, Wilmington, USA) and with 6000 Nano chips (Bioanalyzer 2100; Agilent), respectively. RNA was judged as being suitable for array hybridization only if samples showed intact bands corresponding to the 18S and 28S ribosomal RNA subunits, displayed no chromosomal peaks or RNA degradation products, and

had an RIN (RNA integrity number) above 8.0.
The Ambion WT Expression kit (Life Technologies, P/N 4411974) in conjunction with the Affymetrix GeneChip WT Terminal Labeling kit (Affymetrix, Santa Clara, CA; P/N 900671) was used for the preparation of labeled cDNA from 100ng of total RNA without rRNA reduction. Because of the large number of samples (i.e. 154), RNA labeling was performed in three rounds using a complete block design. Labeled samples were hybridized on Affymetrix GeneChip Mouse Gene 1.1 ST arrays, provided in plate format. Hybridization, washing, and scanning of the array plates was performed on an Affymetrix GeneTitan Instrument, according to the manufacturer's recommendations. Detailed protocols can be found in the Affymetrix WT Terminal Labeling and Hybridization User Manual (P/N 702808 revision 4), and are also available upon request.
Quality control of the datasets obtained from the scanned Affymetrix arrays was performed using Bioconductor (Gentleman RC 2004) packages integrated in an on-line pipeline (Lin, Kools et al. 2011). Various advanced quality metrics, diagnostic plots, pseudo-images, and classification methods were applied to ascertain only excellent quality arrays were used in the subsequent analyses (Heber and Sick 2006). An extensive description of the applied criteria is available upon request. Ten of the 154 arrays did not pass the quality control, and were therefore not included in the subsequent analyses.
The more than 825.000 probes on the Mouse Gene 1.1 ST array were redefined according to Dai et al. (Dai, Wang et al. 2005) utilizing current genome information. In this study, probes were reorganized based on the Entrez Gene database, build 37, version 1 (remapped CDF v13). Normalized expression estimates were obtained from the raw intensity values using the robust multiarray analysis (RMA) preprocessing algorithm available in the Bioconductor library AffyPLM using default settings (Bolstad, Collin et al. 2004). Next, an empirical Bayes method, called ComBat (Johnson, Li et al. 2007), was used to correct for the systematic error (batch effect) introduced during labeling.
Differentially expressed probe sets were identified using linear models, applying moderated t-statistics that implemented empirical Bayes regularization of standard errors (Storey and Tibshirani 2003). The moderated t-test statistic has the same interpretation as an ordinary t-test statistic, except that the standard errors have been moderated across genes, i.e. shrunk to a common value, using a Bayesian model. To adjust for both the degree of independence of variances relative to the degree of identity and the relationship between variance and signal intensity, the moderated t-statistic was extended by a Bayesian hierarchical model to define a intensity-based moderated T-statistic (IBMT) (Sartor, Tomlinson et al. 2006). IBMT improves the efficiency of the empirical Bayes moderated t-statistics and thereby achieves greater power while correctly estimating the true proportion of false positives. P-values were corrected for multiple testing using a false discovery rate (FDR) method proposed by Storey et al. (Storey and Tibshirani 2003). Only probe sets with a fold-change (FC) of at least 1.2 (up/down) and FDR < 0.05 were considered to be significantly regulated.

Biological Interpretation of Expression Datasets
Several complementary methods were applied to relate changes in gene expression to functional changes. Hierarchical clustering of modulated genes in the mucosa that were unique for each time-point (or several time-points) were generated by MeV (Multi-experiment Viewer) (Saeed, Hagabati et al. 2006). Temporal and spatial comparative analysis were carried out using STEM (Short Time-series Expression Miner), which differentiates between real and random

gene expression patterns from short (up to 8 time-points) time-series microarray experiments (Ashburner, Ball et al. 2000). The statistical significance of the profiles generated by STEM was calculated via a permutation test (n=1000) corrected using a false discovery rate (FDR <0.001) (Ernst and Bar-Joseph 2006).

Biological interaction networks among regulated genes activated in response to conventionalization were identified using Ingenuity Pathways Analysis (IPA) (Ingenuity Systems). IPA utilizes a large expert-curated repository of molecular interactions, regulatory events, gene-to-phenotype associations, and chemical knowledge, mainly obtained from peer-reviewed scientific publications, that provides the building blocks for network construction. IPA annotations follow the GO annotation principle, but are based on a knowledge base of > 1,000,000 protein–protein interactions. The IPA output signaling pathways with statistical assessment of the significance of their representation being based on Fisher's Exact Test. Our IPA analyses included comparison of differentially regulated genes in the jejunum, ileum, and colon in days 1, 2, 4, 8, 16, and 30 in each case relative to expression observed in the control group (germfree=day 0). The input was all differentially regulated genes (p value $\leq$ 0.001, FC $\geq$ 1.2 and intensity $\geq$ 20) of jejunum, ileum, and colon after 1, 2, 4, 8, 16, and 30 days post-conventionalization.

To improve bayesian clustering, it is necessary to remove those genes that hardly change across time and location from the analysis. Cluster 3.0 (de Hoon, Imoto et al. 2004) was used to filter for uninformative gene expression data. As input, log2 gene expression fold-change data were used and genes that had FC higher than 1.2 in at least 8 microarrays, and that showed at least 1 fold-change difference between the highest and the lowest values were selected. The 4506 genes that passed these filtering criteria were used as input for clustering.

Identification of clusters containing genes that participate in the immune response was performed by using as gene sets collections of *Mus musculus* genes that make up Gene Ontology categories (http://www.geneontology.org). These categories contained 2475 mouse-specific annotations. To identify the arrays in which each gene set (GO category) was significantly induced or repressed, the induced (or repressed) genes in each array were defined to be those genes whose change in expression was greater than twofold. For each gene set and each array, the fraction of genes was calculated from that gene set that was induced (or repressed) in that array and used the hypergeometric distribution to calculate a P value for this fraction (compared with the null hypothesis of choosing the same number genes at random). FDR correction of 5% was used to correct for multiple tests. To determine statistical significance of array–gene set pairs, the number of array–gene set pairs in which the gene set was significantly induced (or repressed) in the array was evaluated.

To identify gene set clusters, (bottom-up) hierarchical clustering of the gene sets in the matrix of all significant array–gene set pairs was carried out. This resulted in a tree in which each leaf node, corresponding to some gene set G, is associated with a vector (indexed by arrays) that is zero everywhere except for entries that correspond to arrays in which set G was significantly induced (or repressed). In the latter case, the entry contains the fraction (or negative fraction) of genes from set G that are induced (or repressed) in an array. Each internal node is associated with a vector representing the average of the entire gene set vectors at its descendant leaves. Each interior node was annotated with the Pearson correlation between the vectors associated with its two children in the hierarchy. A cluster was defined as each interior node whose Pearson correlation differed by more than 0.05 from the Pearson correlation of its parent node in the hierarchy. Such interior nodes represent points in the tree with a large gap between the

similarities in expression of the node's children and the similarity in expression of the node and its sibling. To evaluate the consistency of a gene with expression of a gene set, given a gene set G and a gene g, we tested whether the expression of g was consistent with the significant changes in the expression of G (for statistics, see below).
In order to find clusters of genes that together participate in a GO category and that could be involved in changing gene expression at later time-points of the mouse conventionalization experiment, we wanted to derive modules from clusters of gene sets. Modules were defined as sets of co-regulated genes that share a common function and/or that respond together to changes in the environment. For each cluster of gene sets, G was defined to be the union of the gene sets in the cluster. Each gene in G was then tested for consistency (as described above). The resulting module consists of genes whose expression is significantly consistent with the expression of the gene set (after FDR correction for multiple hypotheses using a 5% FDR).
All analyses and heat map visualizations used for bayesian clustering were performed using Genomica. This software tool identifies arrays in which gene sets are significantly expressed, the GO annotations enriched in these arrays, and generates heat maps of gene clusters. Genomica is freely available for academic use at http://genomica.weizmann.ac.il/.

SUPPLEMENTAL RESULTS

Gene Sets that Mediate Localization-Specific Regulation of Intestinal Immune Cell Development

Comparing changes in GO-based gene clusters across intestinal regions and time-points could help to find distinct gene regulatory networks expected to derive the changes seen in immune-related GO sets. To this end, we first normalized gene expression using the expression data of mice at day 0 (germfree state) and prefiltered all microarray data to remove genes that did hardly change across time-points and locations. Clustering of the prefiltered gene expression data resulted in 282 clusters of genes that show significant co-regulated changes. In order to find the genes that are most basal to the co-regulated changes in the clusters, a module map (Segal, Friedman et al. 2004) was created; 48 modules were found. Some of the modules contained genes that were co-regulated in a specific intestinal region or showed a separation in expression at early versus later time-points. Interestingly, one module included genes that were near-always down-regulated in colon and were differentially regulated at earlier versus later time-points in ileum and jejunum (Figure S2.10A). The differential expression was predicted to be dependent upon expression of the mitogen-activated protein kinase kinase kinase 9 (*Map3k9*) that regulates cell fate, and the extracellular protease inhibitor *Expi* (now named Psmc6 or proteasome (prosome, macropain) 26S subunit, ATPase, 6). *Expi* (*Psmc6*) is part of the immuno-proteasome, the protein degradation complex which main function is the processing of class I MHC peptides. Regulatory network analysis showed that in this module, expression of several other regulators (including two RIO kinases, melanoregulin Mreg and the DEAH box polypeptide 35 *Dhx35* that are all involved in cell differentiation) was dependent on the transcription factor hepatocyte nuclear factor 4 alpha (*Hnf4a*) (Figure S2.10B).
The prefiltered list of genes was then used to perform GO-enriched bayesian clustering and to identify significantly modulated GO categories (for more details see supplemented experimental procedures). 164 GO categories were significantly modulated in at least one microarray (Figure S2.4). The most strongly upregulated GO categories included immune system processes and cell differentiation, especially of immune cells (Figure S2.4). These categories contained sets of

genes including chemokines, transcription factors, cell surface markers, kinases, and structural proteins such as enzymes. Several immunity-related GO gene sets that were of particular interest to our research questions were then explored as shown in the main text.

SUPPLEMENTAL FIGURES

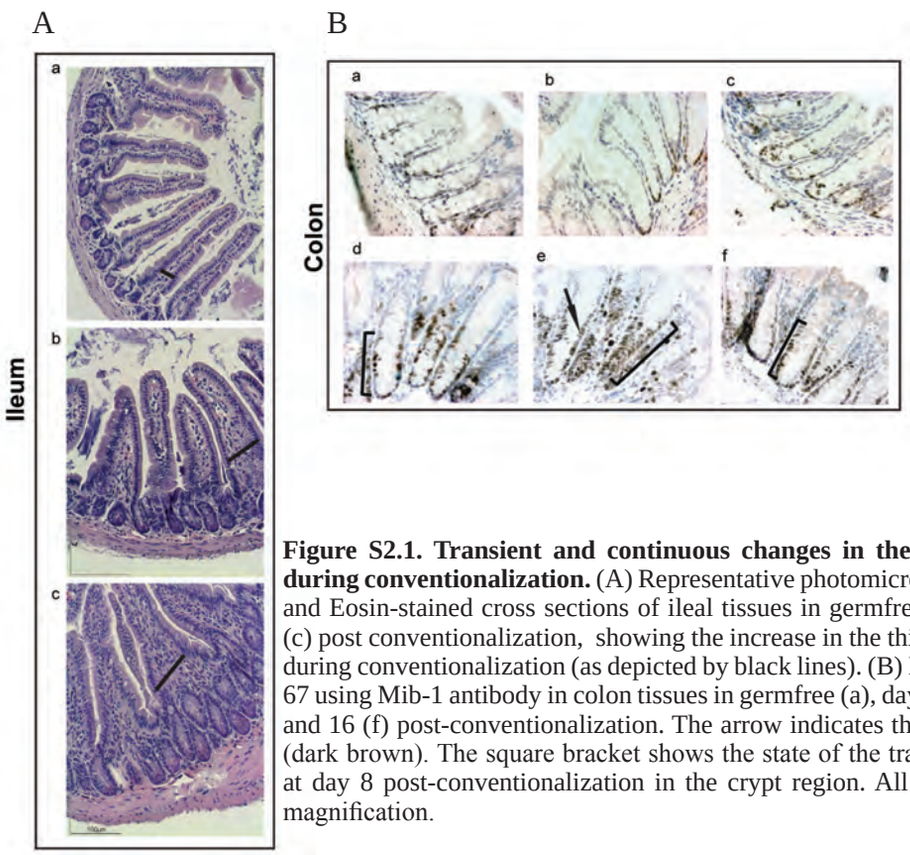

Figure S2.1. Transient and continuous changes in the intestinal morphology during conventionalization. (A) Representative photomicrographs of Haematoxylin and Eosin-stained cross sections of ileal tissues in germfree (a), days 4 (b), and 30 (c) post conventionalization, showing the increase in the thickness of lamina propria during conventionalization (as depicted by black lines). (B) IHC determination of Ki-67 using Mib-1 antibody in colon tissues in germfree (a), days 1 (b), 2 (c), 4 (d), 8 (e), and 16 (f) post-conventionalization. The arrow indicates the positively stained cells (dark brown). The square bracket shows the state of the transient crypt lengthening at day 8 post-conventionalization in the crypt region. All images are of the same magnification.

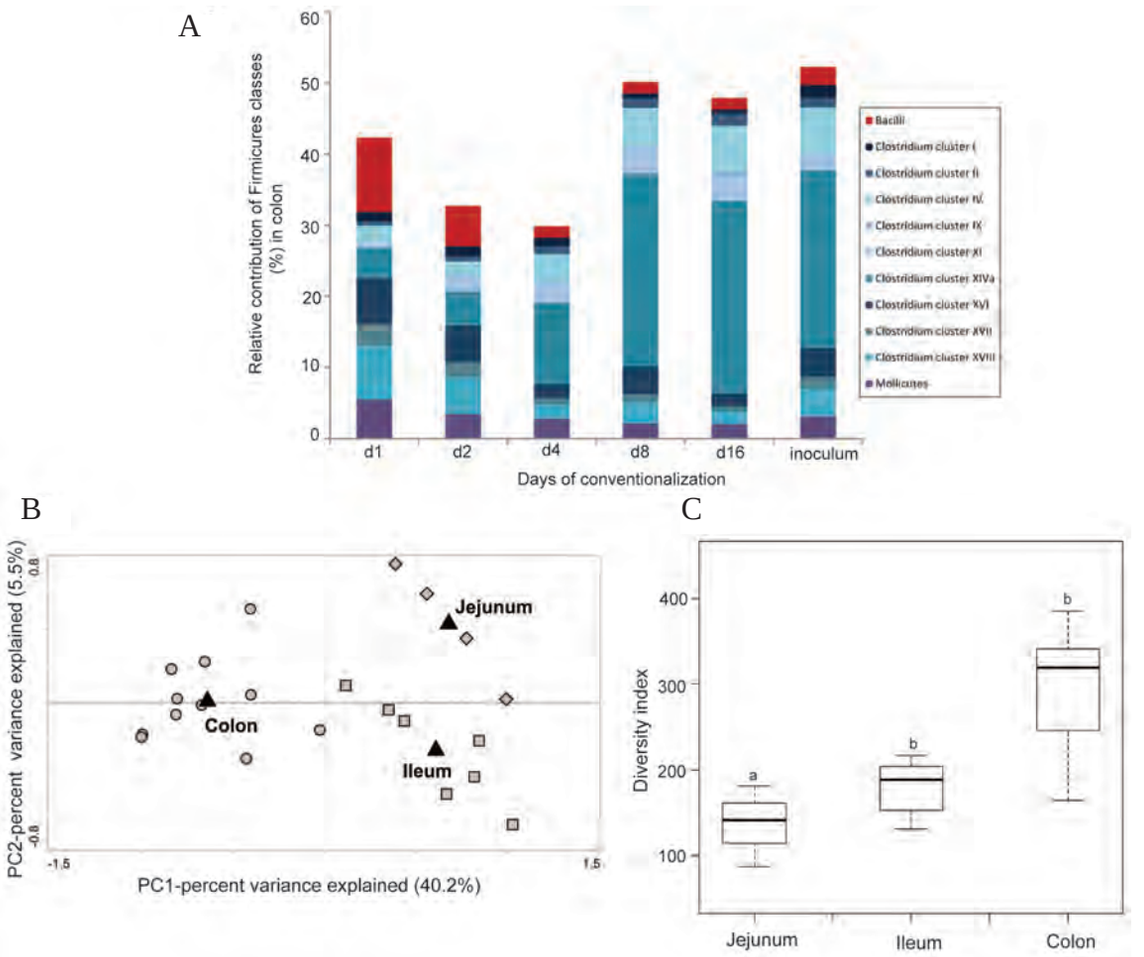

Figure S2.2. Temporal and local dynamics of the colonizing microbiota. (A) Relative contribution of the detected level 1 phylogenetic groups (Class- like) with Firmicutes (Bacilli, Clostridium clusters, and Mollicutes) with MITChip in colon samples over time. (B) RDA triplot representing the effect of intestinal locations on microbiota, projecting the averaged hybridization signals of 94 genus-like groups on the two canonical axes that had the highest explanatory potential (accounting for 39.3% of the total variance in the species). The intestinal locations are the environmental variables [(ileum (□), jejunum (♦), colon (•)], represented as centroids. Percentage values at the axes indicate contribution of the principal components to the explanation of the total variance of the species in the dataset. MCPP indicated that source of the sample (colon versus small intestine) had a significant effect of the intestinal microbiota composition (MCPP=0.001). (C) Diversity of the jejunum, ileum, and colon microbiota at days 8 and 16 post-conventionalization, expressed as Simpson index of the hybridization profiles analyzed by the MITChip.

Figure S2.3

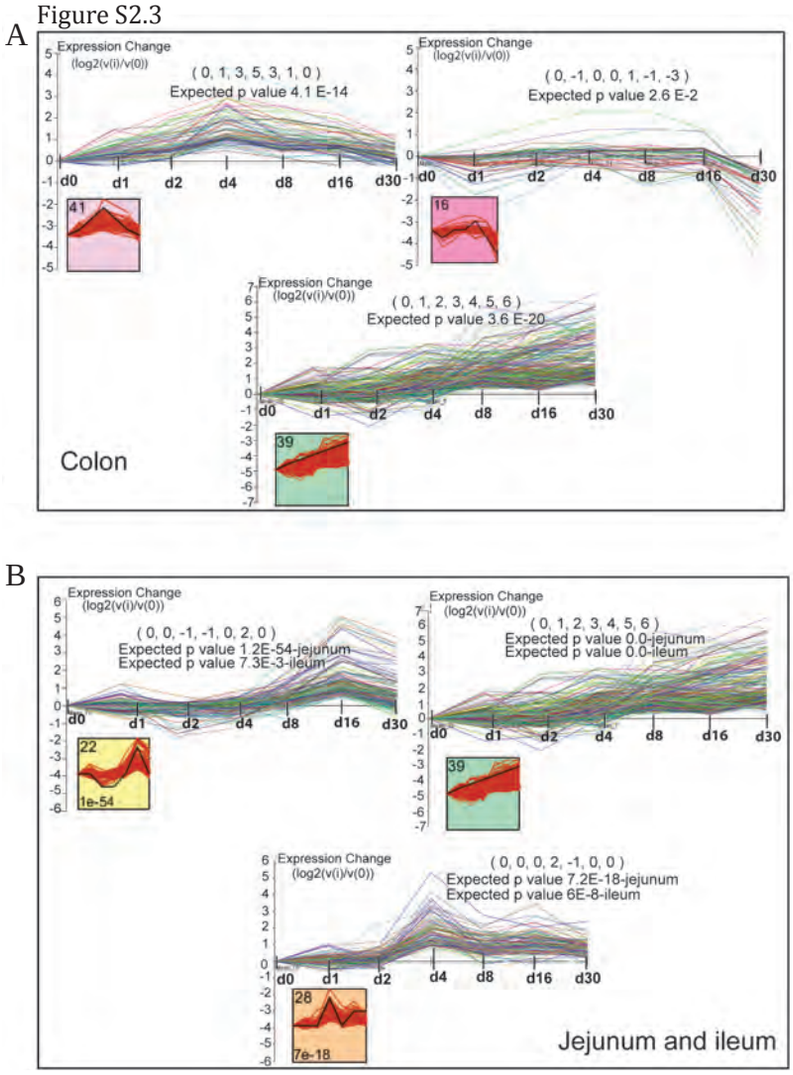

Figure S2.3. Comparison of the temporal expression profiles of genes associated with immune response. Screenshots of detailed model profile windows for the data of STEM. The profiles shown were those which had the majority of genes assigned for the GO "immune response". STEM filtered the input data (gene expression data for all genes) to find those genes that show significant differential expression across all time-points. All profiles were significant. Along the top of each window are the temporal expression patterns and the statistical analysis for the enrichment p-value based on the permutation test. The colored boxes at the bottom-left of each window correspond to the model expression profile available in STEM. The data is drawn from the response of colonic (A), jejunal and ileal (B) tissue to conventionalization.

Figure S2.4

Figure S2.4. Induction of immune system process during conventionalization. Graphical overview of GO enrichment categories (listed at the right of the graph) across all arrays (listed at the bottom part of the graph). A black square indicates that the indicated GO category was not significantly ($p < 0.05$) enriched; a color indicates that the GO category was enriched; a red square indicates that the respective pathway or process was induced; blue indicates that the pathway or process was repressed.

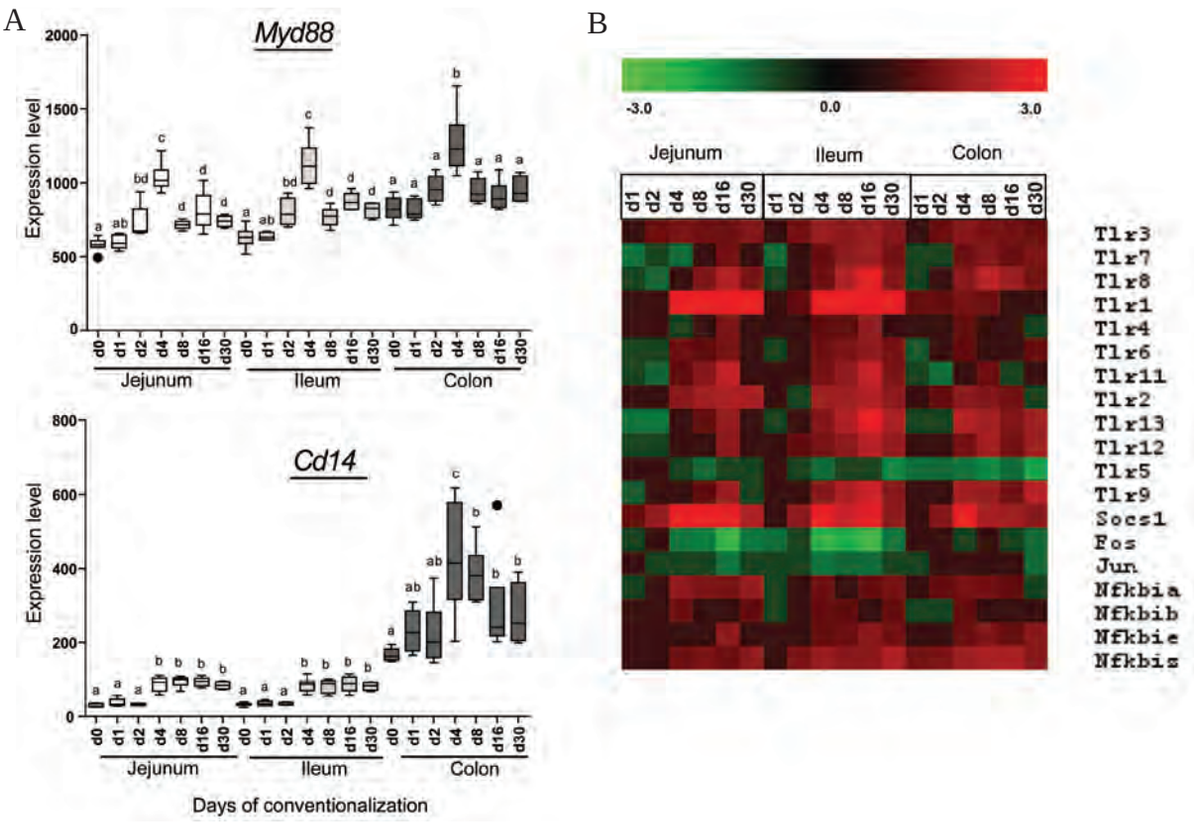

Figure S2.5. Modulation of bacterial recognition receptors and signaling pathways during conventionalization. (A) Jejunum, ileum, and colon gene expression levels of *Myd88* and *Cd14* were analyzed in germfree and conventionalized mice at indicated days post-conventionalization. Values are depicted as box-and whisker diagrams (top to bottom; maximum value, upper quartile, median, lower quartile, and minimal value, respectively). Any data not included between the whiskers is plotted as an outlier with a dot. Significant differences between time-points are indicated by distinctive characters above the measurement groups ($p < 0.05$). (B) Heat map of Toll-like receptors (*Tlr*) and their regulators representing the changes in their expression level at days 1, 2, 4, 8, 16, and 30 post-conventionalization in comparison to the germfree state.

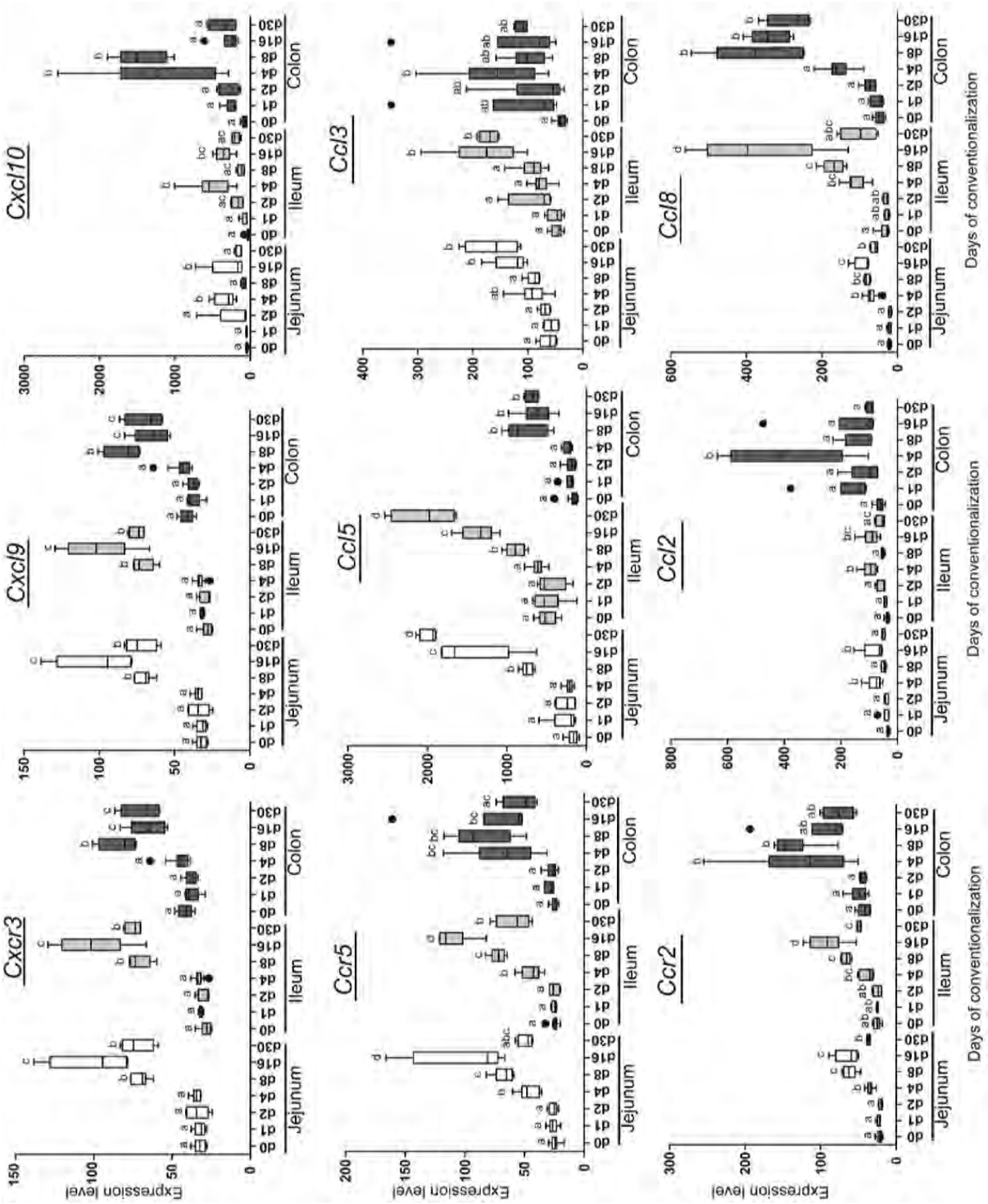

Figure S2.6. Microbial colonization results in region-specific regulation of chemokines. Jejunum, ileum, and colon gene expression levels of inflammatory chemokines and their receptors were analyzed in germfree and conventionalized mice at indicated days post-conventionalization. Values are depicted as box and whisker diagrams (top-to-bottom, maximum value, upper quartile, median, lower quartile, and minimal value, respectively). Any data not included between the whiskers is plotted as an outlier with a dot. Significant differences between time-points are indicated by distinctive characters above the measurement groups ($p < 0.05$).

A

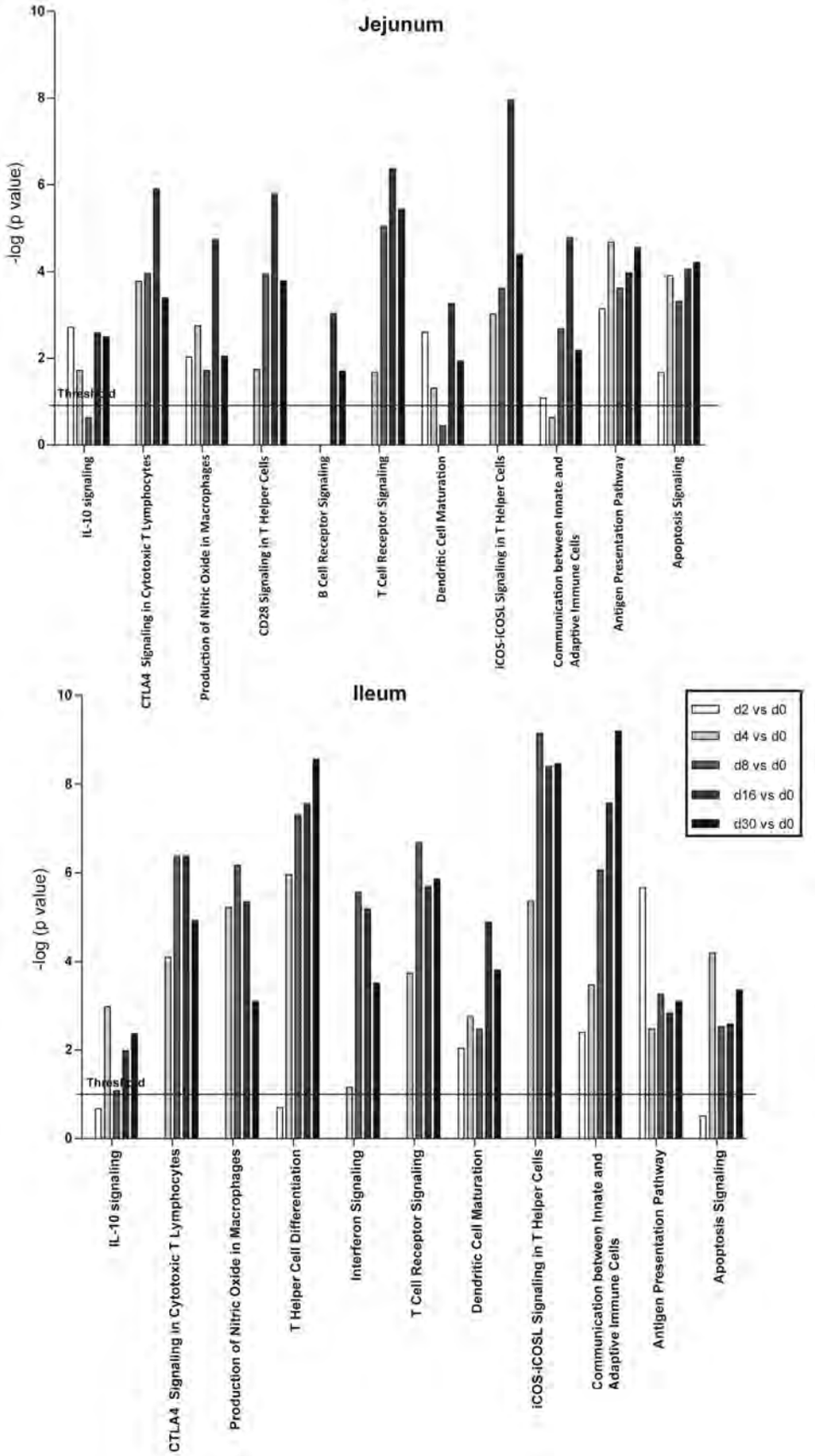
Jejunum
-log (p value)
10
8
6
4
2
0
Threshold
IL-10 signaling
CTLA4 Signaling in Cytotoxic T Lymphocytes
Production of Nitric Oxide in Macrophages
CD28 Signaling in T Helper Cells
B Cell Receptor Signaling
T Cell Receptor Signaling
Dendritic Cell Maturation
iCOS-iCOSL Signaling in T Helper Cells
Communication between Innate and Adaptive Immune Cells
Antigen Presentation Pathway
Apoptosis Signaling
Ileum
-log (p value)
10
8
6
4
2
0
Threshold
d2 vs d0
d4 vs d0
d8 vs d0
d16 vs d0
d30 vs d0
IL-10 signaling
CTLA4 Signaling in Cytotoxic T Lymphocytes
Production of Nitric Oxide in Macrophages
T Helper Cell Differentiation
Interferon Signaling
T Cell Receptor Signaling
Dendritic Cell Maturation
iCOS-iCOSL Signaling in T Helper Cells
Communication between Innate and Adaptive Immune Cells
Antigen Presentation Pathway
Apoptosis Signaling

B

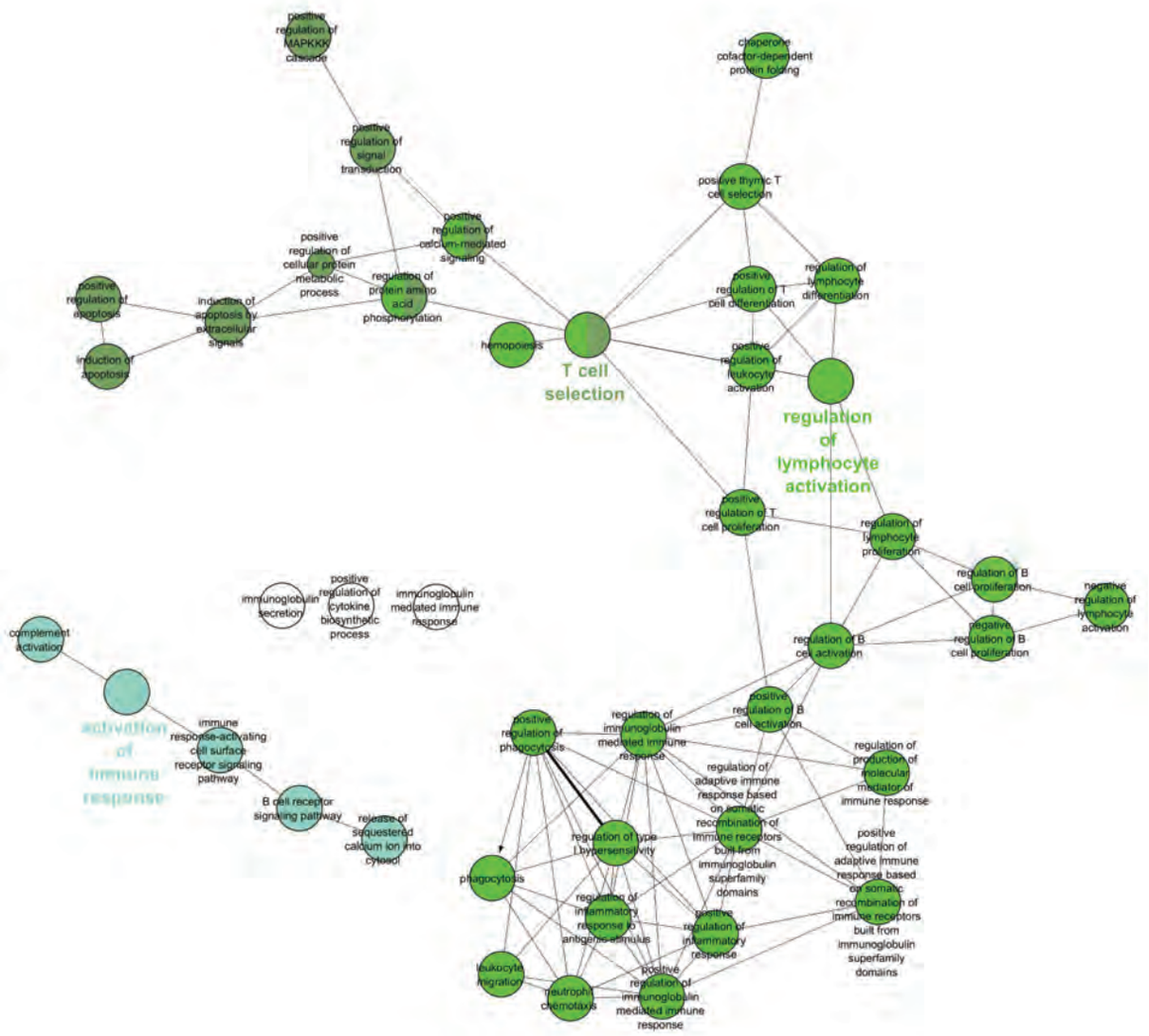
positive regulation of MAPKKK cascade
chaperone cofactor-dependent protein folding
positive regulation of signal transduction
positive thymic T cell selection
positive regulation of calcium-mediated signaling
positive regulation of cellular protein metabolic process
regulation of lymphocyte differentiation
positive regulation of apoptosis
induction of apoptosis by extracellular signals
regulation of protein amino acid phosphorylation
positive regulation of T cell differentiation
induction of apoptosis
hemopoiesis
T cell selection
positive regulation of leukocyte activation
regulation of lymphocyte activation
positive regulation of T cell proliferation
regulation of lymphocyte proliferation
regulation of B cell proliferation
negative regulation of lymphocyte activation
immunoglobulin secretion
positive regulation of cytokine biosynthetic process
immunoglobulin mediated immune response
negative regulation of B cell proliferation
regulation of B cell activation
complement activation
positive regulation of B cell activation
regulation of immunoglobulin mediated immune response
positive regulation of phagocytosis
activation of immune response
immune response-activating cell surface receptor signaling pathway
regulation of production of molecular mediator of immune response
regulation of adaptive immune response based on somatic recombination of immune receptors built from immunoglobulin superfamily domains
B cell receptor signaling pathway
release of sequestered calcium ion into cytosol
regulation of type I hypersensitivity
phagocytosis
positive regulation of adaptive immune response based on somatic recombination of immune receptors built from immunoglobulin superfamily domains
regulation of inflammatory response to antigenic stimulus
positive regulation of inflammatory response
leukocyte migration
neutrophil chemotaxis
positive regulation of immunoglobulin mediated immune response

C

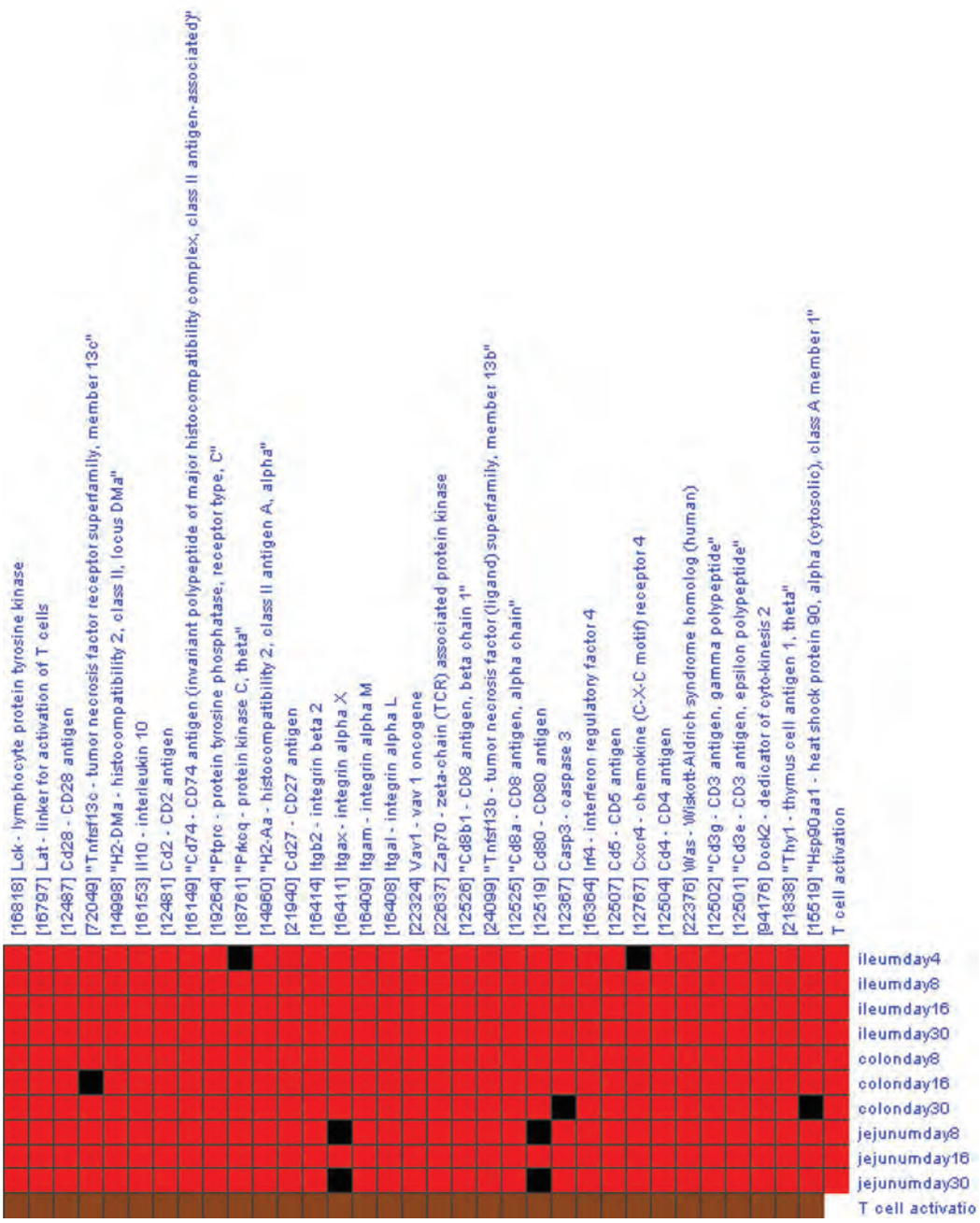

Figure S2.7. Enriched biological functions and pathways modulated during mouse conventionalization.
(A) Cellular pathways significantly modulated in the jejunum and ileum during conventionalization was calculated via a one-tailed Fisher's Exact test in IPA and represented as -log (p value); -log values exceeding 1.30 were significant ($p < 0.05$). (B) Cytoscape graph showing the interrelationships between GO categories. Representation of the GO subcategories belonging to the major enriched GO category "Immune response" that was identified using Genomica software. Here, the nodes indicate GO subcategories, and the edges between nodes indicate that nodes are interrelated (the GO system is hierarchical). The network shows that the major GO categories within the "Immune response" category correspond to the biological processes "T cell selection", "regulation of lymphocyte activation" and "activation of the immune response". (C) Gene list for the enriched GO category "T cell activation" that was identified using Genomica software. The genes are listed at the top of the graph, and the arrays on which the respective genes were significantly induced (squares in red) are indicated to the right of the graph. Black squares indicate that a gene was not significantly expressed on the respective array.

A

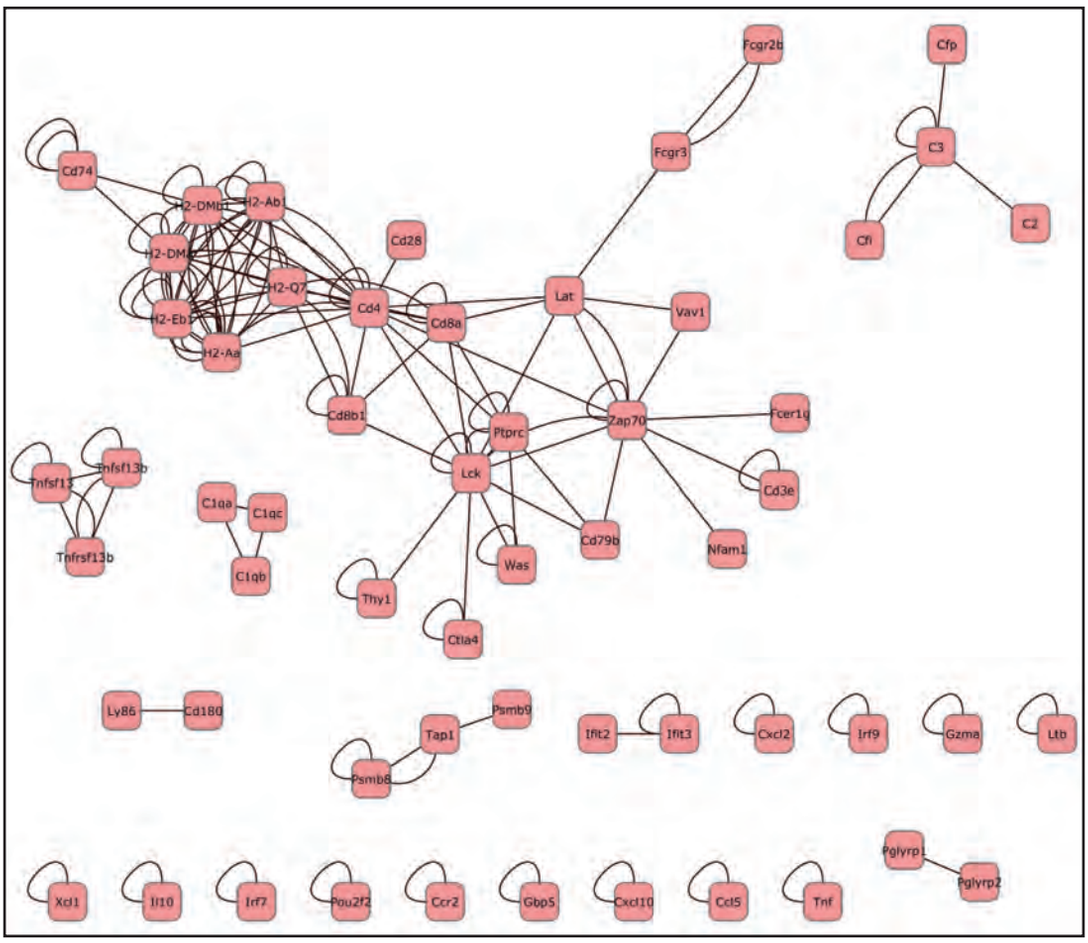
Fcgr2b
Cfp
Fcgr3
C3
Cd74
H2-DMb1
H2-Ab1
Cfi
C2
Cd28
H2-DMa
H2-Q7
Lat
Vav1
Cd4
Cd8a
H2-Eb1
H2-Aa
Cd8b1
Ptprc
Zap70
Fcer1g
Tnfsf13
Tnfsf13b
Lck
Cd3e
C1qa
C1qc
Tnfrsf13b
Cd79b
Nfam1
Was
C1qb
Thy1
Ctla4
Ly86
Cd180
Psmb9
Tap1
Ifit2
Ifit3
Cxcl2
Irf9
Gzma
Ltb
Psmb8
Pglyrp1
Pglyrp2
Xcl1
Il10
Irf7
Pou2f2
Ccr2
Gbp5
Cxcl10
Ccl5
Tnf

B

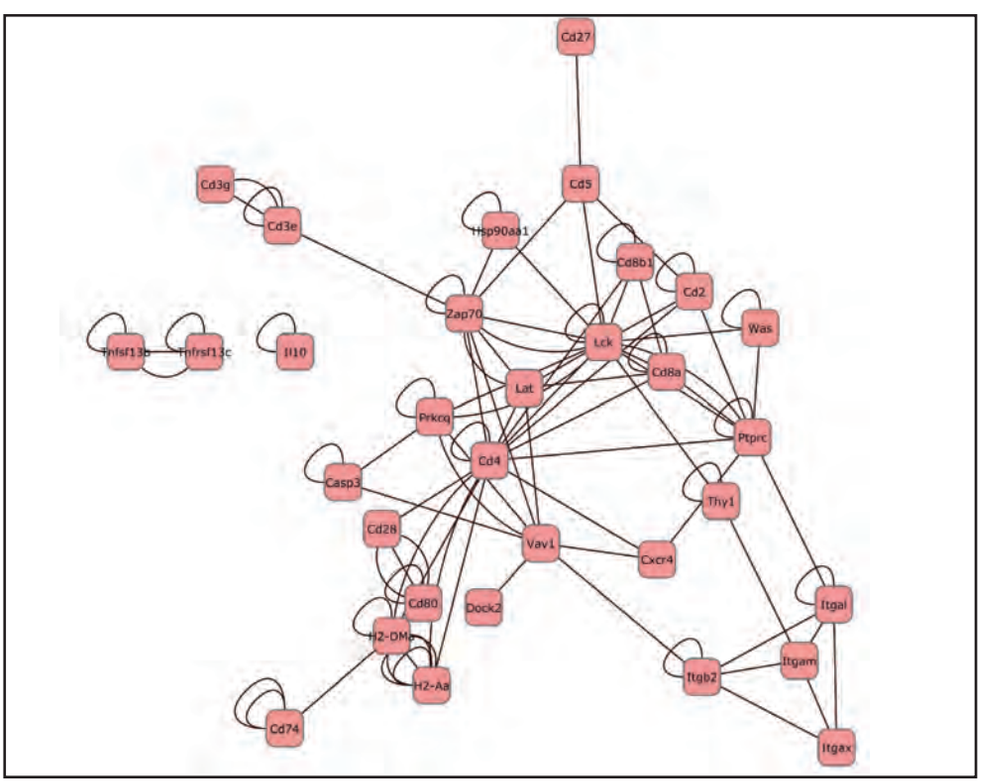
Cd27
Cd3g
Cd5
Cd3e
Hsp90aa1
Cd8b1
Cd2
Zap70
Was
Tnfsf13b
Tnfrsf13c
Il10
Lck
Cd8a
Lat
Prkcq
Ptprc
Cd4
Casp3
Thy1
Cd28
Vav1
Cxcr4
Cd80
Dock2
Itgal
H2-DMa
Itgam
Itgb2
H2-Aa
Cd74
Itgax

C

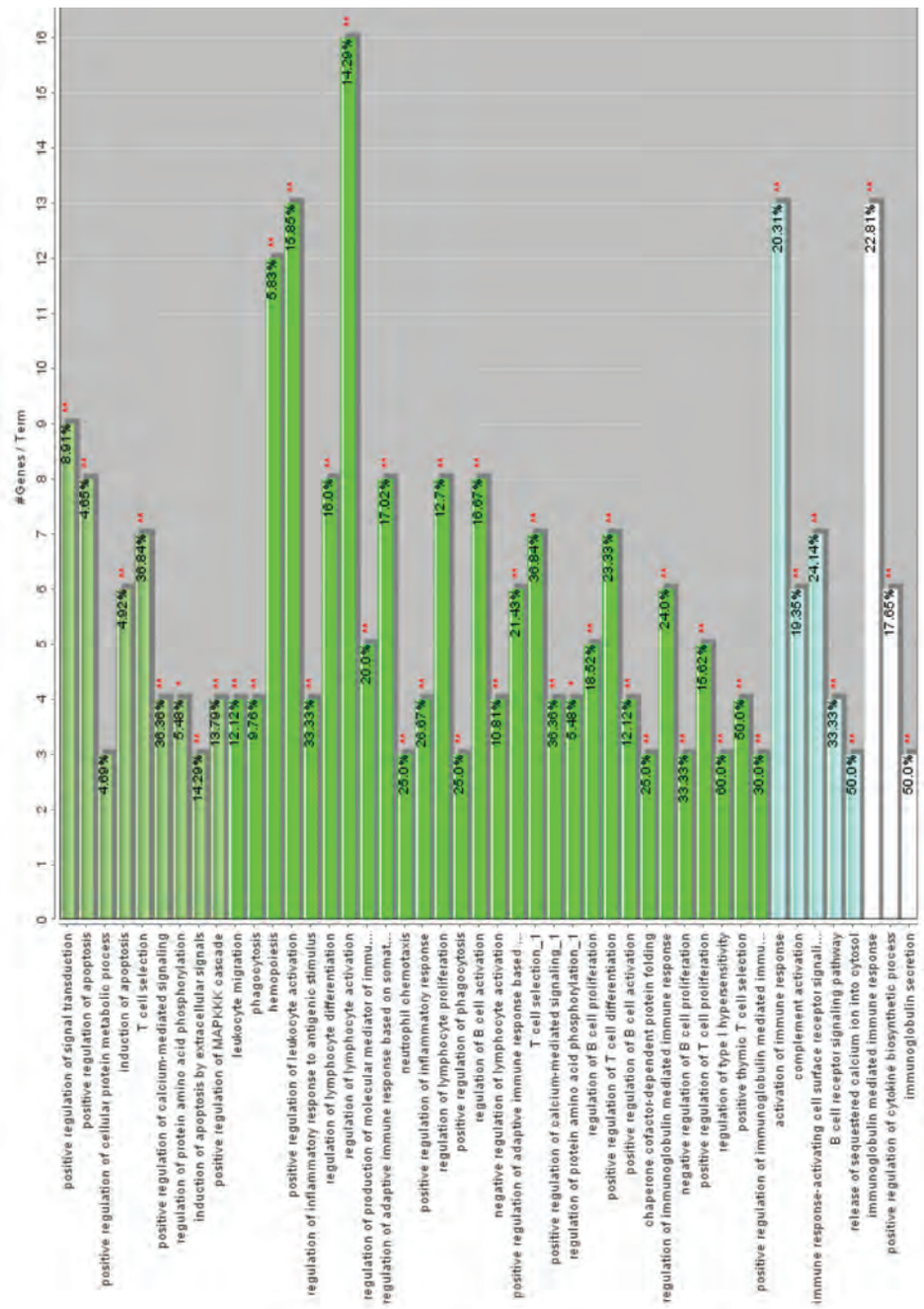

Figure S2.8. Protein-protein interaction networks representing the enriched GO categories "immune response" and "T cell activation". (A) Cytoscape protein-protein interaction (PPI) map of the GO category "Immune response" that was significantly enriched across all arrays, calculated using Genomica. Here, nodes indicate proteins and edges between nodes indicate a functional relationship between the nodes, e.g. protein-protein binding or phosphorylation. Note the similarity between the genes included in this network and the genes included in the network shown in Figure 2.7, although both networks were calculated by two very different methods. (B) Cytoscape PPI network for the significantly induced genes belonging to the GO category "T cell activation". Gene induction significance was calculated using Genomica software. (C) Statistics for the GO category "immune response". Bar height corresponds to the number of genes annotated with the respective GO term; the % corresponds to the number of genes from the dataset belonging to a GO term relative to the total number of genes in the human genome that were annotated with that GO term. The asterisks represent Fisher's exact statistics; * corresponds to $p < 0.05$, and ** corresponds to $p < 0.001$.

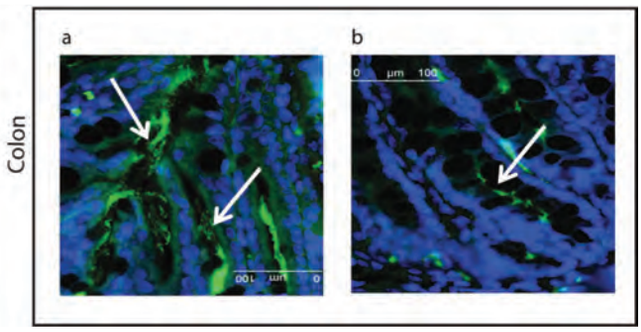

Figure S2.9. Transient intense microbiota-host epithelium contact during conventionalization. Fluorescent in situ hybridization (FISH) in mouse colonic sections with the bacterial universal probe EUB338. The colon exhibits microbiota in close proximity to the epithelia and goblet cells (as depicted by white arrows) at day 4 (a) which was remarkably reduced at day 8 post-conventionalization (b).

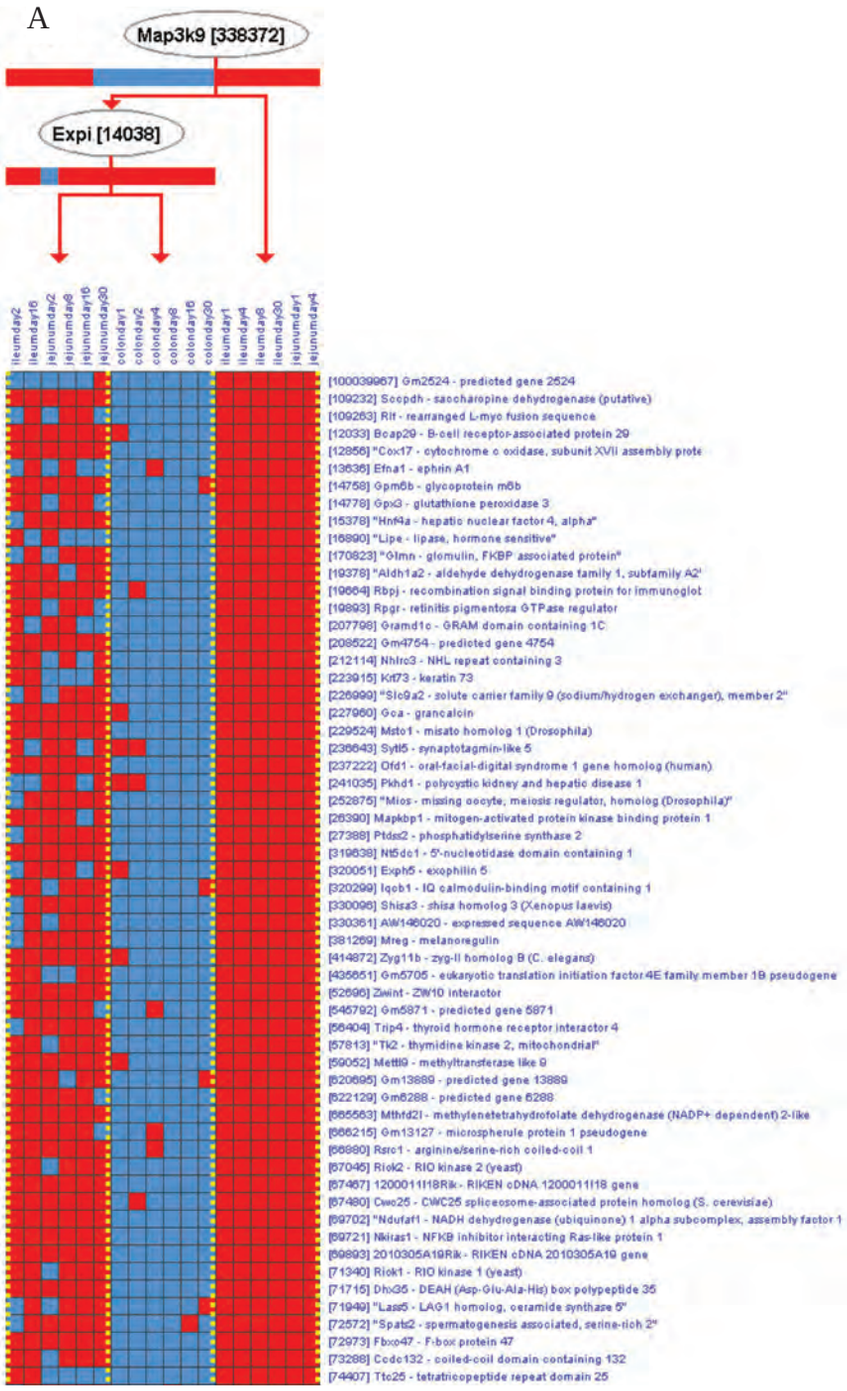

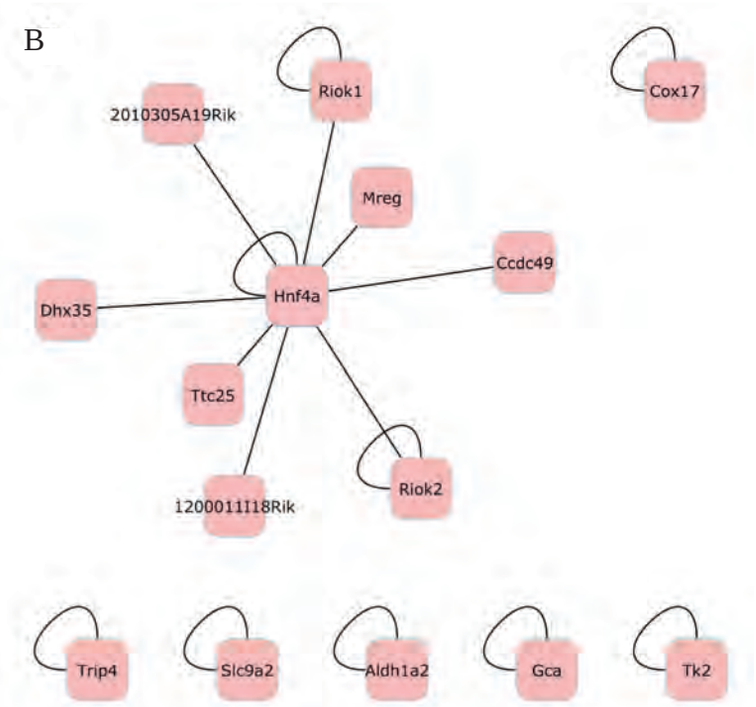

Figure S2.10. Differential expression of genes belonging to a Genomica module, predicted to be driven by the genes *Map3k9* and *Expi.* (A) The graph lists genes (at the right) that are induced (indicated by red squares) or repressed (blue squares) on the arrays that are listed at the top of the graph. The yellow interrupted lines separate groups of arrays that show significantly ($p < 0.05$) distinct expression patterns. The *Map3k9* gene encoding a mitogen-activated protein kinase (3) member 9 was predicted to determine the complete induction (rightmost) or induction or repression (leftmost and central group) of the set of genes listed at the right of the graph. The *Expi* gene, encoding a extracellular proteinase inhibitor, was predicted to determine the induction-repression pattern (leftmost) or the near-complete repression (middle) of the same set of genes. Note that the central group corresponds to microarrays that measured gene expression in the colon, whereas the left- and rightmost groups correspond to arrays from the small intestine. This graph shows a set of genes that were repressed in the colon and much more often induced in the small intestine, thereby exemplifying location- and time-specific gene expression patterns. (B) The corresponding PPI network belonging to the genes listed in (A). This PPI network shows that the transcription factor *Hnf4a* was in the center of a small gene regulatory network that also included two Rio kinases (*Riok1, 2*) that are involved in ribosome biogenesis and cell cycle progression.

References

Abraham, C. and J. H. Cho (2009). "Mechanisms of disease. Inflammatory bowel disease." New England Journal of Medicine **361**(21): 2066-2078.

Ashburner, M., C. A. Ball, et al. (2000). "Gene Ontology: tool for the unification of biology." Nature Genetics **25**(1): 25-29.

Atarashi, K., T. Tanoue, et al. (2011). "Induction of Colonic Regulatory T Cells by Indigenous Clostridium Species." Science **331**(6015): 337-341.

Baumgart, D. C. and S. R. Carding (2007). "Gastroenterology 1 - Inflammatory bowel disease: cause and immunobiology." Lancet **369**(9573): 1627-1640.

Bogomoletz, W. V., G. T. Williams, et al. (1987). "High iron diamine-alcian blue and histochemistry of mucins in colic diseases-20 years later." Gastroenterologie Clinique Et Biologique **11**(12): 865-868.

Bolstad, B. M., F. Collin, et al. (2004). Experimental design and low-level analysis of microarray data. DNA Arrays in Neurobiology, Vol 60. M. F. Miles. **60:** 25-58.

Bouma, G. and W. Strober (2003). "The immunological and genetic basis of inflammatory bowel disease." Nature Reviews Immunology **3**(7): 521-533.

Chen, G., M. H. Shaw, et al. (2009). NOD-Like Receptors: role in innate immunity and inflammatory disease. Annual Review of Pathology-Mechanisms of Disease. **4:** 365-398.

Cherbuy, C., E. Honvo-Houeto, et al. (2010). "Microbiota matures colonic epithelium through a coordinated induction of cell cycle-related proteins in gnotobiotic rat." American Journal of Physiology-Gastrointestinal and Liver Physiology **299**(2): G348-G357.

Dai, M. H., P. L. Wang, et al. (2005). "Evolving gene/transcript definitions significantly alter the interpretation of GeneChip data." Nucleic Acids Research **33**(20).

de Hoon, M. J. L., S. Imoto, et al. (2004). "Open source clustering software." Bioinformatics **20**(9): 1453-1454.

DeJarnette, J. B., C. L. Sommers, et al. (1998). "Specific requirement for CD3 epsilon in T cell development." Proceedings of the National Academy of Sciences of the United States of America **95**(25): 14909-14914.

Deplancke, B. and H. R. Gaskins (2001). "Microbial modulation of innate defense: goblet cells and the intestinal mucus layer." American Journal Of Clinical Nutrition **73**(6): 1131S-1141S.

Deretic, V. and B. Levine (2009). "Autophagy, immunity, and microbial adaptations." Cell Host & Microbe **5**(6): 527-549.

Ernst, J. and Z. Bar-Joseph (2006). "STEM: a tool for the analysis of short time series gene expression data." BMC Bioinformatics **7**: 191.

Falk, P. G., L. V. Hooper, et al. (1998). "Creating and maintaining the gastrointestinal ecosystem: What we know and need to know from gnotobiology." Microbiology And Molecular Biology Reviews **62**(4): 1157-1170.

Fijneman, R. J. A., J. R. Peham, et al. (2008). "Expression of Pla2g2a prevents carcinogenesis in Muc2-deficient mice." Cancer Science **99**(11): 2113-2119.

Fujio, K., T. Okamura, et al. (2010). The Family of IL-10-Secreting CD4(+) T Cells. Advances in Immunology **105:** 99-130.

Gaboriau-Routhiau, V., S. Rakotobe, et al. (2009). "The key role of segmented filamentous bacteria in the coordinated maturation of gut helper T cell responses." Immunity **31**(4): 677-689.

Gentleman RC, C. V., Bates DM, Bolstad B, Dettling M, Dudoit S, Ellis B, Gautier L, Ge Y, Gentry J, Hornik K, Hothorn T, Huber W, Iacus S, Irizarry R, Leisch F, Li C, Maechler M, Rossini AJ, Sawitzki G, Smith C, Smyth G, Tierney L, Yang JY, Zhang J. (2004). "Bioconductor: open software development for computational biology and bioinformatics." Genome Biol. **5**(10:R80).

Geuking, M. B., J. Cahenzli, et al. (2011). "Intestinal Bacterial Colonization Induces Mutualistic Regulatory T Cell Responses." Immunity **34**(5): 794-806.

Geurts L, V. Lazarevic , et al (2011). "Altered gut microbiota and endocannabinoid system tone in obese and diabetic leptin-resistant mice: impact on apelin regulation in adipose tissue." Frontiers in Cellular and Infection Microbiology.

Hayden, M. S. and S. Ghosh (2008). "Shared principles in NF-kappa B signaling." Cell **132**(3): 344-362.

Heber, S. and B. Sick (2006). "Quality assessment of affymetrix GeneChip data." Omics-a Journal of Integrative Biology **10**(3): 358-368.

Hori, S., T. Nomura, et al. (2003). “Control of regulatory T cell development by the transcription factor Foxp3.” Science **299**(5609): 1057-1061.

Irizarry, R. A., B. M. Bolstad, et al. (2003). “Summaries of affymetrix GeneChip probe level data.” Nucleic Acids Research **31**(4).

Ivanov, I. I., K. Atarashi, et al. (2009). “Induction of Intestinal Th17 Cells by Segmented Filamentous Bacteria.” Cell **139**(3): 485-498.

Johnson, W. E., C. Li, et al. (2007). “Adjusting batch effects in microarray expression data using empirical Bayes methods.” Biostatistics **8**(1): 118-127.

Krimi, R. B., L. Kotelevets, et al. (2008). “Resistin-like molecule beta regulates intestinal mucous secretion and curtails TNBS-induced colitis in mice.” Inflammatory Bowel Diseases **14**(7): 931-941.

Lee, Y. K. and S. K. Mazmanian (2010). “Has the microbiota played a critical role in the evolution of the adaptive immune system?” Science **330**(6012): 1768-1773.

Lin, K., H. Kools, et al. (2011). “MADMAX – Management and analysis database for multiple ~omics experiments.” Journal of integrative bioinformatics **8**(2): 160.

Linden SK, S. P., Karlsson NG, Korolik V, McGuckin MA. (2008). “Mucins in the mucosal barrier to infection.” Mucosal Immunol. **1**(3): 183-197.

Macpherson, A. J. and N. L. Harris (2004). “Interactions between commensal intestinal bacteria and the immune system.” Nature Reviews Immunology **4**(6): 478-485.

Miller, S. A. and A. S. Weinmann (2010). “Molecular mechanisms by which T-bet regulates T-helper cell commitment.” Immunological Reviews **238**: 233-246.

Rajilic-Stojanovic, M., H. G. H. J. Heilig, et al. (2009). “Development and application of the human intestinal tract chip, a phylogenetic microarray: analysis of universally conserved phylotypes in the abundant microbiota of young and elderly adults.” Environmental Microbiology **11**(7): 1736-1751.

Saeed, A. I., N. K. Hagabati, et al. (2006). TM4 microarray software suite. Methods Enzymology. **411:** 134-193.

Sansonetti, P. J. and J. P. Di Santo (2007). “Debugging how bacteria manipulate the immune response.” Immunity **26**: 149-161.

Sartor, M. A., C. R. Tomlinson, et al. (2006). “Intensity-based hierarchical Bayes method improves testing for differentially expressed genes in microarray experiments.” Bmc Bioinformatics **7**:538.

Schroder, K., P. J. Hertzog, et al. (2004). “Interferon-gamma: an overview of signals, mechanisms and functions.” Journal of Leukocyte Biology **75**(2): 163-189.

Segal, E., N. Friedman, et al. (2004). “A module map showing conditional activity of expression modules in cancer.” Nature Genetics **36**(10): 1090-1098.

Simpson, E. H. (1949). “MEASUREMENT OF DIVERSITY.” Nature **163**(4148): 688-688.

Storey, J. D. and R. Tibshirani (2003). “Statistical significance for genomewide studies.” Proceedings of the National Academy of Sciences of the United States of America **100**(16): 9440-9445.

Suzuki, M. T., L. T. Taylor, et al. (2000). “Quantitative analysis of small-subunit rRNA genes in mixed microbial populations via 5 ‘-nuclease assays.” Applied and Environmental Microbiology **66**(11): 4605-4614.

Valbuena, G., W. Bradford, et al. (2003). “Expression analysis of the T-cell-targeting chemokines CXCL9 and CXCL10 in mice and humans with endothelial infections caused by rickettsiae of the spotted fever group.” American Journal of Pathology **163**(4): 1357-1369.

West, A. P., A. A. Koblansky, et al. (2006). Recognition and signaling by toll-like receptors. Annual Review of Cell and Developmental Biology. **22:** 409-437.

Wilson, C. L., A. J. Ouellette, et al. (1999). “Regulation of intestinal alpha-defensin activation by the metalloproteinase matrilysin in innate host defense.” Science **286**(5437): 113-117.

Zhu, Y., S. Yao, et al. (2011). “Cell surface signaling molecules in the control of immune responses: a tide model.” Immunity **34**(4): 466-478.

Chapter 3

Molecular Dynamics of Microbiota Sensing in the Mouse Jejunal Mucosa during Conventionalization Support a Prominent Role of the Jejunum in Systemic Metabolic Control

Sahar El Aidy, Claire A. Merrifield, Muriel Derrien, Peter van Baarlen, Guido Hooiveld, Florence Levenez, Joël Doré, Jan Dekker, Elaine Holmes, Sandrine P. Claus, Dirk-Jan Reijngoud, and Michiel Kleerebezem

Submitted

ABSTRACT

Proper interactions between the intestinal mucosa, gut microbiota, and nutrient flow are relevant to establish homeostasis of overall host physiology, immune status, and metabolism. Since the proximal part of the small intestine is the first region where these interactions take place, it is important to understand the molecular dynamics of metabolic responses in the mucosa of this region.

Combined transcriptome, histological, ^{1}H NMR metabonomics, and microbiota analyses in ex-germfree mice highlighted the acute response of jejunal mucosa to the microbiota after only 1 day of conventionalization. These acute responses led to major altered gene expression and metabolic profiles after 4 days of conventionalization upon which a novel, permanent homeostatic state was established. These secondary responses included a drastic transcriptome shift in genes that control the rate of key metabolic pathways, including fatty acid oxidation, glycolysis, gluconeogenesis, amino acid, and nucleotide metabolism. The transcriptional changes in metabolic pathways could be confirmed at the mucosal tissue metabolite level. Detailed transcriptomic analysis throughout the 30-day period of conventionalization identified a central regulatory network that appears to be involved in dynamic control of the reorientation of the metabolic response to the colonizing microbiota in the jejunal mucosa. The majority of the genes in the identified network participate in human metabolic disorders, including insulin sensitivity and type 2 diabetes mellitus. These results illustrate the molecular dynamics of microbiota sensing by the mouse jejunal mucosa, and support a prominent role of the jejunum in systemic metabolic control, including glucose homeostasis.

INTRODUCTION

The gut microbiota is recognized as a key determinant in the regulation of host metabolism including energy harvest from the diet and fat storage (Bäckhed and Crawford 2010). A large proportion of the microbiota metabolism is beneficial to the host and contributes to its nutritional demand by supplying essential nutrients. The microbiota can also convert and neutralize potentially harmful metabolites from the dietary flow and enhance energy harvest from the diet (Bäckhed, Ley et al. 2005). For example, the gut microbiota modulates the absorption of dietary lipids (Bäckhed, Ley et al. 2005), affects glucose absorption (Bäckhed, Ding et al. 2004), and metabolizes indigestible polysaccharides to absorbable nutrients including monosaccharides and short chain fatty acids (SCFAs) (Hooper, Midtvedt et al. 2002). It is now firmly established that the gut microbiota has a major impact on the host phenotype in humans and mice (Bäckhed, Ding et al. 2004; Dumas, Barton et al. 2006; Turnbaugh, Ley et al. 2006). In a pioneering study by Bäckhed and colleagues, it was shown that conventionalization of adult germfree C57 BL/6 J mice with a normal mouse microbiota leads to a nearly 60% increase in body fat content and insulin resistance within 14 days, despite a reduced food intake (Bäckhed, Ding et al. 2004). This study showed that suppression of Fasting-induced adipocyte factor (*Fiaf*, or *Angptl4*) is essential for the induction of *de novo* hepatic lipogenesis, which is triggered by the induction of elevated absorption of monosaccharides such as glucose from the gut lumen and is a prominent factor in obesity (Bäckhed, Ding et al. 2004). Subsequent studies in ex-germfree mice revealed the important roles of SCFA- and endocrine hormone-binding G–protein coupled receptors, Gpr41 and 43, in microbial modulation of host energy balance (Tilg and Kaser 2011). Notwithstanding the recognition of the crucial importance of host-microbiota interaction in controlling metabolic changes in the intestinal mucosa, these insights are mainly derived from studies focused on the ileal or colonic intestinal tissues in studies comparing germfree, and conventional, or conventionalized ex-germfree mice. However, the impact of the microbiota on metabolism in more proximal parts of the small intestine (such as the jejunum), has so far remained largely unexplored. The relatively diminutive microbial community residing in this intestinal region may have been the rationale behind the lack of interest in this region in terms of host-microbe communication. The luminal microbiota encompasses 10^3-10^7 bacterial cells per gram in the human jejunum (O'Hara and Shanahan 2006), and comprises a relatively simple community that is dominated by aerotolerant microbial species like the streptococci and other members of the bacilli (Hayashi, Takahashi et al. 2005). The role of the jejunum as an intestinal region that controls systemic metabolic responses is illustrated by the observation that gastric bypass surgery, which allows nutrients to bypass the duodenum and proximal small bowel (Rubino, Moo et al. 2009), leads to improvement or resolution of type 2 diabetes in both obese and non-obese individuals. Gastric bypass surgery ensures the persistence of normal concentrations of plasma glucose and insulin in 80–100% of the cases (Rubino 2006). Although the mechanisms underlying the increased insulin sensitivity following gastric bypass surgery remain obscure, changes in lipid metabolism (Williams, Hagedorn et al. 2007), intestinal gluconeogenesis (Troy, Soty et al. 2008), as well as altered secretion of gut hormones (Korner, Bessler et al. 2005), have been suggested to be involved.

Recently, we described the molecular dynamics of host immune response development in ex-germfree mice upon conventionalization in different regions of the GI tract, over a time-span of 30 days (Chapter 2). This study illustrated the prominent responsiveness of the jejunal mucosa to the colonizing microbiota. Therefore, the current study focuses on this intestinal region,

and employs tissue-transcriptome, tissue-metabonome (^{1}H NMR), and microbiota profiling, in combination with histological analysis, to improve our understanding of the molecular dynamics involved in microbiota-mediated control of jejunal metabolism. Our findings demonstrate that the mouse jejunum has a unique sensory role in monitoring the luminal microbiota-diet interplay. The results showed that one day of microbial colonization of germfree mice induced an acute and transient response in the jejunal mucosa that was followed by a secondary response starting on day 4 post-conventionalization. After four days, gene metabolic profiles and metabolic fluxes suggested that the original homeostasis representing the germfree state had been replaced by a novel state of homeostasis that appeared to be established and sustained throughout the 30-day period of conventionalization. Detailed mining of the jejunal transcriptomes during the 30-days of conventionalization allowed the reconstruction of a core gene-regulatory network that is proposed to govern the jejunal metabolic changes in response to the colonizing microbiota. Of the genes encompassed in the network, 26 % is reported to play a role in glucose homeostasis and insulin control, indicating that this network with its core regulatory nodes could be used to further improve our understanding on the genetic regulation involved in type 2 diabetes development.

RESULTS

Conventionalization Elicits Early and Late-Adjustments in Jejunal Tissue Morphology

This study comprised three independent experiments aimed to identify the dynamics of jejunal mucosal changes in germfree and conventionalized mice. The jejunal mucosal response to conventionalization characteristically proceeded through two distinct phases: an early (acute) response at day 1 post-conventionalization that is associated with transient alterations in secretory cell-lineages and repression of nuclear receptors involved in the regulation of gut hormones and fatty acid metabolism, and a second response at four days post-conventionalization that is characterized by persistent changes in pathways involved in energy and anabolic metabolism.

At one day post-conventionalization, the colonizing microbiota had induced acute changes in the secretory cell-lineages within the jejunal tissues (Figure 3.1). The most distinguishable morphological change in the secretory cells on day 1 post-conventionalization (and to a lesser extent day 2 post-conventionalization) was the increase (approximately 40%, $p < 0.05$ as compared to the germfree state) in the number of swollen, mucin-filled goblet cells in the villus epithelia that were detected by Alcian blue (AB-PAS) staining. Extending the conventionalization period to four days led to an overall decrease of goblet cells that stained only weakly and appeared to be smaller with a more columnar morphology as compared to days 1 and 2 post-conventionalization. This change in morphology was transient since the number of large, mucin-filled goblet cells recovered to a level that slightly exceeded that of germfree mice from day 16 post-conventionalization onward (Figure 3.1).

Response to Danger Signals Dominates the Acute Transcriptional Response in Jejunal Tissue

Ingenuity Pathways Analysis (IPA) (www.ingenuity.com) was employed to further elucidate the cellular functions and signaling pathways involved in the acute responses of the jejunal mucosa. The first day post-conventionalization was most prominently associated with the induction of tissue damage response pathways, e.g., the P2Y pyrogenic receptor and HMGB1 signaling pathways, as well as the repression of pathways involved in regulation of cell cycle control,

e.g., Notch and P53 signaling pathways (Figure 3.2A).
To further investigate the genes and pathways underlying this acute jejunal response, the day 1 post-conventionalization transcriptomes were compared to those of the control animals (germfree). Short term conventionalization led to an immediate repression of genes encoding enteroendocrine hormones, including cholecystokinin (*Cck*), pancreatic and duodenal homeobox 1 (*Pdx1*), gastric inhibitory peptide (*Gip*), and ghrelin (*Ghrl*) (Figure 3.2B). These changes coincided with the reduced expression of several Notch pathway genes, including the Notch gene homologue 1 *(Notch1)*, the hairy and enhancer of split 1 (*Hes1)*, and neurogenin 3 (*Neurog3)*, but not the atonal homolog 1 *(Atoh1)*, (Figure S3.1A).
Short term conventionalization also elicited a strong repression of specific metabolic function-encoding genesets, such as genes involved in complex I of the oxidative phosphorylation pathway (Figure S3.1B) and the fumarate hydratase gene (*Fh1*) involved in the citrate cycle (TCA), which converts fumarate to malate and is known as a tumor suppression gene. Taken together, the transcriptional changes that characterized the acute phase of conventionalization (day 1 post-conventionalization) in jejunal tissues suggest an early response to danger signals which could be endogenous or derived from the microbiota, its metabolites, and its interaction with nutrient flow or both. These danger signals activated tissue damage response pathways and that co-mediated repression of the cell cycle and parts of basal metabolism.

Microbial Colonization Resulted in a Gradual Reorientation of Jejunal Metabolic Homeostasis

Gene expression time series analysis using the STEM software (Ernst and Bar-Joseph 2006) was performed in order to monitor changes in gene ontology (GO) categories during 30-days of conventionalization. STEM clustering of gene expression indicated that GO terms related to metabolism were strongly enriched over the timespan of the experiment ($p < 0.001$). The majority of the metabolic genes that were differentially expressed in time, particularly those that belonged to the GO categories lipolysis, oxido-reductase activity and transport, displayed a gradual down-regulation during the 30 days of conventionalization. The repression of genes associated with metabolism (that was apparent at day 1 post-conventionalization) became more pronounced during extended periods of conventionalization, and was mainly characterized by gradual repression of fatty acid oxidation and transport (Figure S3.2). This is illustrated by the continuous repression (up to day 30 post-conventionalization) of the major regulator of fatty acid oxidation, *Ppar-α* (peroxisome proliferator activated receptor alpha) and its downstream target genes, including the fatty acid transporter *Cd36* and *Angptl4*. Concurrent with the repression of *Ppar-α*, other genes involved in fatty acid oxidation were also downregulated, including *Hmgcs2* (Hydroxy-3-methylglutaryl-coenzyme A synthase 2) that facilitates the synthesis of ketone bodies (Vila-Brau, Luisa De Sousa-Coelho et al. 2011). Conversely, the expression of *HmgCoA* reductase that encodes the rate-limiting step of steroid synthesis (Dempsey 1974) was induced. These data suggest that the lipolysis, an important source of cellular energy, is repressed during conventionalization, together with fatty acid oxidation and transport. Consequently, the jejunal metabolism appears to shift towards an alternative energy source. This proposed reorientation is supported by the remarkable downregulation of the *Ppar-α* downstream target gene, *Pdk4* (pyruvate dehydrogenase), suggesting the conversion of pyruvate into acetyl-CoA in the jejunal mucosa (figure S3.3), which in turn would affect glucose metabolism.
To further refine our understanding of the postulated metabolic reorientation, expression changes of metabolic genes were projected onto metabolic maps (Figure S3.3). These projections

showed that the suppression of fatty acid oxidation parallels an induction of glycolytic, lipogenic, amino acid, and nucleotide metabolism pathways. This induction was apparent at day 4 and persisted up to day 30 post-conventionalization. The continuous downregulation of the gene encoding *Pck1* (phosphoenolpyruvate carboxykinase 1), suggested repression of gluconeogenesis, while the cellular demand for glucose appeared to be induced by elevated expression of the transporter *Slc2a1* (also known as *Glut1*). The imported glucose appeared to be converted through both the oxidative arm of the pentose phosphate pathway (PPP), as illustrated by elevated expression of *G6pd* (Glucose-6-phosphate dehydrogenase), and the non-oxidative arm of the PPP that generates the ribose that serves as a substrate for nucleic acid synthesis. The significant induction of nucleotide synthesis and metabolism was exemplified by the induction of thymidylate synthase (*Tyms*), ribonucleotide reductase (*Rrm1, 2*), *Pola, e,* and *h* (DNA polymerase a, e, and h), and *Dnmt* (DNA methyltransferase) (Figure S3.3). In addition, the metabolic mapping of transcriptome changes also highlighted the impact of conventionalization on lipogenesis by the induction of *Acly* (ATP citrate lyase), *Acaca* (acetyl-CoA carboxylase alpha), and, *Fasn* (fatty acid synthase) (Figure S3.3).
In addition to the above-detailed fatty acid oxidation, carbohydrate and nucleotide metabolic adaptations, the jejunal metabolism also underwent dynamic changes in expression of genes involved in amino-acid metabolism, including the glutamine, glutamate, and glutathione associated pathways. This was apparent from the induction of *Asns* (asparagine synthetase), and the repression of the *Gclc* and *Gclm* (glutamate consuming γ-glutamylcysteine), *Glul* (glutamine synthetase), and the *Glud1* (mitochondrial glutamate dehydrogenase) genes. Moreover, the mitochondrial *Bcat1* (branched-chain amino acid transaminase), *Tat* (tyrosine transaminase), and *Shmt2* (serine-glycine hydroxymethyl transferase) were induced, while several additional steps in tryptophan, tyrosine, phenylalanine, and branched chain amino acid (BCAA) metabolism were repressed (Figure S3.3). These transcriptome changes support the dynamic modulation of jejunal metabolism during conventionalization. Bacterial colonization of the jejunum induced changes in a variety of metabolic pathways and suggested a reorientation of both energy generating and biosynthetic pathways, presumably to maintain overall mucosal energy homeostasis.

A Possible Association of Jejunal Responses with a Shift in the Colonizing Microbiota

The jejunum is colonized by a relatively low-diversity and relatively small-sized bacterial community compared to the ileum and colon (O'Hara and Shanahan 2006). Molecular analysis by qPCR detection of the 16 S rRNA gene copies in jejunum samples indicated that a mouse microbial community of the density that is expected in the jejunum was already established on day 1; this community contained approximately 4.9±0.3 16 S rRNA copies/ml jejunal content (expressed as log10). This microbial count did not significantly change during the duration of conventionalization. To investigate which bacterial taxa were specifically associated with the acute and subsequent secondary responses observed, the jejunal microbiota composition at days 1 and 4 post-conventionalization, respectively, was analyzed at the various levels of phylogenetic based on the MITChip profiles. At level 0 (phylum-like), day 1 post-conventionalization jejunal microbiota consisted mainly of Firmicutes, Bacteroidetes, Proteobacteria, and Actinobacteria (Figure 3.3A). Interestingly, at level 1, which equates to bacterial class, members of the Firmicutes such as Clostridium clusters XIVa (9.4±1.6 %), XVI (12.9±3.1 %), XVII (6.8±1.3 %), XVIII (17.2±5.6 %) as well as Bacilli (5.2±2.5%) dominated the jejunal microbiota at day 1 post-conventionalization (Figure 3.3B). Moreover, level-2 (genus-like) analysis, the

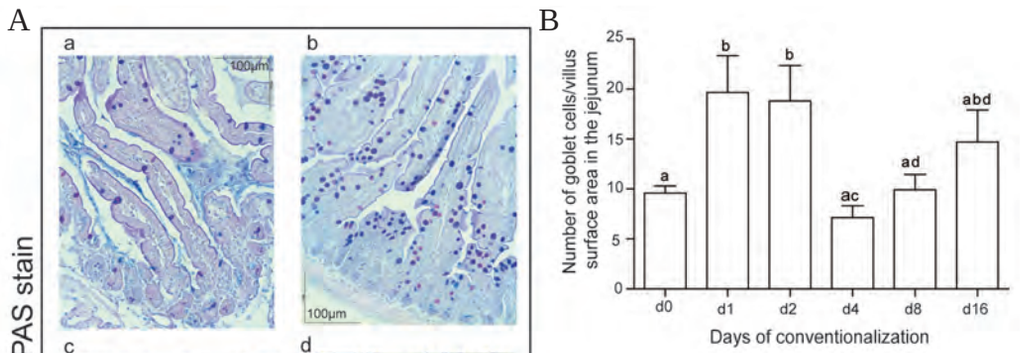

Figure 3.1. Early and late morphological changes in jejunal mucosa in response to conventionalization. (A) Representative AB-PAS stain photomicrographs from the jejunum showing the dynamics of mucin subtypes distribution in germfree (a) and conventionalized mice at days 1 (b), 4(c), and 16(d). (B) The individual goblet cells scores in the jejunum. Significant differences between time-points are indicated by distinctive characters above the measurement clusters ($p < 0.05$). (Score germfree: 9.6 ± 0.7) , (score day 1: 19.7± 3.6), (score day 4: 7.1 ± 1.1), and (score day 16: 14.7 ± 3.2).

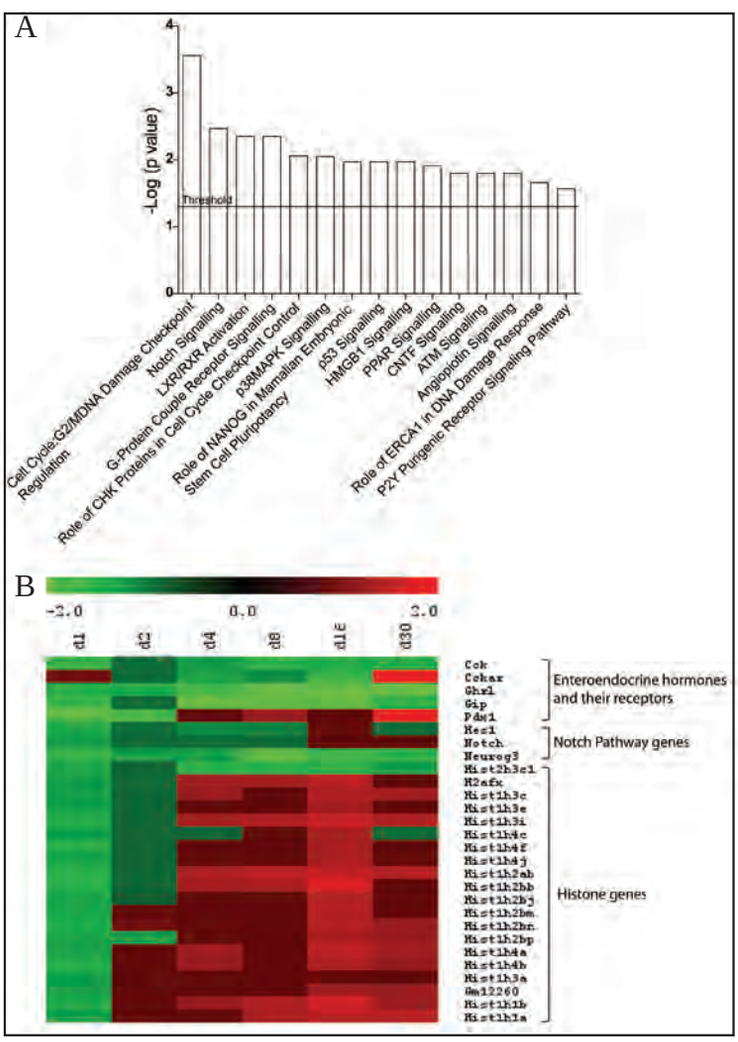

Figure 3.2. Acute jejunal transcriptome response to the colonizing microbiota. (A) Cellular pathways significantly modulated in the jejunum at day 1 post-conventionalization, calculated via a one-tailed Fisher's Exact test in IPA and represented as -log (p value); -log values exceeding 1.30 were significant ($p < 0.05$). (B) Heat map of the expression values for genes encoding enteroendocrine hormones, genes involved in Notch signaling pathway, and histone variants. The data represent the changes in gene expression levels at days 1-30 post-conventionalization in comparison to germfree. Notably, the lower expression levels of histone signaling pathway genes was transient and only measured at day 1 post-conventionalization in contrast to the persistent downregulation of genes encoding enteroendocrine hormones.

deepest level of phylogenetic assignment that can be reliably deduced from MITChip datasets, indicated that the phylotypes belonging to the *Clostridium* clusters were related to *Coprobacillus cateniformis*, *Clostridium leptum*, while the members of the bacilli were mostly assigned to *Lactobacillus plantarum* and relatives (Figure S3.4). This microbiota composition at day 1 post-conventionalization appeared to be specific for the jejunum, since the ileal microbiota comprised the prominent presence of gamma-proteobacteria, mainly members of *Clostridium* cluster XIVa and the colon microbiota were dominated by *Bacteroidetes* (data not shown). These two groups appeared to be much less abundant in the jejunal communities.
Microbial composition of samples collected at day 4 post-conventionalization was significantly different from the composition of the day 1 post-conventionalization samples with a clear shift in microbiota already apparent at the crude phylogenetic level-0. While Firmicutes accounted for the largest proportion of the jejunal microbiota at day 1 post-conventionalization, the abundance of members of the *Bacteroidetes* increased significantly ($p=0.01$) to account for 39.08±7.48% of the total population (Figure 3.3A). Remarkably, the subgroups within this phylum increased simultaneously indicating that the impact was not related to specific subgroups. This contrasted to the Firmicutes, in which only a few genera decreased, especially the members of the *Clostridium* cluster XVI (Figure 3.3). In conclusion, microbiota analysis of these samples showed that the jejunum is colonized by low amounts of bacteria with relatively low diversity and a community structure that is distinct from that in the ileum and colon (Chapter 2), which was apparent throughout the conventionalization course (data not shown).

Jejunal Tissue Metabolic Profiling during Conventionalization Confirms its Metabolic Reorientation

Metabolic phenotyping by ^{1}H NMR of jejunal tissues obtained from germfree and the time-resolved post-conventionalization animals was conducted to delineate the effects of the colonizing microbiota on jejunum metabolism throughout the conventionalization process. These analyses provided insight into the dynamic alteration of amino acid and energy metabolism. Orthogonal partial least-square discriminant analysis (OPLS-DA) models were constructed focusing on the differences between germfree and conventionalized mice over time. The analysis showed that the presence of the gut microbiota was reflected by relatively increased levels of ascorbate, ethanolamine, aspartate, fumarate, glutamate, glutamine, inosine, dihydroxyacetone† (†=tentative assignment), and hypoxanthine also increased over time and the levels of tauro-conjugated bile acids and glycerol were found to decrease. A number of metabolites such as guanosine and glycine were transiently altered during conventionalization (Figure 3.4). The altered metabolic profile of the majority of assigned tissue metabolites seem to correlate well with the differential regulation of the corresponding genes (Figure S3.3 and Table S3.1).
In order to investigate whether there are any statistical correlation between ^{1}H NMR metabolic spectra and transcriptome data obtained from jejunal tissues, computed correlations were modeled by using O2PLS regression (Trygg and Wold 2003). The relationships between the ^{1}H NMR spectra and the transcriptome data were visualized in the form of correlation heat maps, which revealed a negative correlation between the ^{1}H NMR identified metabolite glutathione and a set of 128 genes that are mainly involved in amino acid and purine and pyrimidine metabolism, that were expressed at elevated levels starting at day 4 post-conventionalization onward (Figure S3.5). Taken together, the identified changes in metabolic profiles at the jejunal

tissue level confirm the remarkable transcriptome shift in genes particularly those involved in energy, amino acid, and nucleotide metabolism.

A Core Regulatory Network Orchestrates the Microbiota Driven Metabolic Reorientation of the Jejunal Mucosa

Proper regulation of animal physiology relies for an important part on gene regulatory networks (Davidson 2010). To evaluate whether a central regulatory network could specify the metabolic reorientation observed, STEM time series analyses were mined for metabolic-related GO assignments in the jejunal mucosa. The genes recovered were used to construct a protein-protein interaction network in IPA. The resulting network (Figure 3.5) contains genes involved in the regulation of various cellular pathways, including xenobiotic metabolism, fatty acid metabolism, glutathione and arachidonic acid metabolism, amino acid metabolism, ammonia detoxification, glycolysis and gluconeogenesis (Figure S3.6). The network encompassed 76 nodes that had at least 110 connections, the largest number for any node was 20. These central regulatory nodes belonged to the nuclear receptor subfamily, including *Ppar-α* and *Ppar-γ, Nr1i3* (nuclear receptor subfamily 1-group I-member 3), *Nr0b1* (nuclear receptor subfamily 0-group B-member 2), as well as *Insr* (insulin receptor), and *Thr*β (thyroid hormone receptor beta) (Figures 3.5 and 3.6). These central regulators and their known downstream target genes were included together in the regulatory network (Figure 3.5). Presence of regulators and downstream genes in the identified GO: metabolism corroborates the observed reorientation of the metabolism associated transcriptional profiles and the corresponding tissue-metabolites. Interestingly, IPA analysis of the association of the constituents of the regulatory network with functionality and disease exemplified the involvement of 20 genes of the 76 core regulatory genes in metabolic disorders including type 2 diabetes and insulin resistance (indicated by red arrows in Figure 3.5). This suggests that the core regulatory genes that play roles in the systemic metabolic control of glucose homeostasis in response to microbial colonization of the intestine could also be used to investigate metabolic dysregulation.

A

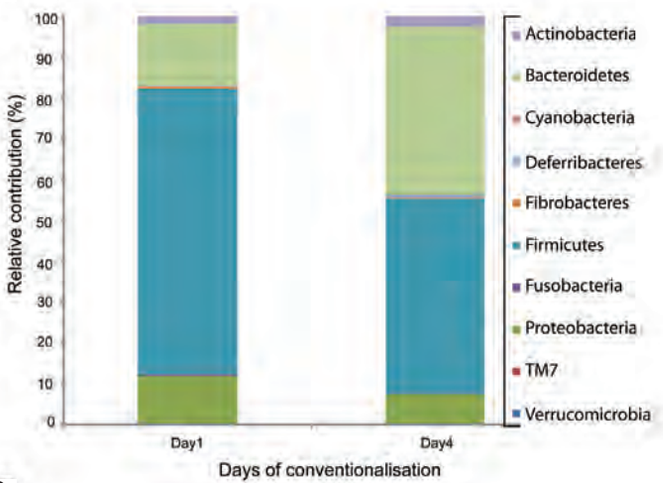

B

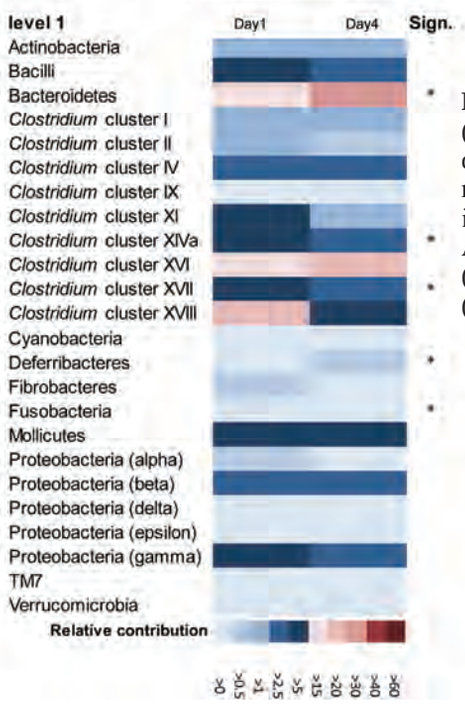

Figure 3.3. Establishment of the colonizing jejunal microbiota (A) Bar plot depicting the relative abundance of bacterial phyla at days 1 and 4 post-conventionalization. (B) Heat map showing the relative contribution of specific bacterial classes (level 1 group) in the jejunal lumen at days 1 and 4 post-conventionalization. Asterisks indicate significant differences between both days ($p < 0.05$) assessed by t test executed in SPSS Statistics 17.0 (SPSS Inc., Chicago, IL).

Figure 3.4. Correlation coefficient heat map that shows that relative increase or decrease of concentrations of respective metabolites during conventionalisation compared to the germfree state. A series of pair-wise OPLS-DA models were constructed from which the correlation coefficients of the significantly altered metabolites in jejunum tissues during days 1-16 post-conventionalization were extracted. Red color represents an increased level and green color represents a decreased level. (†) indicates tentative assignment.

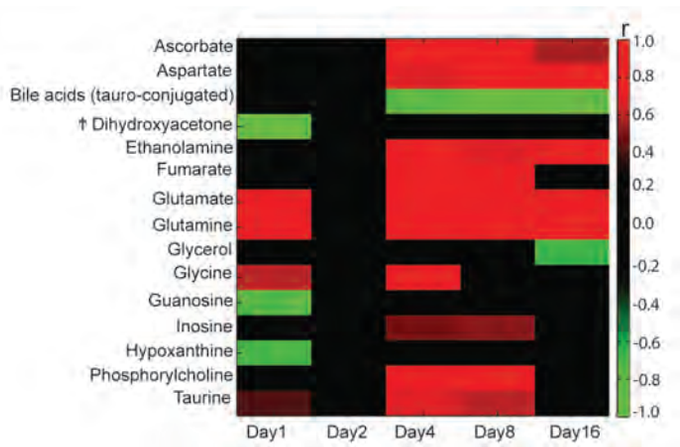

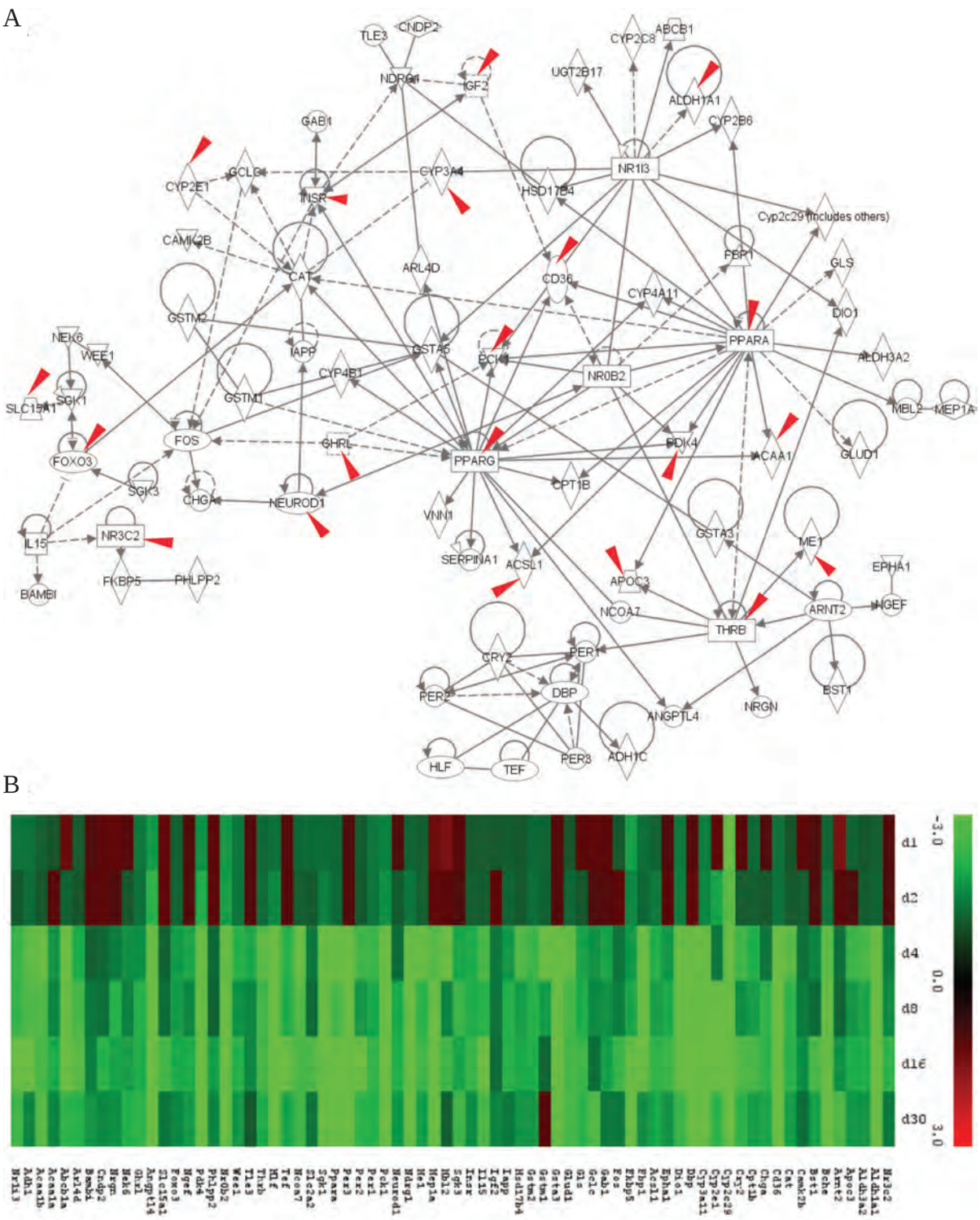

Figure 3.5. A core regulatory network governs the dynamics of jejunal metabolic adaptation during conventionalization. (A) The Ingenuity protein-protein interaction (PPI) network generated by mining STEM time series analyses for metabolic-related GO assignments in the jejunal mucosa. Red arrows refer to genes known to be associated to human insulin resistance and type 2 diabetes based on IPA disease annotation. (B) Heat map diagram of the genes involved in the regulatory network, representing the changes in their jejunum expression level during days 1-30 post-conventionalization in comparison to germfree state.

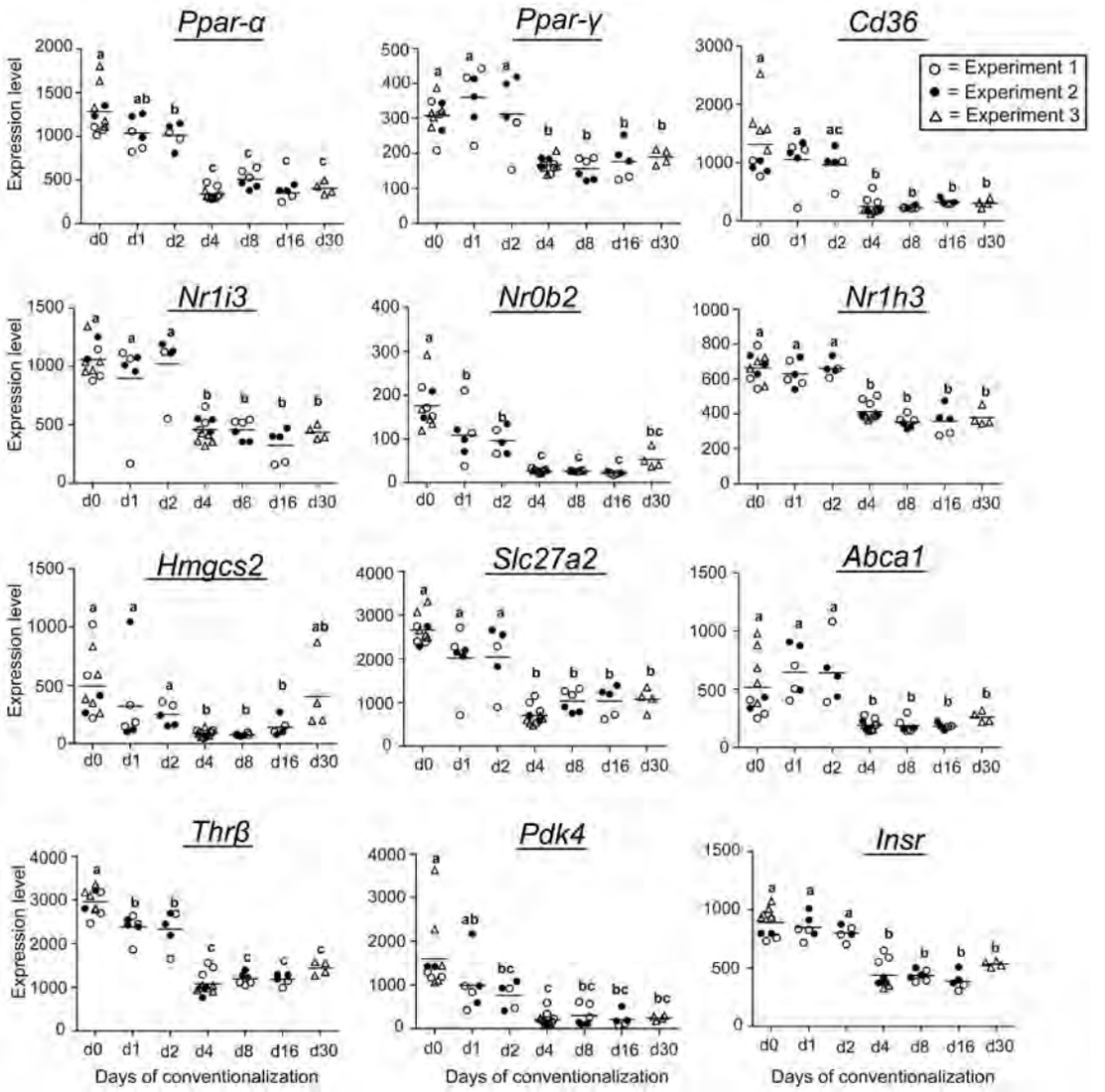

Figure 3.6. Nuclear receptors which regulate gut hormones and fatty acid metabolism constitute the major nodes in the identified regulatory network. Jejunal gene expression levels of nuclear receptors and their target genes were analyzed in germfree and conventionalized mice at indicated days of conventionalization. Values are depicted as dot plots. Significant differences between time-points are indicated by distinctive characters above the measurement groups ($p < 0.05$).

DISCUSSION

The gut microbiota has been recognized to play a prominent role in the modulation of intestinal and systemic energy and lipid metabolism in healthy hosts. In addition, improper host-microbiota interactions have been suggested to underlie the development of metabolic disorders (Bäckhed, Ding et al. 2004; Claus, Ellero et al. 2011). The proximal intestine, and in particular the jejunum can be considered as the initial site of intestinal interaction between the host mucosa, the microbiota and ingested food. Therefore, it may be anticipated that especially this part of the intestinal tract will respond strongly to the presence of microbiota, despite the fact that the microbial densities in this intestinal region are relatively low (O'Hara and

Shanahan 2006).

In a recent study, it was reported that metabolic changes in liver tissues in response to intestinal conventionalization involved two distinct temporal phases, which were characterized by a shift from glycolysis (observed at 5 days post-conventionalization) to triglyceride biosynthesis (at 20 days post-conventionalization) (Claus, Ellero et al. 2011). The present study focuses on time-resolved analysis of metabolic responses in the jejunal mucosa and confirms a two-phase response to conventionalization. The jejunal response to conventionalization was characterized by an acute and transient phase, which was followed by a secondary stable phase, as evidenced by both transcriptomic and metabonomic analyses of the jejunal tissue (Figure 3.7). This rapid and dynamic metabolic response to conventionalization was not observed in the ileum or colon (data not shown) lending further support to the unique role of the proximal intestine in sensing and monitoring the luminal microbiota-diet interplay. During the acute response (day 1 post-conventionalization), "danger signals" appeared to have played important biological roles, judged by the induction of IPA danger signal pathways such as HMGB1, and P2Y pyrogenic receptor signaling cascades (Kono and Rock 2008; Kouzaki, Iijima et al. 2011). The bacterial groups that dominated at day 1 post-conventionalization (e.g. Bacilli), produce TCA cycle intermediates which have been reported to act as "alarm or danger signals" (Poelstra, Heynen et al. 1992; Rubic, Lametschwandtner et al. 2008) and are associated with the induction of rescue pathways and hypoxia associated metabolic responses in host cells (Oppenheim and Yang 2005), suggesting that these bacterial groups participated in the induction of danger signals in this study. The strikingly increased number of mucin-filled goblet cells observed in the jejunum during the acute response (day 1 and to a lesser extent on day 2) could reflect a physiological defence mechanism in response to accumulating "danger signals" during the early days of conventionalization.

Transcriptome analysis including GO enrichment and pathway and gene regulatory network analysis showed that the secondary phase of response to conventionalization (days 4-30) was characterized by molecular changes illustrative of the metabolic reorientation of jejunal tissue. Notably, the repression of the nuclear receptors involved in the regulation of this secondary metabolic response had been already initiated during the first day of conventionalization. The secondary phase of jejunal responses was consolidated during extended periods of conventionalization (up to day 30), illustrating the establishment of a novel metabolic homeostasis that accommodates the microbiota in this region of the intestinal tract. This novel homeostasis included the repression of genes belonging to fatty acid oxidation, lipid absorption (*Pnliprp2*, *Clps*, and *Apoa4*), lipid transport (*Cd36*), but also included 14 important regulators, among which *Ppar-α, Ppar-γ,* and *Angptl4*. Repression of lipid metabolism pathways appeared to favour glucose utilization in the jejunal tissues, which is supported by the increased expression of (among others) *G6pd*, and *Slc2a1*, and repression of *Pck1*, *G6Pc* (glucose-6-phosphatase), and *Pdk4*. The transcriptome changes appear to describe a shift in the jejunal metabolism from an oxidative energy supply to an anabolic metabolism that may be required to meet the energy demand of the mucosal tissue and its epithelial cells that goes through drastic morphological changes and increase in the turnover rate during later stages of conventionalization (Chapter 2). Proliferating cells require nucleotide supplies that are synthesized from precursors derived from glycolytic and TCA cycle intermediates (Tong, Zhao et al. 2009). Indeed, the induced phosphoglycerate dehydrogenase (Phgdh), phosphoserine aminotransferase 1 (Psat1), and Shmt2, may have participated in glycine biosynthesis, which was confirmed on the metabolite level (Figure 3.4). Moreover, the induction of Ripa (ribose-5-phosphate isomerase) and

Pgd (6-phosphogluconate dehydrogenase) may have led to increased ribose-5-phosphate biosynthesis. Both glycine and ribose-5-phosphate are important precursors of nucleotide biosynthesisintermediate 3-phosphoglycerte to glycine, and ribose-5-phosphate biosynthesis (Snell and Weber 1986; DeBerardinis, Sayed et al. 2008). These adaptations resemble the so-called "Warburg effect" that is described to occur in the highly proliferating cancer cells, which produce energy via an increase in glycolysis followed by lactic acid production in the cytosol. This energy-limited anabolism observed in cancer cells is clearly different from the comparatively low rate of glycolysis coupled to mitochondrial oxidative phosphorylation that is exhibited by normal cells (Kim and Dang 2006).

Metabolic tissue profiling by ^{1}H NMR confirmed the induction of anabolic metabolism, illustrated by the accumulation of glutamine, glutamate, and aspartate, which is in agreement with their previously reported elevated levels in the ileum and colon upon colonization of germfree mice (Claus, Tsang et al. 2008). Glutamine has been shown to be extensively utilized by the highly proliferating cells of the intestine and is an important substrate for the anabolic metabolism (Wu 1998) to sustain the increased epithelial turnover and the development of the immune system during conventionalization (Chapter 2). Notwithstanding the decreased expression levels of *Glud1* gene encoding the enzyme that is involved in glutamine production during the metabolic reorientation phase, consistent elevation of glutamine level in jejunal tissue was detected by ^{1}H NMR at day 4 post-conventionalization onward. These results suggest that upon conventionalization the proliferating intestinal cells require the import of glutamine to meet their highly anabolic demands. This finding is in agreement with the notion that glutamine is mainly taken up by jejunal mucosa from the blood circulation (Windmuel and Spaeth 1974). In addition, the remarkable decreased expression of *Glud1* (Fold change ranges from -2.8 at day 4 and -2.5 at day 30 post-conventionalization) implies a repressed replenishment of TCA cycle intermediates using glutamate as a substrate in conventionalized mice (Brosnan 2000).

At day 4 post-conventionalization, genes encoding glutathione reductase (*Gsr*), and peroxidases were up-regulated, presumably because of their involvement in the protection of intestinal tissues against oxidative stress and tissue damage (Dahm and Jones 1994). Two associated genes encoding subunits of γ-glutamyl cysteine ligase (*Gclc* and *Gclm*) were downregulated. γ-glutamyl cysteine ligase is the rate-limiting enzyme in the *de novo* synthesis of glutathione (Krzywanski, Dickinson et al. 2003). Downregulation of *Gclc* and *Gclm* correlates with the observed accumulation of glutamate. Remarkably, conventionalization led to strong repression of two glutathione transferases (*GST-α* and μ) which are involved in phase II metabolism of xenobiotics (Waxman 1990) and in the biosynthesis of arachidonic acid metabolites like prostaglandins and leukotrienes (Vessey and Zakim 1981). Suppression of prostaglandin and leukotriene synthesis by reduced GST expression may have contributed to avoidance of excessive inflammatory reactions from day 4 post-conventionalization onward (Chapter 2). We propose that the protection of tissue injury from oxidative stress contributes to maintenance of tissue integrity towards a novel state of homeostasis that accommodates the microbiota and its metabolites.

Using gene ontology (GO) enrichment and IPA-driven biological annotations of genes, pathways, and processes, we obtained an integrative view of the jejunal transcriptomes and metabolites that were modulated upon colonization of germfree mice. Data integration allowed the reconstruction of a gene regulatory protein-protein interaction network that included repression of genes involved in hormonal regulation and key metabolic genes that play important roles in (among others) fatty acid oxidation and gluconeogenesis. Of note, the identified regulatory

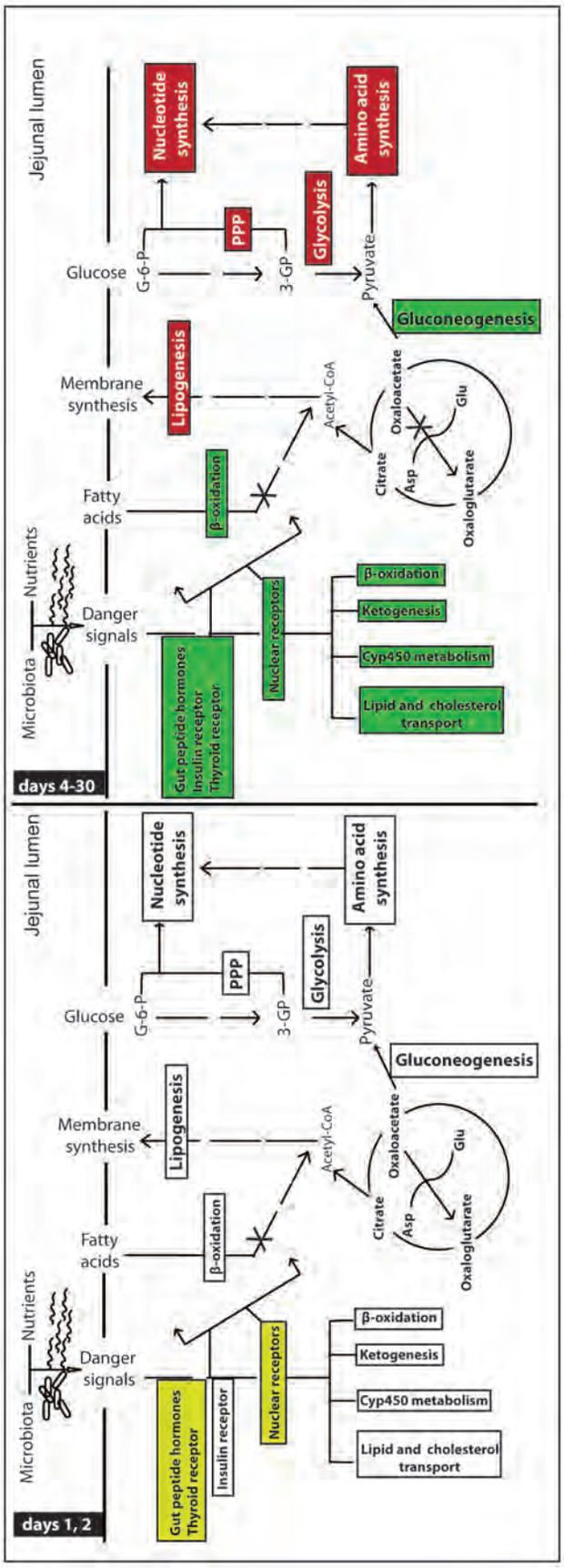

Figure 3.7. Dynamics of the metabolic response in jejunal mucosa during conventionalization. A schematic model of the time-resolved jejunal mucosal changes of fat, energy, and amino acids and nucleotide metabolism during conventionalization. Color coded boxes represent changes in metabolic processes at early (1-2) and late (4-30) days of conventionalization. Red color represents up-regulated processes, green color represents down-regulated processes, over control (germfree=day 0). The intensity of the green color depicted in the figure is proportional to the relative decrease in gene expression.

network comprised genes of which the human orthologues are dysregulated in metabolic disorders, including insulin resistance and type 2 diabetes. In addition, on the basis of genome-wide association studies (GWAS), at least 26 % of the regulatory genes were associated with metabolic diseases. One extrapolation that could harness the linkage between the jejunum and its microbiota with basic systemic metabolic processes and diseases, may come from the study of possible mechanisms by which gastric bypass rapidly improves insulin sensitivity (Troy, Soty et al. 2008). It has been reported that the enhanced intestinal gluconeogenesis that is observed post-surgery stimulates portal sensing of glucose and rapidly modifies the insulin sensitivity of hepatic glucose production (Troy, Soty et al. 2008). The prominent effect of the colonizing microbiota on the host genes that are essential for proper glucose metabolism that was observed in this study, suggests that the microbiota is a key determinant of proper jejunal glucose metabolism. Apparently exclusion of the jejunum together with its microbiota from the nutrient flow can promote recovery of insulin sensitivity (Pories, Swanson et al. 1995; Troy, Soty et al. 2008). It is tempting to speculate that specific microbiota changes that are caused by the exclusion of the nutrient-flow contribute to jejunal responses that may underlie the major health promoting effect of a gastric bypass. Taken together, the present study supports a critical sensory role

of the jejunum in the perception of the local nutrient-microbiota interplay, which is a major determinant of systemic glucose homeostasis.

EXPERIMENTAL PROCEDURES

Animals, Experimental Design, and Sampling

All procedures were carried out as previously described (Chapter 2). In brief, germfree and conventionalized mice (male, C57 BL/6 J) were maintained in sterile conditions, on a commercial laboratory chow diet. Three independent biological experiments were performed using mice of different age after 2 weeks of acclimatization and diet adaptation. The first and second experiments of the three performed independent biological experiments included 36 mice obtained in 2 biologically independent batches of 18 mice each, aged 8 and 10 weeks, respectively. The third experiment included 14 mice, aged 10 weeks old. The jejunum from each mouse was removed and divided into 2 cm segments that were immediately: stored in RNAlater® at room temperature for 1 h prior to subsequent storage at -80°C for RNA isolation, fixed overnight (O/N) in 4% (wt/vol) paraformaldehyde (PFA) followed by paraffin embedding for histological analysis, or snap frozen and stored at -80°C for metabolic analysis. Luminal content from jejunal segments was removed by gentle squeezing, snap frozen, and stored at -80°C for microbiota analysis.

Histological Staining

Cross sections (4 μm-thick) of the intestinal tissue segments were stained with Alcian Blue (AB) followed by the periodic acid-Schiff's reaction (periodic acid-Schiff (PAS) stain); to stain neutral and acid mucins as previously described (Spicer 1965). Since the villus length in the different jejunal tissue samples was not identical, it was important to define a common denominator to determine the number of positively stained goblet cells. Therefore the number of goblet cells was expressed relative to the villus surface area. All data are presented as means ± SD for the number of animals indicated. Comparative analyses of the histochemical and cell-enumeration data were performed at each time-point using one-way analysis of variance (ANOVA) followed by Tukey's Studentized range test (SPSS program, Chicago, IL), and for all variables $p < 0.05$ was considered significant.

Transcriptome Analysis

High quality total RNA was isolated from a 2 cm segment jejunum by extraction with TRIzol reagent, followed by DNAse treatment and column purification. Samples were hybridized on Affymetrix GeneChip Mouse Gene 1.1 ST arrays. Quality control, statistical analysis, and complementary methods for the biological interpretation for the transcriptome data, were performed as previously described (detailed descriptions are provided in the supplemental material of Chapter 2).

Microbial Profiling of Jejunal Luminal Contents

Luminal contents of the jejunum were analyzed by Mouse Intestinal Tract Chip (MITCHip), a diagnostic 16S rRNA array that consists of 3,580 unique probes especially designed to profile mouse intestine microbiota (Geurts, Lazarevic et al. 2011) in analogy to the human intestinal tract (HIT)Chip (Rajilic-Stojanovic, Heilig et al. 2009). In short, 20 ng of jejunal DNA extract was used to amplify the 16S rRNA genes with the primers T7prom-Bact-27-for and Uni-1492-

rev (Chapter 2). Subsequently, an in vitro transcription and labeling with Cy3 and Cy5 dyes was performed. Fragmentation of Cy3/Cy5-labeled target mixes was followed by hybridization on the arrays at 62.5˚C for 16 h in a rotation oven (Agilent Technologies, Amstelveen, The Netherlands). The slides were washed and dried before scanning. Signal intensity data were obtained from the microarray images using Agilent Feature Extraction software, version 9.1 (http://www.agilent.com). Microarray data normalization and further analysis were performed using a set of R-based scripts (http://r-project.org) in combination with a custom-designed relational database, which operates under the MySQL database management system (http://www.mysql.com).
Of note, microbial analysis should be interpreted with particular caution due to the technical challenges encountered in handling the small sized and low density samples obtained from the jejunum.

Tissue Metabolite Profiling
Tissue samples were homogenized and extracted in acetonitrile/water (1:1), as previously described (Waters, Holmes et al. 2002). The supernatant containing the aqueous phase was collected, freeze-dried and dissolved in 600 µl of D_2O. Samples were centrifuged for 10 min at 15,000 g, and 500 µl of the supernatant and 50 µl of water were transferred into 5mm (outer diameter) NMR tubes for analysis by ^{1}H-NMR spectroscopy. All spectra were acquired on an Avance II 600MHz NMR spectrometer (Bruker Biospin, Rheinstetten, Germany) equipped with a Bruker 5mm TXI triple resonance probe operating at 600.13 MHz, and using a BACS auto-sampler. Spectral acquisition of the aqueous phase was performed using the first increment of a standard nuclear Overhauser enhancement scpectroscopy (NOESY) 1-dimensional ^{1}H NMR experiment ((noesypr1D)(RD-90°-t_1-90°-t_m-90°-acquisition), where RD is a relaxation delay, t_1 is a short delay of 2 µs and t_m is a mixing time of 100 ms. Water suppression was applied during the RD and a 90° pulse set at 10 µs. For each spectrum, a total of 256 scans (16 dummy scans) were collected into 64k data points over a spectral width of 20 ppm.
Data were analyzed by applying an exponential window function with a line broadening of 0.3 Hz prior to Fourier transformation to all 1D NMR spectra. The resultant spectra were phased, baseline corrected and calibrated to lactate (δ 1.33) manually using Topspin (2.0a, Bruker BioSpin 2006). The spectra were subsequently imported into MatLab (R20010aSV, The MathsWorks inc.) where the region containing the water resonance (δ 4.6-5.2) was removed. The data were then normalized to the probabilistic quotient (Dieterle, Ross et al. 2006) to minimize the effects of inter-sample variation due to phenomena such as disparate sample volume, although every effort was made to keep this constant during sample preparation.
Metabonomic data were visualized by Principal Component Analysis (PCA). OPLS-DA models (Trygg and Wold 2003) were then fitted between successive time-points in order to highlight discriminant metabolites. PCA, O-PLS, O-PLS-DA and Statistical total correlation spectroscopy (STOCSY) were performed in Matlab (using an in-house routine) (Cloarec, Dumas et al. 2005). Permutation testing of the Y matrix for PLS-based models was conducted using an in-house algorithm (Cloarec, Dumas et al. 2005) to determine whether the Q^2Y (predictive ability) of the model was significantly different from the Q^2Y calculated from 100 random permutations of Y. Variables with a correlation coefficient $|r| > 0.4$ were reported in Figure 3.4 to ascertain an overview of temporal metabolic changes. Assignments were made using additional two-dimensional NMR experiments and reference to databases of spectra of authentic compounds.
An O2PLS model was conducted to integrate metabonomic and transcriptomic datasets as

described by Li *et al* (Li, Wang et al. 2008) using an in-house algorithm (Cloarec, Dumas et al. 2005). The O2PLS model was calculated for pairwise datasets (metabolome and transcriptome) and displayed .O2PLS models were fitted on tables built from 2 merged datasets reflecting the 2 phases of conventionalization: (1) d0, d1 and d2 (n=18) and (2) d4, d8 and d16 (n=14). The first model on d0, d1 and d2 was not significant and is not discussed in the chapter. The second model computed with 1 predictive component, 1 orthogonal component and a 7-fold cross-validation procedure had a good predictive ability, as reflected by the following parameters: $R^2Y=0.36$ and $Q^2Y=0.15$. The significant variables were then selected based on their correlation with the scores of the model ($p < 0.01$).

Accession Numbers
The mouse microarray dataset was deposited in the Gene Expression Omnibus (GEO) with accession number GSE32513.

ACKNOWLEDGMENTS

The authors thank several members of the team of J. Doré (INRA, Jouy en Josas) for assistance with animal sacrifice and sampling, Dicky J. Lindenbergh-Kortleve (Department of Pediatrics, Erasmus Medical Center) for assistance with histological staining, J. Jansen, M. Grootte-Bromhaar, M. Boekschoten and P. de Groot (Division for Human Nutrition, Wageningen University) for their technical support in microarray hybridization and microarray data-quality control and processing.

CHAPTER 3
Supplemental Material

Molecular Dynamics of Microbiota Sensing in the Mouse Jejunal Mucosa during Conventionalization Support a Prominent Role of the Jejunum in Systemic Metabolic Control

SUPPLEMENTAL FIGURES

A

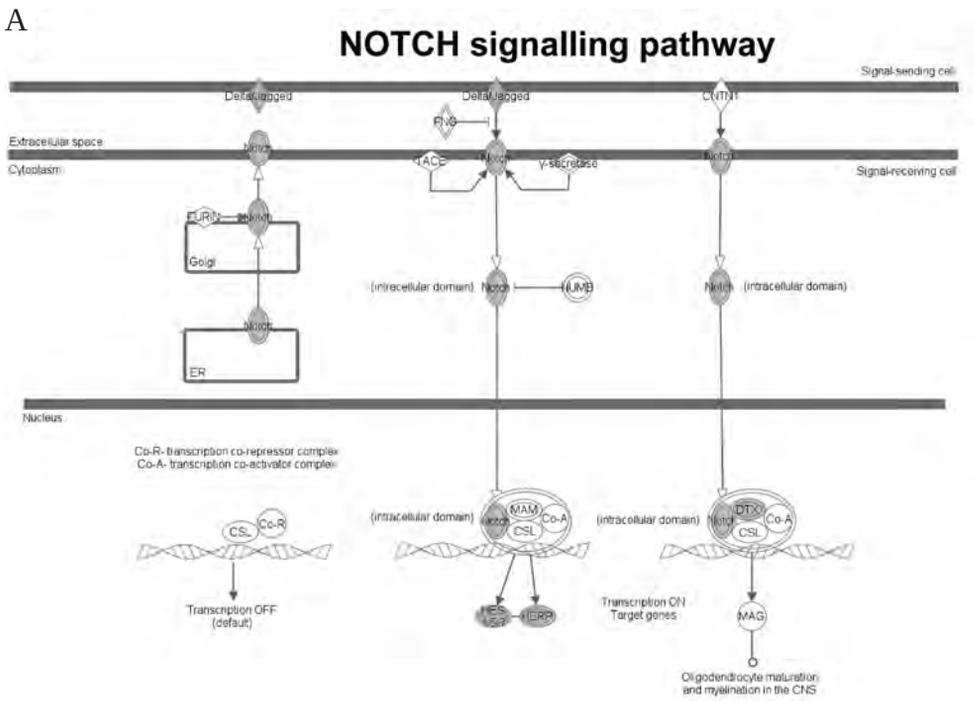

B

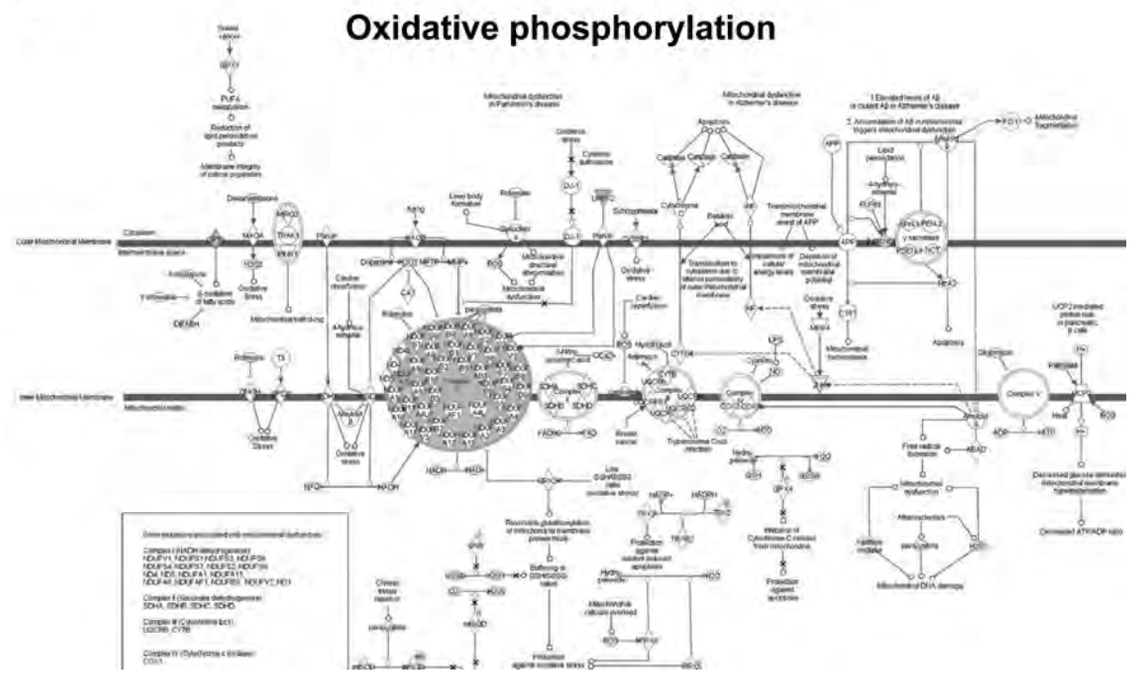

Figure S3.1. Pathway maps analysis of Ingenuity's canonical Notch signaling pathway (A) and mitochondrial dysfunction pathway (B) including the genes that were differentially expressed in the jejunal tissue at day 1 post-conventionalization. The grey color depicts a decrease in gene expression.

Category Name	#Genes Category	p-value	Corrected p-value
carboxylic acid metabolic process	595	5.80E-11	<0.001
oxoacid metabolic process	595	5.80E-11	<0.001
organic acid metabolic process	608	1.00E-10	<0.001
monooxygenase activity	127	1.30E-10	<0.001
cellular ketone metabolic process	617	1.50E-10	<0.001
tetrapyrrole binding	167	9.70E-10	<0.001
oxidoreductase activity	744	1.50E-09	<0.001
organic substance transport	397	3.20E-09	<0.001
heme binding	160	3.90E-09	<0.001
nitrogen compound transport	164	5.60E-09	<0.001
carboxylesterase activity	39	6.30E-09	<0.001
monocarboxylic acid metabolic process	310	1.70E-08	<0.001
active transmembrane transporter activity	316	2.40E-08	<0.001
vitamin metabolic process	62	3.50E-08	<0.001
oxidoreductase activity	194	6.10E-08	<0.001
secondary active transmembrane transporter activity	186	2.10E-07	<0.001
carboxylic acid transport	138	2.30E-07	<0.001
small molecule metabolic process	1644	2.40E-07	<0.001
establishment of localization	2808	2.50E-07	<0.001
transmembrane transport	640	2.50E-07	<0.001
transport	2761	2.60E-07	<0.001
lipid metabolic process	833	2.60E-07	<0.001
organic acid transport	140	2.80E-07	<0.001
fatty acid metabolic process	248	3.40E-07	<0.001
iron ion binding	249	3.60E-07	<0.001
amine transport	145	4.10E-07	<0.001
transmembrane transporter activity	856	4.90E-07	<0.001

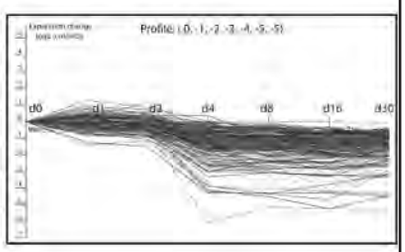

Figure S3.2. Gene Ontology enrichment analyses of jejunum during the time course of 30 days experiment. The table shows the GO enrichment results for the set of genes shown in the graph right to the table. The graph shows the expression patterns for all the genes assigned to the profile. The table shows a count of the number of genes assigned, and the STEM profile's p-value.

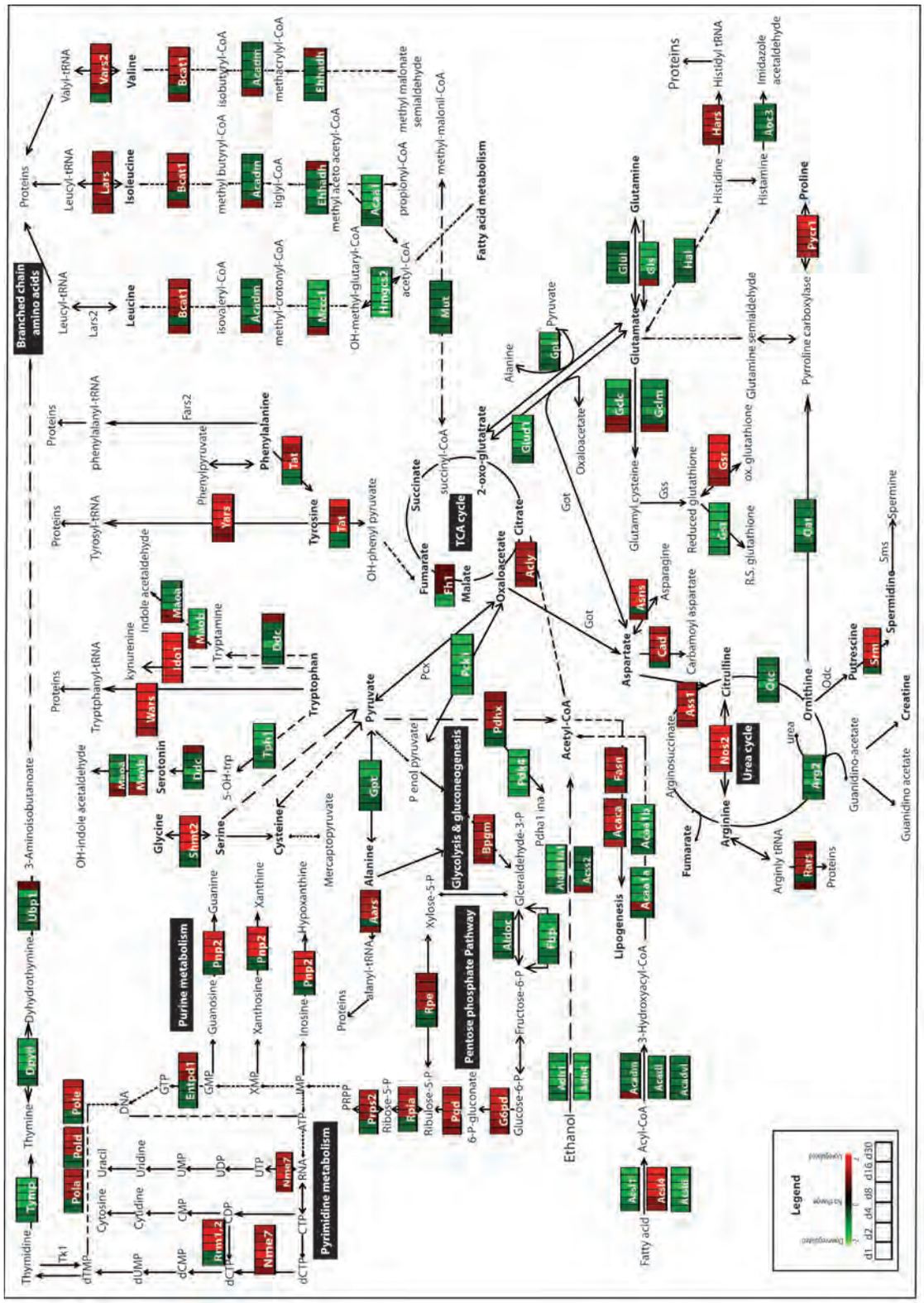

Figure S3.3. Schematic map indicating the changes in the expression of genes encoding metabolic enzymes at days 1-30 post-conventionalization versus germfree mice. Each gene box is divided into six sub-boxes with color codes representing the changes observed for each of the six time-points. Red color represents upregulated genes and green color represents downregulated genes (relative to germfree mice).

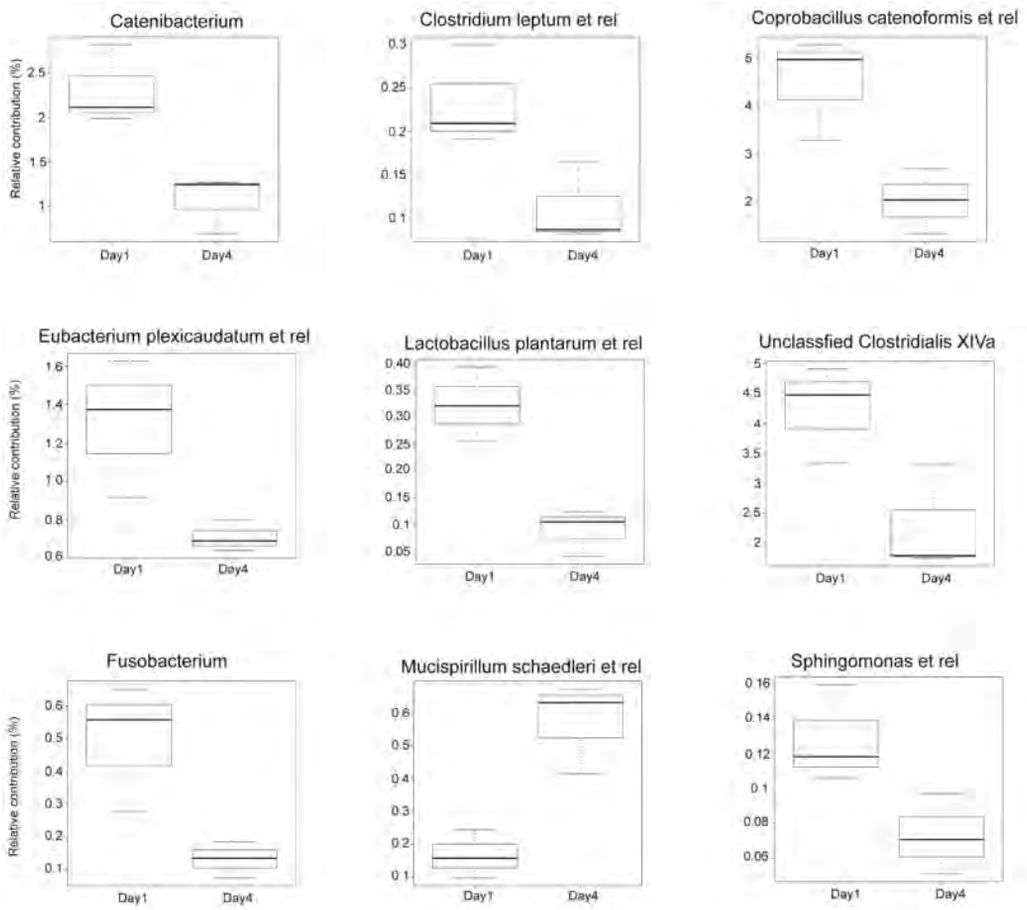

Figure S3.4. Bacterial genera (level 2 data, genus-like) that were significantly different when comparing microbiota profiles of jejunal lumen samples obtained on days 1 and 4 post-conventionalization ($p < 0.05$).

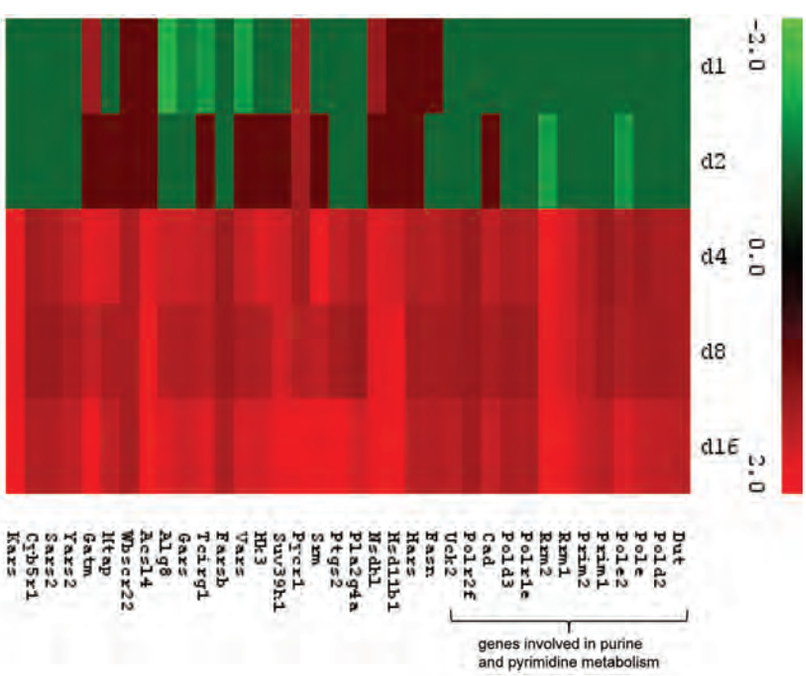

Figure S3.5. Genes negatively correlated with glutathione metabolite at the second phase of conventionalization. Heat map of the genes which were significantly anti-correlated with glutathione metabolite detected by ^{1}H NMR in jejunal tissue samples. The heat map represent the changes in gene expression levels at days 1-16 post-conventionalization.

A

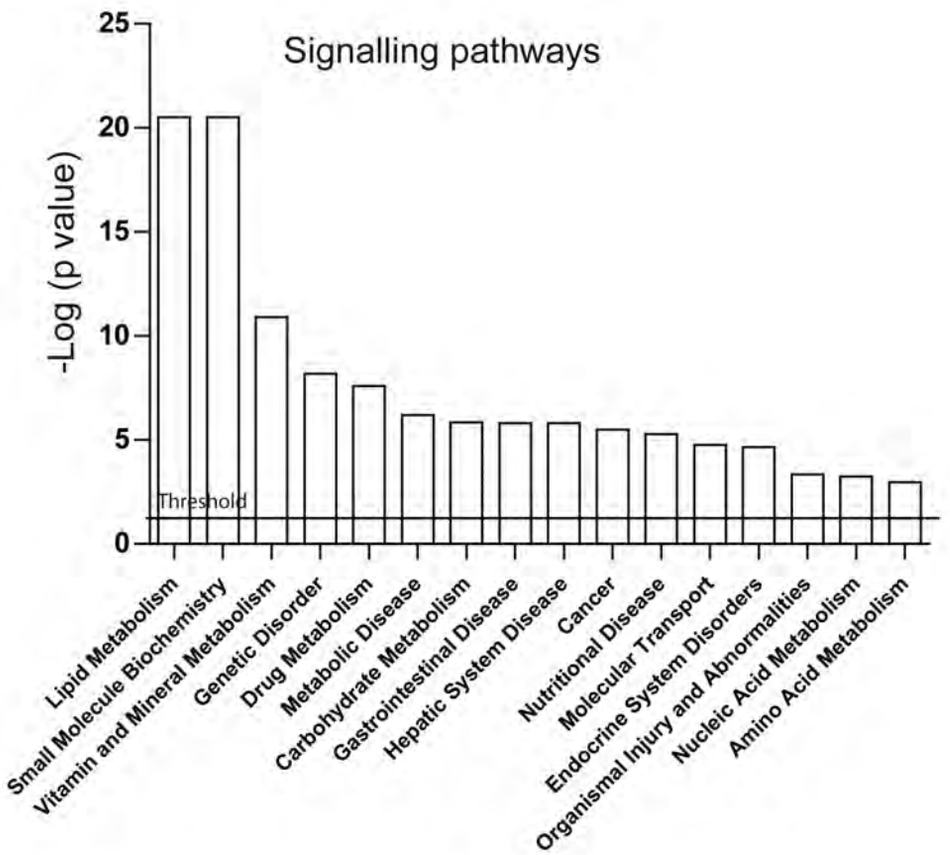
Signalling pathways
-Log (p value)
25
20
15
10
5
0
Threshold
Lipid Metabolism
Small Molecule Biochemistry
Vitamin and Mineral Metabolism
Genetic Disorder
Drug Metabolism
Metabolic Disease
Carbohydrate Metabolism
Gastrointestinal Disease
Hepatic System Disease
Cancer
Nutritional Disease
Molecular Transport
Endocrine System Disorders
Organismal Injury and Abnormalities
Nucleic Acid Metabolism
Amino Acid Metabolism

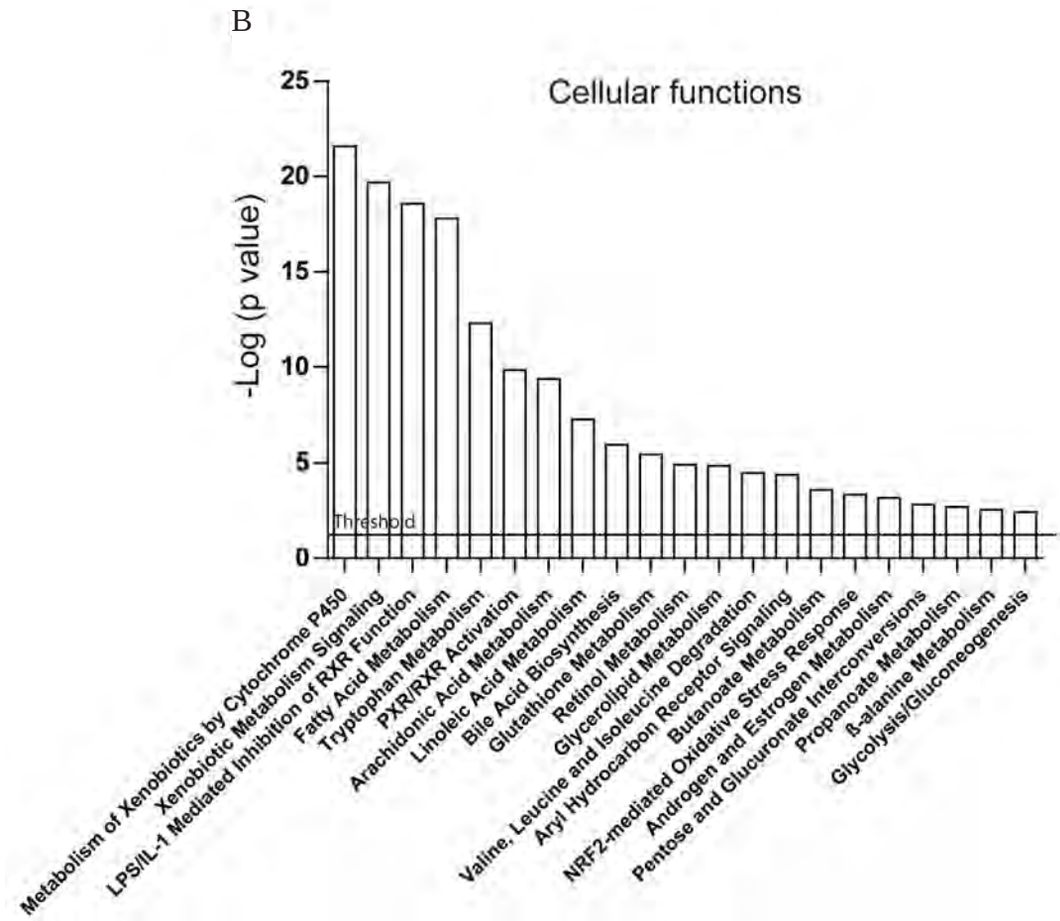

Figure S3.6. Ingenuity canonical pathways (A) and cellular functions (B) that were significantly modulated in the jejunum during conventionalization. Significance was calculated via a one-tailed Fisher's Exact test in IPA and is represented as -log (p value); -log values exceeding 1.30 were significant ($p < 0.05$).

Table S3.1. Correlation between the identified jejunal tissue metabolites and the corresponding genes involved in the metabolic reactions of which the metabolites are end- or by-products. The heat map of the expression values for the genes represents the changes in gene expression levels at days 1-16 post-conventionalization in comparison to germfree as depicted by MADMAX analysis. Red color depicts upregulation and green color depicts downregulation

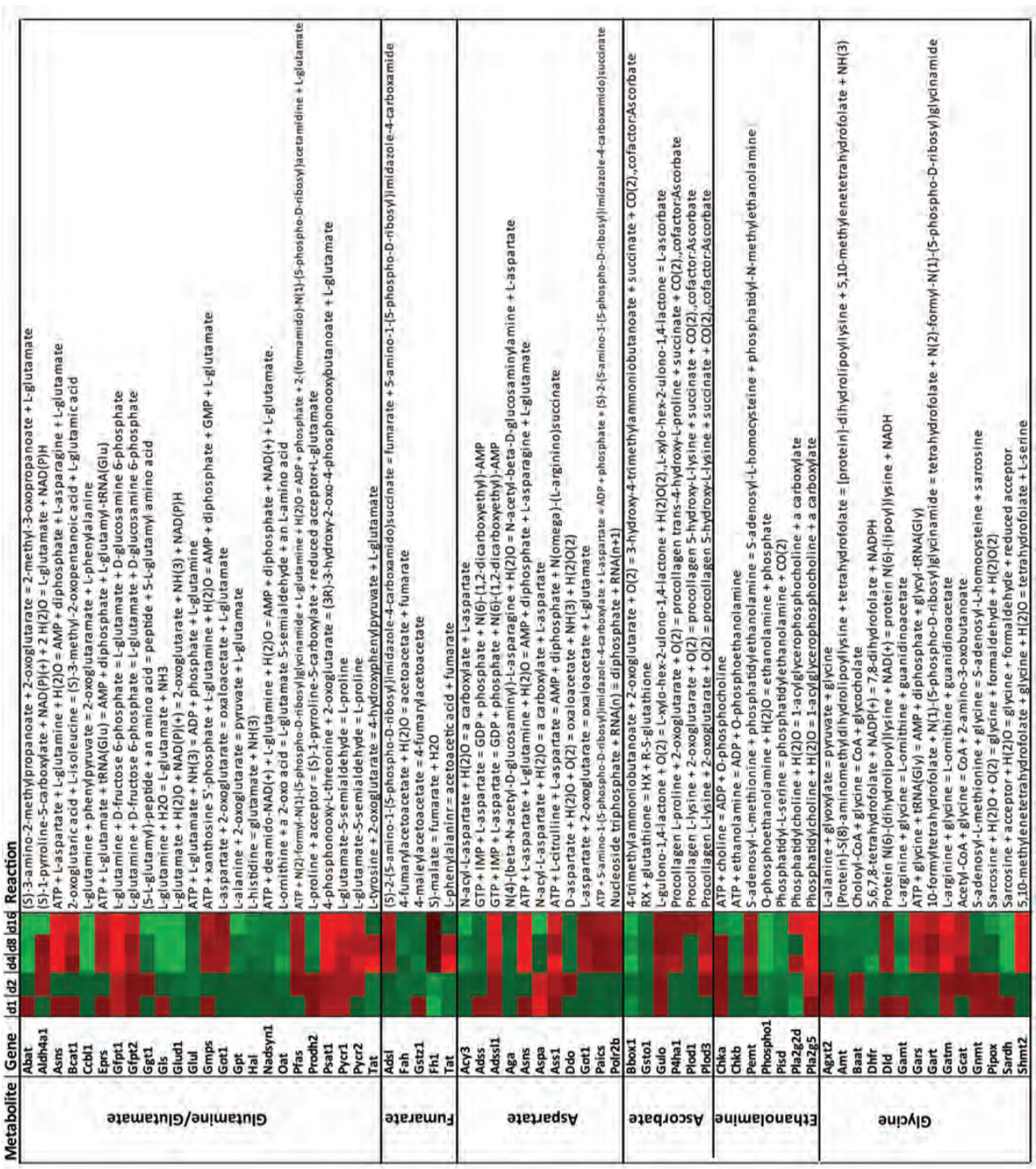

REFERENCES

Bäckhed, F. and P. A. Crawford (2010). "Coordinated regulation of the metabolome and lipidome at the host-microbial interface." Biochimica Et Biophysica Acta-Molecular and Cell Biology of Lipids **1801**(3): 240-245.

Bäckhed, F., H. Ding, et al. (2004). "The gut microbiota as an environmental factor that regulates fat storage." Proceedings of the National Academy of Sciences of the United States of America **101**(44): 15718-15723.

Bäckhed, F., R. E. Ley, et al. (2005). "Host-bacterial mutualism in the human intestine." Science **307**(5717): 1915-1920.

Brosnan, J. T. (2000). "Glutamate, at the interface between amino acid and carbohydrate metabolism." Journal of Nutrition **130**(4): 988S-990S.

Claus, S. P., S. L. Ellero, et al. (2011). "Colonization-induced host-gut microbial metabolic interaction." mBio **2**(2).

Claus, S. P., T. M. Tsang, et al. (2008). "Systemic multicompartmental effects of the gut microbiome on mouse metabolic phenotypes." Molecular Systems Biology **4.**

Cloarec, O., M. E. Dumas, et al. (2005). "Statistical total correlation spectroscopy: an exploratory approach for latent biomarker identification from metabolic 1H NMR data sets." Analytical chemistry **77**(5): 1282-1289.

Cloarec, O., M. E. Dumas, et al. (2005). "Statistical total correlation spectroscopy: An exploratory approach for latent biomarker identification from metabolic H-1 NMR data sets." Analytical Chemistry **77**(5): 1282-1289.

Dahm, L. J. and D. P. Jones (1994). "Secretion of cysteine and glutathione from mucosa to lumen in rat small-intestine." American Journal of Physiology **267**(2): G292-G300.

Davidson, E. H. (2010). "Emerging properties of animal gene regulatory networks." Nature **468**(7326): 911-920.

DeBerardinis, R. J., N. Sayed, et al. (2008). "Brick by brick: metabolism and tumor cell growth." Current Opinion in Genetics & Development **18**(1): 54-61.

Dempsey, M. E. (1974). "Regulation of steroid biosynthesis " Annual Review of Biochemistry **43**: 967-990.

Dieterle, F., A. Ross, et al. (2006). "Probabilistic quotient normalization as robust method to account for dilution of complex biological mixtures. Application in 1H NMR metabonomics." Analytical chemistry **78**(13): 4281-4290.

Dumas, M.-E., R. H. Barton, et al. (2006). "Metabolic profiling reveals a contribution of gut microbiota to fatty liver phenotype in insulin-resistant mice." Proceedings of the National Academy of Sciences of the United States of America **103**(33): 12511-12516.

Ernst J. and Z. Bar-Joseph (2006). "STEM: a tool for the analysis of short time series gene expression data." BMC Bioinformatics **7**: 191.

Geurts L, V. Lazarevic, et al. (2011). "Altered gut microbiota and endocannabinoid system tone in obese and diabetic leptin-resistant mice: impact on apelin regulation in adipose tissue." Frontiers in Cellular and Infection Microbiology.

Hayashi, H., R. Takahashi, et al. (2005). "Molecular analysis of jejunal, ileal, caecal and recto-sigmoidal human colonic microbiota using 16S rRNA gene libraries and terminal restriction fragment length polymorphism." Journal of Medical Microbiology **54**(11): 1093-1101.

Hooper, L. V., T. Midtvedt, et al. (2002). "How host-microbial interactions shape the nutrient environment of the mammalian intestine." Annual Review of Nutrition **22**: 283-307.

Kim, J.-w. and C. V. Dang (2006). "Cancer's molecular sweet tooth and the Warburg effect." Cancer Research **66**(18): 8927-8930.

Kono, H. and K. L. Rock (2008). "How dying cells alert the immune system to danger." Nature Reviews Immunology **8**(4): 279-289.

Korner, J., M. Bessler, et al. (2005). "Effects of Roux-en-Y gastric bypass surgery on fasting and postprandial concentrations of plasma ghrelin, peptide YY, and insulin." Journal of Clinical Endocrinology & Metabolism **90**(1): 359-365.

Kouzaki, H., K. Iijima, et al. (2011). "The Danger signal, extracellular ATP, is a sensor for an airborne allergen and triggers IL-33 release and innate Th2-Type responses." Journal of Immunology **186**(7): 4375-4387.

Krzywanski, D. M., D. A. Dickinson, et al. (2003). "Oxidative stress elevates the molar ratio of glutamate cysteine ligase (GCL) catalytic to modulatory subunits." Free Radical Biology and Medicine **35**: S69-S69.

Li, M., B. Wang, et al. (2008). "Symbiotic gut microbes modulate human metabolic phenotypes." Proceedings of the National Academy of Sciences of the United States of America **105**(6): 2117-2122.

O'Hara, A. M. and F. Shanahan (2006). "The gut flora as a forgotten organ." Embo Reports **7**(7): 688-693.

Oppenheim, J. J. and D. Yang (2005). "Alarmins: chemotactic activators of immune responses." Current Opinion in Immunology **17**(4): 359-365.

Poelstra, K., E. R. Heynen, et al. (1992). "Modulation of anti-Thy1 nephritis in the rat by adenine-nucleotides-evidence for and antiinflammatory role for nucleotidases." Laboratory Investigation **66**(5): 555-563.

Pories, W. J., M. S. Swanson, et al. (1995). "Who would have thought it-An operation proves to be the most effective therapy for adult-Onset diabetes mellitus." Annals of Surgery **222**(3): 339-352.

Rajilic-Stojanovic, M., H. G. H. J. Heilig, et al. (2009). "Development and application of the human intestinal tract chip, a phylogenetic microarray: analysis of universally conserved phylotypes in the abundant microbiota of young and elderly adults." Environmental Microbiology **11**(7): 1736-1751.

Rubic, T., G. Lametschwandtner, et al. (2008). "Triggering the succinate receptor GPR91 on dendritic cells enhances immunity." Nature Immunology **9**(11): 1261-1269.

Rubino, F. (2006). "Bariatric surgery: effects on glucose homeostasis." Current Opinion in Clinical Nutrition and Metabolic Care **9**(4): 497-507.

Rubino, F., T. A. Moo, et al. (2009). "Diabetes surgery: a new approach to an old disease." Diabetes Care **32**: S368-S372.

Snell, K. and G. Weber (1986). "Enzymatic imbalance in serine metabolism in rat hepatomas " Biochemical Journal **233**(2): 617-620.

Spicer, S. S. (1965). "Diamine methods for differentiating mucosubstances histochemically." Journal of Histochemistry & Cytochemistry **13**(3): 211-34.

Tilg, H. and A. Kaser (2011). "Gut microbiome, obesity, and metabolic dysfunction." Journal of Clinical Investigation **121**(6): 2126-2132.

Tong, X., F. Zhao, et al. (2009). "The molecular determinants of de novo nucleotide biosynthesis in cancer cells." Current Opinion in Genetics & Development **19**(1): 32-37.

Troy, S., M. Soty, et al. (2008). "Intestinal gluconeogenesis is a key factor for early metabolic changes after gastric bypass but not after gastric lap-band in mice." Cell Metabolism **8**(3): 201-211.

Trygg, J. and S. Wold (2003). "O2-PLS, a two-block (X-Y) latent variable regression (LVR) method with an integral OSC filter." Journal of Chemometrics **17**(1): 53-64.

Turnbaugh, P. J., R. E. Ley, et al. (2006). "An obesity-associated gut microbiome with increased capacity for energy harvest." Nature **444**(7122): 1027-1031.

Vessey, D. A. and D. Zakim (1981). "Inhibition of glutathione S-transferase by bile-acids." Biochemical Journal **197**(2): 321-325.

Vila-Brau, A., A. Luisa De Sousa-Coelho, et al. (2011). "Human HMGCS2 Regulates Mitochondrial Fatty Acid Oxidation and FGF21 Expression in HepG2 Cell Line." Journal of Biological Chemistry **286**(23): 20423-20430.

Waters, N. J., E. Holmes, et al. (2002). "NMR and pattern recognition studies on liver extracts and intact livers from rats treated with alpha-naphthylisothiocyanate." Biochemical Pharmacology **64**(1): 67-77.

Waxman, D. J. (1990). "Glutathione S-transferases-Roles in alkylating agent resistance and possible target for modulation chemotherapy-A review." Cancer Research **50**(20): 6449-6454.

Williams, D. B., J. C. Hagedorn, et al. (2007). "Gastric bypass reduces biochemical cardiac risk factors." Surgery for Obesity and Related Diseases **3**(1): 8-13.

Windmuel.Hg and A. E. Spaeth (1974). "Uptake and metabolism of plasma glutamine by small-intestine " Journal of Biological Chemistry **249**(16): 5070-5079.

Wu, G. Y. (1998). "Intestinal mucosal amino acid catabolism." Journal of Nutrition **128**(8): 1249-1252.

Chapter 4

The Interplay between Gut Microbiota, Host-Transcriptome, and Metabolism in the Mouse Colon during Conventionalization

Sahar El Aidy, Muriel Derrien, Claire A. Merrifield, Mark Boekschoten, Florence Levenez, Joël Doré, Jan Dekker, Elaine Holmes, Erwin Zoetendal, Sandrine P. Claus, Peter van Baarlen, and Michiel Kleerebezem

To be submitted

ABSTRACT

The interplay between dietary nutrients, gut microbiota, and mammalian host tissues of the gastrointestinal tract is recognized as highly relevant for host health. In this study, we employed a combination of transcriptomic, metabonomic, and microbial profiling tools to analyze the dynamic responses of germfree C57/BL6 J mouse colonic mucosa to conventionalization by normal mouse microbiota at different time-points during 16 days. The colonizing microbiota showed a shift from low (days 1 and 2) towards a high diversity (days 8 and 16). The dynamic changes in the microbial community were rapidly reflected by the urine metabolic profiles (day 1) and at later stages (day 4 onward) by the colon mucosa transcriptomes, and metabolic profiles. A major part of the dynamic transcriptome alterations in the colon mucosa included gene expression that control key metabolic pathways, including glycolysis, glycan biosynthesis and degradation, and amino acid and nucleotide metabolism. Altered gene expression correlated with altered levels of specific tissue metabolites that all participated in the metabolic pathways listed above. Correlations of host transcriptomes, metabolite patterns, and microbiota composition were modeled and revealed correlations between Bacilli and Proteobacteria and differential expression of host genes involved in energy and carbohydrate, glycerophospholipid, and anabolic metabolism. Differential gene expression did strongly correlate with *scyllo*-, and *myo*-inositol, glutamine, glycine, and alanine levels in colonic tissues during the time span of conventionalization. The results of the time-resolved multi-variate analyses that were applied here may help to expand our knowledge of host-microbe molecular interactions during the microbial establishment.

Introduction

The mammalian gastrointestinal (GI) tract is home to an estimated 100 trillion microbial cells, representing the largest microbial community associated with the mammalian body (Savage 1977; Lee and Mazmanian 2010). This complex ecosystem provides a vast reservoir of metabolic capabilities that complement the metabolism of the host (Bäckhed, Ding et al. 2004; Nicholson, Holmes et al. 2005; Turnbaugh, Hamady et al. 2009) and plays a crucial role in several developmental and nutritional processes in the intestine (Kau, Ahern et al. 2011). The colon is the most prominent site of microbial colonization, with bacterial densities reaching up to 10^{12} per gram of content (O'Hara and Shanahan 2006). Nevertheless, the effects of the intestinal microbiota can be observed in diverse regions of the host. "Top-down" systems biology using metabolic profiling of conventional mice revealed large, systemic effects of the microbial community on absorption, storage, and metabolism of dietary compounds in the blood, urine, liver, and feces (Martin, Wang et al. 2007; Claus, Tsang et al. 2008). These, and other studies, have demonstrated that host metabolism is responsive to intestinal-microbial metabolism which provides complementary pathways for dietary ingredients and drugs (Nicholson, Holmes et al. 2005).

There has been a clear influence of changes in the human diet on gut microbiota, to the extent that there appears to have been a coevolution between the diet, human population, and the composition of the human microbiota (Walter and Ley 2011). The microbiota is composed of well-established, resident bacteria that form long-term associations with the host, as well as transient bacteria that do not colonize the GI tract permanently. This large and dynamic community undergoes dramatic changes after initial colonization of the sterile-born host (Hooper 2004; Palmer, Bik et al. 2007). During colonization, all microbes compete with other residing microbes and are under attack by the host's defense systems (Ley, Peterson et al. 2006). Stable establishment of microbial groups requires cooperation in food networks, where metabolites from one organism can act as a substrate for another (cross-feeding) (Duncan, Holtrop et al. 2004; Fischbach 2011).

In the intestinal microbial ecosystem, the most prominent microbial activity is the fermentation of dietary or host-derived components, in particular, the conversion of non-digestible carbohydrates and host glycans into short chain fatty acids (SCFAs) (Bäckhed, Ding et al. 2004). SCFAs activate a G-protein coupled receptor 43 (*Gpr43*), which has been reported to play an important role in immune modulation (Maslowski, Vieira et al. 2009) and plays a key-role in the regulation of energy balance (Bjursell, Admyre et al. 2011). In addition to fermentation of dietary or host glycans, the microbiota synthesizes essential vitamins such as vitamin k and certain B vitamins; these vitamins have to be supplemented in higher amounts in diets for germfree animals (Hooper, Midtvedt et al. 2002). The extensive chemical and macromolecular cross-talk between the microbiota and the host has a marked impact on the host mucosa and its local and systemic metabolic profile (Bäckhed, Ley et al. 2005) to such extent that the co-evolution of the host-microbe interaction has enabled mammals to harvest nutrients from novel sources (Bäckhed, Ley et al. 2005; Walter and Ley 2011). In return, the gut microbiota are provided with a ''protected'', nutrient-rich niche that enables bacterial multiplication (Hooper, Midtvedt et al. 2002), and that has been proposed to provide high-affinity adhesion sites for specific microorganisms to accommodate their persistence in the intestine (Bäckhed, Ley et al. 2005). Such adaptive accommodation of specific microbes by the host stimulates their colonization thereby contributing to the colonization resistance against incoming pathogenic

bacteria (Hultgren, Abraham et al. 1993, Salyers and Pajeau 1989).
There is increasing evidence for an association between interference in the symbiotic microbiota-host relations via changes in proper microbial colonization (dysbiosis) and development of human disease (Neish 2009). Dysbiosis of the microbial community has been associated with a variety of diseases including inflammatory bowel disease and colon cancer (Azcárate-Peril Andrea M. 2011) along with systemic diseases (Huycke and Gaskins 2004) such as obesity (Bäckhed, Ding et al. 2004; Bäckhed, Manchester et al. 2007). In view of the increasing awareness of disease-associated shifts in intestinal microbiota communities, it is important to improve our understanding of the molecular basis and dynamics of the 'normal' interrelations governing intestinal homeostasis. To this end, we aimed to monitor the succession of microbial colonization and the dynamic molecular alterations in the host-microbe metabolic relationship. Following conventionalization, the time-resolved composition of colonic microbial communities was determined in parallel with colon mucosa transcriptomes and ^{1}H NMR spectroscopic profiling of the colonic tissue and urine. Statistical modeling showed correlations between microbial diversity and host transcriptomics and metabonomics and allowed us to reconstruct a comprehensive overview of the transient and more permanent alterations in the symbiotic host-microbe relationship.

RESULTS

Dynamic Establishment of Microbial Communities
The colonic microbiota composition of conventionalized mice was assessed for five time-points post-conventionalization using the mouse intestinal tract (MIT)Chip phylogenetic platform that allows profiling of murine gut microbiota. Previously, we described a composition shift in the microbiota during the conventionalization period (Chapter 2). The colonic microbiota of conventionalized mice proceeded through two major stages discriminated by low diversity of the microbiota during early stages (days 1-2) and increasing microbial diversity at later stages (days 8 and 16) of conventionalization, ultimately reaching levels similar to those observed in conventional animals. MITChip analysis confirmed that this early-to-late shift is characterized by early, rapid colonizers (days 1-2) belonging predominantly to the phyla Bacteroidetes, Firmicutes, Proteobacteria, and Actinobacteria, while at later stages (days 4, 8, and 16 post-conventionalization) specific subgroups of the Firmicutes, particularly the members of *Clostridium* clusters IV and XIVa increased in abundance, (Figure 4.1). Days 1 and 2 post-conventionalization were characterized by relatively high abundance of genera like *Enterococcus (Enterococcus urinaeequi et rel), Bacteroides fragilis et rel., Prevotella, and Lactobacillus salivarius* (Table S4.1). Days 8 and 16 post-conventionalization were typically characterized by an increased abundance of genera such as *Dorea, Butyrivibrio crossotus et rel,* and unclassified TM7 (Table S4.1). Taken together, MITChip analysis identified the microbial communities that had established in the colon of mice over time during conventionalization. Moreover, the detailed analysis identified the dynamic abundance of the microbial groups that comprised the climax community. This community appeared to be established from day 8 post-conventionalization onward, and strongly resembled the inoculum (conventional) microbiota in terms of composition and abundance. The established microbial community was characterized by a general increase of anaerobes and distinct colonization patterns of the major groups Bacteroidetes and *Clostridium* clusters IV and XIVa.
In addition to determination of the phylogenetic composition of the microbiota, gene-specific

qPCR was employed to quantify the relative abundance of the 16 S rRNA gene and specific functional genes within the intestinal microbiota ecosystem. For the latter, well-studied marker key-genes that belong to the pathways of sulfate reduction (dissimilatory sulfite reductase *(dsr)* gene); (Ben-Dov, Brenner et al. 2007)) and methanogenesis (methyl coenzyme-M reductase *(mcrA)* gene); (Steinberg and Regan 2008)) were used. *Dsr* and *McrA* were targeted to monitor the succession of hydrogen-utilizing species (sulfate reducers and methanogens), which ensure efficient H_2 removal to maintain fermentation balance in the colon (Gibson, Macfarlane et al. 1993). Butyrate producers were detected by butyrate production and *butyryl-CoA-transferase* (Louis and Flint 2007). The overall microbial community size as estimated by 16S rRNA gene copy number per gram of colonic content was stable at a level of approximately 11.63±0.59 (expressed as log10) during conventionalization experiment (Chapter 2). In agreement with this apparent stable 16 S rRNA gene abundance, the relative abundance of the *mcrA* gene appeared to be stable and stayed at low levels (4.82±0.82 at day 1, 5.2±0.26 at day2, 5.15±0.76 at day 4, 3.82±1.18 at day 8, and 4.93±0.64 at day16) (expressed as log10), over the entire duration of the conventionalization, suggesting that the methanogen population was among the early colonizers and had already reached its final population site early in the experiment. In contrast, the *dsr* gene appeared to be approximately 100-fold more abundant in the ecosystem during later stages of the conventionalization (Figure 4.2A), increasing from approximately 2.54±0.2 (expressed as log10) during days 1-2 to 4.4±0.86 (expressed as log10) at days 4, 8 and 16 post-conventionalization. Additionally, the *butyryl-CoA* gene abundance in the ecosystem increased more than 100 folds from approximately 9.3±0.42 at days 1-2 to 11.87±0.78 (expressed as log10) on days 8 and 16 post-conventionalization, while the microbial ecosystem on day 4 post-conventionalization appeared to contain an intermediate abundance of this gene (10.5±0.96 (expressed as log10)). These results are in accordance with phylogenetic analysis of the community where the relative populations of typical sulfate reducing organisms such as *Bilophila* and *Desulfovibrio* and butyrate producing organisms like *Roseburia intestinalis et rel*, *Subdoligranulum*, *Faecalibacterium prausnitzii et rel*, and *Butyrivibrio* (Table S4.1) appeared to increase during later stages of conventionalization (days 4, 8, and 16 for the sulfate reducers and days 8 and 16 for butyrate producers).

Dynamics of Microbial Fermentation End-Products The phylogenetic analysis predicted a change in global fermentative capacities of the microbiota, with a shift towards increased production of butyrate at later time-points. To assess the fermentative capacities of the successive microbial communities, concentrations of the short-chain fatty acids (SCFAs) acetate, propionate, butyrate, as well as lactate and succinate were determined in cecal contents. Especially lactate and succinate, together with relatively high amounts of acetate and propionate dominated the microbial fermentation-profile measured during the early stages of conventionalization (days 1-2 and to lesser extend day 4), whereas butyrate concentrations were below the detection limit (0.11 μmole/mg). The concentrations of fermentation metabolites drastically shifted at later stages of conventionalization (days 8 and 16 post-conventionalization) when lactate and succinate levels were decreased below the detection limit and acetate and propionate were significantly increased (Figure 4.2B). Moreover, butyrate was also clearly detected at these later stages, which correlates very well with the increased abundance of butyrate producers (as shown above).

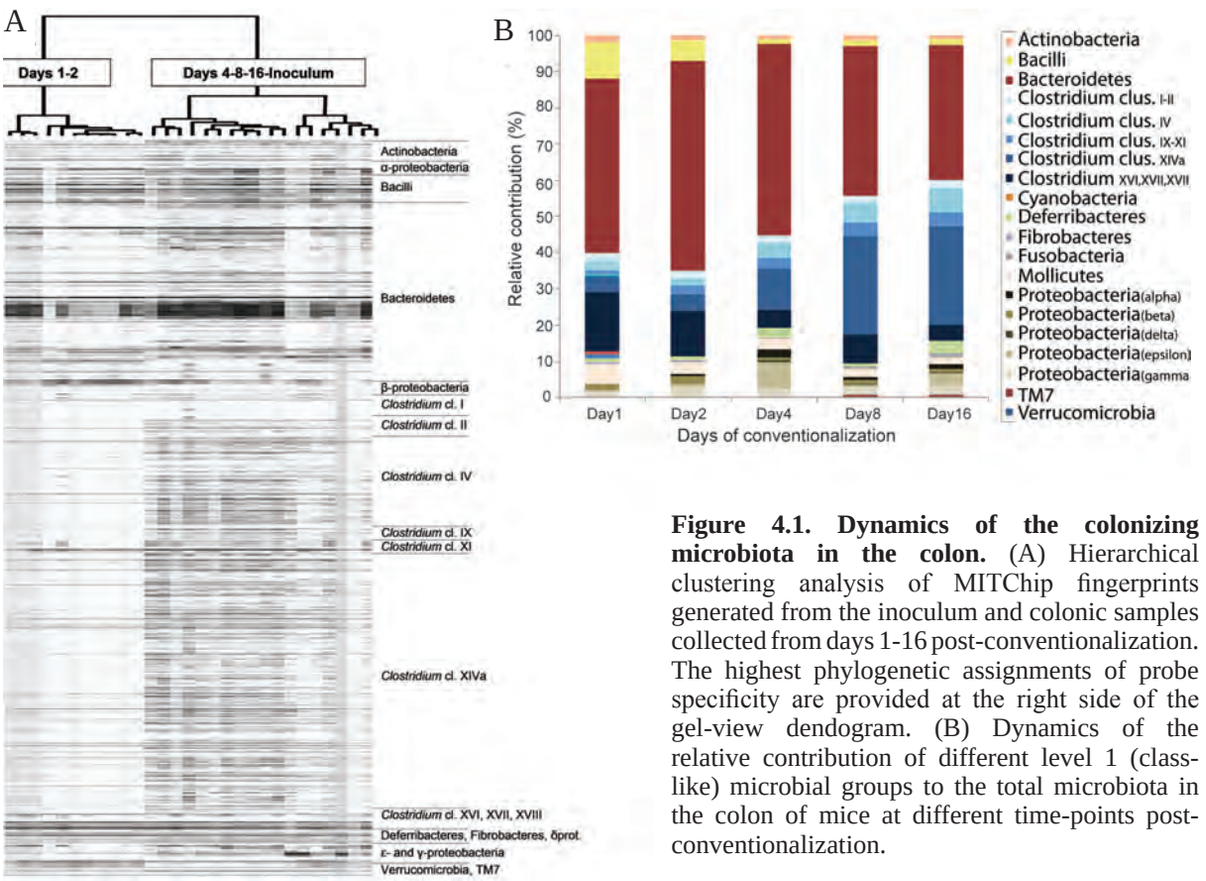

Figure 4.1. Dynamics of the colonizing microbiota in the colon. (A) Hierarchical clustering analysis of MITChip fingerprints generated from the inoculum and colonic samples collected from days 1-16 post-conventionalization. The highest phylogenetic assignments of probe specificity are provided at the right side of the gel-view dendogram. (B) Dynamics of the relative contribution of different level 1 (class-like) microbial groups to the total microbiota in the colon of mice at different time-points post-conventionalization.

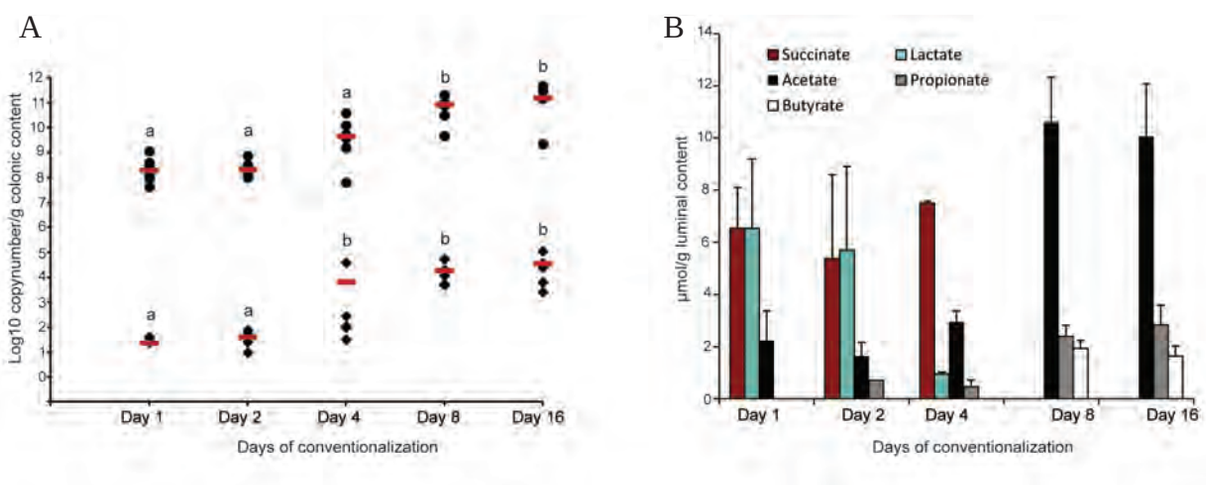

Figure 4.2. **Dynamics of specific functional gene abundance in the microbiota.** (A)Quantification of butyrate producers and sulfate reducers expressed as mean ± SD log10 number of *ButyrylCoA*(•) and *dsr* (♦) genes /g content respectively. Statistical analysis was performed using a one-way ANOVA test executed in SPSS Statistics 17.0 (SPSS Inc., Chicago, IL). Significant differences between time-points are indicated by distinct characters above the measurement groups ($p < 0.05$). (B) HPLC analysis of the large intestinal content for SCFAs including acetate, butyrate, propionate, lactate, and succinate.

Colon Mucosa Transcriptome Profiling Focusing on Metabolic Functions

Previously we established a time- and location-dependent modulation of gene expression profiles during conventionalization, in which the colon mucosa transcriptomes supported the establishment of a novel state of homeostasis within 16 days of conventionalization (Chapter 2). One set of genes that showed time-dependent differential expression in the colon was significantly enriched ($p < 0.001$) for the gene ontology (GO) category "metabolic processes". The genes belonging to this GO category were further analyzed by ingenuity pathway analysis (IPA), which illustrated their involvement in a variety of carbohydrate, lipid, glycolysis/gluconeogenesis, amino acid, and nucleotide metabolism associated pathways (Figure 4.3).

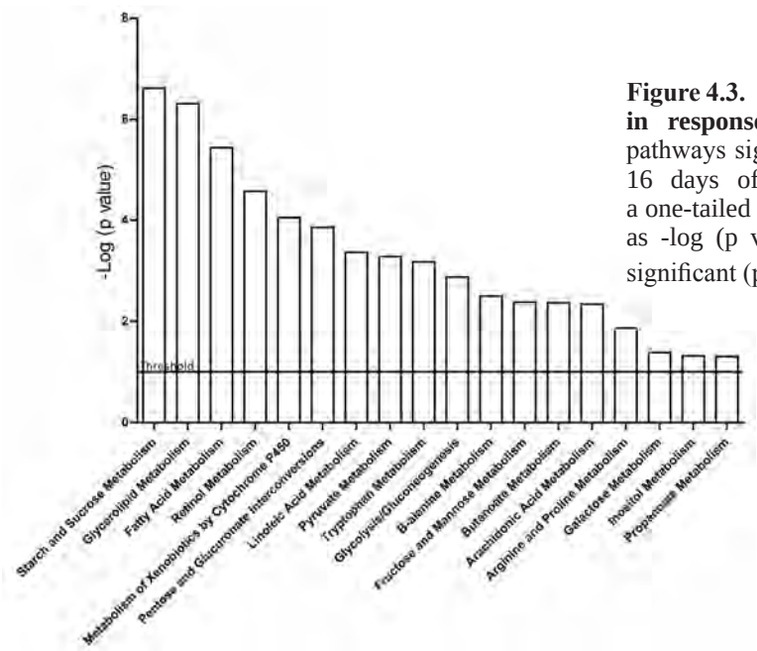

Figure 4.3. Significantly altered signaling pathways in response to microbial colonization. Cellular pathways significantly modulated in the colon during 16 days of conventionalization as calculated via a one-tailed Fisher's Exact test in IPA and represented as -log (p value); -log values exceeding 1.30 were significant ($p < 0.05$).

To predict possible metabolic consequences of the changing metabolic gene expression profiles during conventionalization, gene expression changes were projected onto KEGG metabolic maps (Figure 4.4). These projections showed a significant modulation of glycolytic, amino acid, and nucleotide metabolic pathways on days 4, 8, and 16, in comparison to day 0 (germfree mice) and earlier days (1 and 2) post-conventionalization. The significant induction of nucleotide synthesis and metabolism pathways were illustrated by the induction of thymidylate synthase (*Tyms*) and ribonucleotide reductase (*Rrm1* and *2*), which is an essential enzyme for the production of deoxyribonucleotides (Parker, Begley et al. 1995). The colonic metabolism also underwent dynamic changes in expression of genes involved in amino-acid metabolism, including the glutamine and glutamate associated pathways. This was apparent from the induction of *Asns* (asparagine synthetase), and the repression of the *Glul* (glutamine synthetase), *Glud1* (mitochondrial glutamate dehydrogenase), and *Abat* (4-aminobutyrate aminotransferase or GABA transaminase), which converts 4-aminobutyrate into oxaloglutarate and glutamate. The strong downregulation of the genes encoding *Sord* (sorbitol dehydrogenase), *Sis* (sucrase isomaltase), and *Gbe1* (glucan [1,4-alpha-], branching enzyme 1), suggests that carbohydrate metabolism is repressed. Moreover, also inositol and choline metabolism appeared to be repressed, which was inferred from decreased expression of *Chpt1* (choline phosphotransferase 1) and *Chkb* (choline kinase beta). *Fut2* (fucosyltransferase 2) and *B3galt5* (UDP-Gal:betaGlcNAc

beta 1,3-galactosyltransferase, polypeptide 5) involved in glycosphingolipid biosynthesis were upregulated from day 1 post-conventionalization onward. These transcriptome changes illustrate the dynamic changes in the expression of metabolic pathway genes in the colon mucosa upon conventionalization, which encompass a broad area of intracellular (amino acid, glycolysis, and nucleotide metabolism) as well as membrane (sphingolipid) and extracellular matrix (glycan biosynthesis) metabolic pathways.

The Dynamics of Local and Systemic Metabolic Profiles

Metabolic phenotyping using ^{1}H NMR, was performed on colonic tissue and urine samples from germfree and conventionalized mice to investigate the impact of the colonizing gut microbiota on host colonic metabolism during conventionalization. Tissue metabolic profiling was performed to measure changing concentrations of metabolites as a result of changes in the mucosal amino acid and energy metabolism, while urine metabolic profiling was employed as a proxy for the systemic metabolic changes. The time-resolved metabolite datasets were used to build orthogonal partial least-square discriminant analysis (OPLS-DA) models, focusing on the differences between germfree and conventionalized animals over time. The analysis showed that the presence of microbiota was not significantly reflected by the colonic mucosa metabolic profiles during the first two days of conventionalization (days 1-2). However, during the later time-points (days 8 and 16) of conventionalization, the microbial colonization was detectable in the mucosal metabolite profiles through significantly increasing levels of alanine, fumarate, glycine, uracil, and methylmalonate† (†=tentative assignment), and decreasing levels of glycerol, glucose, and formate. Some, but not all, changes in these metabolic profiles appeared to be initiated at day 4 post-conventionalization (Figure 4.5A). In addition, concentrations of several mucosal metabolites appeared to transiently respond to conventionalization, including modulated levels of acetate, aspartate, glutamine, *scyllo*-inositol, tyrosine, and choline, taurine, and phosphorylcholine (Figure 4.5A). Contrary to the tissue metabolite data, urine metabolite profiles appeared to reflect the consequences of microbial colonization during the early time-points (days 1-2), where the excretion of metabolites such as creatine and formate were increased on day 1 and days 1-2 post-conventionalization, respectively. Whereas concentrations of the urine metabolites 2-hydroxy-3-methylvalerate, trimethylamine, TMAO, β-aminoisobutyrate and β-hydroxybutyrate†, appeared to fluctuate (Figure 4.5 B), the metabolites tryptophan and phenylacetylglycine were consistently detected at a higher level during conventionalization as compared to germfree animals. The identified changes in the local and systemic metabolic profiles appeared to coincide with the transcriptome shifts and the succession of the microbial communities that established during the conventionalization period. Statistical modeling (using O2PLS methods) was employed to detect significant correlations between microbial groups and the mucosal transcriptomes, the mucosal and urine metabolic profiles.

Microbiota, Metabolite, Transcriptome Correlation Mining

O2-PLS regression-models (Trygg and Wold 2003) between ^{1}H NMR urine spectra and level-2 (genera-like) MITChip absolute abundance scores were performed to search for statistically and biologically meaningful correlations between microbial taxa in the colon, colon transcriptomes, and concentrations of specific metabolites. The MITChip probe intensities that were best predicted by the variation in the ^{1}H NMR data were assigned to level-2 groups within the phylum *Bacteroidetes*. The closest relative isolates of the identified genera included, *Prevotella ruminicola et rel., Alistipes, Rikenella,* and *unclassified Porphyromonadaceae.* O2-PLS

modeling found multiple correlations between these microbial groups and the urine metabolites, fumaric acid, 2-oxo-glutaric acid, and malic acid† (Figure S4.1).

A similar modeling strategy was also employed to search for correlations between colonic tissue ^{1}H NMR metabolomes and transcriptomes. The positive and negative correlations that could be identified were visualized by correlation heat maps (Figure S4.2). During conventionalization, the metabolites glutamate, alanine, and glycine were significantly correlated with a set of induced genes that play role in multiple metabolic pathways, including nucleotide metabolism, and O- and N-glycan biosynthesis and degradation. In contrast, the tissue concentrations of *scyllo*- and *myo*-inositol were positively correlated with a set of repressed genes that also played roles in multiple metabolic pathways, including phosphoglycerolipid metabolism, sialylated glycan biosynthesis and degradation, and glycine and serine metabolism.

Correlation analysis of changes in colonic tissue metabolites, host metabolic gene expression, and microbiota taxonomical assignments illustrated that level-1 (MITChip level-1, class-like) microbial groups correlated to subsets of genes within the mucosal transcriptome data. More specifically, a positive correlation between Bacilli with a subset of the genes of which expression was positively correlated with *scyllo*- and *myo*-inositol concentrations was identified. Analogously, a positive correlation between alpha- and epsilon-proteobacteria and a subset of the genes of which the expression correlated with tissue concentrations of glutamate, alanine, and glycine (Figure S4.3). The O2-PLS correlation analysis found strong correlations between changes in the microbial colonizers of the colon, subsets of genes from the tissue transcriptomes and concentrations of specific tissue metabolites. These statistical correlations can be assumed to be of biological relevance since the differentially expressed genes and the correlating metabolites belong to coherent metabolic pathways.

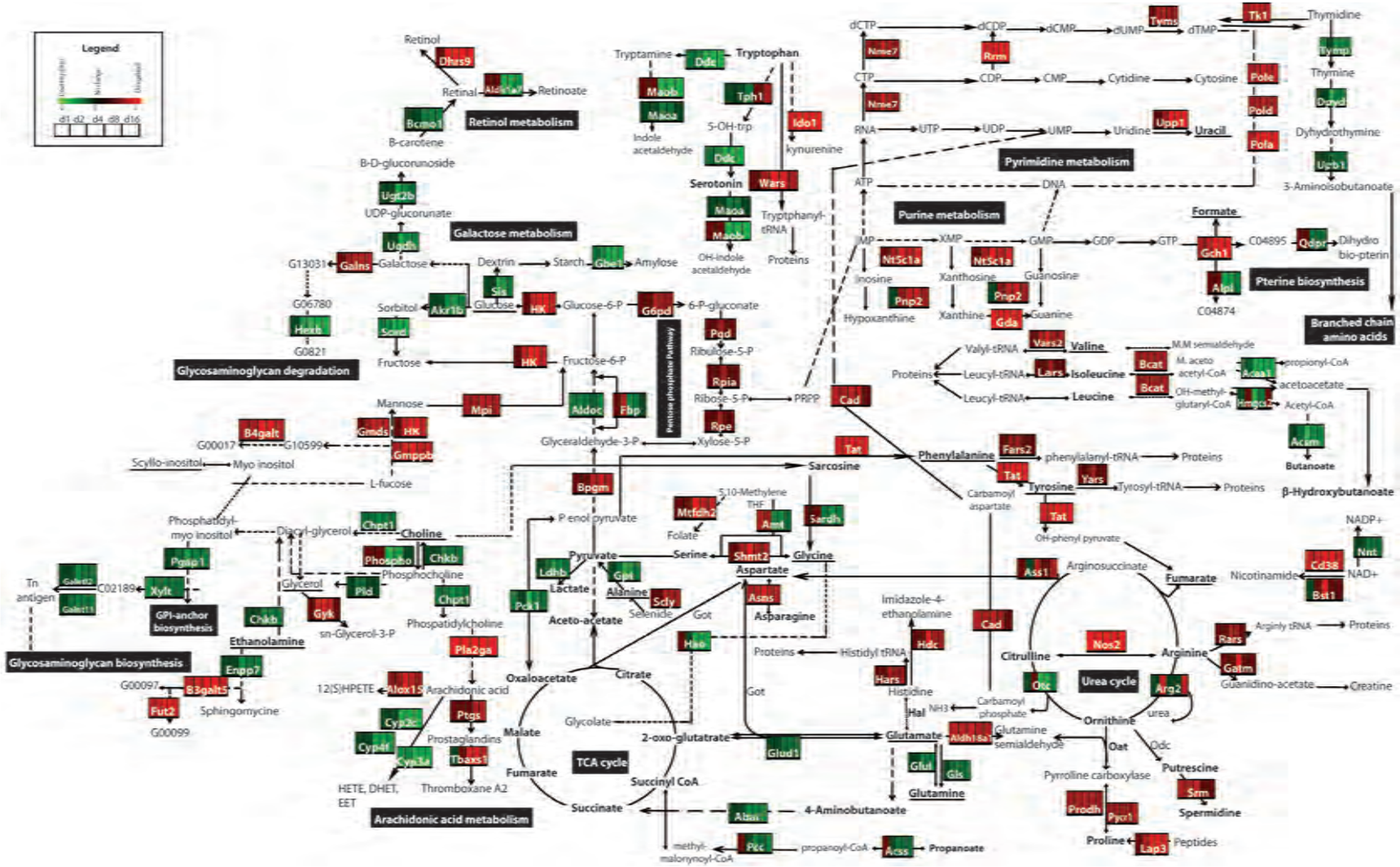

Figure 4.4. Metabolic pathway map including the genes that participate in certain metabolic pathways conversions. Genes are indicated in box symbols; each box is divided into 5 sub-boxes with color codes representing the changes observed at days 1, 2, 4, 8, and 16 post-conventionalization, respectively. Red color represents upregulated genes and green color represents downregulated genes over control (germfree). The metabolites that changed during conventionalization in the colonic tissue as detected by ^{1}H NMR are underlined. Direct and indirect interactions are depicted by solid and dashed arrows respectively.

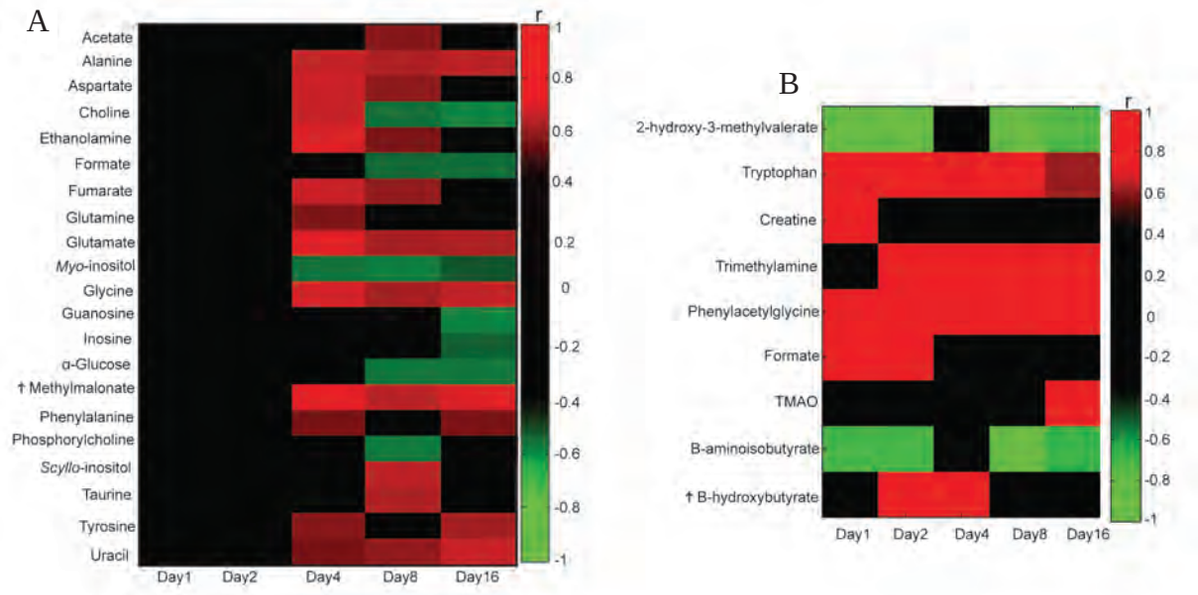

Figure 4.5. Heat map summarizing the colonic metabolic variation during conventionalization. A series of pair-wise OPLS-DA models were constructed for (A) colon tissue, and (B) urine metabolite profiles with significant modulation during the days(d) 1-16 post-conventionalization period, compared to germfree. Red color represents an increased level and green color represents a decreased level. (†) refers to tentative assignment.

DISCUSSION

Several studies have shown that interactions between colonic microbes and germfree mice, lead to basal changes in host metabolism (Bäckhed, Ding et al. 2004; Nicholson, Holmes et al. 2005; Turnbaugh, Hamady et al. 2009). However these changes have hardly been investigated at a multi-variate and time-resolved molecular level. Here a time-resolved multi variate approach was employed to investigate the interactions between colonizing microbes and colonic transcriptome and metabonome, as well as systemic changes in metabonome based on urine metabolites. Our study employed a reductionist experimental design, using germfree mice that were conventionalized and taking samples at specific time-points over a period of 16 days. Detailed analysis of the composition of the colonizing microbiota demonstrated that the establishment of microbiota in the mouse colon is characterized by two major phases. The early, transient phase (days 1 and 2) showed low microbial diversity with typical formate, lactate, and succinate production, while the later phase that appeared to be more stable showed more diverse microbial communities that resembled the inoculum. The latter state is characterized by expansion of the sulfate reducers such as *Desulfovibio spp.* and the strict anaerobic species belonging to the major Clostridia clusters such as *Clostridium* cluster IV and XIVa that contain butyrate producers. This bacterial expansion was confirmed by the qPCR detection of the genes associated with these bacterial groups (*dsr* and *butyryl CoA*, respectively). At day 4 post-conventionalization, transient colonization by some Proteobacteria was found. These microbiota colonization succession showed statistically significant and biologically relevant correlations with alterations in the gene-expression patterns and metabolite profiles from the colonic-tissue . These colonic mucosa correlations were especially significant from day 4 post-conventionalization and onward. In contrast, statistical correlations between systemic

metabolite concentrations that were measured in urine samples could be detected at earlier time-points during conventionalization (i.e., days 1-2), suggesting a rapid and transient systemic metabonome-change by altered metabolite absorption from the gut. This implies that already 1 day after microbial colonization of the intestine, the presence of the microbiota led to changed systemic metabolites profiles that are most likely due to altered luminal metabolite profiles and their absorption by the intestine. Remarkably, such absorption changes did not appear to induce changes in gene expression profiles in the colon mucosa, and may therefore derive from more proximal regions of the intestine (Chapter 3).

Clear correlation was found between the abundance of *Prevotella ruminicola et rel.* with the urine concentrations of the metabolites, fumaric acid and 2-oxo-glutaric acid. This correlation may have reflected a temporarily decreased utilization of tricarboxylic acid (TCA) cycle intermediates by the host. Alternatively, these metabolites could have been derived from the bacterial metabolism, which would be in agreement with the capacity of the correlated bacterial groups to produce oxaloglutarate by reductive carboxylation of succinate (Henderson 1980). Succinate was detected at high levels in the cecal lumen from 1 to 4 days post-conventionalization. The early stages of conventionalization of the colon were also characterized by accumulation of lactate, which can be formed by intestinal lactic acid bacteria or by a variety of other microorganisms in the gut ecosystem (Barcenilla, Pryde et al. 2000). It is of relevance that the results have shown that the initial microbial ecosystem that establishes during the first days of conventionalization (days 1-2) appears to be relatively ineffective in the extraction of energy from dietary materials, which is exemplified by the accumulation of "high-energy fermentation metabolites" such as lactate and succinate. At later days, the subsequent establishment of typical secondary fermenters in the microbial ecosystem such as the members of the *Clostridium* clusters IV, XIVa, and sulfate reducers led to depletion of lactate and succinate in the colonic lumen. The increasing concentrations of typical secondary metabolites such as propionate, butyrate, and acetate in the colon lumen, known to be produced by the Clostridia and sulfate reducers (Falony, Vlachou et al. 2006; Flint, Bayer et al. 2008; Marquet, Duncan et al. 2009), provides support for the secondary conversion of lactate and succinate by these bacteria. These later stage developments in the microbiota community are paralleled by prominent changes in the colon-mucosa transcriptome- and metabolite-profiles. One gene of which the expression showed a reasonable association with the microbial colonization was *Gpr43* , a gene encoding a GPCR that can recognize SCFAs (Brown, Goldsworthy et al. 2003) , and has been proposed to constitute a molecular link between diet, microbiota, and immune responses (Maslowski, Vieira et al. 2009). *Gpr43* play a key-role in the resolution of inflammatory responses, which is in agreement with our previous findings that highlighted the development of adaptive immune responses, including the development of tolerance that accommodated the microbiota by day 16 post-conventionalization (Chapter 2). The established homeostasis was also associated with the appearance of butyrate in the colon where it has been proposed to serve as the primary energy source for colonocytes (Donohoe, Garge et al. 2011) and plays an important role in regulation of fatty acid oxidation (Vanhoutvin, Troost et al. 2009). The mitochondrial hydroxy-3-methylglutaryl-CoA synthase (*Hmgcs2*), which is involved in fatty acid oxidation (Scheppach W 1995) has been shown to be regulated by butyrate production by the intestinal microbiota (Cherbuy, Andrieux et al. 2004). The temporarily decreased expression of *Hmgcs2* at day 4 post-conventionalization but not at later time-points may illustrate a transient impairment in β-oxidation.

The decreasing concentrations of inositol metabolites was strongly correlated with the decreased

expression of genes encoding enzymes involved in metabolism of inositol, choline, and related metabolic pathway involved in the assimilation of sarcosine, glycine, and betaine. These modulations of the inositol- and related metabolic pathways could also be associated with the intestinal colonization by bacteria that can metabolize choline into methylamines (Kiene 1998). This may be reflected by the increased levels of its derivative-metabolites, TMA and TMAO that were identified in the urine samples of conventionalized mice which is in agreement with previous reports (Nicholls, Mortishire-Smith et al. 2003). Interestingly, TMA and subsequent TMAO production by gut microbiota has recently been reported to promote atherosclerosis and cardiovascular diseases (Wang, Klipfell et al. 2011). This further supports the importance of improved understanding of the microbe-host metabolic interaction in view of its link to risk of disease of the host.
This study also identified a statistical correlation between the transiently increased abundance of alpha- and epsilon-proteobacteria, and alterations in tissue and luminal metabolite levels (increased levels of glutamate, alanine, lactate, and glycine, decreased levels of glucose) as well as specific changes in expression of metabolic pathways genes (increased expression of genes involved in the rate limiting steps of glycolysis, amino acid, and nucleotide metabolic pathways). This association appears to be of biological relevance in that it suggests that the colonic metabolism is shifting towards increased energy production via glycolysis and assimilation, via anabolic metabolism, of novel cell components starting at day 4 onward. This proposed assimilation and production of novel cell components correlates well with the morphological changes observed in the tissue during later time-points of conventionalization (Chapter 2).

In conclusion, the time-resolved, multi-variate analysis applied in this study demonstrated statistically significant and biologically relevant correlations between the dynamics of microbiota establishment and the corresponding local host responses in terms of colon tissue transcriptomes and –metabolite profiles as well as systemic adaptations of host metabolism as detected in urine metabolite profiles. We inferred from these correlations that the changes in host transcriptomes and metabolites are exemplary for the establishment of a novel homeostasis that accommodates the microbiota. Based on changes in gene expression and metabolite concentrations, homeostasis was reached in the colon of the mice after 16 days post-conventionalization (Figure 4.6). The transient phases prior to this novel state of homeostasis appeared to include a transient state of dysbiosis apparent from the inefficiency of early colonizing communities to effectively extract energy from the dietary components, leading to accumulation of "high energy metabolites" and impaired fatty acid oxidation. After this initial, transient state, establishment of later colonizers depleted the high-energy metabolites and generated second-stage fermentation SCFAs that can be efficiently metabolized by colonic epithelia. We propose that the dynamic molecular interactions between the microbiota and their hosts presented here revealed metabolic pathways and processes that contributed to the molecular definition of symbiotic, homeostatic interrelations between intestinal microbiota and the colon mucosa.

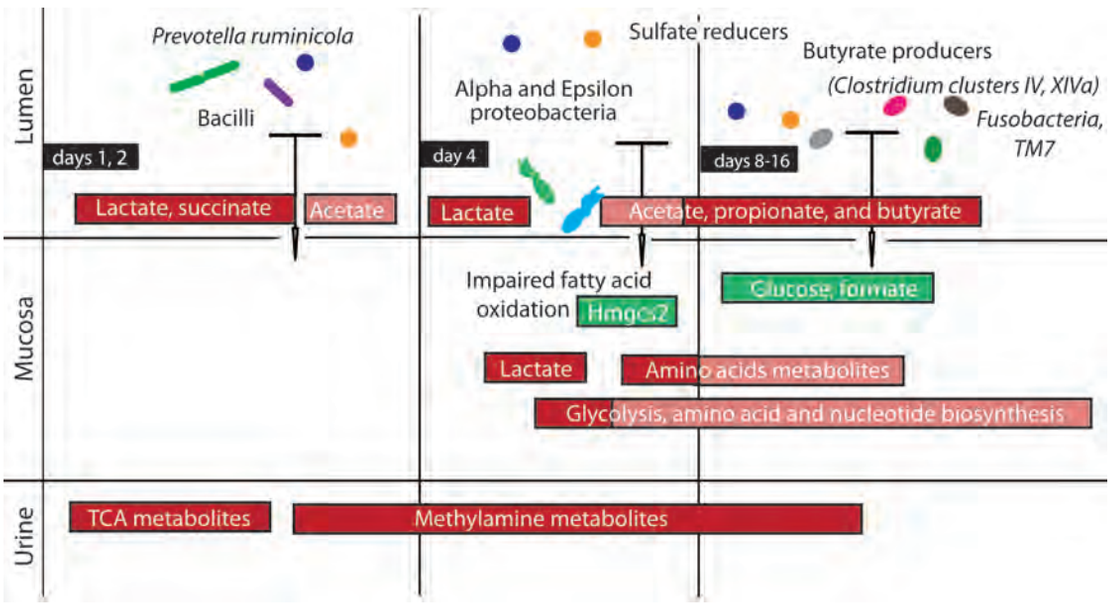

Figure 4.6. Dynamics of the colonizing microbiota and the associated host response. A schematic model of the time-resolved colonic mucosal and urine metabolites changes showing significant correlations with the microbial community. Green color depicts lower levels, red color depicts high levels compared with the germfree measurements . Shades of red depicts the degree of increase (darker = more pronounced effect).

EXPERIMENTAL PROCEDURES

Animals, Experimental Design, and Sampling

All procedures were carried out as previously described (Chapter 2). In brief, germfree and conventionalized mice (male, C57 BL/6 J) were maintained in sterile conditions, on a commercial laboratory chow diet. Two independent biological experiments were performed using mice of different age after 2 weeks of acclimatization and diet adaptation. The first and second experiments included 36 mice obtained in 2 biologically independent batches of 18 mice each, aged 8 and 10 weeks, respectively. The colon from each mouse was removed and divided into 2 cm segments that were immediately: stored in RNAlater® at room temperature for 1 h prior to storage at -80°C for RNA isolation or snap frozen and stored at -80°C for metabolic profiling. Luminal content from colonic segments and cecum was removed by gentle squeezing, snap frozen, and stored at -80°C for microbiota analysis and SCFAs HPLC analyses, respectively. Urine samples (50-70 µl) were collected from the bladder directly after sacrifice and stored at -80°C for metabolites analysis.

Microbial Profiling of Colonic Contents

Luminal contents from colon were analyzed by Mouse Intestinal Tract Chip (MITCHip), a diagnostic 16S rRNA arrays that consists of 3,580 unique probes especially designed to profile murine gut microbiota as previously described and in analogy to the human intestinal tract (HIT)Chip (Rajilic-Stojanovic, Heilig et al. 2009; Geurts Lazarevic et al. 2011). Statistical analysis was performed as previously mentioned (Chapter 2) between all conventionalization days using Kruskal Walis executed in SPSS Statistics 17.0 (SPSS Inc., Chicago, IL).

Quantitative PCR analyses included quantification of total bacteria using 16 S rRNA-specific

primers and gene-specific qPCR, targeting bacterial groups with the following capacity: sulfate reduction, methane production, or butyrate production. QPCR was performed using an IQ5 Cycler apparatus (Bio-Rad, Veenendaal, The Netherlands). Reactions were performed in triplicate in a single run. Samples were analyzed in a 25 µl reaction mixture consisting of 12.5 µl Bio-Rad master mix SYBR Green (50 mM KCl, 20 mM Tris-HCl, pH 8.4, 0.2 mM of each dNTP, 0.625 U iTaq DNA polymerase, 3 mM MgCl2, 10 nM fluorescein), 0.1 µM of each primer (Table S4.2) and 5 µl of template colonic DNA diluted 100 or 1000 times. Standard curves of 16 S rRNA PCR product from pure cultures were created using serial 10-fold dilution of the purified PCR product corresponding to 10^8 to 10^0 16 S rRNA or specific gene. Standards included *Lactobacillus casei* (total bacteria), *Methanobrevibacter arboriphilus* (methanogen), *Desulfovibrio spp*. (sulfate reducer) and *Faecalibacterium prausnitzii* (butyrate producer). The following qPCR conditions were used: 95°C for 10 min, followed by 35 cycles of denaturation at 95°C for 15 sec, annealing temperature for 20 sec, extension at 72°C for 30 sec and a final extension step at 72°C for 5 min. A melting curve was determined at the end of each run to verify the specificity of the PCR amplicons. Data analysis was performed using the Bio-Rad software supplied with the IQ5 Cycler apparatus.

Microbial fermentation product analysis. Cecal content samples were analyzed for SCFAs profiles, including the quantitative detection of acetate, butyrate, propionate as well as lactate and succinate using HPLC (Spectra System, RI-150). Samples of intestinal content (approximately 0.1 g) were thoroughly mixed with four volumes of distilled water. Insoluble residue was removed by centrifugation (15 min at 13,000 g, 4°C). The subsequent supernatant was mixed with the same volume of 1M $HCLO_4$ and mixed organic acid analyses by HPLC as previously described (Starrenburg and Hugenholtz 1991).

Transcriptome Analysis

High quality total RNA was isolated from a 2 cm segment colon by extraction with TRIzol reagent, followed by DNAse treatment and column purification. Samples were hybridized on Affymetrix GeneChip Mouse Gene 1.1 ST arrays. Quality control and statistical analysis were performed using Bioconductor packages integrated in an on-line pipeline (Lin, Kools et al. 2011) as previously described (Chapter 2). Probesets were redefined according to (Irizarry, Bolstad et al. 2003; Heber and Sick 2006). Several complementary methods were used for the biological interpretation for the transcriptome data; gene clustering using Multi-experimental Viewer (MeV) (Saeed, Hagabati et al. 2006) , overrepresentation analysis of Gene Ontology (GO) terms using temporal and location comparative analysis using STEM (Ernst and Bar-Joseph 2006), and construction of biological interaction networks using Ingenuity Pathways Analysis (for detailed descriptions see supplemental material of Chapter 2).

Metabolite Profiling

Urine samples (25-30 µl) were added to 50 µL of phosphate buffer 0.2 M (pH 7.4) in D_2O plus 0.05% 3-(tri-methylsilyl) propionate-2,3-d4 (TSP) before transferring to capillary tubes for analysis by ^1H NMR spectroscopy. Tissue samples were homogenized and extracted in acetonitrile/water (1:1), as previously described (Waters, Holmes et al. 2002). The supernatant containing the aqueous phase was collected, freeze-dried and dissolved in 600 µl of D_2O. Samples were centrifuged for 10 min at 15,000 g, and 500 µl of the supernatant and 50 µl of water were transferred into 5mm (outer diameter) NMR tubes for analysis by ^1H NMR

spectroscopy. All spectra were acquired on an Avance II 600MHz NMR spectrometer (Bruker Biospin, Rheinstetten, Germany) equipped with a Bruker 5mm TXI triple resonance probe operating at 600.13 MHz, and using a BACS auto-sampler. Spectral acquisition of the aqueous phase was performed using the first increment of a standard nuclear Overhauser enhancement scpectroscopy (NOESY) 1-dimensional ^{1}H NMR experiment ((noesypr1D)(RD-90°-t_1-90°-t_m-90°-acquisition), where RD is a relaxation delay, t_1 is a short delay of 2 μs and t_m is a mixing time of 100 ms. Water suppression was applied during the RD and a 90° pulse set at 10 μs. For each spectrum, a total of 256 scans (16 dummy scans) were collected into 64k data points over a spectral width of 20 ppm.

Data were analyzed by applying an exponential window function with a line broadening of 0.3 Hz prior to Fourier transformation to all 1D NMR spectra. The resultant spectra were phased, baseline corrected and calibrated to lactate (δ 1.33) (for tissue samples) and TSP (δ 0.00) (for urine samples), manually using Topspin (2.0a, Bruker BioSpin 2006). The spectra were subsequently imported into MatLab (R20010aSV, The MathsWorks inc.) where the region containing the water resonance (δ 4.6-5.2) was removed. The data were then normalized to the probabilistic quotient (Dieterle, Ross et al. 2006) to minimize the effects of inter-sample variation due to phenomena such as disparate sample volume, although every effort was made to keep this constant during sample preparation.

Metabonomic data were visualized by Principal Component Analysis (PCA). OPLS-DA models (Trygg and Wold 2003) were then fitted between successive time-points in order to highlight discriminant metabolites. PCA, O-PLS, O-PLS-DA and Statistical total correlation spectroscopy (STOCSY) were performed in Matlab (using an in-house routine)(Barnes 2009). Permutation testing of the Y matrix for O-PLS/PLS models was conducted using an in-house algorithm (Barnes 2009) to determine whether the Q^2Y (predictive ability) of the model was significantly different from the Q^2Y calculated from 100 random permutations of Y. Assignments were made using additional two-dimensional NMR experiments and reference to databases of spectra of authentic compounds.
O2-PLS models were used to integrate metabonomic, transcriptomics, and microbiota datasets as described by Li *et al* (Li, Wang et al. 2008). O2-PLS models were calculated for pairwise datasets. Significant variables were then selected based on their correlation with the scores of the model ($p < 0.01$).

Accession Numbers
The mouse microarray dataset was deposited in the Gene Expression Omnibus (GEO) with accession number GSE32513.

ACKNOWLEDGMENTS

The authors thank several members of the team of Dr. Joël Doré (INRA, Jouy en Josas) for assistance with animal sacrifice and sampling, J. Jansen and M. Grootte Bromhaar (Division of Human Nutrition, Wageningen University) for excellent microarray hybridization, P. de Groot (Division of Human Nutrition, Wageningen University) for performing microarray quality control and primary data processing.

Chapter 4
Supplemental Material

The Interplay between Gut Microbiota, Host-Transcriptome, and Metabolism in the Mouse Colon during Conventionalization

SUPPLEMENTAL FIGURES

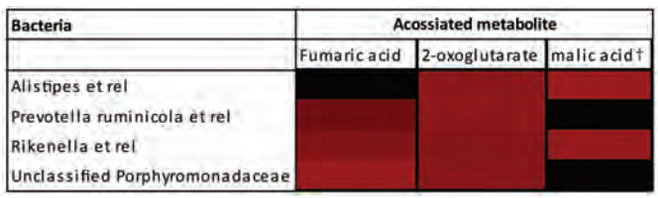

Figure S4.1. Association of early colonizers and urine metabolites. Correlation heat map between urine metabolites and the bacterial taxonomical level from MITChip data (level 2-genus like). The heat map represents correlations across 16 days of conventionalization. Red color depicts positive correlation. Black color indicates no change compared to the control (germfree) mice.

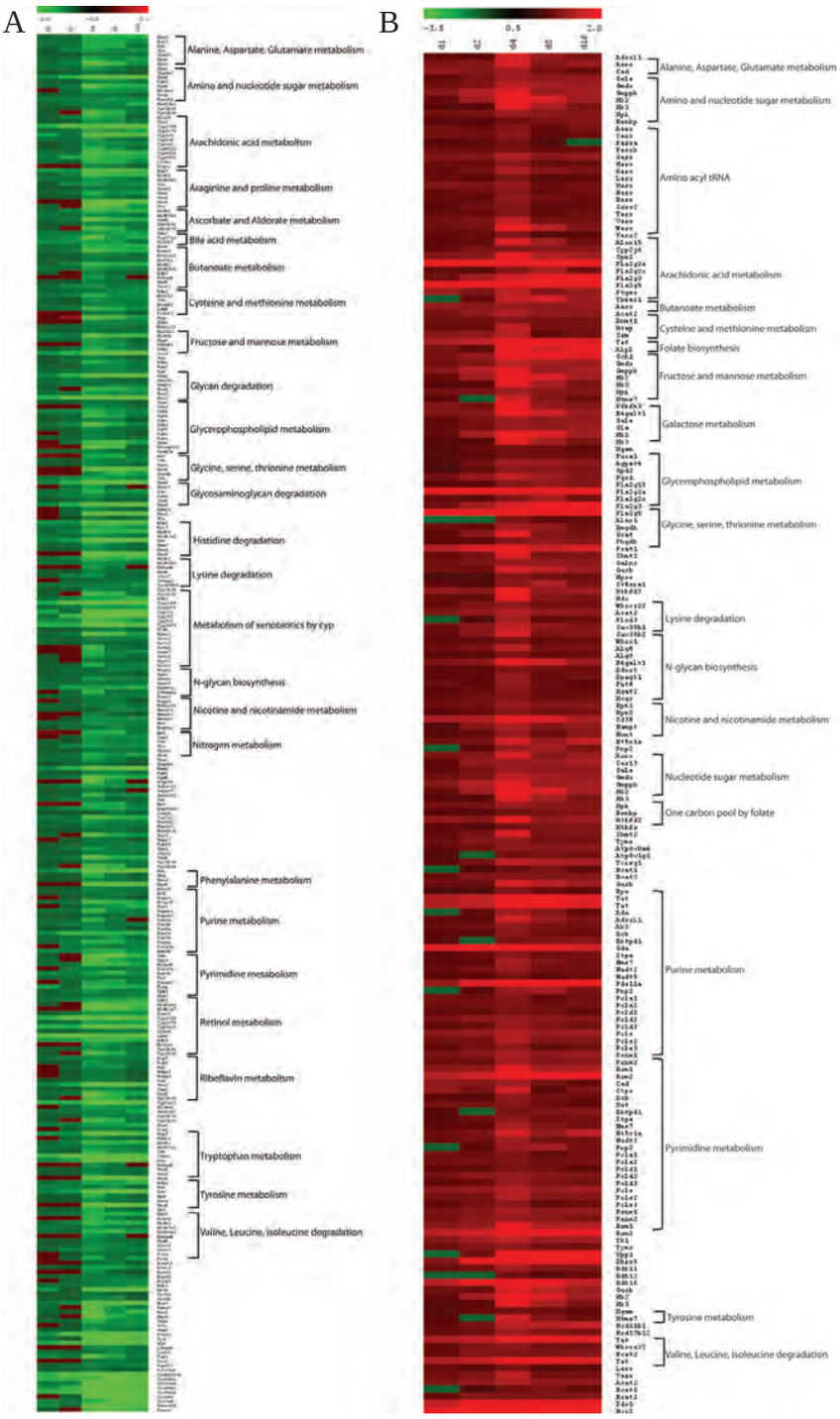

Figure S4.2. Transcriptome-metabolite correlations. Heat maps of (A) downregulated genes of which the expression was positively correlated with the concentrations of *myo*- and *scyllo*-inositol, (B) upregulated genes of which expression was positively correlated with the concentrations of glutamate, alanine, and glycine.

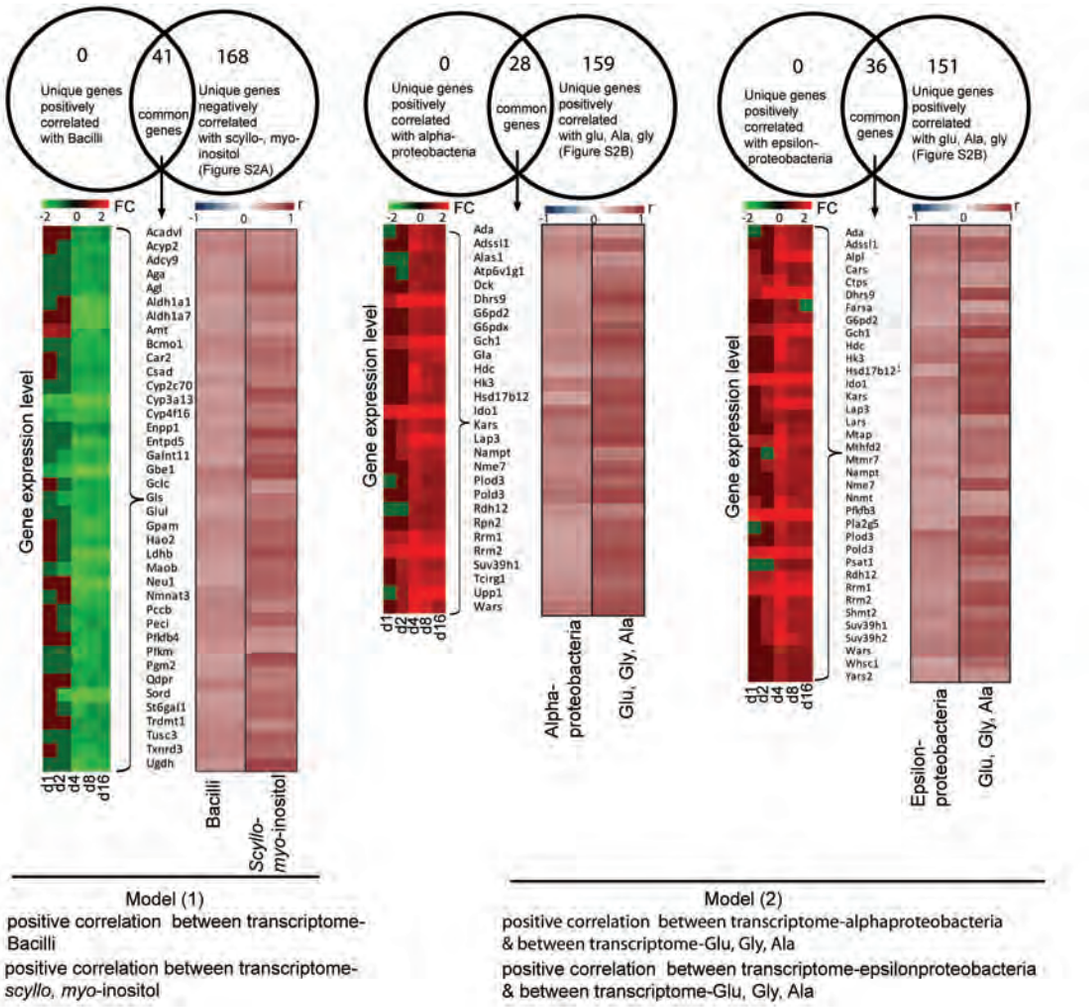

Figure S4.3. Microbiota-transcriptome-metabolite correlations. Correlation heat maps showing (A) **Model (1):**Correlation computed between transcriptome and I-Bacilli (positive correlation), II-*scyllo*- and *myo*-inositol (positive correlation). (B) **Model (2):**Correlation computed between transcriptome and I-alpha and epsilonproteobacteria (positive correlation) and II-glutamate (Glu), glycine (Gly), and alanine (Ala) (positive correlation).

Table S4.1. Relative contribution of significant (Kruskal Walis) level 2 groups between early (days 1 and 2) and later (days 4, 8, and 16) time-points superior to 0.1%. Light grey filling of the taxonomic level represents early colonizers while dark grey represent late colonizers.

Taxonomic level	Conventionalization days (average relative contribution ± SEM)				
	Day 1	Day 2	Day 4	Day 8	Day 16
Actinobacteria					
Catenibacterium	1.24 ± 0.28	0.80 ± 0.17	0.27 ± 0.10	0.36 ± 0.11	0.25 ± 0.05
Bacilli					
Enterococcus	3.96 ± 1.78	2.10 ± 0.53	0.44 ± 0.17	0.01 ± 0.00	0.01 ± 0.00
Lactobacillus acidophilus et rel.	0.02 ± 0.00	0.03 ± 0.01	0.01 ± 0.00	0.01 ± 0.00	0.12 ± 0.11
Lactobacillus plantarum et rel.	0.10 ± 0.05	0.06 ± 0.03	0.03 ± 0.01	0.02 ± 0.00	0.47 ± 0.45
Lactobacillus salivarius et rel.	4.20 ± 0.92	2.40 ± 1.21	0.45 ± 0.32	0.85 ± 0.56	0.37 ± 0.23
Staphylococcus aureus et rel.	0.66 ± 0.34	0.26 ± 0.07	0.05 ± 0.02	0.01 ± 0.00	0.01 ± 0.00
Bacteroidetes					
Bacteroides distasonis et rel.	1.54 ± 0.59	2.85 ± 0.48	1.57 ± 0.46	0.90 ± 0.42	0.43 ± 0.23
Bacteroides fragilis et rel.	6.49 ± 1.45	8.18 ± 1.37	7.05 ± 1.74	1.98 ± 0.56	1.90 ± 0.60
Bacteroides plebeius et rel.	0.93 ± 0.21	0.99 ± 0.18	0.88 ± 0.27	0.37 ± 0.16	0.31 ± 0.09
Bacteroides vulgatus et rel.	2.04 ± 0.53	2.25 ± 0.32	2.98 ± 0.84	1.41 ± 0.62	1.05 ± 0.27
Porphyr. asaccharolytica et rel.	1.49 ± 0.40	0.86 ± 0.24	0.44 ± 0.09	0.41 ± 0.12	0.28 ± 0.10
***Clostridium* cluster II**					
Unclassified Clostridiales II	0.52 ± 0.12	0.69 ± 0.21	0.84 ± 0.30	1.10 ± 0.19	1.55 ± 0.17
***Clostridium* cluster IV**					
Clostridium leptum et rel.	0.05 ± 0.02	0.05 ± 0.01	0.05 ± 0.01	0.23 ± 0.04	0.30 ± 0.12
Sporobacter termitidis et rel.	0.53 ± 0.05	0.72 ± 0.19	1.76 ± 0.43	3.56 ± 0.59	4.34 ± 0.42
***Clostridium* cluster IX**					
Peptococcus niger et rel.	0.03 ± 0.01	0.03 ± 0.00	0.08 ± 0.03	0.19 ± 0.06	0.30 ± 0.10
***Clostridium* cluster XI**					
Anaerovorax et rel.	0.02 ± 0.00	0.24 ± 0.18	0.74 ± 0.54	0.98 ± 0.59	0.12 ± 0.04
Clostridium difficile et rel.	0.73 ± 0.19	2.03 ± 0.97	2.16 ± 0.91	2.62 ± 0.56	3.55 ± 0.24
***Clostridium* cluster XIVa**					
Bryantella et rel.	0.15 ± 0.02	0.24 ± 0.07	1.04 ± 0.45	3.22 ± 0.94	2.64 ± 0.60
Butyrivibrio crossotus et rel.	0.19 ± 0.04	0.43 ± 0.17	0.82 ± 0.25	1.20 ± 0.24	1.66 ± 0.15
Clostridium sphenoides et rel.	0.39 ± 0.06	0.39 ± 0.08	0.73 ± 0.23	1.47 ± 0.42	1.79 ± 0.29
Clostridium symbosium et rel.	0.01 ± 0.00	0.01 ± 0.00	0.06 ± 0.03	0.07 ± 0.03	0.17 ± 0.10
Dorea et rel.	0.10 ± 0.02	0.13 ± 0.03	1.07 ± 0.31	3.13 ± 0.79	2.25 ± 0.43
Eubacterium plexicaudatum et rel.	0.89 ± 0.21	0.77 ± 0.22	1.95 ± 0.66	3.81 ± 0.94	4.17 ± 0.24
Lachnobacillus bovis et rel.	0.05 ± 0.01	0.05 ± 0.01	0.28 ± 0.10	0.83 ± 0.19	0.84 ± 0.11
Lachnospira pectinoschiza et rel.	0.06 ± 0.01	0.06 ± 0.01	0.20 ± 0.03	1.06 ± 0.41	0.68 ± 0.20
Unclassified Clostridiales XIVa	2.23 ± 0.37	2.34 ± 0.42	4.56 ± 1.40	9.54 ± 1.79	11.50 ± 0.56
***Clostridium* cluster XVI**					
Allobaculum et rel.	0.81 ± 0.17	1.70 ± 0.69	0.41 ± 0.14	1.70 ± 1.08	0.32 ± 0.13
Unclassified Clostridiales XVI	5.49 ± 0.74	3.39 ± 0.91	1.52 ± 0.45	2.14 ± 0.70	1.44 ± 0.37
***Clostridium* cluster XVII**					
Coprobacillus catenoformis et rel.	1.81 ± 0.25	1.36 ± 0.30	0.58 ± 0.16	0.86 ± 0.27	0.50 ± 0.12
***Clostridium* cluster XVIII**					

Clostridium ramosum et rel.	7.68 ± 0.93	5.18 ± 1.23	2.07 ± 0.66	2.92 ± 1.03	1.74 ± 0.44
Deferribacteres					
Mucispirillum schaedleri et rel.	1.14 ± 0.13	1.03 ± 0.22	2.73 ± 0.50	0.60 ± 0.09	3.72 ± 3.04
Fibrobacteres					
Fibrobacter succinogenes et rel.	0.46 ± 0.12	0.28 ± 0.07	0.09 ± 0.03	0.21 ± 0.03	0.21 ± 0.09
Fusobacteria					
Fusobacterium	0.15 ± 0.03	0.16 ± 0.03	0.37 ± 0.16	0.66 ± 0.12	0.77 ± 0.07
Mollicutes					
Acholeplasma et rel.	0.12 ± 0.03	0.07 ± 0.01	0.02 ± 0.00	0.02 ± 0.01	0.01 ± 0.00
Solobacterium moorei et rel.	1.41 ± 0.30	0.88 ± 0.21	0.29 ± 0.10	0.42 ± 0.13	0.28 ± 0.07
Unclassified Mollicutes	3.92 ± 0.94	2.52 ± 0.63	2.48 ± 0.81	1.69 ± 0.32	1.78 ± 0.31
Proteobacteria (alpha)					
Sphingomonas	0.15 ± 0.02	0.16 ± 0.02	1.93 ± 1.28	0.30 ± 0.05	0.74 ± 0.49
Labrys methylaminiphilus et rel.	0.02 ± 0.00	0.22 ± 0.13	0.38 ± 0.17	0.60 ± 0.12	0.57 ± 0.10
Proteobacteria (beta)					
Sutterella wadsorthia et rel.	1.54 ± 0.24	2.13 ± 0.56	0.72 ± 0.18	1.11 ± 0.46	0.72 ± 0.27
Vibrio	0.21 ± 0.06	0.39 ± 0.09	0.33 ± 0.10	0.52 ± 0.11	0.53 ± 0.08
Proteobacteria (delta)					
Bilophila	0.01 ± 0.00	0.01 ± 0.00	0.38 ± 0.14	0.19 ± 0.12	0.14 ± 0.07
Desulfovibrio	0.01 ± 0.00	0.01 ± 0.00	0.11 ± 0.04	0.08 ± 0.03	0.08 ± 0.03
Proteobacteria (epsilon)					
Helicobacter	0.80 ± 0.17	0.94 ± 0.14	7.42 ± 4.46	0.52 ± 0.08	3.33 ± 2.82
Proteobacteria (gamma)					
Pasteurella	0.10 ± 0.03	0.16 ± 0.04	0.25 ± 0.09	0.47 ± 0.09	0.48 ± 0.07
TM7					
Unclassified TM7	0.02 ± 0.00	0.04 ± 0.02	0.35 ± 0.13	0.67 ± 0.13	0.81 ± 0.02

Table S4.2. Primers used for the quantification of butyrate producers *(ButyrilCoA* gene*)*, sulfate reducers (*dsr* gene), and *Methanogens* (*McrA* gene), by qPCR.

	Primer name	Primer sequence (5'-3')	Annealing temperature	References
Methanogens	mlas F mcrA-R	GGTGGTGTMGGDTTCAC MCARTA CGTTCATBGCGTAGTTVGGRTAGT	55°C	(Steinberg and Regan, 2008)
Sulfate reducers	RH1dsr-F RH3-dsr-R	GCCGTTACTGTGACCAGCC GGTGGAGCCGTGCATGTT	60°C	(Ben-Dov et al., 2007)
Butyrate producers	BcoATscr-F BcoATscr-R	GCIGAICATTTCACITGGAAYWSITGGCAYATG CCTGCCTTTGCAATRTCIACRAANGC	53°C	(Louis and Flint, 2007)

REFERENCES

Azcárate-Peril Andrea M., S. M., and Bruno-Bárcena José M. (2011). "The intestinal microbiota, gastrointestinal environment and colorectal cancer: A putative role for probiotics in prevention of colorectal cancer?" Am J Physiol Gastrointest Liver Physiol **In press.**

Bäckhed, F., H. Ding, et al. (2004). "The gut microbiota as an environmental factor that regulates fat storage." Proceedings of the National Academy of Sciences of the United States of America **101**(44): 15718-15723.

Bäckhed, F., R. E. Ley, et al. (2005). "Host-bacterial mutualism in the human intestine." Science **307**(5717): 1915-1920.

Bäckhed, F., J. K. Manchester, et al. (2007). "Mechanisms underlying the resistance to diet-induced obesity in germ-free mice." Proceedings Of The National Academy Of Sciences Of The United States Of America **104**(3): 979-984.

Barcenilla, A., S. E. Pryde, et al. (2000). "Phylogenetic relationships of butyrate-producing bacteria from the human gut." Applied and Environmental Microbiology **66**(4): 1654-1661.

Barnes, P. J. (2009). "Intrinsic asthma: not so different from allergic asthma but driven by superantigens?" Clinical and Experimental Allergy **39**(8): 1145-1151.

Ben-Dov, E., A. Brenner, et al. (2007). "Quantification of sulfate-reducing bacteria in industrial wastewater, by real-time polymerase chain reaction (PCR) using dsrA and apsA genes." Microbial Ecology **54**(3): 439-451.

Bjursell, M., T. Admyre, et al. (2011). "Improved glucose control and reduced body fat mass in free fatty acid receptor 2-deficient mice fed a high-fat diet." American Journal of Physiology-Endocrinology and Metabolism **300**(1): E211-E220.

Brown, A. J., S. M. Goldsworthy, et al. (2003). "The orphan G protein-coupled receptors GPR41 and GPR43 are activated by propionate and other short chain carboxylic acids." Journal of Biological Chemistry **278**(13): 11312-11319.

Cherbuy, C., C. Andrieux, et al. (2004). "Expression of mitochondrial HMGCoA synthase and glutaminase in the colonic mucosa is modulated by bacterial species." European Journal of Biochemistry **271**(1): 87-95.

Claus, S. P., T. M. Tsang, et al. (2008). "Systemic multicompartmental effects of the gut microbiome on mouse metabolic phenotypes." Molecular Systems Biology **4**.

Dieterle, F., A. Ross, et al. (2006). "Probabilistic quotient normalization as robust method to account for dilution of complex biological mixtures. Application in 1H NMR metabonomics." Analytical chemistry **78**(13): 4281-4290.

Donohoe, D. R., N. Garge, et al. (2011). "The microbiome and butyrate regulate energy metabolism and autophagy in the mammalian colon." Cell Metabolism **13**(5): 517-526.

Duncan, S. H., G. Holtrop, et al. (2004). "Contribution of acetate to butyrate formation by human faecal bacteria." British Journal of Nutrition **91**(6): 915-923.

Ernst J. and Z. Bar-Joseph (2006). "STEM: a tool for the analysis of short time series gene expression data." BMC Bioinformatics **7**: 191.

Falony, G., A. Vlachou, et al. (2006). "Cross-feeding between Bifidobacterium longum BB536 and acetate-converting, butyrate-producing colon bacteria during growth on oligofructose." Applied and Environmental Microbiology **72**(12): 7835-7841.

Fischbach, M. A. a. S., J.L (2011). "Eating for two: how metabolism establishes interspecies interactions in the gut." Cell Host & Microbe **10**: 336-347.

Flint, H. J., E. A. Bayer, et al. (2008). "Polysaccharide utilization by gut bacteria: potential for new insights from genomic analysis." Nature Reviews Microbiology **6**(2): 121-131.

Geurts L, V. Lazarevic, et al. (2011). "Altered gut microbiota and endocannabinoid system tone in obese and diabetic leptin-resistant mice: impact on apelin regulation in adipose tissue." Frontiers in Cellular and Infection Microbiology.

Gibson, G. R., S. Macfarlane, et al. (1993). "Metabolic interactions involving sulfate-reducing and methanogenic bacteria in the human large-intestine." Fems Microbiology Ecology **12**(2): 117-125.

Heber, S. and B. Sick (2006). "Quality assessment of affymetrix GeneChip data." Omics-a Journal of Integrative Biology **10**(3): 358-368.

Henderson, C. (1980). "The influence of extracellular hydrogen on the metabolism of Bacteroides ruminicola,

anaerovibrio lipolytic and selenomonas ruminantium." Journal of General Microbiology **119**(AUG): 485-491.
Hooper, L. V. (2004). "Bacterial contributions to mammalian gut development." Trends in Microbiology **12**(3): 129-134.
Hooper, L. V., T. Midtvedt, et al. (2002). "How host-microbial interactions shape the nutrient environment of the mammalian intestine." Annual Review of Nutrition **22**: 283-307.
Hultgren, S. J., S. Abraham, et al. (1993). "Pilus and nonpilus bacterial adhesins- assembly and function in cell regulation." Cell **73**(5): 887-901.
Huycke, M. M. and H. R. Gaskins (2004). "Commensal bacteria, redox stress, and colorectal cancer: Mechanisms and models." Experimental Biology and Medicine **229**(7): 586-597.
Irizarry, R. A., B. M. Bolstad, et al. (2003). "Summaries of affymetrix GeneChip probe level data." Nucleic Acids Research **31**(4).
Kau, A. L., P. P. Ahern, et al. (2011). "Human nutrition, the gut microbiome and the immune system." Nature **474**(7351): 327-336.
Kiene, R. P. (1998). "Uptake of choline and its conversion to glycine betaine by bacteria in estuarine waters." Applied and Environmental Microbiology **64**(3): 1045-1051.
Lee, Y. K. and S. K. Mazmanian (2010). "Has the microbiota played a critical role in the evolution of the adaptive immune system?" Science **330**(6012): 1768-1773.
Ley, R. E., D. A. Peterson, et al. (2006). "Ecological and evolutionary forces shaping microbial diversity in the human intestine." Cell **124**(4): 837-848.
Li, M., B. Wang, et al. (2008). "Symbiotic gut microbes modulate human metabolic phenotypes." Proceedings of the National Academy of Sciences **105**(6): 2117-2122.
Lin, K., H. Kools, et al. (2011). "MADMAX – Management and analysis database for multiple ~omics experiments." Journal of integrative bioinformatics **8**(2): 160.
Louis, P. and H. J. Flint (2007). "Development of a semiquantitative degenerate real-time PCR-based assay for estimation of numbers of butyryl-coenzyme A (CoA) CoA transferase genes in complex bacterial samples." Applied and Environmental Microbiology **73**(6): 2009-2012.
Marquet, P., S. H. Duncan, et al. (2009). "Lactate has the potential to promote hydrogen sulphide formation in the human colon." Fems Microbiology Letters **299**(2): 128-134.
Martin, F.-P. J., Y. Wang, et al. (2007). "Effects of probiotic Lactobacillus Paracasei treatment on the host gut tissue metabolic profiles probed via magic-angle-spinning NMR spectroscopy." Journal of Proteome Research **6**(4): 1471-1481.
Maslowski, K. M., A. T. Vieira, et al. (2009). "Regulation of inflammatory responses by gut microbiota and chemoattractant receptor GPR43." Nature **461**(7268): 1282-U1119.
Neish, A. S. (2009). "Microbes in Gastrointestinal Health and Disease." Gastroenterology **136**(1): 65-80.
Nicholls, A. W., R. J. Mortishire-Smith, et al. (2003). "NMR spectroscopic-based metabonomic studies of urinary metabolite variation in acclimatizing germ-free rats." Chemical Research in Toxicology **16**(11): 1395-1404.
Nicholson, J. K., E. Holmes, et al. (2005). "Gut microorganisms, mammalian metabolism and personalized health care." Nature Reviews Microbiology **3**(5): 431-438.
O'Hara, A. M. and F. Shanahan (2006). "The gut flora as a forgotten organ." Embo Reports **7**(7): 688-693.
Palmer, C., E. M. Bik, et al. (2007). "Development of the human infant intestinal microbiota." Plos Biology **5**: 1556-1573.
Parker, N. J., C. G. Begley, et al. (1995). "Human gene for the large subunit of ribonucleotide reductase (RRM1)-Functional-analysis of the promoter." Genomics **27**(2): 280-285.
Rajilic-Stojanovic, M., H. G. H. J. Heilig, et al. (2009). "Development and application of the human intestinal tract chip, a phylogenetic microarray: analysis of universally conserved phylotypes in the abundant microbiota of young and elderly adults." Environmental Microbiology **11**(7): 1736-1751.
Saeed, A. I., N. K. Hagabati, et al. (2006). TM4 microarray software suite. Methods Enzymology. **411:** 134-193.
Salyers, A. A. and M. Pajeau (1989). "Competitiveness of different polysaccharide utilization mutants of Bacteroides-Thetaiotaomicron in the intestinal tracts of germfree-mice." Applied and Environmental Microbiology **55**(10): 2572-2578.
Savage, D. C. (1977). "Microbial ecology of gastrointestinal-tract " Annual Review of Microbiology **31**: 107-133.

Scheppach W, B. P., Richter A (1995). Management of diversion colitis, pouchitis and distal ulcerative colitis. Physiological and clinical aspects of short-chain fatty acids. R. J. Cummings JH, Sakata T. Cambridge University Press, Great Britain**:** 353–360.

Starrenburg, M. J. C. and J. Hugenholtz (1991). "Citrate fermentation by lactococcus and leuconostoc spp." Applied and Environmental Microbiology **57**(12)**:** 3535-3540.

Steinberg, L. M. and J. M. Regan (2008). "Phylogenetic comparison of the methanogenic communities from an acidic, oligotrophic fen and an anaerobic digester treating municipal wastewater sludge." Applied and Environmental Microbiology **74**(21)**:** 6663-6671.

Tlaskalova-Hogenova, H., R. Stepankova, et al. (2011). "The role of gut microbiota (commensal bacteria) and the mucosal barrier in the pathogenesis of inflammatory and autoimmune diseases and cancer: contribution of germ-free and gnotobiotic animal models of human diseases." Cellular & Molecular Immunology **8**(2)**:** 110-120.

Trygg, J. and S. Wold (2003). "O2-PLS, a two-block (X-Y) latent variable regression (LVR) method with an integral OSC filter." Journal of Chemometrics **17**(1)**:** 53-64.

Turnbaugh, P. J., M. Hamady, et al. (2009). "A core gut microbiome in obese and lean twins." Nature **457**(7228)**:** 480-U487.

Vanhoutvin, S. A. L. W., F. J. Troost, et al. (2009). "Butyrate-induced transcriptional changes in human colonic mucosa." Plos One **4**(8).

Walter, J. and R. Ley (2011). "The human gut microbiome: ecology and recent evolutionary changes." Annual Review of Microbiology **65**: 411-429.

Wang, Z., E. Klipfell, et al. (2011). "Gut flora metabolism of phosphatidylcholine promotes cardiovascular disease." Nature **472**(7341)**:** 57-U82.

Waters, N. J., E. Holmes, et al. (2002). "NMR and pattern recognition studies on liver extracts and intact livers from rats treated with alpha-naphthylisothiocyanate." Biochemical Pharmacology **64**(1)**:** 67-77.

Chapter 5

A Transient State of Microbial Dysbiosis and Inflammation is Pivotal in the Establishment of Homeostasis during Conventionalization of Mice

Sahar El Aidy, Muriel Derrien, Ronald Aardema , Guido Hooiveld, Selena E. Richards, Adrie Dane, Jan Dekker, Rob Vreeken, Florence Levenez, Erwin G. Zoetendal, Joël Doré, Peter van Baarlen, and Michiel Kleerebezem

Submitted

ABSTRACT

Gut microbiota is increasingly recognized as a key-player in defining the health status of the gastrointestinal tract. Recently we demonstrated that conventionalization of germfree mice with normal fecal microbiota elicits the temporal and region-specific dynamic host-microbe communication pathways that establish a homeostatic state of tolerance towards the microbiota in healthy mice within 30 days post-conventionalization. To decipher the specific features of the time-point that showed the largest shift in mucosal response during this process at four days post-conventionalization, multi-variate mining of a combination of colon transcriptome data, plasma cytokines, and amine metabolites, and gut microbiota profiling were employed. Transcriptome analyses highlighted the strong induction of genes involved in innate immune functions, pro-inflammatory responses, and cell cycle regulation, suggesting that day 4 post-conventionalization represents a transient state of inflammation that is necessary to stimulate development of adequate innate and adaptive immunity. This transient state of inflammation was characterized by the expression of inflammatory cytokines and amines, in response to a temporal domination of the microbial genera *Helicobacter, Sphingomonas,* and *Mucispirillum*. *Helicobacter* and *Sphingomonas* are known as so-called "pathobionts" and can activate specific immune cells and could bring about a state of dysbiosis, or a state with an imbalanced representation of microbial taxa in the intestine. Our results propose that the mucosal parameters measured at day 4 post-conventionalization of germfree mice reflect the boundary of homeostasis and dysbiosis in host-microbe interplay and that certain microbial genera are potent stimulators of the developing immune system.

INTRODUCTION

The intimate contact between the microbiota and host provides vital functions for the host including the digestion of complex dietary compounds, and resistance to colonization of pathogens (Bäckhed, Ley et al. 2005). The gastrointestinal (GI) tract is the initial site of interaction between the host immune system and its colonizing microbiota (Macpherson, Geuking et al. 2005) . To preserve homeostasis, immune responses need to be tightly controlled (O'Connor, Taylor et al. 2006) so that the immune system mounts appropriate, tolerant responses to the colonizing gut microbiota. During the past decade, several studies in humans, mice, and other mammals have supported the role of gut microbiota especially its Gram-negative members in activating the immune system and eliciting inflammatory responses that may lead to disease in genetically predisposed persons (Solnick and Schauer 2001; Fox 2002; On, Hynes et al. 2002; Manco, Putignani et al. 2010). Representative examples of commensals that promote gut inflammatory responses are segmented filamentous bacteria (Stepankova, Powrie et al. 2007) , *Helicobacter* species (Erdman, Rao et al. 2009), *Clostridium difficile* (Palmer 2011), *Prevotellacae,* TM7, and *Klebsiella pneumoniae* (Elinav, Strowig et al. 2011). These potential pathogenic symbionts were previously termed "pathobionts" referring to their ability to induce tissue damage under certain conditions (Chow and Mazmanian 2010). "Pathobionts" are prominent species in the GI tract of healthy humans and animals that trigger disease in response to changes in the environment, including the diet and shifts in microbial composition, and/or a transiently weakened immune response. Inappropriate shifts in the composition of the intestinal microbial community, termed dysbiosis, can deplete the microbiota from competing symbionts, some of which promote intestinal anti-inflammatory responses (Sokol, Pigneur et al. 2008).

Studies looking into the complex interactions between hosts and changes in the microbiota have been extremely challenging since such studies required a genome-wide determination of host responses to simultaneous changes in the microbiota. Moreover, the host response to changes in the microbiota contains local and systemic changes in metabolism and immunity. Systemic responses include both mobile chemical signals such as hormones and chemokines carried by the blood, but also immune cells that respond to changes in chemokine gradients. The rapid technological development of functional genomics provides novel opportunities for the identification of molecular signatures that represent homeostasis and dysbiosis situations. Therefore, the application of transcriptomics in colonic tissues, combined with simultaneous microbiota characterization and analysis of blood analytes such as cytokines and amines, should allow us to unravel the molecular mechanisms underlying gut homeostasis or dysbiosis.

This notion prompted us to employ a germfree mouse model to study the dynamics of the regulated mucosal responses to the microbiota during conventionalization (Chapter 2). This study comprehensively analyzed how microbiota accommodating homeostasis is established. In this study, we found at four days post-conventionalization, a strong induction of innate immunity including the production of antimicrobial molecules. These innate immune-related responses appeared to have stabilized from day 8 onward in the colon. Stabilization of innate immunity coincided with activation of adaptive immunity (Chapter 2). Here, we focus on the features of the transient state of inflammation observed four days after the initiation of conventionalization. Parallel determination of colon tissue transcriptomes, gut microbiota composition, and systemic plasma cytokines and metabolic markers enabled the characterization of this transient state. We propose that the early colonizing genera activate specific parts of the innate (days 1-4) and adaptive (days 8-16) immune system and that these immune responses

elicit subsequent tolerant immune responses to the commensal microbiota. We further propose that day 4 marks a stage of strong "physiological" inflammation (Sansonetti and Di Santo 2007; Medzhitov 2008) that activated the immune (mainly T) cell development pathways that were observed from days 8 onward.

RESULTS

Comprehensive Colon-Transcriptome Analysis of a Transient Conventionalization State that is Characterized by a Gene Regulatory Network Associated with Pro-Inflammatory Responses

Recently we established that relatively short term conventionalization (4 days) of germfree mice was characterized by a drastic transcriptome pattern shift, where some genes stopped being expressed while others were induced for the first time (Chapter 2). The functional annotations of the genes involved in the transcriptional shift suggested that day 4 may mark a distinct transient state that occurs during conventionalization. To characterize the biological processes associated with this transcriptomic shift, the Short Time Series Expression Miner (STEM) software (Ernst and Bar-Joseph 2006) was employed in this study to identify genes that display their highest expression at day 4 post-conventionalization. The genes that met this criterion were used to construct a protein-protein interaction network in ingenuity pathway analysis (IPA) software (www.ingenuity.com). Gene-function annotation of the resulting network (Figure 5.1A) showed that most genes belonged to two major biological processes: induction of pro-inflammatory responses and cell cycle regulation. The pro-inflammatory response network part included genes that play a key role in the induction of T helper (Th1) responses, such as lipopolysaccharide recognition (*Cd14*), pro-inflammatory cytokines, tumor necrosis factor-alpha (*Tnf-α*) and interferon gamma (*Ifn-γ*), chemokines (*Ccl5, Ccl7, Ccr5, Cxcl9, Cxcr3,* and *Ccl8*), and activators of MHC Class I, transporters 1,2 (*Tap1* and *2*), and the proteasome subunit beta, type 8, 9 (*Psmb8* and *9*). The cell cycle control and proliferation network part also included genes encoding "hub" proteins with key-functions, like Aurora kinase A (*Aurka*), Cyclin a, b, and d (*Ccna, b,* and *d*), Pim-1 oncogene (*Pim1*), and Baculoviral IAP repeat-containing 5 (*Birc5*) (Figure 5.1A). Notably, all the genes in this network were induced. Statistical analysis of GO annotation enrichment for genes that were differentially expressed at day 4 post-conventionalization confirmed that the majority of the modulated biological processes were involved in cell signaling including cell cycle control and inflammatory responses (Figure 5.1B). Among the most significantly ($p < 0.05$) altered signaling pathways were two pathways involved in an inflammatory response: *Ifn-γ* signaling and cross talk between dendritic cell and natural killer cells, and cell cycle regulation (Figure 5.1C). IPA found significant ($p < 0.05$) associations of the regulatory network genes with disease: 37 associated core genes in the regulatory network are known to promote or co-mediate gastrointestinal disorders including inflammatory bowel disease and colon cancer (indicated with red arrows in Figure 5.1A). In summary, the biological and functional annotations of the genes modulated at the identified intermediate state and the network shown in Figure 5.1 (A) support the hypothesis that this transient state during conventionalization marks the boundaries of balanced physiological responses, typical of healthy hosts, to gut microbiota.

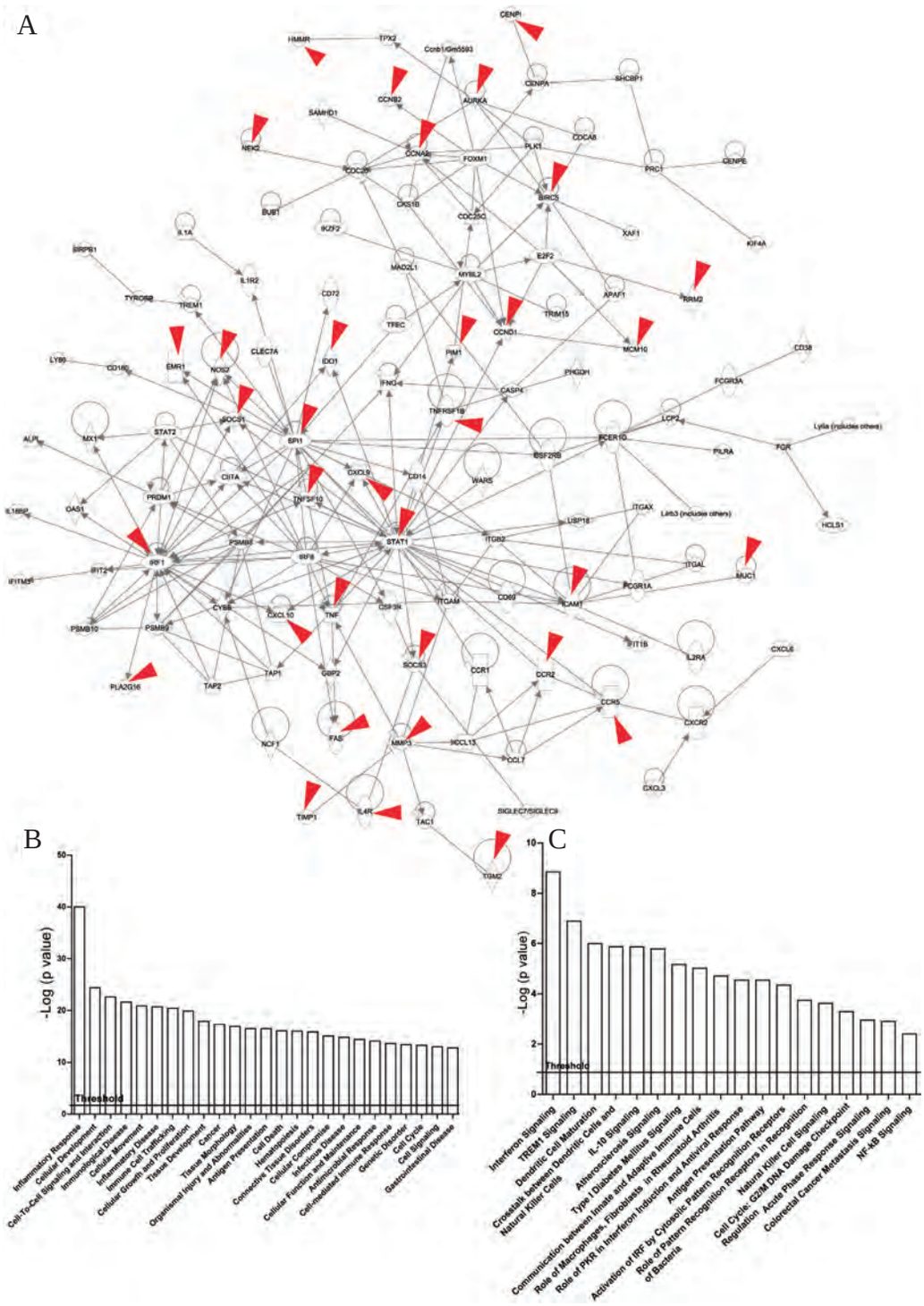

Figure 5.1. The core regulatory network that is specifically modulated during day 4 post-conventionalization and associates with inflammatory cascades. (A) The core regulatory network that is based on IPA protein-protein interaction network reconstruction that is characteristic for day 4 post-conventionalization. This network exemplifies the transition towards a new state of intestinal homeostasis during the process of conventionalization. Arrow heads indicate genes associated with human inflammatory bowel disease and colon cancer. (B) Cellular functions and disease annotations calculated using IPA. (C) Cellular pathways significantly modulated in the colon at day 4 post-conventionalization. Pathways were determined using IPA and significance of pathway modulation was calculated via a one-tailed Fisher's Exact test in IPA and represented as -log (p value); -log values exceeding 1.30 were significant ($p < 0.05$)**.**

Distinct Microbial Diversity Features the Transient State of Mucosal Response in the Colon

Previous experiments have shown that the gut microbiota composition is succeeding in time after the initiation of conventionalization, and that a microbiota resembling that of conventional mice is established already after approximately eight days post-conventionalization (Chapter 2). Based on the transcriptome findings (presented above), we assumed that also the changes in microbiota composition during conventionalization may pass through a transient state, analogous to the mouse transcriptomic changes. To explore this possibility, the composition of the luminal colon microbiota at day 4 post-conventionalization was compared to earlier and later time-points using a 16S rRNA based phylogenetic array, mouse intestinal tract (MIT) chip. The microbiota composition at day 4 post-conventionalization differed significantly ($p < 0.01$) from all other time-points analyzed in the experiment (Figure 5.2). The bacterial genera that were significantly and specifically associated with day 4 were predominated by Gram-negative groups, belonging mainly to the Proteobacteria with high abundance of *Helicobacter* (7.42%±4.46) (Epsilonproteobacteria), *Sphingomonas* (1.93%±1.28) (Alphaproteobacteria), *Mucispirillum* (2.37%±0.50) (Deferribacteres). Next to these changes, the relative abundance of *Streptococcus* (Firmicutes) also appeared to increase specifically on day 4 post-conventionalization, but this group only appeared at low abundance (<0.001%), suggesting that this reflects only a marginal modulation. Several additional genera appeared to be more abundant in the microbiota on day 4 post-conventionalization (*Desulfovibrio;* 0.11%±0.03 and *Bilophila* 0.38%±0.14), but these groups remained present in the microbiota at higher levels also on later time-points post-conventionalization (i.e., days 8 and 16). Taken together, the increased absolute and relative abundance of the genera *Helicobacter, Sphingomonas,* and *Mucispirillum* specifically characterized the microbiota found at day 4 post-conventionalization.

Increased numbers of Proteobacteria and Deferribacteres are correlated with pro-inflammatory cytokine expression networks

Possible association of colon microbiota members with colonic gene expression patterns were explored using a false discovery rate (FDR) method (details are presented in the experimental procedures). Colonic gene expression profiles that peaked at day 4 post-conventionalization as identified by STEM analysis were correlated to the changes in the composition of colonizing microbiota members identified by MITChip over the first 16 days of conventionalization. Significant correlations (corrected FDR <0.01; Benjamini–Yekutieli correction) between microbiota members and specific mucosal genes expression changes were only detected for *Helicobacter, Sphingomonas,* and *Mucispirillum* that displayed a positive correlation with several inflammation-related cytokines such as matrix metallopeptidase 3 and 10 (*Mmp3* and *10*), metallopeptidase inhibitor 1 (*Timp1*), transglutaminase 2 (*Tgm2*), chemokine (C-X-C motif) ligands 10 and 11, (*Ip-10* or *Cxcl10*), (*Cxcl11*), suppressor of cytokine signalling 1 (*Socs1*), monocyte chemoattractant protein 3 (*MCP-3* or *Ccl7*), and C-type lectin domain family 4 (*Clec4e*) (Figure 5.3). Notably, the genes with peak expression at day 4 that show significant correlations with microbiota were also part of the regulatory network identified by IPA analysis (Figure 5.1A). In addition, the correlated microbial groups were also shown to be most abundant at day 4 post-conventionalization (Figure 5.2), strongly supporting the validity of these correlations between colonic gene expression and colonic microbiota members.

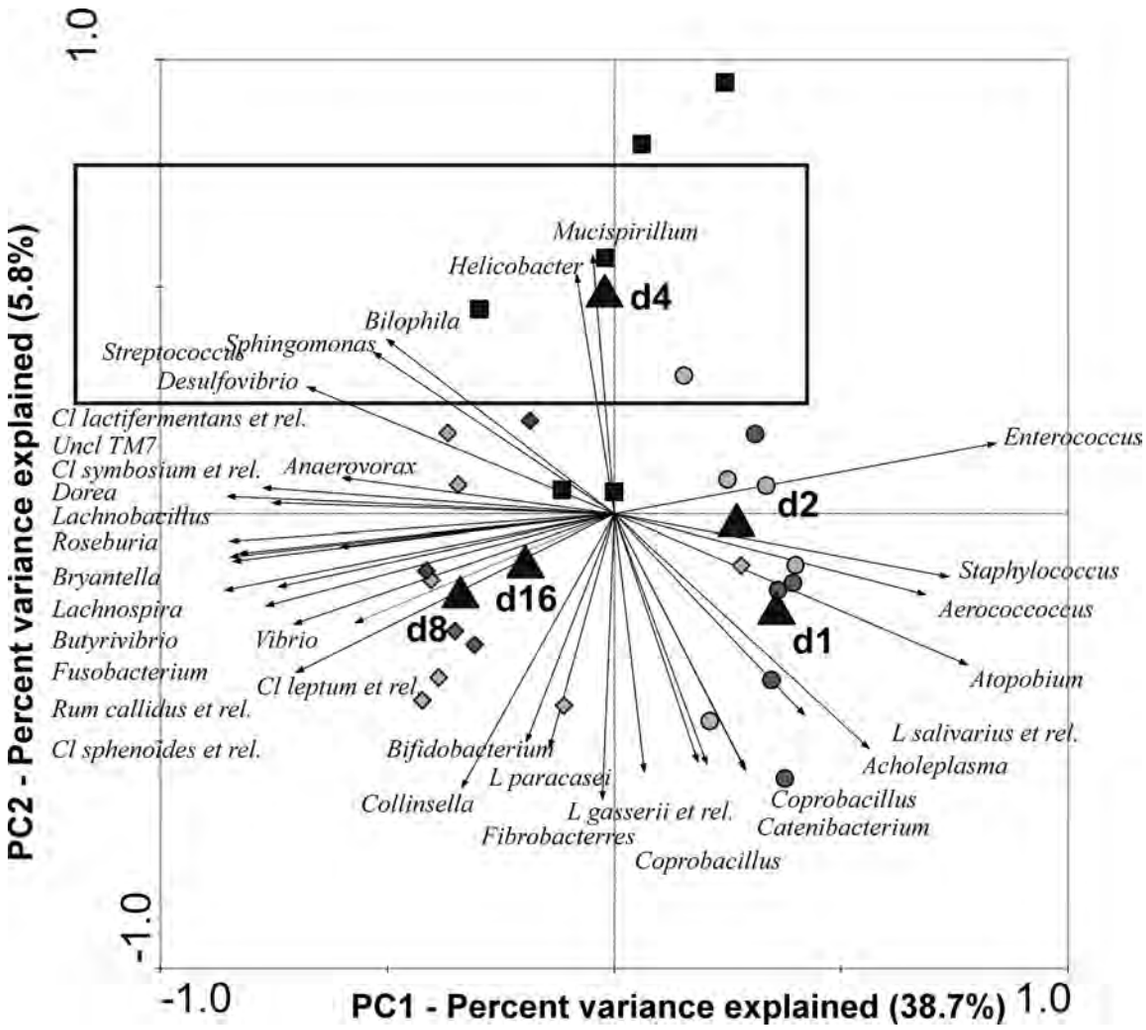

Figure 5.2. Selected microbial genera marks the transient state of mucosal response in the colon. Redundancy analysis triplot of the colonic lumen microbiota composition, as measured by MITChip analysis (level 2 data). Days of conventionalization are represented as centroids, (◦= samples of day 1, •=samples of day 2, □= samples of day 4, ♦=samples of day 8, and ♦=samples of day 16). Microbial groups that contributed to at least 70% to the explanatory axes are represented as vectors. Monte Carlo Permutation Procedure (MCPP) revealed that day 4 post-conventionalization is characterized by a distinct microbial groups (p=0.003) indicated within the black framed rectangle.

Changes in the plasma levels of pro-inflammatory cytokines and amines at day 4 post-conventionalization

To investigate whether the specific status of day 4 post-conventionalization had a systemic impact on the overall host physiology and could be determined in the blood cytokines and amine metabolites, analytes levels were determined in the blood plasma from germfree mice (germfree homeostasis), at day 4 (transient state) and day 30 (homeostasis as described in Chapter 2). Plasma cytokine levels of Ifn-γ, IP-10, monocyte chemo attractant proteins 1, 3, 5 (MCP-1 or Ccl2, MCP-3, MCP-5 or Ccl12), macrophage inflammatory proteins 2, 3β (MIP-2 or Ccl3, MIP-3β), growth-regulated alpha protein (KC/GRO), colony stimulating factor 2 (granulocyte-macrophage) (GM-CSF or Csf2), and oncostatin M (OSM) were significantly elevated at day 4 in comparison with germfree and day 30 post-conventionalization mice ($p < 0.05$) (Figure 5.4; Figure S5.2A). The transient elevated level of the plasma cytokines is in agreement with

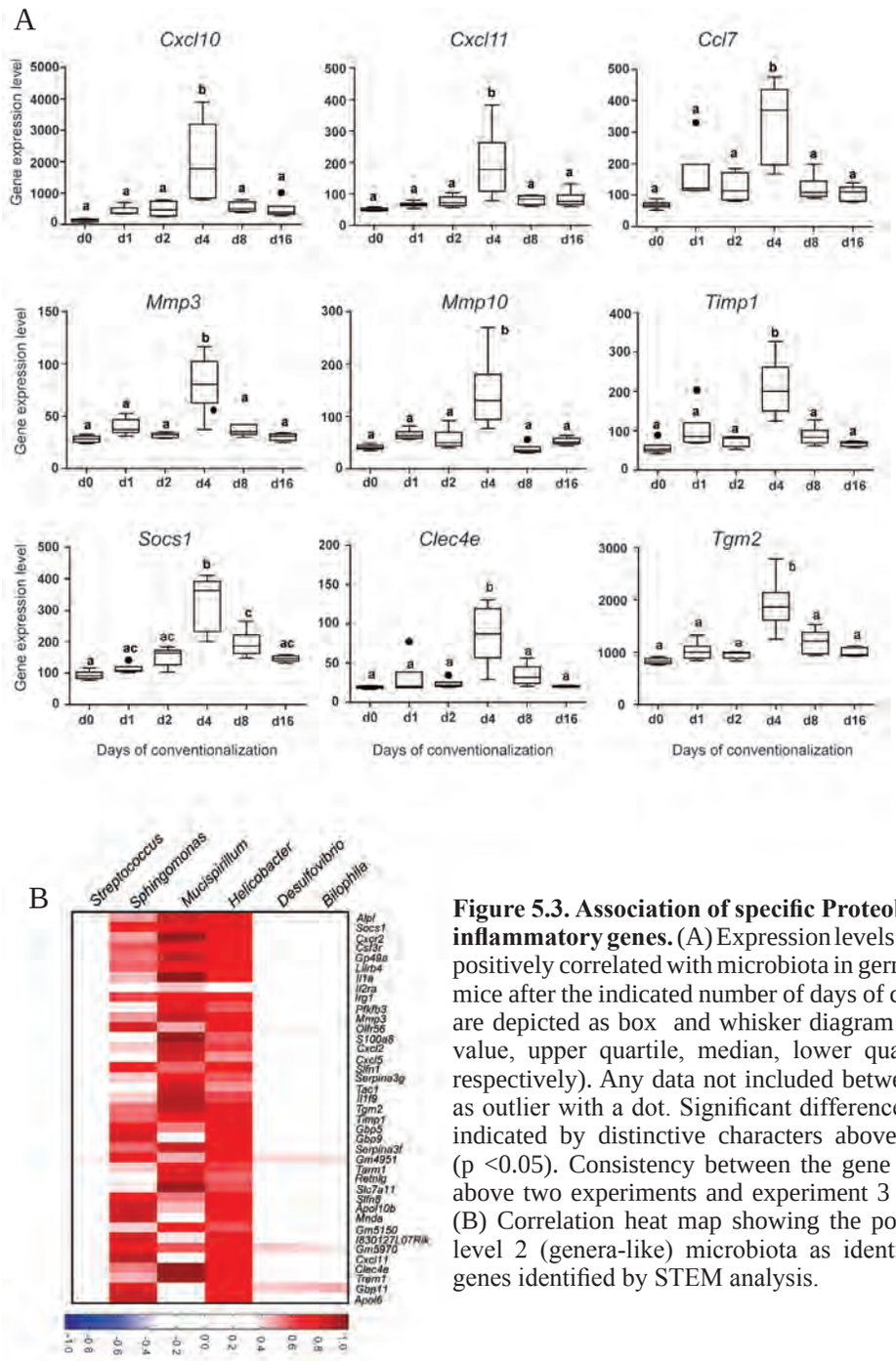

Figure 5.3. Association of specific Proteobacteria groups with pro-inflammatory genes. (A) Expression levels of the colonic genes that are positively correlated with microbiota in germfree and conventionalized mice after the indicated number of days of conventionalization. Values are depicted as box and whisker diagram (top-to-bottom, maximum value, upper quartile, median, lower quartile, and minimal value, respectively). Any data not included between the whiskers is plotted as outlier with a dot. Significant differences between time-points are indicated by distinctive characters above the measurement groups ($p < 0.05$). Consistency between the gene expression patterns in the above two experiments and experiment 3 are shown in Figure S5.1. (B) Correlation heat map showing the positive association between level 2 (genera-like) microbiota as identified by MITchip and the genes identified by STEM analysis.

a transient increase in the level of the corresponding transcripts that were also included in the day 4 post-conventionalization gene-regulatory network (Figure 5.4). Collectively, the data illustrated that the plasma cytokine profile of the transient state of mucosal response during conventionalization exemplifies that of an inflammatory state, with elevated levels of pro-inflammatory cytokines. This state is transient and clearly distinct from the germfree and day 30 post-conventionalization homeostatic states (see discussion).

In addition to the cytokines, amine metabolites were determined in the plasma samples. A specific subset of these metabolites appeared to be significantly ($p < 0.05$) and specifically elevated on

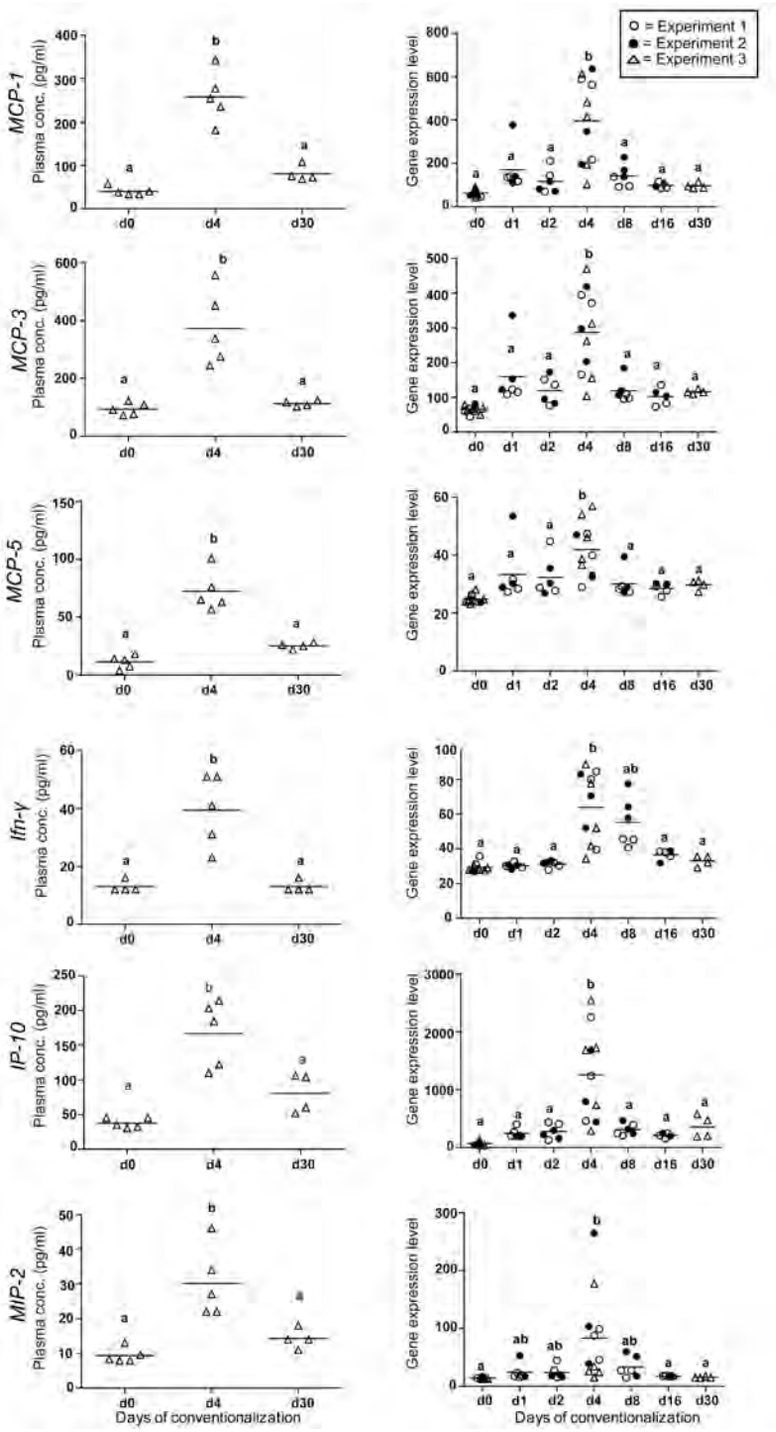

Figure 5.4. Plasma cytokine profile of day 4 post-conventionalization displays properties that are found in tissues in a state of inflammation. Plasma levels of inflammation-associated cytokines measured by Mouse MAP multiplexed immunoassay systems. The elevated level of inflammation-associated cytokines detected in the plasma obtained on day 4 post-conventionalization is corroborated by the expression levels of the corresponding transcripts as shown in the dot-plots where individual expression values obtained for individual mice are plotted for each of the experiments. Significant difference between time-points are indicated by distinctive characters above the measurement groups ($p < 0.05$).

day 4 relative to germfree and day 30 post-conventionalization mice. These metabolites included elevated levels of o-phosphoethanolamine, cystine, taurine, L-kynurenine-to-tryptophan (Kyn/Trp) ratio, and L-glutamine (Figures 5.5 and S5.2B). In contrast, citrulline, L-serine, and L-tryptophan were present at lower levels (Figures 5.5 and S5.2B). The altered concentrations of these amine metabolites correlated strongly with the colonic tissue transcriptome, plasma cytokines, and microbiota composition observed on day4 post-conventionalization. For example, the transient increase in Kyn/Trp ratio which determines the activity of indoleamine

2,3-dioxygenase (IDO) enzyme corroborates the induction of the gene expression level of *Ido* which catalyzes the rate limiting step of tryptophan degradation along the kynurenine pathway (Suzuki, Suda et al. 2010) (Figure 5.5A). In addition, the altered plasma levels of citrulline and L-glutamine, a precursor of arginine and nitric oxide production through citrulline in the

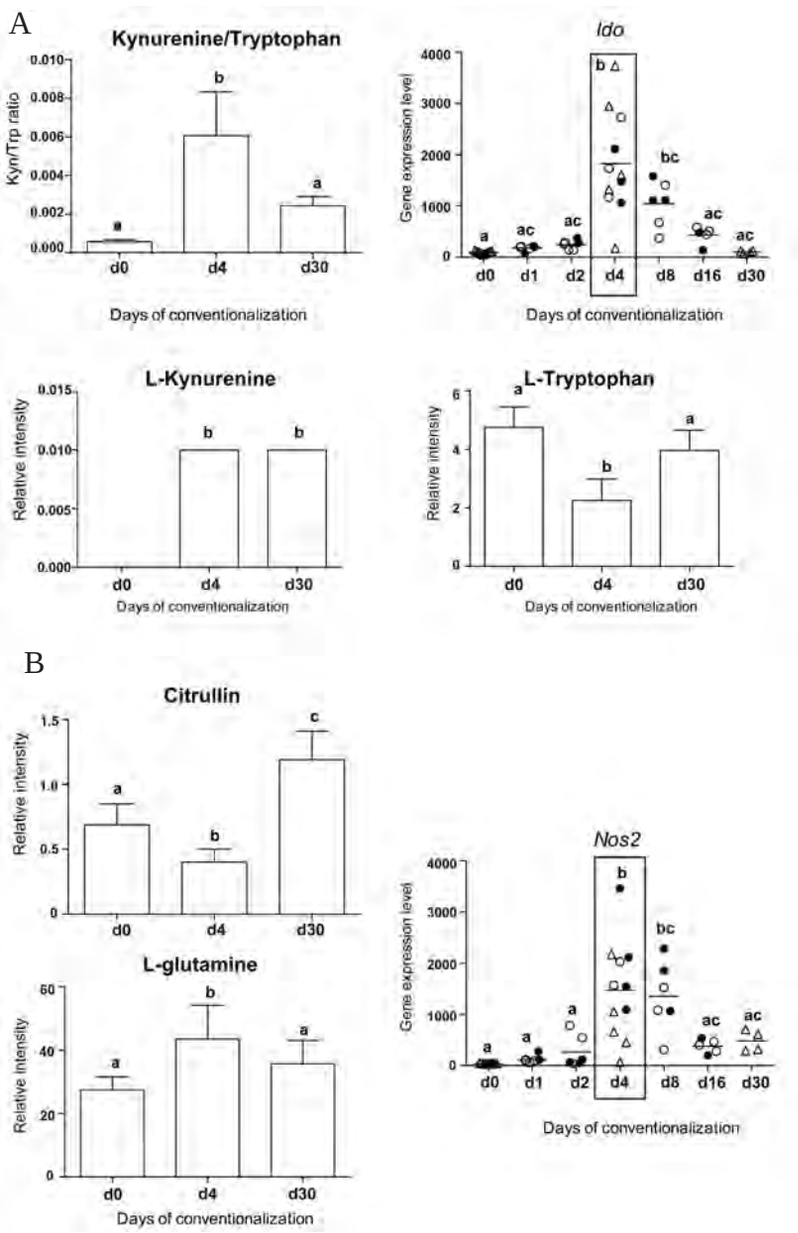

Figure 5.5. Modulation of amine metabolites in plasma samples of day 4 post-conventionalization. Relative intensities of amine metabolites, determined by LC-MS/MS. Comparisons are shown for plasma samples of germfree (day 0), days 4 and 30 post-conventionalization (mean ± SD values). The transient significant increase of Kyn/Trp ratio (A) which determine the activity of indoleamine 2,3-dioxygenase (IDO) enzyme corroborates the induction of the gene expression level of *Ido* as depicted by dot-plots where individual expression values obtained for individual mice are plotted for each of the experiments. The modulated levels of citrulline and L-glutamine (B), which are involved in nitric oxide production coincided with the transient induction of *Nos2* gene, which encodes for nitric oxide enzyme. Significant difference between time-points are indicated by distinctive characters above the measurement groups ($p < 0.05$). The unit of the Y-axis (relative intensity) a.u. "arbitrary unit".

intestine (Bellows and Jaffe 1999), coincided with the induced gene expression level of inducible nitric oxide (*Nos2*) (Figure 5.5B). Taken together, the measured changes in accumulation of specific metabolites supports the hypothesis that day 4 post-conventionalization represents a transitional state between physiological and pathological inflammation.

DISCUSSION

It is widely accepted that the use of simplified model systems can enable the comprehensive analysis of extremely complex biological processes including the intestinal homeostatic mechanisms. Previously, it has been established that conventionalization of germfree mice is associated with a transient inflammation that, on histology, has similarity to ulcerative colitis (Fukushima, Sasaki et al. 1999). The present study demonstrates that mining of multivariate datasets in a similar germfree mouse conventionalization model provides an attractive reductionist-model to identify the molecular events underlying the transient changes that reflect the transient state of "inflammation" by dysbiosis of host-microbe interplay. The analysis of colonic transcriptome data, plasma cytokines, and amine metabolites, as well as gut microbiota composition consistently indicated that a transient state (day 4) during conventionalization precedes the establishment of a novel state of microbiota accommodating homeostasis reached at day 30 post-conventionalization (Chapter 2).

The microbial communities that were specifically associated with the transient state of inflammation included *Helicobacter* and *Sphingomonas.* These genera were shown to have specific characteristics that enable them to colonize the intestinal mucus layer and tolerate the strong innate immune response (Sarma-Rupavtarm, Ge et al. 2004) observed at this time-point (this study and Chapter2). *Helicobacter* species have been found in close proximity to the intestinal mucosal epithelium in crypts of the mouse colon and cecum, thereby are capable of evading the innate immune system (Sarma-Rupavtarm, Ge et al. 2004). Although they are among the natural inhabitants of the intestine of mice (Sterzenbach, Lee et al. 2007), and can peacefully co-exist with the host, they still retain pathologic potential via their ability to induce inflammatory responses and were therefore designated "pathobionts" (Chow and Mazmanian 2010; Lee and Mazmanian 2010; Chow, Tang et al. 2011). *Helicobacter hepaticus* has been associated with dysbiosis (Dieleman, Arends et al. 2000) and is capable of inducing T-cell dependent (induction of Th1 and Th17) and T-cell independent (via TLRs) inflammatory responses in immunocompromised and *IL 10* $^{-/-}$ and lymphocyte-deficient *Rag* $^{-/-}$ *Myd88* $^{-/-}$ mice but not in wild-type mice (Erdman, Rao et al. 2003; Kullberg, Jankovic et al. 2006; Erdman, Rao et al. 2009). The abundance of *Sphingomonas* could be linked to the subsequent induction of natural Killer T cells as previously described (Chapter 2), since *Sphingomonas* has been associated with activation of natural killer T cells in humans via their glycosphingolipids (Mattner, DeBord et al. 2005). Interestingly, glycolipids produced by *Sphingomonas* induced an increased production of typical Th1 chemokines in human and mouse (Chang, Huang et al. 2007) which was also observed in our study.

The correlation between expansion of *Helicobacter* and *Sphingomonas* and a Th1-type immune response was also exemplified by a gene regulatory network where the typical gamma-interferon activated-Th1 type chemokines *Cxcl10* (*IP-10*), *Cxcl11*, *Clec4e*, *Tgm2*, and *Mmp3, 10* constituted an important part of the total network. The Th1 part of the network represented a characteristic gene-expression signature for day 4. This particular transient response was also observed in bacterial infections where peak expression of the pro-inflammatory chemokine *Cxcl10* preceded

T cell infiltration by four days prior to the activation of $Cd8^+$ T cells (Valbuena, Bradford et al. 2003). Importantly, two major negative regulators of the pro-inflammatory genes, *Socs1*, a potent negative regulator of cytokines including *Ifn-γ* and downstream target genes (Kinjyo, Hanada et al. 2002), and *Timp-1*, the natural inhibitor of *Mmp3* (Heuschkel, MacDonald et al. 2000) were co-induced with their target genes. Asynchronous expression of *Socs1* and *Timp1* has been shown in chronic inflammatory bowel disease in humans (Heuschkel, MacDonald et al. 2000; Chinen, Kobayashi et al. 2006) and the induction of *Socs1* was proposed to be a potentially effective treatment (Chinen, Kobayashi et al. 2006) . The co-induction of *Socs1* and *Timp1* inhibitor genes together with the pro-inflammatory cytokines that are antagonized by *Socs1* and *Timp1* might have contributed to the controlled state of inflammation that did not lead to tissue damage, as concluded from the histological staining (Chapter 2).

This absence of tissue damage throughout the intestine at day 4 comes as no surprise since our study used healthy mice, with mucosa that apparently possessed sufficient plasticity to tolerate the microbiota. Mild inflammatory responses to commensal bacteria while maintaining the integrity of the intestinal barrier is a major hallmark of physiological inflammation (Sansonetti and Di Santo 2007). These findings, together with the expansion of T cells and the corresponding increased T cell-specific gene expression profiles propose that this transient state of inflammation was pivotal for appropriate immune system development. It is conceivable that the correlating genetic regulation of expansion of tolerant T cells is somehow lost in patients that suffer from inflammatory bowel diseases. Supporting this hypothesis are reports that link the transiently elevated pro-inflammatory cytokines that we measured in plasma to inflammation in experimental animals and in human inflammatory bowel disease (e.g.; *Mip-1,-2 Ifn-γ, Ip-10, Mip-3β*, and *Mcp-3*) (Dieleman, Ridwan et al. 1994; Banks, Bateman et al. 2003; Demierre, Higgins et al. 2005; Singh, Venkataraman et al. 2007; Torrence, Brabb et al. 2008; Nishimura, Kuboi et al. 2009; Wang, Pezo et al. 2010).

Evidence for a regulation of immune cell numbers (proliferation) and behavior (immune suppression) was also found at the metabonome level. Among the detected plasma amines specifically induced on day 4 post-conventionalization were L-kynurenine and L-tryptophan, metabolites that potentially inhibit immune cell proliferation and induce apoptosis and immune suppression (Suzuki, Suda et al. 2010). We also observed an increased plasma glutamine level that, under conditions of cell proliferation and growth as observed during conventionalization (Chapter 2), plays a crucial role in T cell activation and nucleic acids biosynthesis (Wu 1998), and the elevation of nitric oxide levels (Akobeng, Miller et al. 2000). Nitric oxide is a reactive free radical which acts as a messenger in several processes including antimicrobial and antitumoral activities. A drop in citrulline levels was observed at day 4 (Figure 5.5). The changes in plasma levels of glutamine and citrulline were associated with a correlating transient increase in the colon in the expression level of the expression of *Nos2* (also known as *iNos*) that is induced by bacterial LPS and cytokines such as *Ifn-γ, Tnfα* and *Il-1β*. We did not determine if nitric oxide did accumulate since its short half-life (minutes) precluded its detection in our experiments.

In conclusion, the transient peak of three microbial genera, the corresponding initiation of inflammatory cascades, and the temporal induction of identified plasma analytes, illustrates that day 4 post-conventionalization of mice by their natural microbiota marks a stage where resilience of healthy mice to inflammatory stimuli is most strongly challenged. The changes in gene expression and plasma metabolites at day 4 show very strong correlations with a transient expansion of the three microbial genera and an activation and expansion of innate but especially, adaptive immune (T) cells from day 8 onward (Chapter 2). Especially microbes

belonging to two of these thee genera, *Helicobacter* and *Sphingomonas*, are known to promote activation of multiple T cell types, including NK T cells, by glycolipids that increase tissue concentrations of Th1 cytokines. We propose that the strong Th1 response that we measured at day 4 and the concurrent expansion and activation of T cells that we measured from day 8 onward were induced by at least these two microbial genera, but may also include others like *Mucispirillum*, which is known to colonize the mucus layer (Robertson, O'Rourke et al. 2005). This activation of the (adaptive) immune system is in good agreement with the pathobiont hypothesis of (Lee and Mazmanian 2010). Our study provides an extensive resource of genes, pathways, and metabolites that together very well illustrate how this activation is regulated at the tissue level. In the healthy mice that we used, the transient inflammatory responses that led to expansion and activation of T cells did not lead to tissue damage but rather, to a state of apparent physiological inflammation and homeostasis. It is of interest that the identified regulatory gene expression profiles and concentrations of several blood plasma metabolites show similarities with loss of homeostasis as it has been described in mouse models of inflammation as well as in patients with inflammatory disorders. Of note, in our study these molecules and regulatory gene expression profiles were identified in a context of mucosal and physiological responses to commensal microbiota in ex-germfree but otherwise healthy animals, with no genetic background for inflammatory diseases. In this context, it is of interest that the multi-variate approach chosen here shows that a combination of genomics (transcriptomics), plasma analytes measurements (metabolomics and immune cytokines), and microbial profiling techniques can provide potential human inflammation risk indicators of the intestinal mucosa.

Experimental Procedures

Animals, Experimental Design, and Sampling

All procedures were carried out as previously described (Chapter 2). In brief, germfree and conventionalized mice (male, C57 BL/6 J) were maintained in sterile conditions, on a commercial laboratory chow diet. Three independent biological experiments were performed using mice of different age after 2 weeks of acclimatization and diet adaptation. The first and second experiments of the three performed independent biological experiments included 36 mice obtained in 2 biologically independent batches of 18 mice each, aged 8 and 10 weeks, respectively. The third experiment included 14 mice, aged 10 weeks old. The colon from each mouse was removed and divided into 2 cm segments that were immediately: stored in RNA-Later at room temperature for 1 h prior to storage at -80°C for RNA isolation. Luminal content from colonic segments was removed by gentle squeezing, snap frozen, and stored at -80°C for microbiota analysis. Plasma samples (150-300 µl) were collected from germfree and conventionalized mice directly after sacrifice and stored at -80°C for cytokine and amine measurements.

Transcriptome Analysis

High quality total RNA was isolated from a 2 cm segment colon by extraction with TRIzol reagent, followed by DNAse treatment and column purification. Samples were hybridized on Affymetrix GeneChip Mouse Gene 1.1 ST arrays. Several complementary methods were used for the biological interpretation for the transcriptome data; gene clustering using Multi-experimental View (MeV) software (Saeed, Hagabati et al. 2006), overrepresentation analysis of Gene Ontology (GO) terms using temporal and location comparative analysis using STEM (Ernst and Bar-Joseph 2006), and construction of biological interaction networks using Ingenuity

Pathways Analysis (for detailed descriptions see supplemental material of Chapter 2).

Microbial Profiling of Gut Contents
Colon content was analysed by Mouse Intestinal Tract Chip (MITChip), a diagnostic 16S rRNA arrays that consists of 3,580 unique probes especially designed to profile murine gut microbiota (Geurts, Lazarevic et al. 2011) in analogy to the human intestinal tract (HIT)Chip (Rajilic-Stojanovic, Heilig et al. 2009) (for detailed descriptions see supplemental material of Chapter 2). Correlation analysis of MITChip and transcriptome datasets was performed as previously described (Swann et al., 2011). In brief, a correlation matrix between the MITChip level 2 (genera-like) data and the transcriptome was computed using the absolute expression values. To reduce the probability of type I errors (false positives) for multiple testing, the Benjamini–Yekutieli method (Benjamini and Yekutieli 2001) was employed and the data were corrected for multiple testing using an FDR method. FDR was set at < 0.05 % for expected proportion of false positive correlations in the multiple comparison testing.

Plasma Measurements
Cytokines were determined in 70 µl plasma samples using the Mouse MAP multiplexed immunoassay standard operating procedures established at Rules-Based Medicine laboratory (Austin-USA) (www.rulesbasedmedicine.com); (for more detailed descriptions, see supplementary methods). Plasma aliquots of 5 µL were used for quantitative analysis of primary and secondary amines using LC-MS/MS after derivatization using the AccQ·Tag Ultra Derivatization Kit (Waters, UK) as described by Shi et al. (unpublished data). The acquired data was analyzed using Quanlynx (Waters, UK). The quality of the measurements for the individual metabolites was assessed by means of the relative standard deviation (RSD) on the quality controls and replicates (see supplementary methods for detailed procedure description). For data analysis, ANOVA was executed in SPSS Statistics 17.0 (SPSS Inc., Chicago, IL). To correct for multiple testing a Benjamini-Hochberg correction was applied to generate corrected p values. When significant differences ($p < 0.05$) were detected, a Tukey Honestly Significant Difference test was performed to determine which groups were significantly different from each other.

Accession Numbers
The mouse microarray dataset was deposited in the Gene Expression Omnibus (GEO) with accession number GSE32513.

ACKNOWLEDGMENTS

The authors thank the technical staff in the animal facilities in the lab of J. Doré (INRA, Jouy en Josas) for assistance with animal sacrifice and sampling, J. Jansen, M. Grootte-Bromhaar, M. Boekschoten and P. de Groot (Division for Human Nutrition, Wageningen University) for their technical support in microarray hybridization and microarray data-quality control and processing. We are also grateful to E.E.S.Nieuwenhuis (Utrecht medical center, Utrecht) and J.Samsom (Erasmus University Medical Centre, Rotterdam) for critical reading of the manuscript, and T. Hankemeier for providing access to the excellent technical facilities and expertise at the Netherlands Metabolomics Centre, Leiden.

CHAPTER 5
Supplemental Material

A Transient State of Microbial Dysbiosis and Inflammation is Pivotal in the Establishment of Homeostasis during Conventionalization of Mice

SUPPLEMENTAL EXPERIMENTAL PROCEDURES

Plasma Measurements of Amine Metabolites

Quantitative analysis of primary and secondary amines was performed with an aliquot of 5 µL plasma using LC-MS/MS after derivatization using the AccQ·Tag Ultra Derivatization Kit (Waters, UK) as described by Shi et al. (unpublished data). Briefly, this method involves the reaction of primary and secondary amines present in protein precipitated mouse plasma with the AccQ·Tag Reagent, to form stable ureas. The samples were injected onto the AccQ·Tag column (Waters, UK) and 59 primary and secondary amines were detected using the XevoQqQ MS (Waters, UK) in MRM mode. A binary gradient of water – eluent A (10:1, v/v) (AccQ·Tag, Waters) and 100% eluent B (AccQ·Tag, Waters), was used. Elution of the amines was achieved by ramping the percentage of eluent B from 0.1 to 90% in approx. 9.5 minutes. The flow rate was 0.7 ml min^{-1}. An ACQUITY ultra pressure liquid chromatography (UPLC) system (Waters, UK) was hyphenated to a XevoQqQ mass spectrometer, which was operated in positive-ion mode. The desolvation gas flow was 1000 l h^{-1}, and the desolvation temperature was set at 450 °C. The cone gas flow was set at 50 l h^{-1} and the source temperature was 140°C. The cone voltage was set at 52V. The capillary voltage was 3.20 kV. Collision energy and collision gas (Ar) pressure were 22eV and 2.5 mbar, respectively. The samples were analyzed in one batch. Nine samples were at random chosen to be analyzed in duplicate. All samples (including the 9 replicas) were randomized and divided into blocks of 5. Between each block a quality control (QC) sample was analyzed. These QC samples were created by pooling an aliquot of all the samples. Each sample was injected twice in a row. The acquired data was analyzed using Quanlynx (Waters, UK). The automated peak integration was checked manually and when necessary corrected by hand. All peak areas were corrected for system trends by using the QC samples as described by van der Kloet *et al*. (van der Kloet, Bobeldijk et al. 2009) The data was normalized by dividing the intensity of a compound by the mean intensity of all compounds and globally checked on inconstancies. There were no unexpected differences between duplicate samples and the duplicate injections were within range of each other. The quality of the measurements for the individual metabolites was assessed by means of the relative standard deviation (RSD) on the QCs and the replicates. In general, we consider metabolites with RSD values on both below 15% as measured with enough precision.

Plasma Measurements of Cytokines

All samples were stored at -80°C until tested. The samples were thawed at room temperature (RT), vortexed, spun at 13,000 x g for 5 minutes for clarification and 35 µL was removed for MAP analysis into a master microtiter plate. Using automated pipetting, an aliquot of each sample was introduced into one of the capture microsphere multiplexes of the Mouse CytokineMAP A v1.0, Mouse CytokineMAP B v1.0, Mouse CytokineMAP C v1.0 and Rodent CustomMAP: RAMB1, RAMB2 and RAMB5. The mixture of sample and capture microspheres were thoroughly mixed and incubated at RT for 1 h. Multiplexed cocktails of biotinylated, reporter antibodies for each multiplex were then added robotically and after thorough mixing, were incubated for an additional hour at RT. Multiplexes were developed using an excess of streptavidin-phycoerythrin solution which was thoroughly mixed into each multiplex and incubated for 1 h at RT. The volume of each multiplexed reaction was reduced by vacuum filtration and the volume increased by dilution into matrix buffer for analysis. Analysis was performed in a Luminex 100/200 instrument and the resulting data stream was interpreted using proprietary

data analysis software developed at Rules-Based Medicine (www.rulesbasedmedicine.com). For each multiplex, both calibrators and controls were included on each microtiter plate. Eight-point calibrators were run in the first and last column of each plate and three-level controls were included in duplicate. Standard curve, control, and sample QC were performed to ensure proper assay performance. Unknown values for each of the analytes localized in a specific multiplex were determined using 4 and 5 parameter, weighted and non-weighted curve fitting algorithms included in the data analysis package.

SUPPLEMENTAL FIGURES

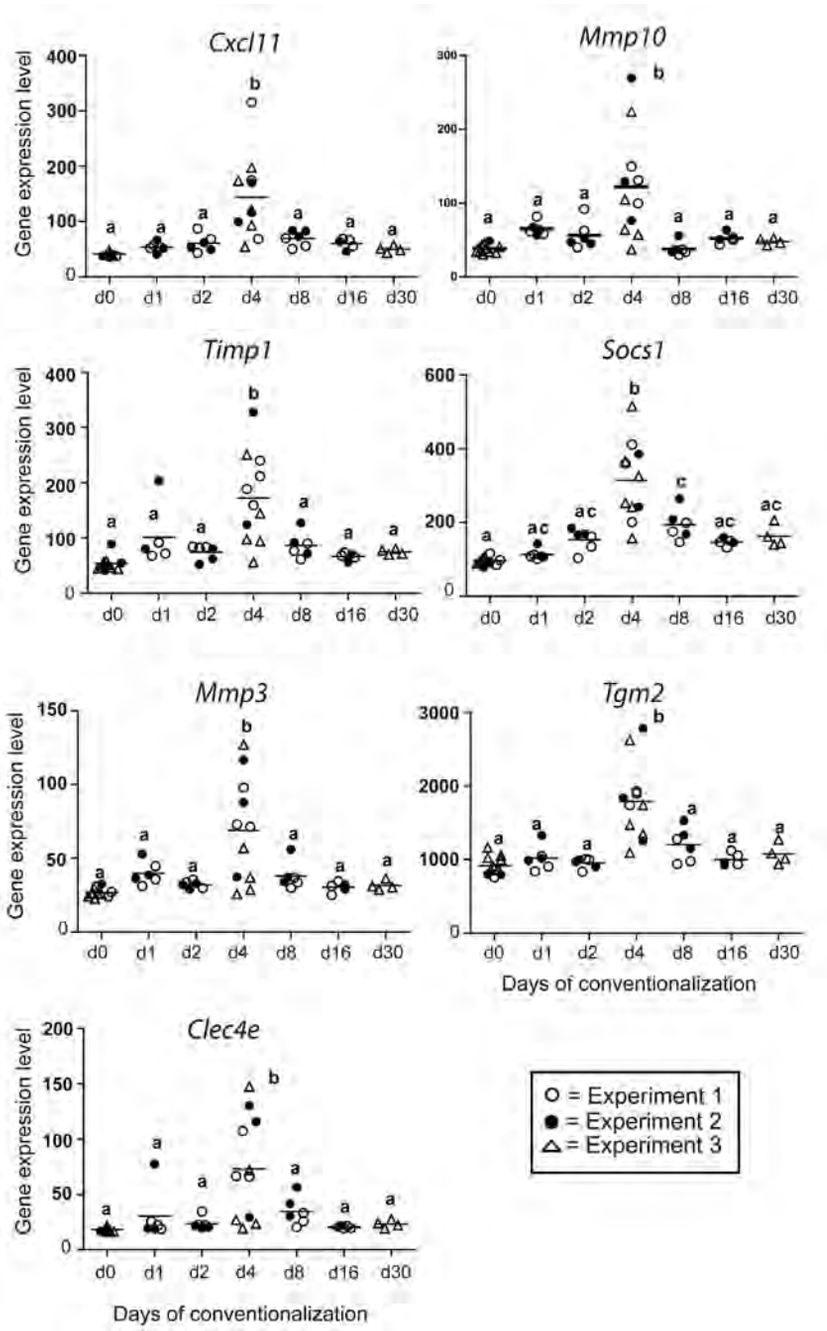

Figure S5.1. Consistency between the gene expression patterns in the three independent conventionalization experiments. Expression levels of the colon genes that are positively correlated with microbiota in germfree and conventionalized mice at indicated days of conventionalization. Values are depicted as dot plots. Significant differences between time-points are indicated by distinctive characters above the measurement groups ($p < 0.05$). The expression levels confirm the similar modularity of transcriptome in experiments 1, 2, and 3 and the consistence presence of transient state of compromised mucosal response during the 30 days of conventionalization. Among the mice sacrificed at day 16, one mouse was excluded as an outlier because the gene expression levels for this mouse were more than 600 SD from the rest of the data for all the pro-inflammatory cytokines. Interestingly, the MITChip data analysis of the same mouse indicated the dominance of *Helicobacter* (17.03%) compared to (0.51% ± 0.08) in the rest of the mice at day 16 post-conventionalization.

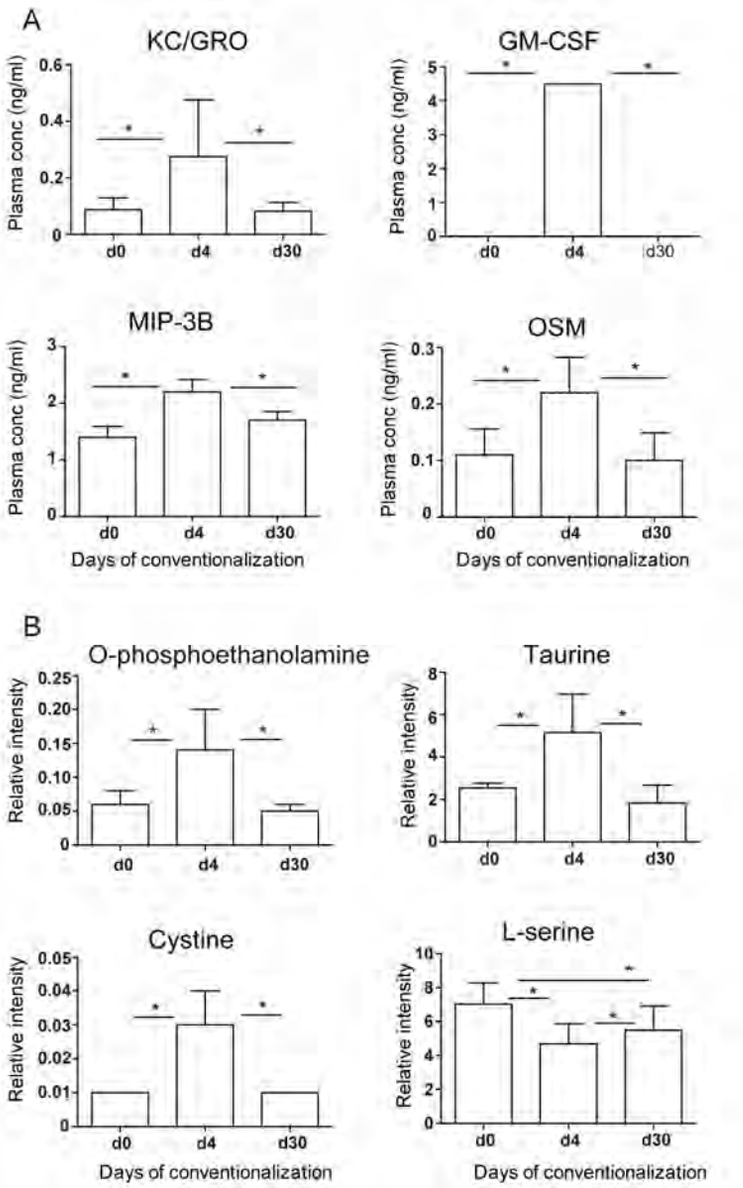

Figure S5.2. Changes in the plasma levels of pro-inflammatory cytokines and amines at day 4 post-conventionalization. Additional plasma analytes including (A) KC/GRO, GM-CSF, MIP-3β, and OSM and (B) o-phosphoethanolamine, Taurine, and Cystine were significantly increased at day 4 when compared to germfree and day 30 post-conventionalization. (*= $p < 0.05$). Although the plasma cytokines (A) are induced upon exposure to inflammatory stimuli as reported in previous studies (Torrence, Brabb et al. 2008; Mentor-Marcel, Bobe et al. 2009), their elevated profile did not correlate with the trend of expression of corresponding genes because the expression level of these genes was very low on the Affymetrix GeneChip Mouse Gene 1.1 ST arrays at all time-points of conventionalization suggesting it could be a background.

REFERENCES

Akobeng, A. K., V. Miller, et al. (2000). "Glutamine supplementation and intestinal permeability in Crohn's disease." Journal of Parenteral and Enteral Nutrition **24**(3): 196-196.

Bäckhed, F., R. E. Ley, et al. (2005). "Host-bacterial mutualism in the human intestine." Science **307**(5717): 1915-1920.

Banks, C., A. Bateman, et al. (2003). "Chemokine expression in IBD. Mucosal chemokine expression is unselectively increased in both ulcerative colitis and Crohn's disease." Journal of Pathology **199**(1): 28-35.

Bellows, C. F. and B. M. Jaffe (1999). "Glutamine is essential for nitric oxide synthesis by murine macrophages." Journal of Surgical Research **86**(2): 213-219.

Benjamini, Y. and D. Yekutieli (2001). "The control of the false discovery rate in multiple testing under dependency." Annals of Statistics **29**(4): 1165-1188.

Chang, Y.-J., J.-R. Huang, et al. (2007). "Potent immune-modulating and anticancer effects of NKT cell stimulatory glycolipids." Proceedings of the National Academy of Sciences of the United States of America **104**(25): 10299-10304.

Chinen, T., T. Kobayashi, et al. (2006). "Suppressor of cytokine signaling-1 regulates inflammatory bowel disease in which both IFN gamma and IL-4 are involved." Gastroenterology **130**(2): 373-388.

Chow, J. and S. K. Mazmanian (2010). "A Pathobiont of the Microbiota Balances Host Colonization and Intestinal Inflammation." Cell Host & Microbe **7**(4): 265-276.

Chow, J., H. Tang, et al. (2011). "Pathobionts of the gastrointestinal microbiota and inflammatory disease." Current Opinion in Immunology **23**(4): 473-480.

Demierre, M. F., P. D. R. Higgins, et al. (2005). "Statins and cancer prevention." Nature Reviews Cancer **5**(12): 930-942.

Dieleman, L. A., A. Arends, et al. (2000). "Helicobacter hepaticus does not induce or potentiate colitis in interleukin-10-deficient mice." Infection and Immunity **68**(9): 5107-5113.

Dieleman, L. A., B. U. Ridwan, et al. (1994). "Dextran sulfate sodium-induced colitis occurs in sever combined immunodefient mice " Gastroenterology **107**(6): 1643-1652.

Elinav, E., T. Strowig, et al. (2011). "NLRP6 inflammasome regulates colonic microbial ecology and risk for colitis." Cell **145**(5): 745-757.

Erdman, S. E., V. P. Rao, et al. (2003). "CD4(+)CD25(+) regulatory lymphocytes require interleukin 10 to interrupt colon carcinogenesis in mice." Cancer Research **63**(18): 6042-6050.

Erdman, S. E., V. P. Rao, et al. (2009). "Nitric oxide and TNF-alpha trigger colonic inflammation and carcinogenesis in Helicobacter hepaticus-infected, Rag2-deficient mice." Proceedings of the National Academy of Sciences of the United States of America **106**(4): 1027-1032.

Ernst J. and Z. Bar-Joseph (2006). "STEM: a tool for the analysis of short time series gene expression data." BMC Bioinformatics **7**: 191.

Fox, J. G. (2002). "The non-H pylori helicobacters: their expanding role in gastrointestinal and systemic diseases." Gut **50**(2): 273-283.

Fukushima, K., I. Sasaki, et al. (1999). "Colonization of microflora in mice: mucosal defense against luminal bacteria." Journal of Gastroenterology **34**(1): 54-60.

Geurts L, V. Lazarevic, et al. (2011). "Altered gut microbiota and endocannabinoid system tone in obese and diabetic leptin-resistant mice: impact on apelin regulation in adipose tissue." Frontiers in Cellular and Infection Microbiology.

Heuschkel, R. B., T. T. MacDonald, et al. (2000). "Imbalance of stromelysin-1 and TIMP-1 in the mucosal lesions of children with inflammatory bowel disease." Gut **47**(1): 57-62.

Kinjyo, I., T. Hanada, et al. (2002). "SOCS1/JAB is a negative regulator of LPS-induced macrophage activation." Immunity **17**(5): 583-591.

Kullberg, M. C., D. Jankovic, et al. (2006). "IL-23 plays a key role in Helicobacter hepaticus-induced T cell-dependent colitis." Journal of Experimental Medicine **203**(11): 2485-2494.

Lee, Y. K. and S. K. Mazmanian (2010). "Has the microbiota played a critical role in the evolution of the adaptive immune system?" Science **330**(6012): 1768-1773.

Macpherson, A. J., M. B. Geuking, et al. (2005). "Immune responses that adapt the intestinal mucosa to commensal intestinal bacteria." Immunology **115**(2): 153-162.

Manco, M., L. Putignani, et al. (2010). "Gut microbiota, lipopolysaccharides, and innate immunity in the pathogenesis of obesity and cardiovascular risk." Endocrine Reviews **31**(6): 817-844.

Mattner, J., K. L. DeBord, et al. (2005). "Exogenous and endogenous glycolipid antigens activate NKT cells during microbial infections." Nature **434**(7032): 525-529.

Medzhitov, R. (2008). "Origin and physiological roles of inflammation." Nature **454**(7203): 428-435.

Mentor-Marcel, R. A., G. Bobe, et al. (2009). "Inflammation-associated serum and colon markers as indicators of dietary attenuation of colon carcinogenesis in ob/ob mice." Cancer Prevention Research **2**(1): 60-69.

Nishimura, M., Y. Kuboi, et al. (2009). "Chemokines as novel therapeutic targets for inflammatory bowel disease." Contemporary Challenges in Autoimmunity **1173**: 350-356.

O'Connor, S. M., C. E. Taylor, et al. (2006). "Emerging infectious determinants of chronic diseases." Emerging Infectious Diseases **12**(7): 1051-1057.

On, S. L. W., S. Hynes, et al. (2002). "Extragastric Helicobacter species." Helicobacter **7**: 63-67.

Palmer, R. (2011). "Fecal matters." Nature Medicine **17**(2): 150-152.

Rajilic-Stojanovic, M., H. G. H. J. Heilig, et al. (2009). "Development and application of the human intestinal tract chip, a phylogenetic microarray: analysis of universally conserved phylotypes in the abundant microbiota of young and elderly adults." Environmental Microbiology **11**(7): 1736-1751.

Robertson, B. R., J. L. O'Rourke, et al. (2005). "Mucispirillum schaedleri gen. nov., sp nov., a spiral-shaped bacterium colonizing the mucus layer of the gastrointestinal tract of laboratory rodents." International Journal of Systematic and Evolutionary Microbiology **55**: 1199-1204.

Saeed, A. I., N. K. Hagabati, et al. (2006). TM4 microarray software suite. Methods Enzymology. **411:** 134-193.

Sansonetti, P. J. and J. P. Di Santo (2007). "Debugging how bacteria manipulate the immune response." Immunity **26**(2): 149-161.

Sarma-Rupavtarm, R. B., Z. M. Ge, et al. (2004). "Spatial distribution and stability of the eight microbial species of the altered Schaedler flora in the mouse gastrointestinal tract." Applied and Environmental Microbiology **70**(5): 2791-2800.

Singh, U. P., C. Venkataraman, et al. (2007). "CXCR3 axis: Role in inflammatory bowel disease and its therapeutic implication." Endocrine Metabolic & Immune Disorders-Drug Targets **7**(2): 111-123.

Sokol, H., B. Pigneur, et al. (2008). "Faecalibacterium prausnitzii is an anti-inflammatory commensal bacterium identified by gut microbiota analysis of Crohn disease patients." Proceedings of the National Academy of Sciences of the United States of America **105**(43): 16731-16736.

Solnick, J. V. and D. B. Schauer (2001). "Emergence of diverse Helicobacter species in the pathogenesis of gastric and enterohepatic diseases." Clinical Microbiology Reviews **14**(1): 59-+.

Stepankova, R., F. Powrie, et al. (2007). "Segmented filamentous bacteria in a defined bacterial cocktail induce intestinal inflammation in SCID mice reconstituted with CD45RB(high) CD4+ T cells." Inflammatory Bowel Diseases **13**(10): 1202-1211.

Sterzenbach, T., S. K. Lee, et al. (2007). "Inhibitory effect of enterohepatic Helicobacter hepaticus on innate immune responses of mouse intestinal epithelial cells." Infection and immunity **75**(6): 2717-2728.

Suzuki, Y., T. Suda, et al. (2010). "Increased serum kynurenine/tryptophan ratio correlates with disease progression in lung cancer." Lung Cancer **67**(3): 361-365.

Swann J., Richards S. E. , et al. (2011). Culture-independent analysis of the human gut microbiota and their activities. Handbook of Molecular Microbial Ecology, Volume II: Metagenomics in different habitats. First edition. E. b. F. J. d. Bruijn. Wiley-Blackwell, John Wiley & Sons, Inc. **II:** 207-218.

Torrence, A. E., T. Brabb, et al. (2008). "Serum biomarkers in a mouse model of bacterial-induced inflammatory bowel disease." Inflammatory Bowel Diseases **14**(4): 480-490.

Valbuena, G., W. Bradford, et al. (2003). "Expression analysis of the T-cell-targeting chemokines CXCL9 and CXCL10 in mice and humans with endothelial infections caused by rickettsiae of the spotted fever group." American Journal of Pathology **163**(4): 1357-1369.

van der Kloet, F. M., I. Bobeldijk, et al. (2009). "Analytical error reduction using single point calibration for accurate and precise metabolomic phenotyping." Journal of Proteome Research **8**(11): 5132-5141.

Wang, D., R. C. Pezo, et al. (2010). “Altered dynamics of intestinal cell maturation in Apc1638N/+ mice.” Cancer Research **70**(13): 5348-5357.
Wu, G. Y. (1998). “Intestinal mucosal amino acid catabolism.” Journal of Nutrition **128**(8): 1249-1252.

Chapter 6

General Discussion, Future Perspectives, and Concluding Remarks

GENERAL DISCUSSION

The importance of the interplay between gut microbiota, diet, metabolism, and immune system for the human health status has become generally accepted during the last five years. Nonetheless, there is a large gap in our knowledge on the genetic regulation of immune tolerance towards the gut microbiota and regulation of homeostasis during simultaneous changes in microbiota composition and intestinal metabolism. The work described in this thesis reports on the outcome of conventionalization studies where a germfree mouse model was used to explore the time- and region-dependent host response, with respect to metabolic and immune processes, to changes in the composition of a *de novo* introduced microbial community.
The major findings described in the experimental chapters of this thesis and their future perspectives will be discussed in the following chapter.

Colonization of Mouse Gut Microbiota Rapidly Establishes a Full-sized, Low Diversity Microbial Community

The basis for this thesis was conventionalization experiments, where healthy germfree mice were inoculated with a standard mouse microbiota at eight-ten weeks of age. The total number of colonizing microbial community very rapidly reached the densities that are normally encountered in conventional mice. Quantitative PCR determination of 16S rRNA gene copies in jejunal, ileal, and colonic luminal samples, indicated that already one day after conventionalization, the estimated copy numbers increased from 4.9 ± 0.3 in the jejunum, to 8.25 ± 1.1 in the ileum, and 10.7 ± 1.2 in the colon (mean ± SD Log10 copy number of 16S rRNA/g content), and these numbers did not drastically change upon prolonged conventionalization periods. As anticipated, the total number of bacteria and the community composition diversity (Figure 6.1) increased significantly along the length of the GI tract. In this thesis research, the extensive microbial profiling throughout the GI tract suggested that the establishment of gut microbiota occurred in two phases **(Chapter 4)**. The microbial population at days 1 and 2 was characterized by a low diversity and mainly consisted of bacteria that failed to efficiently extract energy from the diet. This was inferred from the rapid (after one day) accumulation of fermentation metabolites with a high energy content, such as lactate and succinate, in the lumen of the cecum as well as high concentrations of TCA cycle intermediates in the urine. The latter finding implies that these early bacterial colonizers have a profound effect on systemic metabonomics. Remarkably, this early stage of conventionalization was not reflected in prominent transcriptome or tissue metabolite profile changes in the ileum or colon, suggesting that the microbiota associated metabolites passed the intestinal epithelium without influencing the local intestinal tissues in these intestinal compartments. However, this was not the case in the proximal part of the small intestine, the jejunum, where prominent tissue responses could be detected acutely (one day after introduction of the microbiota) upon conventionalization **(Chapter 3)**.

Jejunum is the Initial Sensor of the Colonizing Microbiota

Despite the relatively low microbial densities in the jejunum, the bacterial presence appeared to elicit “danger signal” responses in the jejunal mucosa (**Chapter 3**). This may involve their metabolites (including some typical TCA-cycle intermediates) that could arise from their interaction and utilization of compounds within the nutrient flow (**Chapter 3**). The induction of canonical pathways associated with “danger signal” responses in the jejunal tissue transcriptome after one day of conventionalization was paralleled by the initiation of repression

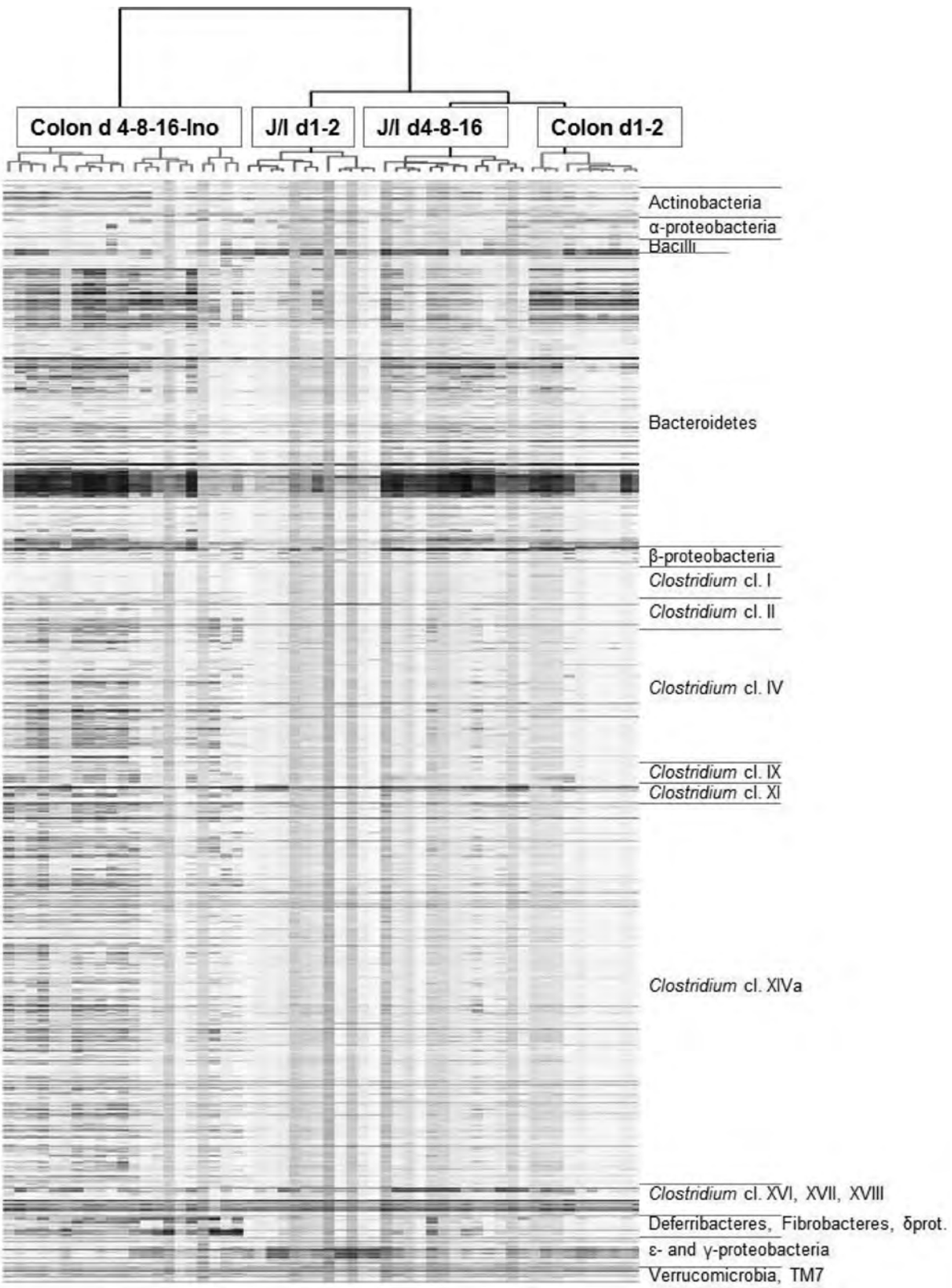

Figure 6.1. Hierarchical clustering analysis of MITChip fingerprints generated from the inoculum (Ino), jejunal (J), ileal (I), and colonic samples collected from the indicated days (d) post-conventionalization. The highest phylogenetic assignments are provided at the right side of the gel-view dendogram.

of genes involved in lipid uptake, transport, and oxidation, including the main regulator of lipid metabolism *Ppar-α* and its downstream target genes. These responses included the repression of *Angptl4*, the gene which is essential for the induction of *de novo* hepatic lipogenesis and elevation of circulating leptin levels (Bäckhed, Ding et al. 2004). By suppressing *Angptl4*, the microbiota indirectly promotes storage of calories harvested from the diet into fat in the liver (Bäckhed, Ding et al. 2004). Since the jejunum is regarded as the main absorptive site in the GI tract, this modulation of energy (fat) storage is intriguing in the light of recent studies that link the gut microbiota to the development of metabolic disorders in genetically susceptible persons (Bäckhed, Ding et al. 2004; Korner, Bessler et al. 2005; Delzenne and Cani 2010; Claus, Ellero et al. 2011).

A Transient State of Inflammation during Conventionalization

The simple composition of the early bacterial community in the colon was succeeded by a transiently increased abundance of particular Gram negative bacteria at day 4 post-conventionalization, which included the genera *Helicobacter* and *Sphingomonas*. These two genera have previously been designated "pathobionts" (Chow and Mazmanian 2010) to emphasize their dualistic role as typical commensals with pathogenic potential (**Chapter 5)**. They are of particular interest since glycosphingolipids produced by members of these genera promote (natural killer) T cell development (Kinjo, Wu et al. 2005; Mattner, DeBord et al. 2005; O'Keeffe and Moran 2008). Intriguingly, at the same time-point, the major changes in intestinal physiology and morphometry were observed throughout the GI tract: a reduction of the cecal size, an increased epithelial cell proliferation, the highest level of antimicrobial peptides production, alterations in the chemical composition of the goblet cells, and the drastic transcriptome shift, in particular for innate immune-associated genes **(Chapter 2)**. Interestingly, *RegIIIγ*, a secreted C-type lectin with antimicrobial activity was among the protective innate molecules that peaked at day 4 post-conventionalization throughout the GI tract. This finding corroborates the recent notion that *RegIIIγ* is required to keep the microbiota at bay by maintaining a spatial segregation between the microbiota and host to prevent the activation of excessive cytotoxic adaptive immune responses in the small intestine (Vaishnava, Yamamoto et al. 2011).

Day 4 post-conventionalization also marked a metabolic shift towards an anabolic metabolism throughout the GI tract (**Chapters 3 and 4)**. The jejunum in particular was characterized by a strong repression of fatty acid uptake, transport, and oxidation that was already initiated at day 1 post-conventionalization **(Chapter 3)**. Moreover, a transient impairment of the fatty acid oxidation was observed in the colon at day 4 post-conventionalization **(Chapter 4)**. This drastic metabolic change pointed to a shift towards an anabolic metabolism that favors glucose utilization, which was confirmed by the increased levels of glutamine, glutamate, and asparate throughout the GI tract and the decreased levels of tissue glucose in the colon. The drastic changes in intestinal morphometry and the cell proliferative phenotype did resemble the highly proliferating tumor cells, which depend on glycolysis as their main source of energy (Heiden, Cantley et al. 2009). It is possible that this metabolic shift correlated with the increase of connective tissue and the simultaneous accumulation of (activated) T cells and innate immune cells in the lamina propria, in that the glycolytic metabolism was necessary to support the activated immune cells. The correlation between the metabolic shift and the activation and accumulation of innate and adaptive immune cells highlights the strong link between metabolism and the immune system. The shifts in the microbiota composition during

the first four days strongly suggest that the changes in metabolism and immunity were driven by the colonizing microbiota.
Intriguingly, a statistical correlation was found between alpha- and epsilon-Proteobacteria classes to which *Helicobacter* and *Sphingomonas spp.* belong, elevated levels of metabolites known to play a key role in anabolic metabolism (glutamate, glycine, and alanine) (Wu 1998), and peak induction of genes involved in nucleotide biosynthesis **(Chapter 4)**. This correlation could be of biological relevance in that it suggests the high requirement of anabolic metabolism during the transient state of inflammation, when the abundance of *Helicobacter* and *Sphingomonas* was specifically enhanced. *Helicobacter spp.* are among the natural inhabitants of the mouse intestine (Sterzenbach, Lee et al. 2007), but can also occur as pathobionts that promote intestinal inflammation (Erdman, Rao et al. 2009; Chow and Mazmanian 2010). *Helicobacter* can induce Th1 type inflammatory responses and can promote the production of *Tnf-α* in immuno-compromised mice (Kullberg, Ward et al. 1998). At day 4 post conventionalization, the induction of a Th1 type immune response was also detected. *Sphingomonas* was shown to activate natural killer cells that promote adaptive immune system activation by its glycoshingolipids, via induction of a T cell receptor (TCR) signalling cascade that involves the MHC class I molecule, *Cd1d1* (Mattner, DeBord et al. 2005). These particular features suggest that the transient expansion of the two bacterial genera were instrumental in activating an inflammatory Th1 type immune response at day 4 post-conventionalization. The Th1 response was inferred from a gene regulatory network that included typical Th1 specific genes and the correlated pro-inflammatory Th1 cytokines and the increased levels of several plasma markers, including inflammatory cytokines and some amines **(Chapter 5)**. The transient features that marked day 4 post-conventionalization, revealed a consistent association with inflammation. Collectively, these findings suggested that the transient state at day 4 marked a transient state of dysbiosis and inflammation where the resilience of the healthy mice to inflammatory stimuli was most strongly challenged. Here it is proposed that the molecules that characterize this transient state could provide useful risk indicators for the loss of homeostasis that is associated with progressive inflammation in individuals that suffer from inflammatory diseases.
During the conventionalization experiments, the mice remained healthy and the integrity of the intestinal mucosal barrier remained intact, as apparent from histological examinations **(Chapter 2).** The results therefore imply that the transient state described above and in **Chapter 5** activated the development of the lamina propria immune function without actual loss of homeostasis. The regulatory network that was induced during the transient dominance of *Helicobacter* and *Sphingomonas* included activators of MHC class I and chemokines. Interestingly, these same chemokines were previously observed to peak at 4 days after bacterial infection in mice and preceded infiltration by activated $Cd8^+$ T cells (Valbuena, Bradford et al. 2003). These results indicate that the induction of pro-inflammatory cytokines and chemokines during the transient dominance of *Helicobacter* and *Sphingomonas* (**Chapters 2 and 5)** without loss of mucosal barrier integrity was part of a natural process leading to the activation and maturation of adaptive immune responses that was measured at days 8 and 16 (**Chapter 2**)(Figure 6.2).

Establishment of Microbiota Accommodating Homeostasis
Day 8, four days following the transient state of dysbiosis and inflammation, was marked by activation of adaptive immunity, in particular T cell activation. At day 8, a gradual increase in T cells that express the surface markers Cd4, Cd8, and the T cell maturation marker Cd3ε was observed. These activated T cells accumulated in the lamina propria over the period of

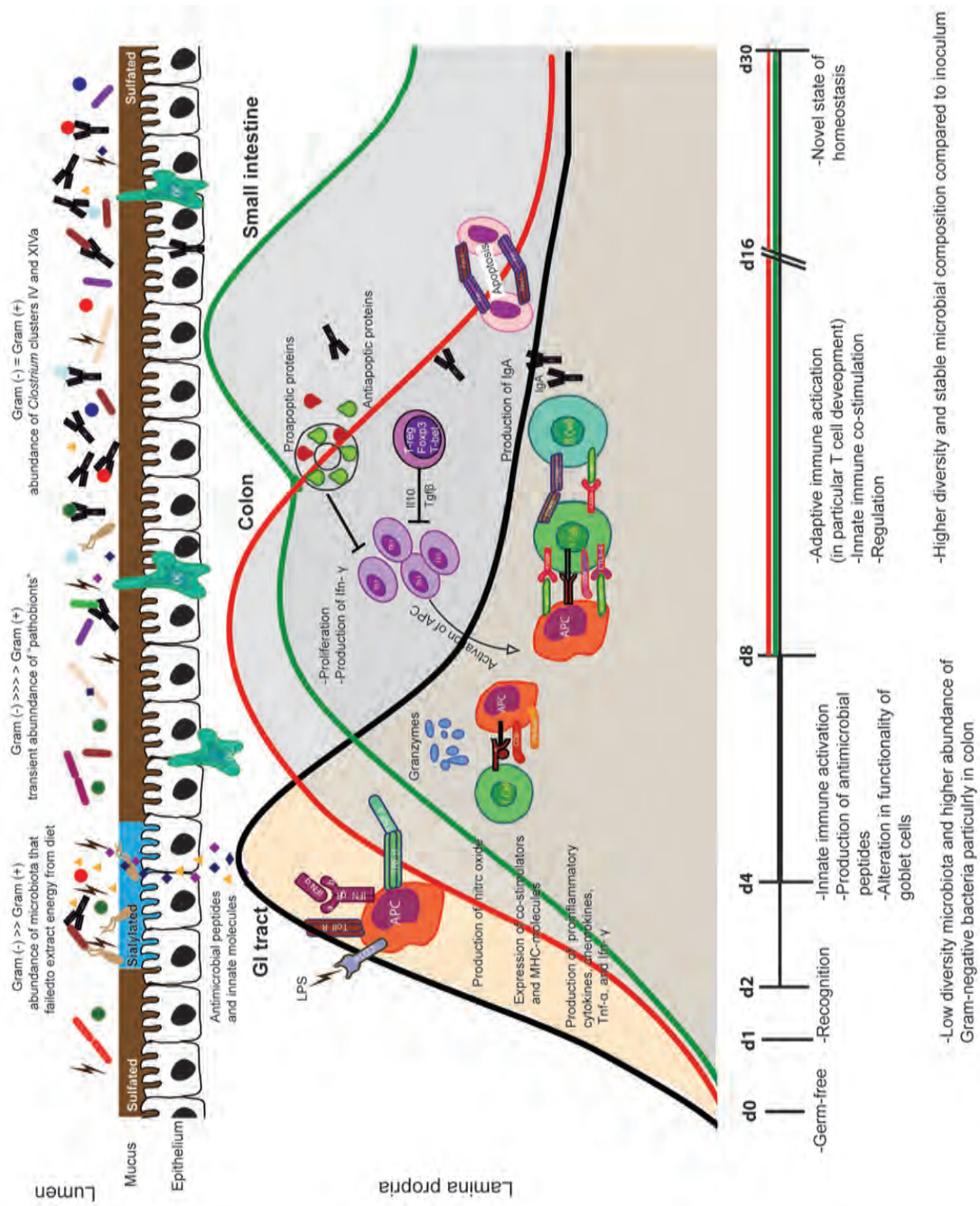

Figure 6.2. Dynamic changes in the regulation of intestinal homeostasis during microbial colonization. The major molecular changes measured in terms of transcriptomes, IHC, and microbiota composition were initiated at day 4 of conventionalization along the GI-tract. These changes correlated with a strong induction of the innate immune response, production of antimicrobial peptides and altered functionality of mucin secreting goblet cells (more sialylated mucins specifically in the colon). Stimulation of adaptive immune response, local immune cell recruitment (in particular T cell development), as well as their regulators followed between days 8 and 16 of conventionalization in the colon, and later between days 16 and 30 in the small intestine. In parallel, establishment of the colonizing microbiota started with a relatively low diversity and higher abundance of Gram-negative bacteria, followed by a transient intermediate diversity and peak of Gram-negative between days 2 and 4 in the colon and days 4 and 8 in the small intestine. This intermediate stage eventually shifted towards high diversity and stable microbial composition (in comparison to the inoculum) between days 8-16 in the colon and at day 16 in the small intestine.

days 8-30 post-conventionalization and displayed the largest abundance in the small intestine **(Chapter 2)**. In parallel, the initial low diversity microbial populations shifted to a high diversity, relatively stable community **(Chapter 4)**. This shift closely resembles the dynamic shift during acquisition of gut microbiota in infants (Pamer 2007; Adlerberth and Wold 2009). The newly established microbiota comprised members that could efficiently deplete the "high energy content metabolites" that were accumulating during the early stages of conventionalization, by converting these metabolites into short chain fatty acids (SCFAs) that can be efficiently used by the host intestinal cells. This scenario was inferred from the high concentrations of the SCFAs butyrate, propionate, and acetate in the large intestinal lumen at days 8 and 16 post-conventionalization. The statistical correlation found between the decreased level of *Myo*-inositol and the repression of host genes involved in choline metabolism could point to the colonization by microbial groups that can metabolize choline and convert it into its derivative metabolites (TMA and TMAO), which were detected in the urine metabolic profiles **(Chapter 4)**. The expansion of Gram- positive Firmicutes, in particular, *Clostridium* clusters IV and XIVa characterized the second stage of conventionalization. These spore-forming Clostridia groups have previously been shown to stimulate regulatory T cell (T_{reg}) population in the colon of mice (Atarashi, Tanoue et al. 2011), which is corroborated by the current finding that T_{reg} population development in the colon mucosa coincided with the abundant colonization of the colon microbiota by the *Clostridium* groups. Expansion of the T_{reg} population was apparent from the increased expression of typical T_{reg} markers, *Il10, Tbx21, Foxp3,* and *Tgfβ1*. Importantly, expansion of T_{reg} continued also during later time-points of conventionalization, illustrating the requirement of T_{reg} to establish tolerance and to maintain microbiota accommodating homeostasis in the intestine.

Establishment of Homeostasis Occurred Earlier in the Colon than in the Small Intestine

Combined analysis of transcriptomics and histological data as shown in **Chapter 2** suggested that a novel state of microbiota-accommodating homeostasis was reached in the colon during the time course of 8 to 16 days post-conventionalization. In contrast, homeostasis was reached in the small intestine after 16 to 30 days post-conventionalization (Figure 6.2). This was supported by the transient changes in small intestinal versus colonic tissue morphology, differences in expression pattern of genes regulating the innate responses, as well as tissue metabolites. Importantly, these molecular differences coincided with the expected (based on gene expression) microscopic differences in the microarchitecture of the small intestine versus colon mucosa **(Chapter 2)**. For instance, the colonic morphology (most notably, crypt depth) and the expression pattern of the antimicrobial *RegIIIγ* returned to the germfree level at 30 days of conventionalization, while small intestinal morphology and elevated *RegIIIγ* expression was maintained throughout the 30 day period, albeit to a lesser extent as compared to days 8 and d16 post-conventionalization. In addition, increases in T cell numbers and the expression of specific chemokines and their receptors increased continuously in the small intestine, while these activities reached a steady level in the colon after eight days of conventionalization. The earlier establishment of a homeostatic state in the colon coincided with the expansion of SCFAs producing bacteria and the parallel increased concentrations of SCFAs, in particular butyrate, in the lumen of the large intestine **(Chapter 4)**. The production of SCFAs could have activated the *Gpr43* (*Ffar2*) receptor, a gene encoding a GPCR that plays a crucial role in modulating inflammatory responses (Maslowski, Vieira et al. 2009). Moreover, the increased levels of aspartate, glutamate, and glutamine remained higher than the germfree levels in the

small intestine during the 16 days of colonization **(Chapter 3)**. In contrast, the level of these metabolites returned to the germfree level after 8 days in the colon (except for glutamate whose expression levels remained higher than in the germfree animals) **(Chapter 4)**. These results coincided with the continuous changes in tissue composition and development in the small intestine. Such regional differences may relate to the higher density of the colon microbiota and could be a prerequisite for the establishment of a microbiota-accommodating homeostasis in this densely populated part of the GI tract.

Establishment of Conventionalized Immune and Metabolic Homeostasis is Governed by Gene Regulatory Networks

Proper regulation of animal physiology relies for an important part on gene regulatory networks (Davidson 2010). The reconstructed gene regulatory networks in **Chapters 2, 3, and 5** appeared to be involved in regulation of the dynamic immune and metabolic adaptation of the intestinal mucosa to the colonizing microbiota**.** The central regulatory network identified in this study throughout the GI tract may therefore serve as a genetic signature for control of intestinal homeostasis in healthy mice and could be used as a hypothesis generating model for further studies into diseases with a clear genetic basis that includes the network genes. Such studies should then investigate the modulations and dysregulation of these networks in patients. Moreover, the intriguing link between the genes in the regulatory network identified for the jejunum in **Chapter 3** and the possible mechanisms by which gastric bypass surgery rapidly improves insulin sensitivity (Troy, Soty et al. 2008) appears to suggest that exclusion of the proximal small-intestine from the nutrient flow and/or the normal microbiota affects the regulation of systemic glucose homeostasis and insulin sensitivity. It is likely that the microbiota-induced changes in the jejunal metabolic profile, more specifically the very low accumulation of glucose compared to the germfree state **(Chapter 3)**, may underlie the health promoting effect of the human duodenal-jejunal by-pass surgery.

FUTURE PERSPECTIVES

The time series approach implemented in the design of this study has brought new insight in the dynamics of host responses to microbial colonization and thereby complements other studies that dissected the intestinal-microbiota interactions in similar models. The vast majority of these studies used only a single time-point for analysis or included only extended periods of conventionalization or colonization to evaluate the host responses. Especially the unique, transient state identified at day 4 post-conventionalization of the mice makes it attractive to design finer sampling strategies (e.g. to include days 3, 5, 6, and 7), to more precisely monitor the molecular dynamics that enable the mucosa to proceed from a transient state of partial dysbiosis and inflammation to a state of homeostasis without loss of barrier function. Such study would also allow further deciphering of the processes involved in the establishment of the "normal" mucosal defense mechanisms that underlie homeostasis in the presence of microbiota. The microbiota studied here appeared to lack the presence of segmented filamentous bacteria (SFB), which have been reported to play a prominent role in the maturation of the immune system. As a consequence our measurements failed to identify differential expression of *Il-17* and the corresponding accumulation of Th17 cells in the mucosa. This is due to the mouse strain used in this study (C57/ BL6 J), which lack SFB in their normal microbial community. The use of other mouse strains that do contain SFB in their microbiota, such as C57/ BL6 supplied by Taconic, in combination with the application of finer sampling time lines could be

of great interest. Such experiments would unravel the impact of colonization by a microbiota that includes SFB on Th17 development, which may drastically affect the typical transient state of dysbiosis and inflammation observed on day 4 post-conventionalization in C57/BL6 J mice. In this study, no tissue damage was observed in the mucosa of the mice during the transient state of inflammation, which may relate to the relatively high resistance to inflammation of C57/BL6 J mice, and could be significantly different in other mouse strains with a higher susceptibility to inflammation.

A Role of the Gut Microbiota in Gut-Brain Interaction?

Recently, a profound interest emerged in the role of intestinal microbiota in brain development and behavior, which was stimulated by observations that showed decreased motor-activity but increased anxiety in conventional mice compared to their germfree counterparts (Husebye, Hellstrom et al. 1994; Heijtza, Wang et al. 2011; Neufeld, Kang et al. 2011). In addition, the bidirectional cross-talk between the immune- and nervous systems, which is influenced by the microbiota, is involved in several neuropsychiatric diseases including autism and depression that were linked to the "compromised gut barrier"(Maes, Kubera et al. 2008; Theoharides and Doyle 2008; de Magistris, Familiari et al. 2010; Yap, Angley et al. 2010). The time-resolved transcriptome analysis performed in this thesis highlighted some intriguing changes in the expression of genes associated with the cholinergic and the adrenergic systems (Figure 6.3A). Surprisingly, conventionalization elicited significant down regulation of the expression of genes involved in nerve growth, neurotransmission, dopamine, histamine, γ-amino butyric acid, serotonin, and acetylcholine synthesis, throughout the GI tract (Figure 6.3A).

The genes encoding Substance P (SP) receptor (also known as tachykinin receptor, *Tacr*), and to lesser extend SP were among the modulated genes during conventionalization (Figure 6.3B). SP plays different roles in the GI tract, including the induction of intestinal secretion of water and electrolytes (Riegler, Castagliuolo et al. 1999) and the inhibition of gastric secretion (Martensson HG 1984). SP also has a major role as an excitatory transmitter that stimulates muscle contraction and intestinal transit (Riegler, Castagliuolo et al. 1999). To evaluate the impact of microbial colonization on substance P , IHC staining of SP in the myenteric plexus (the major nerve supply to the GI tract that also controls GI tract motility), was performed as previously described (Verdu, Bercik et al. 2006). The results showed few (non-significant) differences between the stained myenteric plexus SP from germfree and conventionalized mice at days 4, 8, and 16 post-conventionalization, which seemed to corroborate the slight but non-significant differences observed at the *Tac* transcription level (Figure 6.3A). Strikingly, 30 days after conventionalization a large increase was observed in the level of SP in the myenteric plexus of the colonic mucosa in comparison to germfree mice and other time-points post-conventionalization (Figure 6.4A,B). This finding confirms that the microbiota can significantly influence the development of the enteric nervous system, and may explain its postulated role in modulating the GI tract motility and intestinal transit (Silkoff, Karmeli et al. 1988). Interestingly, Goldin and colleagues reported that elevated levels of SP were observed in patients with ulcerative colitis, which may be correlated with the disease's effect on intestinal transit (Goldin, Karmeli et al. 1989). This tentative link between the intestine microbiota and enteric nervous system modulation may eventually influence the functional properties of the gut-brain axis, which could potentially influence brain function and have some intriguing consequences. Moreover, these findings also support that microbial dysbiosis and/or gastrointestinal inflammatory diseases may influence the gut-brain axis function.

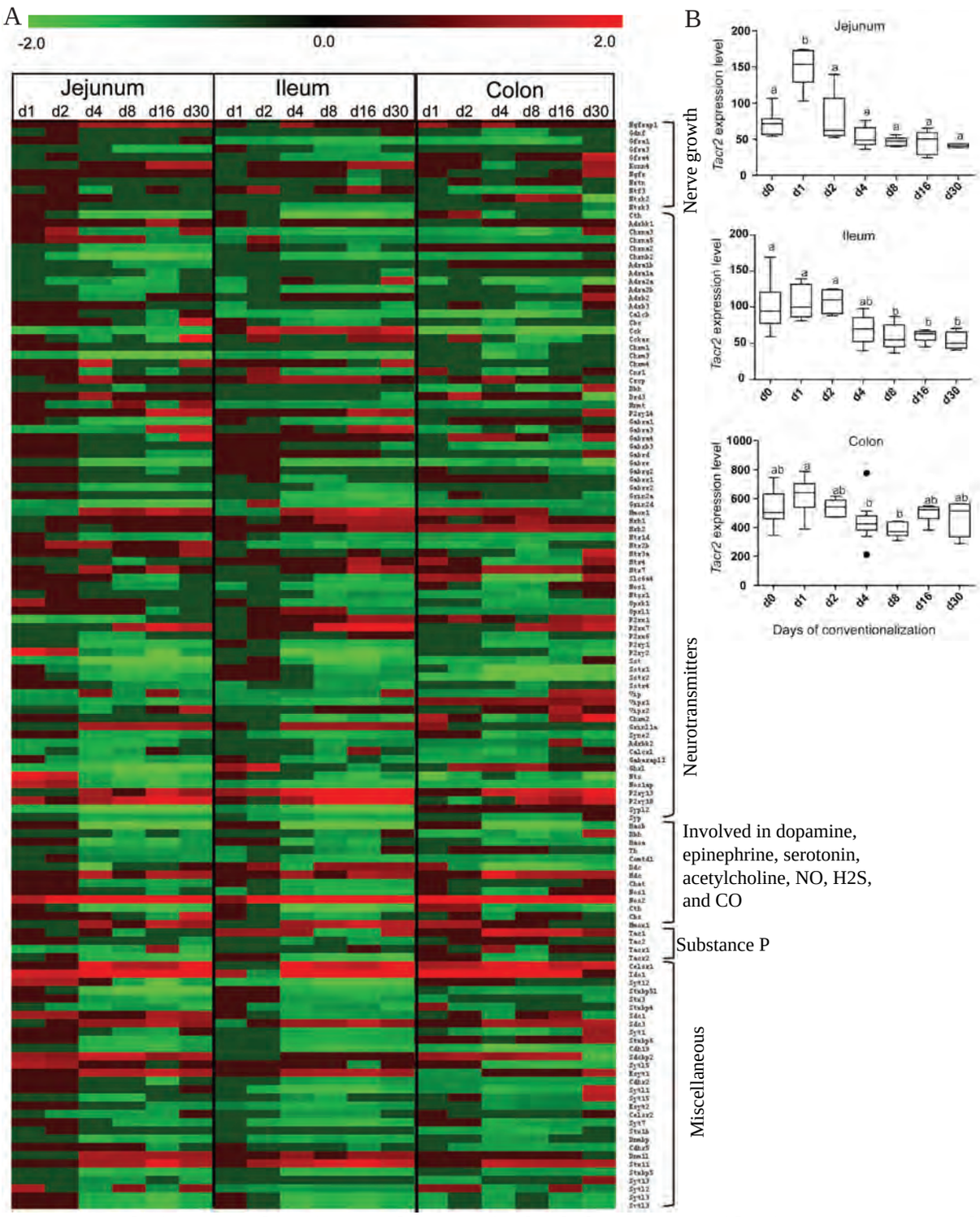

Figure 6.3. Colonizing microbiota impacts the expression level of gut neuropeptides. (A) Heat map generated from the expressed genes involved in neurotransmission and nerve growth, dopamine, epinephrine, serotonin, acetylcholine, nitric oxide (NO), hydrogen sulfide (H_2S), and carbon monoxide (CO) synthesis as well as substance P (SP) and its receptors, between germfree and conventionalized mice at the indicated time-points throughout the GI tract. (B) Gene expression level of SP receptor (*Tacr2)* depicted as box and whisker diagram (top-to-bottom, maximum value, upper quartile, median, lower quartile, and minimal value, respectively). Any data not included between the whiskers is plotted as outlier with a dot. Significant difference between time-points are indicated by distinctive characters above the measurement group ($p < 0.05$).

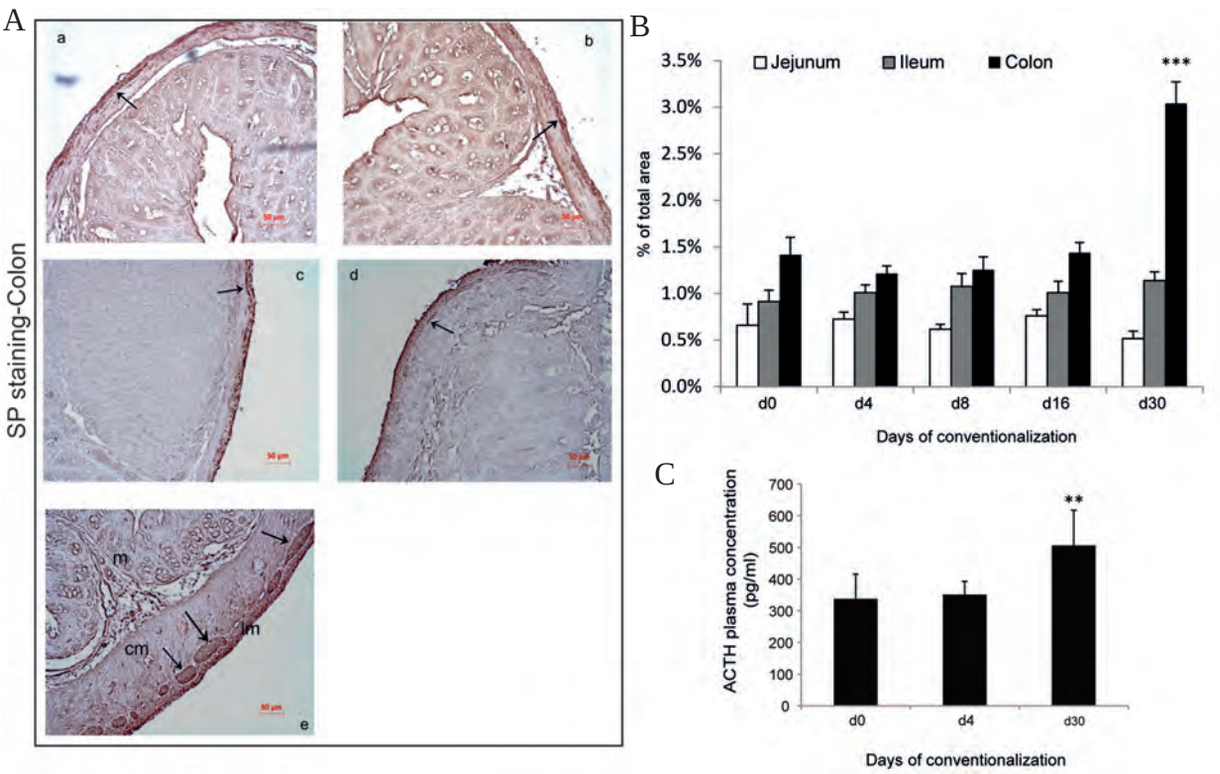

Figure 6.4. Microbiota and gut-brain interaction. (A**)** Representative immunostaining of substance P. The staining was performed as previously described (Verdu, Bercik et al. 2006). In brief, 4 µm-thick paraffin embedded cross sections from jejunum, ileum, and colon of germfree and conventionalized mice were incubated with Rabbit anti-substance P (1:1000) antiserum (Chemicon international, California, USA) as a primary antibody. Negative controls were performed by omitting the primary antibody. Vectastin Elite ABC kit was used for secondary anti substance P antibody and solutions (Vector, Burlingame, California, USA), using the manufacturer's instructions. Stained sections were analysed using light microscopy (Carl Zeiss, Axio 3.1), and quantification of immunostaining was performed on computer using computer software (image J) selecting the area of the myentric and submucous plexus and positive staining was expressed as percentage of total tissue area. (B) % of total surface area of substance P (SP) immunostaining in germfree and conventionalized mice at: a (day 0), b (day 4), c (day8), d (day 16), and e (day 30). M= mucosa; cm=circular muscle; lm=longitudinal muscle. The arrow indicates SP staining in the myenteric plexus. (C) Plasma levels of adrenocorticotrophic hormone (ACTH) measured by Mouse MAP multiplexed immunoassay systems. **=p value <0.001, ***= p value <0.0001.

The plasma analysis performed in germfree mice and after 4 and 30 days of conventionalization revealed the significant up-regulation of adrenocorticotrophic hormone (ACTH) at day 30 of conventionalization when compared to the other mice (germfree and 4 days after mice conventionalization) (Figure 6.4C). ACTH is secreted by the anterior pituitary gland in response to biological stress and is a main component of the hypothalamic-pituitary-adrenal (HPA) axis. Our results are in very good agreement with the previous observations made by Sudo and coworkers, who reported on the role of the gut microbiota on the modulation of the levels of ACTH and HPA in mice (Sudo, Chida et al. 2004). These authors suggested that microbial colonization and the associated immune activation increases the HPA responsiveness via the release of cytokines, which subsequently affect the parts of the central nervous system involved in the HPA regulation (Sudo, Chida et al. 2004). Taken together, these preliminary results suggest that there is a detectable effect of the microbiota on the function and architecture of the enteric nervous system. Such modulations may promote alterations of gut function, including mucosal metabolism and immune repertoire, but may also affect the central nervous system as is suggested by the altered ACTH plasma levels.
In order to unravel the mechanisms of the proposed communication between the microbiota and the enteric nervous system (and the brain), it would be required to carry out dedicated sampling of tissue from the GI tract and other organs (including liver) that are known to participate in hormonal signaling to the brain. In this respect it would be of interest to also sample the mouse brain at different time-points after conventionalization. It has previously been reported that the intestinal microbiota may affect the behavior of its host by activation of the mucosal immune system and neuropeptides (Bercik 2011), which can modulate brain functions and may change mood and behavior. Moreover, O'Connor and colleagues showed that bacterial LPS resulted in depression-like behavior which was linked to cytokine-induced changes in tryptophan metabolism and production of kynurenine (O'Connor, Andre et al. 2009). In light of these observations, it seems interesting to correlate the results of the proposed time-resolved brain analysis to the changes in host metabolism- and immune responses, and also in this respect day 4 post-conventionalization may be of particular interest on basis of the transient increase in the ratio of kynurenine/tryptophan at this time-point post-conventionalization.

Unraveling the Mechanism of Jejunal Control on Systemic Insulin Control

The striking role of the jejunum in perception of the microbiota-diet interplay proposes a crucial impact of the colonizing microbiota in altering host metabolic pathways including systemic glucose homeostasis and insulin control. It is likely that, after efficient microbial conversion of high-energy dietary compounds into low-energy compounds and after depletion of luminal glucose, epithelia store far less energy as fat and are accumulating far less glucose. Unfortunately, the present study did not allow a conclusive assessment of the effect of microbial colonization on gut hormones involved in the modulation of insulin secretion and the absorption of glucose in the proximal small intestine. Precise measurement of these gut hormones over time as well as glucose fluxes in the jejunum would help to explore whether the early microbial signaling seen in the jejunum is achieved through an endocrine mechanism and/or metabolic modulation. The intriguing connection that can be made to human duodenal-jejunal bypass surgery with the hormonal changes that occur prior to body weight modifications (Pories, Swanson et al. 1995), supports the proposed role of the jejunum in nutrient sensing and systemic control. This connection is potentially of utmost importance in diagnostics and/or therapies related

to important emerging diseases in Western Societies like obesity and the associated insulin resistance and type 2 diabetes. The discovery of an "obese microbiota" is of relevance in this context; apparently some microbiota can promote fat storage and insulin resistance as previously reported by Turnbaugh and colleagues who showed that gut microbiota transplantation from obese donor (*ob/ob* genotype) to lean acceptor (wild-type) mice resulted in increased fat deposition and weight gain in the transplanted mice (Turnbaugh, Ley et al. 2006). The observed inability of the first-stage microbiota that we found at days 1-4 to sufficiently deplete high-energy compounds might be seen as displaying characteristics of an "obese microbiota". Of note, the gastric bypass avoids contact between the diet, jejunum microbiota and the intestine. It is attractive to speculate that one reason for the success of gastric bypass surgery to avoid obesity problems is by bypassing an "obese" microbiota but instead, translocating the diet immediately to a more "lean" microbiota that is capable of efficient depletion of dietary glucose and high-energy compounds.

Identifying the Bacterial Effector Molecules; Functional Microbiomics

The application of the MITChip enabled the efficient determination of the dynamics of the establishing gut microbiota throughout the GI tract. Combined with multi-variate correlation analysis the MITChip datasets allowed the identification of specific bacterial groups that correlated with specific host responses. However, the identification of the bacterial effector molecules that are involved in mediation of these host-responses remains a major challenge. To identify such effector molecules one may consider employing large-insert metagenome expression libraries in combination with high throughput screening systems that employ efficient reporter cell-lines. This approach has been shown to allow the detection of specific pathway-activating or pathway-repressing metagenome clones, which paves the way towards identification of specific microbial effector molecules (van der Kleij, Latz et al. 2002; Gloux, Leclerc et al. 2007; Lakhdari, Cultrone et al. 2010). The application of metagenomic screening approaches could for example be employed to search for the microbiota effector molecules that elicit the acute response on day 1 post-conventionalization in the jejunal mucosa. Alternatively, these microbial effector molecules may also be discovered via mono-association or colonization with simplified microbial communities of germfree mice (Hooper, Wong et al. 2001; Mahowald, Rey et al. 2009). Such models may answer the question whether the observed activation of "danger signals" associated responses may be elicited by the diffusion of bacterial secreted metabolites and their uptake by epithelia or may depend on direct interaction of the mucosal tissue with bacterial ligands and their wall components. Provided that the nutrient flow is of importance in eliciting these acute effects, the application of different diets could address their impact on bacterial and metabolic sensing in the proximal part of the small intestine. We therefore propose that more attention should be given to the role and functionality of the small intestine (as opposed to colon) in bacterial and metabolic sensing, including systemic communication to the liver and the brain. It should not be forgotten that the eventual mechanistic insight that one may obtain from animal models needs to be translated into human physiology of health and disease. This requires the design of targeted validation studies in healthy or compromised volunteers in which jejunum biopsies are sampled that can be employed for transcriptome profiling and/or IHC investigations (van Baarlen, Troost et al. 2009; van Baarlen, Troost et al. 2011).

The application of metagenomic screening could also target the identification of microbial effector molecules involved in eliciting the transient state of inflammatory responses that preceded the establishment of tolerance and homeostasis. Such microbial effector molecules

could subsequently be administered to conventional mice, to explore their capacity to modulate the severity of induced inflammatory diseases, as they are applied in the TNBS and/or DSS ulcerative colitis models (Wirtz, Neufert et al. 2007). Another approach of interest could investigate the capacity of specific probiotic strains to modulate the transient inflammatory state that was measured at day 4 **(Chapter 5)**, aiming to (partially) reverse the adverse effects of the transient shift in the microbial community on the host immune response.

Relevance of the identified gene-regulatory networks as gene signatures for human

This study identified several gene regulatory networks that appeared to be involved in regulation of the immune and metabolic adaptation of the mouse intestinal mucosa to the colonizing microbiota. However, the evaluation of the relevance of the identified gene regulatory networks to be used as molecular signatures to monitor the risk of disease in humans is yet a major challenge. This goal could be approached by performing comparative studies of the regulatory networks identified from the mouse model, which appeared to be driven by a core set of regulating genes, and the corresponding human biological and disease regulatory networks. Such comparative studies would tell whether the overlays include essential core or non-essential peripheral genes, and whether they represent known disease genes in humans. Although the existence of complete reliable human regulatory networks and their role in disease is debated (Barabasi, Gulbahce et al. 2011), the identification of common regulators in the mouse model used in this study and of their human orthologues would confirm the validity of the animal-models for human studies. This in turn may inspire molecular hypotheses for human gastrointestinal disease, and may strengthen the accuracy of monitoring progressive clinical disease.

Concluding Remarks

The time-resolved mining of multi-variant datasets applied in this thesis provides a solid catalogue of genes, pathways, histology, metabolites, and plasma analytes that details the processes involved in the establishment of homeostasis in the germfree mouse model upon microbial conventionalization. This approach appears to have been very successful in delivering an important resource that complements previous studies that have targeted the colonization of the intestine in the same or a similar reductionist mouse model. The positive correlations identified in this thesis between the multi-variate datasets, including the linkages identified between microbial groups and specific host functions, support the prominent role of the microbiota in the modulation of the host's physiology. The interplay that was most extensively explored in this thesis focused on mucosal immunity and metabolism, but some impact of the microbiota to other aspects of host physiology may also be of great relevance for the host's health and well-being.

Acknowledgments

The authors thank Prof. J. Bienenstock, Y.K. Mao, and W. Kunze (McMaster University, Ontario) for assistance with histological staining and valuable discussions.

REFERENCES

Adlerberth, I. and A. E. Wold (2009). "Establishment of the gut microbiota in Western infants." Acta Paediatrica **98**(2): 229-238.

Atarashi, K., T. Tanoue, et al. (2011). "Induction of colonic regulatory T cells by indigenous Clostridium Species." Science **331**(6015): 337-341.

Bäckhed, F., H. Ding, et al. (2004). "The gut microbiota as an environmental factor that regulates fat storage." Proceedings of the National Academy of Sciences of the United States of America **101**(44): 15718-15723.

Barabasi, A.-L., N. Gulbahce, et al. (2011). "Network medicine: a network-based approach to human disease." Nature Reviews Genetics **12**(1): 56-68.

Bercik, P. (2011). "The microbiota-gut-brain axis: learning from intestinal bacteria?" Gut **60**(3): 288-289.

Chow, J. and S. K. Mazmanian (2010). "A pathobiont of the microbiota balances host colonization and intestinal inflammation." Cell Host & Microbe **7**(4): 265-276.

Claus, S. P., S. L. Ellero, et al. (2011). "Colonization-induced host-gut microbial metabolic interaction." mBio **2**(2).

Davidson, E. H. (2010). "Emerging properties of animal gene regulatory networks." Nature **468**(7326): 911-920.

de Magistris, L., V. Familiari, et al. (2010). "Alterations of the intestinal barrier in patients with autism spectrum disorders and in their first-degree relatives." Journal of Pediatric Gastroenterology and Nutrition **51**(4): 418-424.

Delzenne, N. M. and P. D. Cani (2010). "Nutritional modulation of gut microbiota in the context of obesity and insulin resistance: Potential interest of prebiotics." International Dairy Journal **20**(4): 277-280.

Erdman, S. E., V. P. Rao, et al. (2009). "Nitric oxide and TNF-alpha trigger colonic inflammation and carcinogenesis in Helicobacter hepaticus-infected, Rag2-deficient mice." Proceedings of the National Academy of Sciences of the United States of America **106**(4): 1027-1032.

Gloux, K., M. Leclerc, et al. (2007). "Development of high-throughput phenotyping of metagenomic clones from the human gut microbiome for modulation of eukaryotic cell growth." Applied and Environmental Microbiology **73**(11): 3734-3737.

Goldin, E., F. Karmeli, et al. (1989). "Colonic substance-P levels are increased in ulcerative-colitis and decreased in chronic severe constipation " Digestive Diseases and Sciences **34**(5): 754-757.

Heiden, M. G. V., L. C. Cantley, et al. (2009). "Understanding the Warburg Effect: The Metabolic Requirements of Cell Proliferation." Science **324**(5930): 1029-1033.

Heijtza, R. D., S. Wang, et al. (2011). "Normal gut microbiota modulates brain development and behavior." Proceedings of the National Academy of Sciences of the United States of America **108**(7): 3047-3052.

Hooper, L. V., M. H. Wong, et al. (2001). "Molecular analysis of commensal host-microbial relations hips in the intestine." Science **291**(5505): 881-884.

Husebye, E., P. M. Hellstrom, et al. (1994). "Intestinal microflora stimulates myoelectric activity of rat small-intestine by promoting cyclic initiation and aboral propagation of migrating myoelectric complex." Digestive Diseases and Sciences **39**(5): 946-956.

Kinjo, Y., D. Wu, et al. (2005). "Recognition of bacterial glycosphingolipids by natural killer T cells." Nature **434**(7032): 520-525.

Korner, J., M. Bessler, et al. (2005). "Effects of Roux-en-Y gastric bypass surgery on fasting and postprandial concentrations of plasma ghrelin, peptide YY, and insulin." Journal of Clinical Endocrinology & Metabolism **90**(1): 359-365.

Kullberg, M. C., J. M. Ward, et al. (1998). "Helicobacter hepaticus triggers colitis in specific-pathogen-free interleukin-10 (IL-10)-deficient mice through an IL-12- and gamma interferon-dependent mechanism." Infection and Immunity **66**(11): 5157-5166.

Lakhdari, O., A. Cultrone, et al. (2010). "Functional metagenomics: a high throughput screening method to decipher microbiota-driven NF-kappa B modulation in the human gut." Plos One **5**(9).

Maes, M., M. Kubera, et al. (2008). "The gut-brain barrier in major depression: Intestinal mucosal dysfunction with an increased translocation of LPS from gram negative enterobacteria (leaky gut) plays a role in the inflammatory pathophysiology of depression." Neuroendocrinology Letters **29**(1): 117-124.

Mahowald, M. A., F. E. Rey, et al. (2009). "Characterizing a model human gut microbiota composed of members of its two dominant bacterial phyla." Proceedings of the National Academy of Sciences of the United States of America **106**(14): 5859-5864.

Martensson HG, A. B., Yeo C, Jaffe BM (1984). "The role of substance P in the control of gastric acid secretion." Surgery. 1984 **95**(5): 567-571.

Maslowski, K. M., A. T. Vieira, et al. (2009). "Regulation of inflammatory responses by gut microbiota and chemoattractant receptor GPR43." Nature **461**(7268): 1282-U1119.

Mattner, J., K. L. DeBord, et al. (2005). "Exogenous and endogenous glycolipid antigens activate NKT cells during microbial infections." Nature **434**(7032): 525-529.
Neufeld, K. M., N. Kang, et al. (2011). "Reduced anxiety-like behavior and central neurochemical change in germ-free mice." Neurogastroenterology and Motility **23**(3).
O'Connor, J. C., C. Andre, et al. (2009). "Interferon-gamma and tumor necrosis factor-alpha mediate the upregulation of indoleamine 2,3-dioxygenase and the induction of depressive-like behavior in mice in response to Bacillus Calmette-Guerin." Journal of Neuroscience **29**(13): 4200-4209.
O'Keeffe, J. and A. P. Moran (2008). "Conventional, regulatory, and unconventional T cells in the immunologic response to Helicobacter pylori." Helicobacter **13**(1): 1-19.
Pamer, E. G. (2007). "Immune responses to commensal and environmental microbes." Nature Immunology **8**(11): 1173-1178.
Pories, W. J., M. S. Swanson, et al. (1995). "Who would have thought it-an operation proves to be the most effective therapy for adult-Onset diabetes mellitus." Annals of Surgery **222**(3): 339-352.
Riegler, M., I. Castagliuolo, et al. (1999). "Effects of substance P on human colonic mucosa in vitro." American Journal of Physiology-Gastrointestinal and Liver Physiology **276**(6): G1473-G1483.
Sarma-Rupavtarm, R. B., Z. M. Ge, et al. (2004). "Spatial distribution and stability of the eight microbial species of the altered Schaedler flora in the mouse gastrointestinal tract." Applied and Environmental Microbiology **70**(5): 2791-2800.
Silkoff, P., F. Karmeli, et al. (1988). "Effect of substance-P on rat gastrointestinal transit." Digestive Diseases and Sciences **33**(1): 74-77.
Sterzenbach, T., S. K. Lee, et al. (2007). "Inhibitory effect of enterohepatic Helicobacter hepaticus on innate immune responses of mouse intestinal epithelial cells." Infection and immunity **75**(6): 2717-2728.
Sudo, N., Y. Chida, et al. (2004). "Postnatal microbial colonization programs the hypothalamic-pituitary-adrenal system for stress response in mice." Journal of Physiology-London **558**(1): 263-275.
Theoharides, T. C. and R. Doyle (2008). "Autism, gut-blood-brain barrier, and mast cells." Journal of Clinical Psychopharmacology **28**(5): 479-483.
Troy, S., M. Soty, et al. (2008). "Intestinal gluconeogenesis is a key factor for early metabolic changes after gastric bypass but not after gastric lap-band in mice." Cell Metabolism **8**(3): 201-211.
Turnbaugh, P. J., R. E. Ley, et al. (2006). "An obesity-associated gut microbiome with increased capacity for energy harvest." Nature **444**(7122): 1027-1031.
Vaishnava, S., M. Yamamoto, et al. (2011). "The antibacterial lectin RegIII gamma promotes the spatial segregation of microbiota and host in the intestine." Science **334**(6053): 255-258.
Valbuena, G., W. Bradford, et al. (2003). "Expression analysis of the T-cell-targeting chemokines CXCL9 and CXCL10 in mice and humans with endothelial infections caused by rickettsiae of the spotted fever group." American Journal of Pathology **163**(4): 1357-1369.
van Baarlen, P., F. Troost, et al. (2011). "Human mucosal in vivo transcriptome responses to three lactobacilli indicate how probiotics may modulate human cellular pathways." Proceedings of the National Academy of Sciences of the United States of America **108**: 4562-4569.
van Baarlen, P., F. J. Troost, et al. (2009). "Differential NF-kappa B pathways induction by Lactobacillus plantarum in the duodenum of healthy humans correlating with immune tolerance." Proceedings of the National Academy of Sciences of the United States of America **106**(7): 2371-2376.
van der Kleij, D., E. Latz, et al. (2002). "A novel host-parasite lipid cross-talk - Schistosomal lyso-phosphatidylserine activates Toll-like receptor 2 and affects immune polarization." Journal of Biological Chemistry **277**(50): 48122-48129.
Verdu, E. F., P. Bercik, et al. (2006). "Specific probiotic therapy attenuates antibiotic induced visceral hypersensitivity in mice." Gut **55**(2): 182-190.
Wirtz, S., C. Neufert, et al. (2007). "Chemically induced mouse models of intestinal inflammation." Nature Protocols **2**(3): 541-546.
Wu, G. Y. (1998). "Intestinal mucosal amino acid catabolism." Journal of Nutrition **128**(8): 1249-1252.
Yap, I. K. S., M. Angley, et al. (2010). "Urinary metabolic phenotyping differentiates children with autism from their unaffected siblings and age-matched controls." Journal of Proteome Research **9**(6): 2996-3004.

Appendices

Nederlandse Samenvatting
الملخص العربي
Co-author affiliations
Acknowledgments
About the Author
List of Publications
Overview of Completed Training Activities

De dynamische interactie van microbiota en mucosa leidt tot vestging van homeostase in geconventionaliseerde muizen

De interacties tussen ons, onze darmbacteriën en de voedingscomponenten die door de darm passeren zijn van cruciaal belang voor onze gezondheid. Introductie van darmbacteriën in kiemvrije muizen (conventionalisering) resulteert in een cascade van strikt gereguleerde moleculaire mechanismen die zorgen voor homeostase en een tolerante respons van het immuunsysteem tegen deze bacteriën. Om de dynamiek van deze communicatie tussen bacteriën en gastheer te bestuderen gedurende conventionalisering op verschillende locaties in de darm is een combinatie van transcriptomics, (immuun)histologie, metabonomics (tissue, plasma en urine) en microbiota profilering met behulp van een muis-specifieke fylogenetische microarray (MITChip) gebruikt. Voor deze studie werden C57/B6 J kiemvrije muizen geconventionaliseerd met ontlasting van een normale C57/B6 J muis en vervolgens gedurende 30 dagen bestudeerd.

Uit deze studie is gebleken dat de diversiteit van de darmbacteriën na conventionalisering in de tijd toeneemt. Al na een dag was het effect van deze conventionalisering te zien in jejunum en urine, waar specifieke metabolieten werden gemeten, alsook in de transcriptionele respons van het jejunum epitheel. Daarentegen werd de transciptoom response in de ileum en colon pas na vier dagen waargenomen, die vervolgens tot een stabiele maar locatie-specifieke moleculaire situatie leiden vanaf dag 16. De belangrijkste moleculaire reacties op conventionalisering waren een sterke inductie van het niet-specifieke immuunsysteem die vervolgens gevolgd werden door adaptieve en regulerende immuunreacties en een verandering van vet-, suiker-, en anabole metabole routes. Convenionalisering werd verder gekenmerkt door twee fasen, die gescheiden worden door een korte intermediaire fase op dag 4 waarop een ontstekingsreactie plaatsvond die waargenomen kon worden in zowel de transcriptoom als specifieke histologische en plasma markers. Tegelijkertijd vond een verschuiving in de samenstelling van de darmbacteriën plaats waarbij vooral bacteriën domineerden die als pathobiont bekend staan, wat aangeeft dat het hier waarschijnlijk een tijdelijke dysbiosis betreft. Extensieve karakterisering van de transcriptoomdata over alle tijdstippen en locaties resulteerde in de identificatie van specifieke centrale genregulatie netwerken die het proces van conventionalisering reguleren en daarmee als genetische signaturen voor controle van homeostase in muizen kunnen worden beschouwd. Veel van deze genetische signaturen hebben ook homologen die in de genoom van de mens zijn gevonden wat suggereert dat deze observaties in muizen ook relevant kunnen zijn voor de darmbiologie van de mens. Deze hypothese wordt verstrekt door het feit dat het genetische regulatore netwerk in het jejunum sterk geassocieerd is met metabole ziekten in mensen, wat suggereert dat de proximale dunne darm een belangrijke rol speelt bij de systemische metabole controle.

Dit proefschrift illustreert de centrale rol van dynamische moleculaire interacties tussen darmbacteriën en darmepitheel in de ontwikkeling en behoud van mucosale homeostase in gezonde muizen. De moleculaire signaturen die in dit proefschrift beschreven staan zouden uiteindelijk kunnen leiden tot nieuwe therapeutische targets en diagnostische toepassingen voor specifieke ziekten die het gevolg zijn van dysbiosis of verlies van homeostase in de darm.

التفاعل الديناميكي بين البكتريا المعوية النافعة (الميكروبايوتا) والغشاء المخاطي وتأثيره علي تحقيق الاتزان البيولوجي للفئران المطعمة بالبكتريا

يعد التفاعل الوثيق بين كل من الميكروبايوتا والعائل والتدفق الغذائي ذى أهمية جوهرية في تعريف الحالة الصحية للعائل .ومن خلال عملية القيام بتطعيم الفئران الخالية من الميكروبات بالبكتريا المعوية النافعة , أمكن دراسة تأثير الاستجابات الجزيئية شديدة التنظيم في تحقيق الاتزان البيولوجي وتفعيل المقاومة المناعية إزاء الميكروبايوتا.

ولاكتشاف العمليات الديناميكية الزمنية والموضعية للتفاعل بين الميكروبايوتا والعائل خلال عملية تطعيم الفئران بالبكتريا تم دراسة مزيج من العناصر الجينية (الترانسكريبتوم) والخلايا والأنسجة المناعية إضافة إلى المواد الناشئة عن الايض (في الأنسجة والبول والدم) علاوة على تعريف الميكروبايوتا. وعقب ذلك تم تطعيم الفئران الخالية من الميكروبات بالبكتريا المعوية النافعة. وقد تمت متابعة نتائج تلك التجارب على مدار فترة زمنية تبلغ ثلاثون يوما متقطعة وقد اتسمت البكتريا المستوطنة بتغير مستوى التنوع من الأقل إلى الأكثر تنوعا على مدار فترة التطعيم. بالإضافة إلى ذلك أنعكس استيطان البكتريا على نمو سريع من خلال ارتفاع تركيزات مواد الأيض في البول والجزء الأوسط من الأمعاء الدقيقة وكذا التغيرات البيولوجية المهمة في جينات نسيج الجزء الأوسط من الأمعاء الدقيقة. وعلى العكس من ذلك أمكن قياس مدى استجابة الجينات في الجزء الأسفل من الأمعاء الدقيقة والقولون ولكن في فترة زمنية أكبر مقارنة بالجزء الأوسط من الأمعاء الدقيقة وقد اشتملت غالبية الاستجابات الجزيئية على زيادة حادة في الاستجابة المناعية غير المتخصصة بتبعها استثارة للوظائف المناعية المنظمة والمتخصصة فضلا عن التعديلات في مسارات ألايض المشتملة على ايض الدهون والكربوهيدرات. وعلى صعيد متصل اشتملت عملية التطعيم خلال مرحلتين منفصلتين يتخللهما مرحلة وسطية تمدد لفترة يوم واحد – وعلي وجة الخصوص في منطقة القولون – حيث تشبه تلك المرحلة إلى حد بعيد مرحلة انتقالية للالتهابات وذلك وفقا للمعدلات الانتقالية المرتفعة لمحددات معينة بالدم.

وقد تزامنت تلك المرحلة مع سيادة مؤقتة لمجموعة بعينها من البكتريا. وقد أتاح التحليل المكثف للجينات في منطقة الأمعاء الفرصة لتعريف شبكات جينية مركزية منظمة تعمل على التحكم في الاستجابات الجزيئية خلال عملية التطعيم.

وأخيرا فان هذا البحث يوضح الدور الحيوي الذي تلعبه التفاعلات الديناميكية فيما بين البكتريا المعوية النافعة والغشاء المخاطي من حيث تحقيق الاتزان البيولوجي في الفئران السليمة . وقد توفر الاستجابات الجزيئية التي توصل إليها البحث من خلال تلك الدراسات على الفئران أدوات تشخيصية موضعية وأهداف علاجية للإنسان عند حدوث بعض الاضطرابات المعوية والمتعلقة باعتلال الأمعاء والغشاء المخاطي.

Co-author Affiliations

Peter van Baarlen[1], Muriel Derrien[2, 3]†, Erwin G. Zoetendal[2, 3], Dicky J. Lindenbergh-Kortleve[4], Janneke N. Samsom[4], Guido Hooiveld[2, 5], Mark Boekschoten[2, 5], Florence Levenez[6], Joël Doré[6], Jan Dekker[2, 7], Claire A. Merrifield[8], Sandrine P. Claus[9], Elaine Holmes[8], Dirk-Jan Reijngoud[10], Ronald Aardema[11,12], Adrie Dane[11, 12], Rob Vreeken[11, 12], Selena E. Richards[13], Edward E.S. Nieuwenhuis[14], and Michiel Kleerebezem[1, 2, 3, 15]

[1] Host-Microbe Interactomics, Wageningen University, Wageningen, The Netherlands
[2] Top Institute Food and Nutrition, Wageningen, The Netherlands
[3] Laboratory of Microbiology, Wageningen University, Wageningen, The Netherlands
[4] Division Gastroenterology and Nutrition, Department of Pediatrics, Erasmus Medical Center, University Medical Center, Rotterdam, The Netherlands
[5] Nutrition, Metabolism and Genomics Group, Division of Human Nutrition, Wageningen University, Wageningen, The Netherlands
[6] INRA, UMR1319, Jouy-en-Josas France
[7] Department of Animal Sciences, Wageningen University, Wageningen, The Netherlands
[8] Biomolecular Medicine, Department of Surgery and Cancer, Faculty of Medicine, Imperial College London, London, United Kingdom
[9] Department of Food and Nutritional Sciences, The University of Reading, reading, UK
[10] Department of Laboratory Medicine, University Medical Centre Groningen, University of Groningen, Groningen, The Netherlands
[11] Division of Analytical Biosciences, LACDR, Leiden University, P.O Box 9502, 2300 RA Leiden, The Netherlands
[12] Netherlands Metabolomics Centre, Leiden, The Netherlands
[13] School of Science and Technology, Nottingham Trent University, Nottinghamshire, Nottingham, United Kingdom
[14] Department of Pediatric Gastroenterology, Wilhelmina Children's Hospital, University Medical Center Utrecht, Utrecht, The Netherlands
[15] NIZO food research, Health Department, Ede, The Netherlands

†Present address: Danone Research, Palaiseau, France

ACKNOWLEDGMENTS

When I was done with the reading version of my Ph.D. thesis, my supervisor said: "Well done to hang on to the finish". Indeed, completing the Ph.D. has been like a marathon event for me, and I would not have been able to complete this journey over the past five years without the help and support of far too many people to mention individually.

I am enormously grateful to my (co-) supervisor(s) who made the long time spent in this Ph.D. seems worthwhile after all. I owe my first and most sincere gratitude towards my supervisor; **Michiel**, you provided me with a step-by-step guide upon my first steps into the "Host-microbe interaction" field. In every sense, none of this work could be carried out without you. Your support, encouraging, constructive criticism, extensive discussions, and tireless help and patience, during my many hard times, had developed my professional qualifications as well as my personality at all levels.
Peter, your considerable and comprehensive knowledge, your creative ideas and logical way of thinking have been of great value to me.
Throughout my work with both of you, **Michiel** and **Peter**, I learnt not to accept only the conventional perception, but rather trust my instincts, the matter which offered me more scope for developing my own speculations.
Erwin, thank you so much for your generous support throughout this work.

Willem and **Hauke**, my sincere thanks for giving me the opportunity to manage my Ph.D. in your laboratory and within the MolEco group.

Je tiens plus particulièrement à remercier **Muriel**. Je suis très heureuse que nous avions pu surmonter tous les moments difficiles que nous avons passés et continuer ainsi notre travail et notre amitié.
Wasma and **Maria**, dear paranymphs, thank you for accepting to accompany me during my defense and to be my ceremonial assistants. I wish you all the best with your own defense very soon.

I would like to thank the cosmopolitan MolEco: **Sebastian, Tom, Susana, Xin, Coline, Clara, Ludmila, Floor, Milkha, Kyle, Naim, Noora, Janneke, Mauricio, Vincent, Detmer, Tian, Jing, Wilma , Hans, Ineke, Philippe, Corina, Monika, and Teresita.** A lot of thanks, particularly, to my (ex)-officemates: **Odette, Gianina, Petia, Farai, Thomas, Rozelin, Sara, Carmen**, **Jose**, and **Hermien**, your relevant insights were invaluable over the past years. Furthermore, I thank **Ton**, **Jannie**, and **Wim** for their substantial assistance. **Iris**, although I had the chance to work with you for only few times, it has been a great pleasure for me, thank you very much.

During this work I have been involved in many collaborations and have got the opportunity to work with several people. I would like to express my great regard and present my warmest thanks to all those who have participated in carrying out this work. Je tiens d'abord à exprimer ma profonde gratitude à **Joel, Florence, Christel, Florence, Pascal, Fabien, Patricia, Tomas, Marion, Sebastian, Antonella, Karien, and Michelle.** Je vous remercie pour l'accueil que vous m'avez réservé, pour l'aide professionnelle que vous m'avez accordée durant les

expérimentations et pour les bons moments que j'ai passé à l'INRA et à Paris. J'exprime aussi ma gratitude à tous ceux qui ont participé de près ou de loin dans l'élaboration de ce mémoire, je ne citerai pas de noms ici, pour ne pas en oublier certains.
I am very grateful to **Edward** at University medical center-Utrecht, **Janneke, Dicky, Roline**, and others, at Erasmus medical center-Rotterdam for providing me with the opportunity to touch on the field of immunology and for the valuable as well as the interesting discussions that greatly improved the immunology part in this work. **Dirk-Jan**, your helpful willingness to offer constructive discussions and comments were of great value in improving the metabolic part in this work through our collaboration with the medical university hospital-Groningen.
Jerry, during the "Introduction Day" of your group, Host-microbe interactomics, and in the beginning of my Ph.D., you introduced me to the cell biology and immunology (CBI) group at Wageningen University. Thank you for facilitating my work there. Concerning the CBI group, I would like to express my deep gratitude to **Henk** and **Anja** for guiding me in preparing such fascinating histological sections.
It has been a true honor **John** to collaborate with you and your team at McMaster university-Canada. Thank you for your encouraging, motivation, and very fast response in spite of your continuous travel schedule.

In addition, I wish to thank **Anja, Mali, Hannie, Carolein, Roelifina, Petra**, **Felice, Luc, Michiel,** and **Rianne** for their expert help in the administrative and secretarial work.

This research was part of the Top Institute of Food and Nutrition, A-1001, project. **Jan,** thank you so much for facilitating the project procedures. I would like to thank all team members of A-1001 and TIFN experts including **Linda, Nicole, Denise, Irene, Anneke, Aat, Shohreh, Mark,** and **Guido** for their valuable participation.

My dear friends, **Judit, Daniela, Laure, Martha, Haisa, Yorgos, Kindel, Lisa, Lidia, Wasma, Patricia, Pieter, Rosemarie, Noriko, Abdelhalim**, **Carien, Oriana, Rafael, May, Audrey,** and **Ola**, although many of you are not or no longer are in the Netherlands, you have played an essential role in my life during the years I spent away from my home country. Thank you all for everything, you made my stay in Holland very special as you all proved to be that a friend in need is a friend indeed!

Finally, my last acknowledgment is to my family. **Ahmed**, dearest brother, thank you for your emotional support and your effective cooperation, while I am away. My most heartfelt thank-you to my parents for instilling in me confidence and a drive for pursuing my Ph.D. My dearest **Papa** and **Mama**, without your continual support, encouraging, and helpful advice, it would have been impossible for me to make it to the end! For always being there when I needed you most, and never once complaining about how busy I am, even during my infrequent visits, you deserve far more credit than I can ever give you.

واخيراً أود أن أتقدم بجزيل شكرى و تقديرى لعائلتى الكريمة التى أمدتنى بالدعم المستمر، فلولا مثابرتهم و تشجعهم الدائم لما استطعت تحقيق هدفي و مبتغاى مهما واجهت من صعاب او اعترضت طريقى المشكلات و المعوقات.
و لقد رأيت أن ما من شئ يمكننى فعله لرد الجميل سوى العودة بدرجة الدكتوراه لأجعلهم جميعاً فخورين بما حققته أثناء غيابى.

Sahar

About the Author

Sahar El Aidy was born on the 10th of January 1980 in Berlin, Germany. Upon graduation in high school in 1996, she started her B.S. studies in pharmaceutical sciences at the Faculty of Pharmacy-Alexandria University during the period from September 1996 to June 2001. From October 2001 till June 2003, Sahar worked as a demonstrator at the department of Pharmacognosy and Medicinal plants, Faculty of Pharmacy-Misr University for Science and Technology, Cairo, Egypt and Faculty of Pharmacy, El-Minya University, Egypt. In June 2003, she continued her work as a demonstrator at the department of Pharmaceutical and Industrial Biotechnology in the Genetic engineering and Biotechnology Research Institute-Minoufya University, Egypt. In September 2004, Sahar was granted a fellowship from the Netherlands Organization for International Cooperation in Higher Education to obtain the master degree (MS.c) in cellular and molecular biotechnology at Wageningen University. Sahar joined the laboratory of microbiology in September 2005 to accomplish her major thesis for a six-month course. Afterwards, she completed her minor thesis at the Microbiology laboratory, University of Illinois at Urbana-Champaign, USA, in a four-month course. In 2007 till now, she returned to the Laboratory of Microbiology at Wageningen University to start her Ph.D. thesis under the supervision of Professor Michiel Kleerebezem. The Ph.D. project was a work-package within one of the Top Institute of Food and Nutrition projects.

List of Publications

Van den Abbeele P, Gérard P, Rabot S, Bruneau A, **El Aidy S**, Derrien M, Kleerebezem M, Zoetendal EG, Smidt H, Verstraete W, Van de Wiele T, Possemiers S. 2011. Arabinoxylans and inulin differentially modulate the mucosal and luminal gut microbiota and mucin-degradation in humanized rats. *Environ Microbiol.***13** (10):2667-80.

Booijink CC, **El Aidy S**, Rajilić-Stojanović M, Heilig HG, Troost FJ, Smidt H, Kleerebezem M, De Vos WM, Zoetendal EG. 2010. High temporal and inter-individual variation detected in the human ileal microbiota-Environmental Microbiology. *Environ Microbiol.* **12** (12):3213-27.

Van den Abbeele P, Grootaert C, Marzorati M, Possemiers S, Verstraete W, Gérard P, Rabot S, Bruneau A, **El Aidy S**, Derrien M, Zoetendal E, Kleerebezem M, Smidt H, Van de Wiele T. 2010. Microbial community development in a dynamic gut model is reproducible, colon-region specific and selects for Bacteroidetes and Clostridium cluster IX. *Appl Environ Microbiol.* **76** (15):5237-46.

El Aidy S, van Baarlen P, Derrien M, Lindenbergh-Kortleve DJ, Hooiveld G, Levenez F, Doré J, Dekker J, Samsom JN, Nieuwenhuis EES, and Kleerebezem M. Identification of the core gene-regulatory network that governs the dynamic establishment of intestinal homeostasis during conventionalization in mice. *Submitted.*

El Aidy S, Merrifield CA, Derrien M, van Baarlen P, Hooiveld G, Levenez F, Doré J, Dekker J, Holmes E, Claus SP, Reijngoud DJ, and Kleerebezem M. Molecular dynamics of microbiota sensing in the mouse jejunal mucosa during conventionalization support a prominent role of the jejunum in systemic metabolic control. *Submitted.*

El Aidy S, Derrien M, Merrifield C.A, Boekschoten M, Levenez F, Doré J, Dekker J, Holmes E, Zoetendal EG, Claus SP, van Baarlen P, and Kleerebezem M. The interplay between gut microbiota, host-transcriptome and metabolism in the mouse colon during conventionalization. *To be submitted.*

El Aidy S, Derrien M, Aardema R, Hooiveld G, Richards S, Dane A, Dekker J, Vreeken R, Levenez F, Zoetendal EG, Doré J, van Baarlen P, and Kleerebezem M. A transient state of microbial dysbiosis and inflammation is pivotal in the establishment of homeostasis during conventionalization of mice. *Submitted.*

El Aidy S and Kleerebezem M. Gut microbiota and the balance between health and disease. *In preparation.*

Overview of Completed Training Activities

Discipline Specific Activities	
Ecophysiology of the GUT	2007
Metabolomics	2007
Design of animal experiments	2008
HITChip course	2008
Food fermentation	2008
Advanced microarray data analysis	2008
Basic statistics	2008
The light in the intestinal tunnel	2009
UEGF Teaching Activity on Basic Science;cell signaling and the gut	2009
Nutrigenomics course	2009
Advanced visualization, integration, and biological interpretation of ~omics data	2010
General Courses	
Techniques of scientific writing	2007
Scientific publication	2007
VLAG Ph.D. week	2007
Writing Grant proposals	2010
Optional Activities	
Preparing Ph.D. research proposal	2007
TIFN project meetings A-1001	2007-11
Ph.D./Postdoc. meetings, Laboratory of Microbiology, Wageningen	2007-11
Symposia/Conferences	
Darmendag, University Medical center, The NL **(Poster presentation)**	2008
Mucosal immunology and intestinal microflora ,UK **(Oral presentation)**	2009
Sackler Colloquium-Microbes and Health, USA **(Poster presentation)**	2009
Darmendag, Unilever, The NL **(Oral presentation)**	2009
1st MetaHit conference, China **(Poster presentation)**	2010
7th Rowett/INRA symposium on Gut microbiology, UK **(Oral presentation)**	2010
3rd ASM-beneficial microbes conference, USA **(Poster presentation)**	2010
Symposium Mucosal immunology, Rotterdam, The NL	2011
2nd Intern. symposium, Microbes for health, France **(Oral presentation)**	2011

The research described in this thesis was financially supported by the Top Institute Food and Nutrition (TIFN).

Cover Design: Sahar El Aidy and Georgios Perrakis

Printed by: GVO drukkers & vormgevers B.V. | Ponsen & Looijen